UNIVERSITÀ VITA-SALUTE SAN RAFFAELE

**CORSO DI DOTTORATO DI RICERCA
IN MEDICINA MOLECOLARE**

Curriculum in Immunologia e Oncologia di Base e Applicate - MMBAIO

Unravelling the role of Integrated Stress Response signalling in metastatic Breast Cancer bioenergetics

Supervisore: Prof. Carlo Tacchetti
Co-supervisore: Prof. Carlotta Giorgi

Tesi di DOTTORATO di RICERCA di Clara Cardella
Matr. 022929

Ciclo di dottorato XXXVIII
SSD BIO/13 – BIOLOGIA APPLICATA

Anno accademico 2024/2025

CONSULTAZIONE TESI DI DOTTORATO DI RICERCA

Il/la sottoscritto ……..Clara Cardella……

Matricola ……022929…….

nata a ……Palermo…….

il ……09/01/1996……

autore della Tesi di Dottorato di Ricerca dal titolo

Unravelling the role of Integrated Stress Response signalling in metastatic Breast Cancer bioenergetics

X AUTORIZZA la Consultazione della Tesi

□ NON AUTORIZZA la Consultazione della Tesi per …… mesi a partire dalla data di sottomissione della domanda di conseguimento titolo

Poiché:

□ l'intera ricerca o parti di essa sono potenzialmente soggette a brevettabilità;

□ ci sono parti di Tesi che sono già state sottoposte a un editore o sono in attesa di pubblicazione;

□ la Tesi è finanziata da enti esterni che vantano dei diritti su di esse e sulla loro pubblicazione.

E' fatto divieto di riprodurre, in tutto o in parte, quanto in essa contenuto

Data .....30/03/2026…. Firma …….....

DECLARATION

Questa Tesi è stata:

- Redatta da me e non è mai stata utilizzata in alcuna precedente richiesta di laurea. Nel testo si utilizza sia il pronome "io" che "noi" in modo intercambiabile.
- Scritta in conformità alle linee guida editoriali approvate dall'Università.

È stata richiesta e ottenuta l'autorizzazione all'uso di immagini e altro materiale coperto da copyright. Per le seguenti immagini 1, 2, 3, 4, 5, 6 and 9 non è stato possibile ottenere il permesso e pertanto, sono incluse nella Tesi in base all'eccezione di “fair use” (Decreto Legislativo italiano n. 633/1941 e successive modifiche).

Tutti i risultati qui presentati sono stati ottenuti da me, ad eccezione di:

1) Analisi bioinformatica, Heatmap da TCGA-BRCA dataset (Risultati, Capitolo 1, Figura 7B), eseguita da Jagat Chauhan (Ludwig Cancer Research, University of Oxford, United Kingdom).

***2)** Ribo-Seq/RNA-Seq e analisi su Reactome (Risultati, Capitolo 2.1, Figura 9 e Figura 10),* eseguiti da Paola Falletta (Vita-Salute San Raffaele University e IRCCS San Raffaele Hospital, Experimental Imaging Center, Milan) e Marco Gaviraghi (Human Technopole, Genomic Research Centre, Milan).

***3)** Microscopia elettronica e analisi (Risultati, Capitolo 2.2, Figura 12),* eseguiti da Alessia Loffreda ed Emanuele Colombo (Vita-Salute San Raffaele University, Experimental Imaging Center, Alembic, Milan).

***4)** Analisi di Metabolomica, Lipidomica e Proteomica (Risultati, Capitolo 2.3, Figura 15C; Capitolo 3.1, Figura 19; Capitolo 3.2, Figura 26)* eseguiti da Eduardo Maria Sommella e altri componenti del gruppo del Prof. Campiglia (University of Salerno, Department of Pharmacy, Fisciano, Salerno, Italy).

***5)** Seahorse XF Cell Mito Stress Test e Metabolomica (Risultati, Capitolo 2.3, Figura 15A,B)* eseguiti da Daniela Gaglio (Institute of Molecular Bioimaging and Complex Biological Systems (IBSBC), National Research Council (CNR), Segrate, Milan, Italy).

6) *3D reconstruction of mitochondrial network and analyses (Risultati, Capitolo 2.2, Figura 11),* eseguiti in collaborazione con il gruppo di ricerca del Prof. Paolo Pinton (Signal Transduction Lab, University of Ferrara, Ferrara, Italy).

7) Calcium flux measurements and live confocal microscopy images (Risultati, Capitolo 2.2, Figura 11, 13 e 14) eseguiti presso il laboratorio del Prof. Paolo Pinton (Signal Transduction Lab, University of Ferrara, Ferrara, Italy).

Tutte le fonti di informazione sono state riconosciute tramite citazioni bibliografiche.

ACKNOWLEDGEMENTS

This PhD project was supported by a 2024 AIRC short-term fellowship, which offered me the opportunity to spend three months in the Signal Transduction Lab led by prof. Paolo Pinton (University of Ferrara). The aim of this period abroad was to investigate how activation of the integrated stress response (ISR) regulates mitochondrial dynamics and functionality.

ABSTRACT- ENGLISH

The Integrated Stress Response (ISR) is an evolutionarily conserved adaptive pathway that mediates translation reprogramming in response to microenvironmental stress, often hijacked by cancer cells to promote metastasis. To reveal novel targetable vulnerabilities in Triple-negative Breast Cancer (TNBC), the most aggressive breast cancer subtype, characterized by high metastatic propensity and limited therapeutic options, here we elucidate the mechanisms by which ISR accommodates the energy demands of metastatic cells. We show that TNBC exhibits the highest level of ISR among all breast cancer subtypes, correlating with reduced overall survival. ISR specifically enhances mitochondrial proteins synthesis, resulting phenotypically in reversible fragmentation and altered cristae morphology and functionally in the suppression of mitochondrial calcium uptake, oxidative and carbon metabolism. Concurrently, ISR promotes a shift towards fatty acid oxidation, upregulating Carnitine Palmitoyltransferase 1A (CPT1A). At the lipid metabolic level, ISR drives depletion of monounsaturated fatty acids through Stearoyl-CoA Desaturase 1 (SCD1) downregulation, establishing a bidirectional feedback loop that stabilizes a mesenchymal, stress-resistant cellular state and promotes TNBC cells invasiveness. Despite the pro-ferroptotic consequences of MUFA depletion, ISR confers ferroptosis resistance through coordinated upregulation of SLC7A11 and downregulation of transferrin receptor 1 (TFR1) and ether-linked phosphatidylcholines (PC-O), establishing a multi-layered ferroptotic barrier that translates into a long-term survival advantage under challenge. Together, these findings define the ISR as a central coordinator of metabolic adaptation in TNBC that simultaneously drives invasive reprogramming and ferroptosis resistance, identifying its downstream effectors as rational therapeutic targets in this aggressive disease.

ABSTRACT- ITALIANO

La risposta integrata allo stress (ISR) è una via adattativa conservata dal punto di vista evolutivo che media la riprogrammazione della traduzione in risposta allo stress microambientale, spesso sfruttata dalle cellule tumorali per favorire la metastasi. Per rivelare nuove vulnerabilità bersagliabili nel carcinoma mammario triplo negativo (TNBC), il sottotipo di carcinoma mammario più aggressivo, caratterizzato da un'elevata propensione alla metastasi e da opzioni terapeutiche limitate, qui chiariamo i meccanismi attraverso i quali l'ISR soddisfa il fabbisogno energetico delle cellule metastatiche. Dimostriamo che il TNBC presenta i livelli più elevati di ISR tra tutti i sottotipi di carcinoma mammario, in correlazione con una ridotta sopravvivenza globale. L'ISR potenzia specificamente la sintesi delle proteine mitocondriali, determinando a livello fenotipico una frammentazione reversibile e un'alterazione della morfologia e della struttura delle creste mitocondriali e, a livello funzionale, la soppressione dell'assorbimento del calcio a livello mitocondriale, del metabolismo ossidativo e di quello del carbonio. Contemporaneamente, l'ISR promuove uno spostamento verso l'ossidazione degli acidi grassi, aumentando l'espressione della carnitina palmitoiltransferasi 1A (CPT1A). A livello del metabolismo lipidico, l'ISR determina la deplezione degli acidi grassi monoinsaturi determinando la riduzione della stearoil-CoA desaturasi 1 (SCD1) e stabilendo un feedback loop bidirezionale che stabilizza uno stato cellulare mesenchimale e resistente allo stress e promuove l'invasività delle cellule di TNBC. Nonostante le conseguenze pro-ferroptotiche della deplezione di MUFA, l'ISR conferisce resistenza alla ferroptosi attraverso una regolazione positiva coordinata di SLC7A11 e una regolazione negativa del recettore 1 della transferrina (TFR1) e delle fosfatidilcoline con legame etere (PC-Os), creando una barriera ferroptotica a più livelli che si traduce in un aumento di sopravvivenza a lungo termine in condizioni di stress. Nel loro insieme, questi risultati definiscono l'ISR come coordinatore centrale dell'adattamento metabolico nel TNBC che guida simultaneamente la riprogrammazione invasiva e la resistenza alla ferroptosi, identificando i suoi effettori a valle come potenziali bersagli terapeutici in questa malattia aggressiva.

TABLE OF CONTENTS

INTRODUCTION

1. Tumour progression and adaptation to microenvironmental stress

Cancer progression is determined by uncontrolled proliferation accompanied by the capacity of transformed cells to survive, adapt, and acquire plasticity under a plethora of stress conditions. As tumours develop, they are exposed to a wide range of fluctuating challenges exacerbated by a profound remodelling of the tumour microenvironment (TME), such as hypoxia, nutrient deprivation, oxidative and proteotoxic stress, acidosis, immune surveillance, and therapy-induced harm. In this context, the most aggressive tumour cells are not merely those with the highest proliferative potential, but those able to exploit stress as a selective force, activating adaptive programs to preserve viability and counteract cell death activation, promote cell plasticity to accommodate microenvironmental metabolic shifts, and support metastatic colonization by activating migratory and invasive programs.

This view places stress adaptation at the core of tumour evolution towards malignancy. From this perspective, tumour aggressiveness arises from the interplay between intrinsic genetic determinants, including the accumulation of oncogenic alterations and loss of tumour-suppressive functions, and adaptive programs that dynamically rewire transcriptional, translational and metabolic processes in response to microenvironmental stress. These adaptive responses are essential throughout metastatic progression, enabling cancer cells to withstand adverse local conditions, survive during detachment and systemic dissemination, and eventually colonize distant organs. At the same time, they affect the crosstalk between cancer cells and the stromal, immune and metabolic components of the TME, contributing to tumour heterogeneity and therapeutic outcomes.

Among solid tumours, Breast Cancer (BC) provides an especially relevant context in which to investigate the relationship between stress adaptation and malignancy progression. In particular, and among the different BC subtypes, Triple-negative Breast Cancer (TNBC) represents a clinically aggressive and biologically heterogenous subtype, characterized by high metastatic propensity, marked metabolic plasticity, and limited therapeutic options. These features make TNBC especially dependent on molecular programs that enable adaptation to hostile microenvironmental conditions. For this reason, TNBC constitutes a valuable model to explore how stress response pathways

orchestrate metabolic rewiring, mitochondrial adaptation, lipid homeostasis, and resistance to regulated forms of cell death.

Within this conceptual framework, the Integrated Stress Response (ISR) should be regarded as one of the principal molecular systems through which tumour cells sense adverse conditions and reorganize their biology accordingly. By coupling environmental and intracellular stress signals to broad changes in translation, transcription, metabolism and cell fate regulation, the ISR stands in a central position at the intersection of the major processes addressed in this thesis. These include metabolic remodelling, mitochondrial function, redox homeostasis, lipid metabolism, ferroptosis susceptibility, and the acquisition of invasive traits. Framing the ISR in this broader context is therefore essential to understand how tumour cells adapt to microenvironmental pressure and how such adaptation may, in turn, create specific vulnerabilities that can be therapeutically exploited.

2. Breast Cancer

BC is a heterogeneous malignancy that, as reported by GLOBOCAN 2022 (Global Cancer Observatory, World Health Organization), ranks as the second most diagnosed cancer globally and the fourth leading cause of cancer-related death across all sexes. Among women specifically, it represents the foremost cause of both cancer incidence and mortality. In 2022 alone, the disease was responsible for 666,103 deaths, accounting for approximately 6.9% of all cancer fatalities. These figures reflect a broader global trend of rising cancer burden, driven by population growth and aging alongside shifts in the prevalence of risk factors that are closely tied to patterns of socioeconomic development. (Bray et al. 2024)

BC arises predominantly from the epithelial compartment of the terminal duct–lobular unit, which represents the functional and anatomical origin of most mammary tumours (Biswas et al. 2022). Histopathological studies indicate that early neoplastic changes frequently develop at the interface between terminal ducts and lobules, where lesions such as hyperplastic enlarged lobular units can be detected (Oyama et al. 2000; Nicosia et al. 2024). These early alterations are considered precursors of hormone-responsive BCs and are often associated with increased expression of estrogen and progesterone receptors, highlighting the importance of histological context in determining endocrine sensitivity and therapeutic response (S. Lee et al. 2005). Accordingly, the anatomical and cellular

origin of breast tumours has long served as a foundation for their classification and clinical management.

From a pathological perspective, BCs are broadly classified by the World Health Organization into carcinomas and sarcomas (Sinn and Kreipe 2013). Carcinomas, which account for most cases, originate from epithelial cells of the ducts and lobules or from mammary stem cells capable of epithelial differentiation, whereas sarcomas arise from mesenchymal components such as connective tissue and represent a rare entity (S. Liu et al. 2005; Voutsadakis et al. 2011). Breast carcinomas display substantial heterogeneity and are further subdivided into *in situ* lesions, which remain confined to their tissue of origin, and invasive carcinomas, which acquire the capacity to infiltrate surrounding tissue and metastasize. Among invasive tumours, carcinoma of no special type (NST) constitutes the most prevalent subtype, while invasive lobular carcinoma (ILC) represents a distinct and clinically relevant entity characterized by unique growth patterns and morphological features (Siegel et al. 2015; Zubair et al. 2021). Although grading systems based on glandular differentiation, nuclear atypia, and mitotic activity contribute to prognostic evaluation, they only partially capture the complexity of invasive BC. The recognition of this heterogeneity has driven the development of molecular classifications that complement traditional histopathological approaches. Advances in genomic and transcriptomic profiling have refined the classification of BC into biologically and clinically meaningful subtypes. While the intrinsic classification is based on transcriptomic signatures, routine clinical practice generally relies on surrogate immunohistochemical markers, including estrogen receptor (ER), progesterone receptor (PR), human epidermal growth factor receptor 2 (HER2), and the proliferation marker Ki67 (Harbeck et al. 2019). Based on the expression of ER and/or PR, BCs are further subdivided into luminal A and luminal B subtypes (Sørlie et al. 2003) (**Figure 1,** (Sheva et al. 2024)). This integrated histological and molecular framework has become central to modern BC management, informing prognosis, guiding therapeutic strategies, and underscoring the need for specialized, multidisciplinary care (Roy et al. 2023).

Luminal A BCs constitute roughly 40–50% of all cases. They are characterized by high hormone receptor expression, low proliferative index, reflected by low Ki67 levels, absence of HER2 amplification, and generally lower histological grade. Clinically, luminal A tumours are associated with a favourable prognosis and high sensitivity to

endocrine therapies (Perou et al. 2000; Sørlie et al. 2003; Xinhui Li et al. 2021; Harbeck et al. 2019).

Luminal B tumours account for approximately 15–20% of BCs. While also hormone receptor–positive, they display higher proliferative activity, reflected by higher levels of Ki67, they may express or not HER2, and often present with higher grade and worse clinical outcomes compared to luminal A tumours. As a result, luminal B cancers frequently require combined endocrine and chemotherapeutic approaches (Perou et al. 2000; Sørlie et al. 2003; Xinhui Li et al. 2021; Harbeck et al. 2019).

The HER2-enriched subtype comprises about 10–15% of BCs. These tumours are defined by amplification or overexpression of HER2, typically lack ER and PR expression, high grade and high proliferative activity, with high Ki67 index. Prior to the introduction of HER2-targeted therapies, this subtype was associated with an aggressive clinical course and poor prognosis. The development of HER2-directed agents has dramatically improved outcomes, illustrating the clinical relevance of molecular stratification (Perou et al. 2000; Sørlie et al. 2003; Xinhui Li et al. 2021; Harbeck et al. 2019).

TNBC accounts for approximately 15–20% of cases and is defined by the absence of ER, PR, and HER2 expression. Although many TNBCs display a basal-like gene expression profile, the two categories are not fully overlapping, indicating biological diversity within this clinical group. This subgroup is characterized by high histological grade, elevated proliferative rates, with high Ki67 index, early recurrence, and a strong propensity for visceral and brain metastases. Due to the lack of actionable receptors, TNBC treatment relies predominantly on chemotherapy, and its aggressive nature underscores the need for novel therapeutic strategies. (Perou et al. 2000; Sørlie et al. 2003; Xinhui Li et al. 2021; Harbeck et al. 2019).

A smaller fraction of tumours, often referred to as normal-like BC, represents less than 5% of cases. This subtype shares gene expression patterns with normal breast tissue; however, its biological and clinical significance remains less well defined, partly due to potential contamination with non-tumour tissue in gene expression analyses. (Perou et al. 2000; Sørlie et al. 2003; Xinhui Li et al. 2021).

Overall, the molecular classification of BC has profoundly influenced clinical management by enabling more accurate prognostication and personalized treatment

selection. Importantly, these subtypes also differ markedly in their metabolic dependencies (Tufail et al. 2024), stress response pathways, and susceptibility to cell death mechanisms, providing a conceptual framework for exploring subtype-specific vulnerabilities, particularly relevant for aggressive forms such as TNBC (Giri et al. 2023).

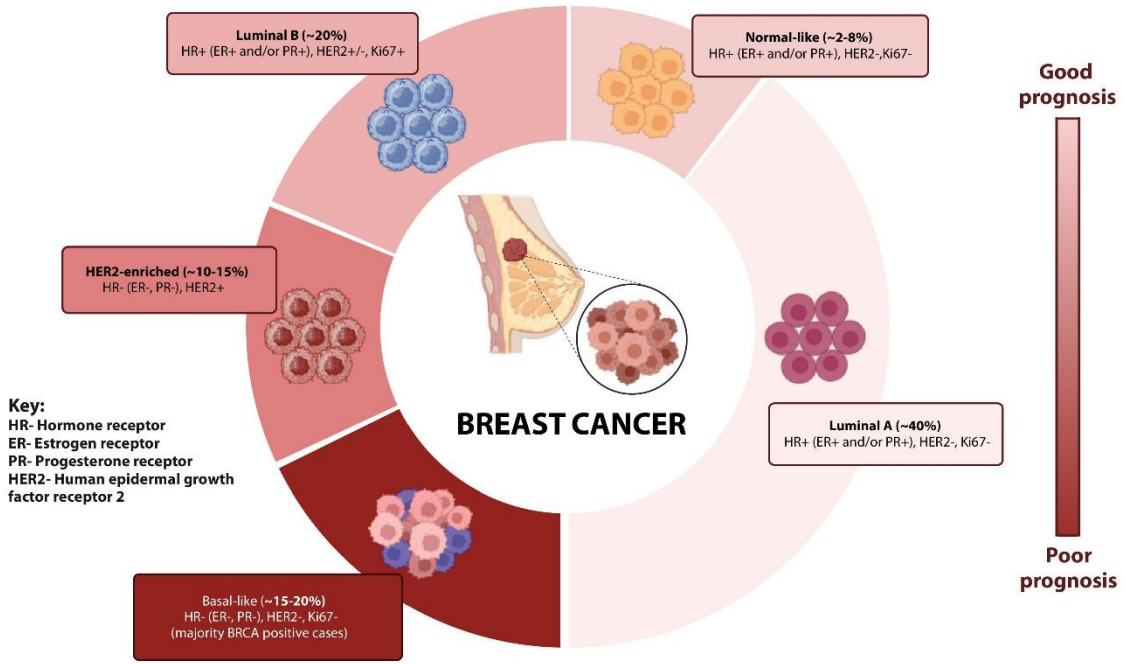

Figure 1. Molecular breast cancer subtypes. *Clinical categorization of breast tumors is determined by the presence or absence of specific biomarkers, including the estrogen receptor (ER), progesterone receptor (PR), human epidermal growth factor receptor 2 (HER2), and the proliferation index Ki-67. These markers distinguish between the Luminal A, Luminal B, Normal-like, HER2-enriched, and Basal-like (TNBC) subtypes. Image from Sheva et al. 2024*

2.1 Triple-negative Breast Cancer

TNBC is the most aggressive subtype of BC, characterized by higher metastatic potential and the absence of effective targeted therapeutic approaches. It occurs more frequently in young, premenopausal women, particularly under the age of 40, and shows a higher incidence in women of African-American ancestry (Dietze et al. 2015; Derakhshan and Reis-Filho 2022).

At the genomic level, TNBC displays a high degree of instability and heterogeneity, with one of the highest mutation rates among BC subtypes (METABRIC Group et al. 2012; Bareche et al. 2018). TP53 is the most frequently altered gene, accompanied by widespread copy number gains and losses reflecting chromosomal instability (Shah et al.

2012; The Cancer Genome Atlas Network 2012; Ellis and Perou 2013). A prominent feature is homologous recombination deficiency (HRD), often associated with germline or somatic alterations in BRCA1/2 and other DNA repair genes, as well as with epigenetic silencing of BRCA1 (Hartman et al. 2012; Couch et al. 2015; Turner 2017). These defects generate characteristic genomic scars collectively referred to as a BRCAness phenotype (Timms et al. 2014; Bianchini et al. 2016), and HRD-positive TNBCs tend to show enhanced sensitivity to DNA-damaging agents such as platinum compounds (Tutt et al. 2018; Bianchini et al. 2022), making HRD-related signatures potential predictive biomarkers. Overall, the complex and variable pattern of genomic alterations in TNBC helps explain its biological aggressiveness and the difficulty in identifying simple markers for clinical stratification.

TNBC is a highly heterogeneous disease at the molecular level, comprising distinct subtypes with specific biological features and clinical behaviours. Gene expression profiling studies by Lehmann et al. in 2011 initially identified up to seven TNBC subgroups, which were subsequently refined in 2016, through histological evaluation and laser microdissection, into four major intrinsic tumour subtypes: basal-like (BL1 and BL2), mesenchymal, immunomodulatory, and luminal androgen receptor (LAR) (Lehmann et al. 2011, 2016). The basal-like subtype accounts for the majority of cases (approximately 70–80%) and is characterized by high proliferative activity, genomic instability, frequent TP53 mutations, expression of basal cytokeratins, and an overall poor clinical outcome. The mesenchymal subtype is defined by activation of epithelial-to-mesenchymal transition (EMT) programs, conferring increased motility, invasiveness, therapy resistance, and an aggressive clinical course. (Lehmann et al. 2011, 2016, 2021; Bareche et al. 2018) The immunomodulatory subtype displays enrichment of immune-related gene signatures, high levels of tumour-infiltrating lymphocytes, and a more favourable prognosis, with enhanced responsiveness to immunotherapeutic approaches; within this group, a basal-like immune-activated (BLIA) phenotype with activation of Signal Transducer and Activator of Transcription (STAT) signalling pathways has been identified later and associated with particularly good outcomes (Burstein et al. 2015). The LAR subtype, which is less frequent, is characterized by androgen receptor expression, a luminal-like transcriptional profile, recurrent alterations in the Phosphoinositide 3-kinase (PI3K) pathway, and a relatively indolent behaviour, suggesting potential sensitivity to

anti-androgen–based therapies (Y.-Z. Jiang et al. 2019; Bareche et al. 2018). Collectively, these transcriptomic classifications demonstrate that the definition “TNBC” includes a spectrum of molecularly distinct subtypes with important implications for pathogenesis, prognosis, and therapeutic stratification rather than being a single biological entity. (Zagami and Carey 2022)

Clinically, TNBC is characterized by high histological grade, elevated proliferative activity, and aggressive biological behaviour, which together account for its poor prognosis compared with other BC subtypes. Patients experience earlier relapse, and distant metastases develop in nearly half of the patients, most commonly affecting visceral organs and the brain, typically within the first three years after diagnosis (N. U. Lin et al. 2008). Once metastatic, survival is markedly limited, with a median overall survival of approximately 13 months and a very high mortality rate shortly after recurrence. The strong propensity of TNBC to colonize distant sites such as brain, lung, and bone largely explains its high lethality, since the metastatic disease remains essentially incurable. A major clinical challenge is posed by the ability of disseminated TNBC cells to persist in a low-proliferative or dormant state within secondary organs, which renders them difficult to detect and relatively insensitive to cytotoxic therapies (Echeverria et al. 2019; Riggio et al. 2021). Quiescent cells can remain clinically silent for prolonged periods before reawakening and giving rise to overt metastatic lesions, a transition that is thought to depend on additional molecular alterations within tumour cells as well as on permissive signals from the local microenvironment.

2.1.1 Therapeutic strategies for TNBC: opportunities and limitations

The clinical management of TNBC is particularly challenging due to its aggressive behaviour, marked heterogeneity, and the absence of established hormone- or HER2-targeted therapies. Treatment relies on a multimodal strategy integrating systemic and local approaches. (Bianchini et al. 2022) Chemotherapy remains the cornerstone across early and advanced stages, with anthracycline–cyclophosphamide regimens, taxanes, and platinum-based agents, particularly effective in tumours harbouring BRCA1/2 mutations or DNA repair defects, achieving substantial tumour regression and high pathological complete response rates (Hurvitz et al. 2021; Mustacchi and De Laurentiis 2015; Vidra et al. 2021). However, chemotherapy is limited by variable efficacy in the metastatic setting by the development of resistance (Nedeljković and

Damjanović 2019). Surgical treatment, consisting in breast-conserving surgery or mastectomy supported by lymph node evaluation, ensures local tumour control but cannot address the high systemic relapse risk, necessitating integration with systemic therapy (Harbeck et al. 2019; Margenthaler and Ollila 2016). Radiotherapy contributes to local control and recurrence risk reduction in both neoadjuvant and adjuvant settings (Y.-H. Lin et al. 2023).

Beyond these established modalities, targeted therapies represent an expanding field driven by the advances in the molecular characterization of TNBC. Poly (ADP-ribose) polymerase (PARP) inhibitors have demonstrated clear benefits in BRCA1/2-mutated disease, leading to FDA approval, (Vinayak and Ford 2010) while immune checkpoint inhibitors targeting PD-1/PD-L1, most notably pembrolizumab, have improved survival outcomes in PD-L1–positive tumours and received regulatory approval in combination with neoadjuvant chemotherapy (T. Yang et al. 2023; Santa-Maria et al. 2022). Emerging targeted agents, including androgen receptor inhibitors, Cyclin-dependent kinase (CDK) inhibitors, PI3K/AKT/mTOR inhibitors, and antibody–drug conjugates, have shown potential in preclinical studies or early trials, but their clinical efficacy in TNBC remains variable or incompletely defined (Powers et al. 2020; Saleh et al. 2021; Yun Li et al. 2022; Keskinkilic and Sacks 2024). Combination immunotherapeutic strategies are under exploration, including CAR-T cell approaches and tumour vaccines (Geng et al. 2023; Sahin et al. 2026).

Despite these advances, targeted therapy and immunotherapy benefit only a subset of patients and treatment resistance remains the major obstacle in TNBC management, arising through tumour heterogeneity, adaptive activation of bypass signalling pathways, and immunosuppressive remodelling of the TME. Combination therapies, integrating targeted agents with conventional chemotherapy or additional targeted drugs, and biomarker-guided treatment approaches to optimize therapeutic selection through the identification of predictive biomarkers are strategies that are being explored to address this challenge. In addition, novel therapeutic modalities, including antibody–drug conjugates, bispecific antibodies, and tumour-targeted nanoparticles, designed to improve drug delivery specificity, maximize tumour cell killing, and reduce off-target toxicity, are emerging as promising strategies to overcome resistance. Precision medicine approaches based on genomic and molecular profiling aim to identify actionable alterations and guide

patient stratification, but their clinical implementation remains limited by incomplete biomarker validation and tumour heterogeneity. (N. Xiong et al. 2024)

Although recent advances have expanded treatment options, TNBC remains the BC subtype with the highest risk of early relapse, metastatic dissemination, and disease-related mortality, underscoring the urgent need to better understand the molecular programs driving metastatic progression and to identify novel therapeutic vulnerabilities, among which the metabolic dependencies and stress response pathways that define this tumour subtype represent particularly promising targets.

2.2 Microenvironmental stress, aggressiveness, and metabolic plasticity in TNBC

The clinical aggressiveness of TNBC cannot be explained only by the absence of ER, PR, and HER2 signalling. TNBC progression is sustained by a remarkable capacity to endure hostile micro-environmental conditions and to exploit them as selective pressures that favour invasive and therapy-resistant states. In this setting, metabolic adaptation is not a secondary consequence of transformation, but a core determinant of tumour fitness.

2.2.1 Adaptive capacity of TNBC cells relies on metabolic reprogramming

A defining feature of TNBC is its remarkable phenotypic plasticity, the capacity to adapt to conditions that would otherwise trigger cell death, including metabolic stress, oxidative stress, and therapy-induced damage (Mardamshina et al. 2025). This adaptability is not merely a passive tolerance but an active reprogramming process, driven by stress adaptation pathways that simultaneously reshape cellular metabolism and modulate the threshold for cell death. Among these, metabolic reprogramming stands as a central adaptive strategy: TNBC cells rewire nutrient utilization, redox homeostasis, and lipid metabolism in response to a hostile microenvironment, acquiring metabolic configurations that sustain proliferation and survival under conditions of nutrient deprivation or therapeutic pressure. Beyond metabolic adaptation, TNBC cells exploit a broader repertoire of stress-responsive mechanisms, including transcriptional reprogramming, epigenetic plasticity, and remodelling of cell death pathways, that collectively stabilize stress-resistant cellular states. A key consequence of this adaptive reprogramming is the dynamic regulation of cell death susceptibility: by modulating the balance between pro-death and pro-survival signals, TNBC cells can shift their

vulnerability to various forms of regulated cell death in a context-dependent manner. Collectively, these adaptive mechanisms do not simply confer survival, they actively promote invasiveness, therapeutic resistance, and metastatic potential, linking stress adaptation to the aggressive clinical behaviour that defines this tumour subtype.

Metabolic reprogramming describes the ability of cells to reorganize metabolic pathways in response to changing physiological or pathological conditions, allowing them to preserve homeostasis while supporting growth and survival. In cancer, this adaptive capacity is markedly enhanced and becomes a central driver of disease progression. Tumour cells develop within a highly dynamic TME, composed of malignant cells together with immune, stromal, and vascular components embedded in the extracellular matrix. Within this context, metabolic rewiring enables cancer cells to engage in reciprocal interactions with surrounding non-malignant cells, generating a metabolic network that sustains tumour growth and promotes progression (Elia and Haigis 2021).

A defining feature of malignant cells is their capacity to thrive in conditions characterized by limited nutrient and oxygen availability. Through metabolic adaptation, cancer cells efficiently acquire and utilize available resources to maintain their transformed state, support biosynthetic demands, and sustain uncontrolled proliferation. The conceptual foundation of cancer-associated metabolic alterations was first established by Otto Warburg, who reported that tumour cells rely heavily on glycolysis for energy production even under aerobic conditions, defining the so called “Warburg Effect” (Warburg 1956). Subsequent work has expanded this paradigm, demonstrating that tumours undergo extensive rewiring of glucose, lipid, and amino acid metabolism, which collectively supports malignant growth and exposes context-specific metabolic vulnerabilities (Vander Heiden et al. 2009; Martínez-Reyes and Chandel 2021).

Beyond fulfilling bioenergetic and anabolic requirements, metabolism exerts a direct influence on cellular phenotypes. Variations in oxygen tension, such as hypoxia, can promote invasive behaviour, while changes in amino acid availability have been shown to affect metastasis therapeutic responses (Bergers and Fendt 2021). These observations underscore the role of metabolism as both a supporter and a determinant of cancer cell fate. Cellular metabolism functions as a flexible and interconnected network capable of integrating intrinsic oncogenic signals with extrinsic stresses imposed by the TME.

Exploiting such metabolic constraints may therefore offer therapeutic opportunities, particularly if malignant cells become reliant on conserved metabolic programs that normal cells can more readily bypass (Hanahan 2022).

2.2.2 Hallmarks of metabolic reprogramming in TNBC

Metabolic reprogramming is a hallmark of aggressiveness. The ability of BC cells to sustain proliferation and survival under adverse conditions relies on the coordinate exploitation of multiple metabolic pathways (Pavlova and Thompson 2016; Luengo et al. 2017). In TNBC, metabolic adaptation involves a broad reprogramming of the principal cellular metabolic networks, indicating that virtually all major metabolic blocks contribute to meeting the elevated energetic, biosynthetic, and redox requirements of BC cells. In this context, the most extensively affected pathways include glucose, amino acid, and lipid metabolism (X. Sun et al. 2020; Gong et al. 2021).

TNBC cells are characterized by a metabolic configuration that largely relies on aerobic glycolysis, commonly referred to as the Warburg effect (Warburg 1956). This metabolic preference is associated with elevated glucose uptake and enhanced glycolytic flux, enabling cancer cells to rapidly generate adenosine triphosphate (ATP) while simultaneously providing intermediates required for anabolic processes (Lunt and Vander Heiden 2011; Shen et al. 2015). In this context, glycolysis is functionally uncoupled from oxidative phosphorylation (OXPHOS), leading to the preferential conversion of glycolysis-derived pyruvate into lactate rather than its oxidation in mitochondria, even under oxygen-rich conditions (Vander Heiden et al. 2009).

The excessive production and export of lactate profoundly influence the TME, promoting extracellular acidification (Fang et al. 2026). This acidic milieu contributes to tumour progression by enhancing invasive behaviour, suppressing anti-tumour immune responses, and facilitating metastatic dissemination (Morais-Santos et al. 2015; De La Cruz-López et al. 2019). Thus, glycolytic metabolism in TNBC supports not only intracellular biosynthetic needs but also the remodelling of the surrounding microenvironment in favour of tumour growth.

At the molecular level, these metabolic features are reflected by the increased expression of glucose transporters, such as Glucose Transporter Type 1 (GLUT1), and key glycolytic enzymes, including hexokinase 2 (HK2) and pyruvate kinase 2 (PKM2), as well as proteins involved in lactate production and export, as lactate dehydrogenase A

(LDHA) and Monocarboxylate transporters (MCTs) (Oh et al. 2017; X. Huang et al. 2016; Lim et al. 2016; C. Ma et al., n.d.; S. Jiang et al. 2012). Together, these changes support high glycolytic throughput and efficient lactate handling, reinforcing the glycolytic phenotype of TNBC cells.

Beyond energy production, glucose-derived metabolites play a central role in sustaining the biosynthetic demands of rapidly proliferating TNBC cells. Intermediates such as glucose-6-phosphate, pyruvate, and acetyl-CoA serve as precursors for the synthesis of nucleotides, amino acids, and lipids, thereby supporting biomass accumulation (Lunt and Vander Heiden 2011). In particular, the diversion of glucose intermediates into the pentose phosphate pathway provides ribose sugars for nucleotide synthesis and contributes to the maintenance of redox homeostasis. Through the generation of reducing equivalents, this pathway supports cellular adaptation to oxidative stress, while additional integration of glucose-derived carbon into the tricarboxylic acid (TCA) cycle and lipid biosynthesis further sustains anabolic requirements (Burns and Manda 2017).

Compared to normal breast tissue, BC displays significant alterations in amino acid metabolism, with increased levels of multiple amino acids that have also been proposed as early diagnostic markers (Feitelson et al. 2015). This metabolic rewiring reflects the increased biosynthetic and redox demands associated with tumour growth and progression.

In this context, glutamine plays a prominent role, as it provides both carbon and nitrogen to support key cellular processes. Through its contribution to the TCA cycle, nucleotide and non-essential amino acid biosynthesis, and redox homeostasis via glutathione production, glutamine supports cancer cell proliferation and survival. In TNBC, glutamine uptake and the expression of glutamine-related enzymes are upregulated, resulting in a glutamine-dependent phenotype that may represent a selective therapeutic vulnerability compared to luminal BC subtypes (Lampa et al. 2017; Kung et al. 2011).

In addition, TNBC cells exhibit an increased requirement for serine and glycine to sustain an active one-carbon metabolic pathway. This pathway supports nucleotide biosynthesis, DNA replication and methylation, and redox balance through NADPH production, thereby enabling rapid cell proliferation and adaptation to oxidative stress.

Consequently, serine and glycine metabolism is particularly important for the growth and progression of TNBC and other aggressive BC subtypes. (Pan et al. 2020; Possemato et al. 2011)

Lipid metabolism represents a fundamental component of the TNBC metabolic phenotype. Both fatty acid synthesis (Giró-Perafita et al. 2017; Sodi et al. 2018) and fatty acid oxidation (FAO) (Camarda et al. 2016; Carracedo et al. 2013; Cheng et al. 2018) contribute to tumour progression, despite traditionally being considered opposing metabolic processes. In TNBC, these pathways operate in a coordinated manner to support energy production, membrane biosynthesis, and signalling functions, further underscoring the metabolic flexibility that characterizes this aggressive BC subtype.

Taken together, these observations indicate that metabolic reprogramming in TNBC is not limited to the deregulation of individual pathways but reflects a broad and coordinated adaptation involving the major metabolic networks that sustain energy production, biosynthesis, and redox balance. Such extensive metabolic plasticity enables TNBC cells to survive and proliferate under hostile microenvironmental conditions, while also contributing to invasion, metastatic progression, and therapy resistance (Bian et al. 2021).

3. The Integrated Stress Response as a central adaptive pathway in cancer

Because aggressive tumors must constantly adapt to nutrient limitation, hypoxia, oxidative damage, and therapy-induced stress, pathways that rapidly couple stress sensing to translational and metabolic remodeling become central determinants of tumor behavior. The Integrated Stress Response (ISR) is one of the most important of these pathways. Introducing its molecular logic at this stage makes it possible to understand how the microenvironmental constraints described above are translated into coordinated survival, plasticity, and cell-death programs in TNBC.

3.1 Molecular mechanisms and regulation

Regulation of protein translation is essential for cellular homeostasis, tissue specification, and the maintenance of cell-type–specific functional and energetic demands. The ISR is an evolutionarily conserved adaptive pathway that allows cells to respond to a broad spectrum of physiological and pathological stresses by dynamically reshaping the translational landscape (Costa-Mattioli and Walter 2020). The ISR

integrates multiple extracellular and intracellular signals, including nutrient deprivation, hypoxia, oxidative stress, endoplasmic reticulum (ER) stress, and viral infection, through the activation of a family of four serine/threonine kinases: protein kinase R–like ER kinase (PERK), a core component of the unfolded protein response (UPR), activated by ER stress; protein kinase R (PKR), activated by double-stranded RNA; heme-regulated inhibitor kinase (HRI), activated by heme deficiency; and general control non-derepressible 2 (GCN2), activated by aminoacids deprivation. Although activated by distinct upstream cues, these kinases converge on a common molecular event that defines ISR initiation: the phosphorylation of the α subunit of eukaryotic initiation factor 2 (eIF2α), a central regulator of translation initiation (**Figure 2**). (J. J. Chen 2007; Deval et al. 2009; Galluzzi et al. 2008; Kaufman 1999; Nakamura et al. 2010)

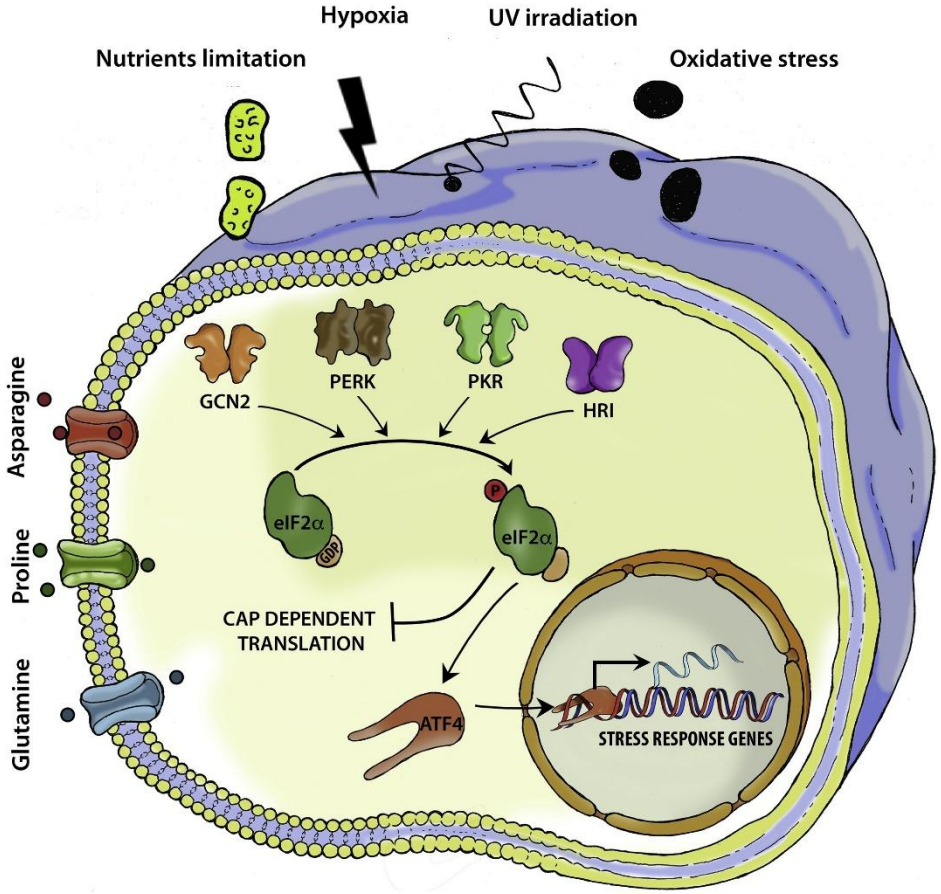

Figure 2. Schematic representation of the Integrated Stress Response (ISR) signalling pathway. *Intracellular and extracellular stressors, including hypoxia, nutrient deprivation, UV radiation, and oxidative stress, trigger the activation of four specialized kinases: GCN2, PERK, PKR, and HRI. These sensors converge on the phosphorylation of the alpha subunit of eukaryotic initiation factor 2 (eIF2α), a key regulatory event that attenuates global cap-dependent protein synthesis while selectively enhancing the translation of specific mRNAs, such as the transcription factor ATF4. Once translocated to the nucleus, ATF4 coordinates an adaptive gene expression program aimed at restoring cellular homeostasis. Image from Licari et al. 2021*

Under basal conditions, canonical cap-dependent translation is initiated through the assembly of the 43S pre-initiation complex (PIC), which is recruited to the 5′ untranslated region (5′-UTR) of mRNAs to scan for the start codon. The PIC consists of the 40S ribosomal subunit associated with the ternary complex composed of eukaryotic translation initiation factor 2 (eIF2) (a heterotrimer of eIF2α, eIF2β, and eIF2γ), guanosine triphosphate (GTP), and the initiator methionyl-tRNA (Met-tRNAi), together with additional translation initiation factors. A critical step in this process is the recycling of eIF2 from its inactive guanosine diphosphate (GDP)-bound form to its active GTP-bound state, that allows the binding to 40S ribosomal subunit. Nucleotide exchange is

catalysed by its dedicated guanine nucleotide exchange factor (GEF), eIF2B, as the intrinsic release of GDP from eIF2 is inefficient. (Pestova et al. 1998; Jackson et al. 2010)

Upon stress, phosphorylation of eIF2α at serine 52 increases the affinity of eIF2 for eIF2B, leading to the formation of an inhibitory eIF2–eIF2B complex. This event results in a rapid and global repression of cap-dependent translation, thereby reducing protein synthesis and cellular energy expenditure. Concomitantly, this translational attenuation selectively favours the cap-independent translation of a subset of stress-responsive mRNAs, enabling the expression of adaptive programs that support cell survival and recovery. (Adomavicius et al. 2019; Pavitt et al. 1998)

Selective translation is an intrinsic property of mRNAs determined by the presence of cis-regulatory elements within their 5′ untranslated regions (5′-UTRs), which control ribosome recruitment and accessibility to the translation initiation machinery. Among these elements, internal ribosome entry sites (IRESs) and upstream open reading frames (uORFs) represent two of the most extensively characterized mechanisms enabling selective translation under stress conditions.

IRESs are structural RNA elements that allow direct recruitment of ribosomes to internal sites within the 5′-UTR, thereby initiating translation independently of 5’ cap structure. IRES-mediated translation initiation relies on the interaction with specific IRES trans-acting factors (ITAFs), which facilitate proper RNA folding and promote the recruitment of the 40S ribosomal subunit together with a limited set of translation initiation factors. Originally identified in viral RNAs, IRES-mediated translation has since been described in a subset of cellular mRNAs, particularly those involved in stress adaptation and survival, including several oncogenes. When global cap-dependent translation is inhibited, this mechanism becomes relevant supporting the synthesis of proteins critical for cell fate decisions. (Weingarten-Gabbay et al. 2016)

uORFs are short open reading frames located upstream of the main coding sequence within the 5′-UTR and are present in a large fraction of mammalian mRNAs. Under basal conditions, uORFs generally act as repressors of translation by limiting ribosomal access to the downstream canonical start codon (Johnstone et al. 2016). However, during stress, uORFs can promote selective translation through regulated reinitiation mechanisms that are tightly linked to phosphorylation of eIF2α. A paradigmatic example is the mRNA encoding activating transcription factor 4 (ATF4), a master regulator of the ISR, whose

uORF architecture enables efficient translation specifically when eIF2α is phosphorylated and global protein synthesis is reduced (Harding et al. 2000).

Termination of the ISR is a tightly regulated process that is essential to restore protein synthesis and normal cellular function once stress conditions are resolved. Central to ISR shutdown is the dephosphorylation of the α subunit of eIF2α, which counteracts the translational repression imposed during stress. This reaction is mediated by protein phosphatase 1 (PP1), whose catalytic subunit (PP1c) acquires specificity for eIF2α through association with one of two regulatory subunits: PPP1R15B (also known as CReP) or PPP1R15A (also known as GADD34) (Costa-Mattioli and Walter 2020). In unstressed cells, the constitutively expressed CReP–PP1 complex maintains low basal levels of eIF2α phosphorylation, thereby sustaining translational homeostasis (Jousse et al. 2003). In contrast, GADD34 expression is induced during the later phases of the ISR and acts as a key negative feedback mechanism. GADD34 is upregulated both transcriptionally by ATF4 and translationally through uORF-dependent mechanisms, resulting in the assembly of the GADD34–PP1 complex that markedly enhances eIF2α dephosphorylation and promotes recovery of global protein synthesis. (Novoa et al. 2001; Young et al. 2015)

3.2 Functional outcomes of ISR activation: adaptation and metabolic rewiring

A central effector of the ISR is the transcription factor ATF4, a member of the ATF/CREB family that functions predominantly as a transcriptional activator downstream of eIF2α phosphorylation (Karpinski et al. 1992; Wek et al. 2023). The controlled induction of ATF4 represents a pivotal adaptive mechanism, coordinating gene expression programs that enable cells to withstand diverse stress conditions. ATF4 drives the transcription of genes involved in antioxidant defence, amino acid transport and biosynthesis, metabolic adaptation, and autophagy, thereby promoting cellular survival under nutrient deprivation, hypoxia, oxidative stress, and ER stress.

One of the major pathways regulated by ATF4 is autophagy, a catabolic process essential for maintaining cellular homeostasis during stress. ATF4 orchestrates an autophagic transcriptional program by directly upregulating multiple autophagy-related genes and autophagy regulatory factors, required for autophagosome biogenesis and function, while also indirectly promoting autophagy through the induction of DNA damage response 1 (REDD1), a negative regulator of mTORC1 signalling (B'Chir et al.

2013; Dikic and Elazar 2018). Through this dual mechanism, the ISR suppresses anabolic signalling and facilitates the recycling of cytoplasmic components, providing amino acids, fatty acids, and metabolic substrates to sustain ATP production and biosynthetic capacity. Notably, phosphorylation of eIF2α constitutes a converging node linking distinct stress-sensing kinases, including PERK and GCN2, to autophagy induction in response to ER stress, hypoxia, amino acid starvation, and proteotoxic insults.

Beyond autophagy, the ISR intersects with multiple pro-survival signalling pathways. Crosstalk with the UPR enables coordinated alleviation of ER stress through translational attenuation (Harding et al. 2000; C. Y. Liu et al. 2000) and enhanced protein folding and degradation, while interactions with PI3K/AKT/mTOR signalling further shape metabolic and survival outcomes (Kazemi et al., n.d.). ATF4-dependent transcriptional programs also modulate apoptosis by upregulating anti-apoptotic factors such as Myeloid Cell Leukemia-1 (MCL-1) (J. Hu et al. 2012), thereby restraining mitochondrial cell death pathways and conferring resistance to metabolic stress and cytotoxic therapies. In parallel, ATF4 activates Nuclear Protein 1, Transcriptional Regulator (NUPR1), a transcriptional regulator implicated in metabolic stress adaptation, DNA repair, and cell cycle control, reinforcing the pro-survival arm of the ISR (H. Jin et al. 2009).

The effect of ISR activation depends also on its duration and severity. In fact, short-lived ISR determines the above mentioned adaptive, pro-survival response aiming at resolving stress and restoring homeostasis, while persistent ISR can signal toward a maladaptive response: if the stress is not resolved, ATF4 can activate molecular pathways promoting cell death (Boone and Zappa 2023).

Although the ISR is primarily activated to promote cellular adaptation, it also contains signalling programs that drive cell death when stress is prolonged or unresolved. These outcomes are largely governed by ATF4 and its downstream transcriptional network, particularly C/EBP homologous protein (CHOP) and ATF3. ATF4 can directly induce pro-apoptotic B-cell lymphoma 2 (BCL-2) family members such as Phorbol-12-myristate-13-acetate-induced protein 1 (PMAIP1) (Armstrong et al. 2010) or indirectly promote apoptosis through the induction and functional cooperation with CHOP and ATF3. CHOP serves as a key mediator of ISR-induced apoptosis by upregulating Bcl-2 Homology 3 (BH3)-only pro-apoptotic BCL-2 family members BCL2L11 and BBC3 (Puthalakath et al. 2007), enhancing death receptor signalling (W. Zou et al. 2008), and

disrupting ER redox homeostasis via Endoplasmic Reticulum Oxidoreductase 1 Alpha (ERO1α) induction (Marciniak et al. 2004). In addition, heterodimerization between ATF4, CHOP, and ATF3 expands the transcriptional output of the ISR toward cell death through the regulation of additional pro-apoptotic factors, including ATF5 and Tribbles Pseudokinase 3 (TRIB3) (Teske et al. 2013; Ohoka et al. 2005). Beyond transcriptional control, sustained ISR signalling contributes to apoptosis by relieving inhibition of caspases through downregulation of anti-apoptotic proteins and by exacerbating proteotoxic stress as translation is reactivated under conditions of impaired protein folding (Hiramatsu et al. 2014). While apoptosis represents the predominant outcome, the ISR can also trigger alternative forms of cell death, such as ATF4-dependent necrosis (León-Annicchiarico et al. 2015), depending on the nature and duration of the stress (Marciniak et al. 2022; Wek et al. 2023).

3.3 The ISR in cancer: from tumour initiation to therapeutic resistance

The regulation of mRNA translation represents a rapid and efficient mechanism by which cells adapt to pathological challenges, enabling swift phenotypic changes that confer survival advantages. This capacity for translational rewiring underlies cellular plasticity, allowing cells to transition between distinct functional states in response to environmental cues and can be used by cancer cells to sustain growth and survival under adverse conditions. In tumours, deregulated cell proliferation, genomic instability, elevated metabolic demands, reduced oxygen availability, and extensive remodelling of the TME impose continuous stress. Under these conditions, activation of adaptive pathways such as the ISR supports cancer cell survival, promotes proliferation, and facilitates tumour progression. (Lines et al. 2023)

The ISR is engaged from early stages of oncogenesis, where ISR-dependent translational rewiring operates at pre-neoplastic stages to support tumour initiation and progression. Consistently, ISR activation is observed downstream of major oncogenic lesions, including MET overexpression (Cerqua et al. 2025) Phosphatase And Tensin Homolog (PTEN) loss combined with MYC amplification (H. G. Nguyen et al. 2018), where early eIF2α phosphorylation and PERK signalling are required for tumour development, and pharmacological restoration of global translation leads to tumour regression (Blais et al. 2006; Hart et al. 2012; Bobrovnikova-Marjon et al. 2010).

Beyond tumour initiation, the ISR promotes cancer cell survival under metabolic and microenvironmental stress by sustaining nutrient homeostasis, regulating amino acid transporter expression, and supporting biosynthetic programs through ATF4-dependent transcription, as observed in solid tumours as lung adenocarcinoma, metastatic prostate cancer and pancreatic cancer (Halbrook et al. 2022; Cordova et al. 2022; Gwinn et al. 2018). The influence of the ISR extends to the TME, where ATF4 regulates amino acid metabolism required for extracellular matrix remodelling by cancer-associated fibroblasts and drives metabolic reprogramming of endothelial cells toward glycolysis, contributing to aberrant vascularization and the formation of an immunosuppressive microenvironment (Verginadis et al. 2022).

A critical consequence of ISR-driven translational control is the facilitation of immune escape through non-canonical translation of PD-L1, bypassing inhibitory uORFs in a process observed in liver and lung cancer models. Increased PD-L1 expression suppresses T cell activity within the TME, impairing immunosurveillance and promoting metastatic dissemination. (Suresh et al. 2020)

Finally, the ISR contributes to tumour plasticity, invasion, and therapeutic resistance.(A. A. H. Patel et al. 2026; Calvo et al. 2023) Hypoxia-, glucose-, and nutrient deprivation–induced ISR activation enhances invasive and metastatic potential in BC and melanoma (Nagelkerke et al. 2013; García-Jiménez and Goding 2019), while ATF4-dependent translation reduces oxidative stress, prevents anoikis, a key requirement for successful metastatic spread and contributes to chemoresistance in multiple cancer types, including pancreatic cancer, melanoma, and gastric cancer, by activating adaptive pathways (Avivar-Valderas et al. 2011) that protect tumour cells from therapy-induced death, regulating autophagy, cystine/glutamate antiporter xCT, and determining the acquisition of mesenchymal-like, therapy-resistant states (Falletta et al. 2017; Corazzari et al. 2015; Nagasawa et al. 2020; S.-F. Wang et al. 2018).

While ISR activation often confers survival advantages to tumour cells, excessive or prolonged ISR signalling can exert tumour-suppressive effects, by attenuating global protein synthesis and engaging pro-apoptotic pathways or modulating chemosensitivity. For example, in a mouse model of HER2-positive BC, the PKR-eIF2α axis exhibits anti-tumour activity, and its activation in combination with targeted therapies suppresses

tumour growth. Elevated eIF2α phosphorylation correlates with improved clinical outcomes and enhanced response to trastuzumab. (Darini et al. 2019)

In summary, the ISR exhibits a dual nature in cancer, acting both as a promoter of tumour survival and a potential therapeutic vulnerability. On one hand, ISR activation enables tumour cells to adapt to adverse conditions such as hypoxia, nutrient deprivation, and chemotherapy, supporting proliferation, metastasis, and chemoresistance. On the other hand, sustained or maladaptive ISR signalling can trigger apoptosis and enhance the effectiveness of anticancer therapies, including targeted agents and chemotherapeutics. This duality underscores the context-dependent role of the ISR in tumour biology and highlights its potential as a target for therapeutic strategies aimed at tipping the balance from survival toward cell death in cancer cells.

3.3.1 ISR and metabolic reprogramming in cancer

In TNBC, the relevance of the ISR is magnified by the marked dependence of tumour cells on metabolic plasticity. The pathway not only buffers acute stress, but also reshapes nutrient utilization, antioxidant defences, and metabolite exchange with the TME. These functions place the ISR at the intersection between adaptive survival and the metabolic liabilities that may be therapeutically exploited.

One major outcome of ISR activation is the regulation of redox homeostasis through modulation of glutathione metabolism. In TNBC, ATF4 promotes the expression of genes involved in glutathione biosynthesis and cystine uptake, including Glutamate-Cysteine Ligase Catalytic Subunit (GCLC), Solute Carrier Family 7 Member 11 (SLC7A11), and Cystathionine Gamma-Lyase (CTH), thereby supporting antioxidant capacity and limiting oxidative damage (Bai et al. 2021). This program is tightly interconnected with Nuclear factor erythroid 2-related factor 2 (NRF2) signalling, which reinforces cystine import through the xCT antiporter and activates complementary antioxidant systems, such as thioredoxin-related pathways. In melanoma it is documented that ATF4 increases the expression of glutathione-degrading enzyme ChaC glutathione specific gamma-glutamylcyclotransferase 1 (CHAC1), which is fundamental for maintaining NRF2 activation (Kreß et al. 2023). Through this coordinated response, ISR activation helps maintain redox balance despite fluctuations in glutathione availability, ultimately enhancing cellular resistance to stress.

In parallel, ISR exerts a profound influence on glutamine metabolism, positioning the ATF4-glutamine axis as a key integrative node linking stress sensing to metabolic adaptation (Yan and Liu 2025). ATF4 enhances glutamine uptake and utilization by regulating amino acid transporters and metabolic enzymes, including Solute Carrier Family 1 Member 5 (SLC1A5), thereby increasing glutamine dependency under metabolic stress (R. Patel et al. 2024; Xiao et al. 2024). Glutamine deprivation itself induces ATF4 expression, leading to the induction of genes involved in amino acid biosynthesis and transport, such as Asparagine Synthetase (ASNS), Pyrroline-5-Carboxylate Reductase 1 (PYCR1), and Solute Carrier Family 7 Member 5 (SLC7A5), and the modulation of growth-regulatory pathways including mTOR signalling, establishing a feedback mechanism that allows cancer cells to dynamically adapt to changes in nutrient availability (Lampa et al. 2017). Importantly, ATF4-dependent control of glutamine metabolism also contributes to redox homeostasis by sustaining cysteine availability and glutathione synthesis, thereby protecting cells from oxidative damage and ferroptotic cell death (N. Zhang et al. 2018).

Together, these observations underscore the ISR as a central adaptive program that integrates metabolic and stress signalling. By coordinating glutamine metabolism and antioxidant defences, ATF4 enables tumour cells to tolerate metabolic stress, resist cell death, and sustain survival in hostile microenvironmental conditions, highlighting ISR-driven metabolic pathways as potential therapeutic vulnerabilities.

3.4 Targeting the ISR in cancer therapy

Current understanding of cancer progression indicates that tumour cells harness the adaptive aspects of the ISR to survive and proliferate, while evading its maladaptive, pro-apoptotic programs. This dual nature of the ISR provides a unique therapeutic window, in which both its pharmacological activation or inhibition can be strategically employed to limit tumour growth and sensitize cancer cells to treatment.

Several anticancer strategies exploit the ISR through context-dependent activation of distinct eIF2α kinases. Nutrient stress–based therapies predominantly engage the GCN2 pathway: L-asparaginase, a well-established clinical example, induces GCN2-dependent ISR activation and apoptosis (Ye et al. 2010; St. Paul et al. 2024), while glutaminase inhibitors such as CB-839 and amino acid starvation–inducing agents such as halofuginone extend this approach to solid tumours by depleting intracellular amino acids

and activating GCN2 to exert cytostatic and cytotoxic effects or enhance chemosensitivity (Yerbes et al. 2022; Keller et al. 2012; Juárez et al. 2012). Notably, drugs with limited clinical efficacy, such as neratinib in glioblastoma, are increasingly recognized for off-target activation of adaptive GCN2–ISR signalling (C. P. Tang et al. 2022).

In parallel, other therapeutic agents activate the ISR through mitochondrial dysfunction and proteotoxic stress. Imipridones, most notably ONC201, hyperactivate the mitochondrial protease ClpP to induce eIF2α phosphorylation, engaging HRI and PKR, and apoptotic cell death, and have progressed to late-stage clinical trials including phase II studies (Stein et al. 2017; Anderson et al. 2022; Shenoy et al. 2025). Pharmacological PERK activation using compounds such as CCT020312 promotes apoptosis, chemosensitivity, and growth inhibition in colorectal and TNBC models (Y. Lei et al. 2021; Xiaoli Li et al. 2020; C. Zhang et al. 2026).

Persistent activation of the ISR can be achieved by limiting eIF2α dephosphorylation through inhibition of its regulatory phosphatase subunits, GADD34 and CReP (Boyce et al. 2005; Bryant et al. 2008; Rojas et al. 2015; C. Zhang et al. 2026). Small molecules such as Salubrinal display antitumor activity across multiple cancer models, including hepatocellular, ovarian, melanoma, cholangiocarcinoma, and inflammatory BC, often showing enhanced efficacy when combined with established chemotherapeutic or targeted agents (Kardos et al. 2020; X. Zhao et al. 2016; Yu et al. 2019). Modified formulations, such as copper-complexed Salubrinal, further increase cytotoxicity in ovarian cancer models (Masuri et al. 2021). Similarly, the antihypertensive drug Guanabenz acetate has been repurposed to inhibit GADD34, inducing ER stress–associated apoptosis and autophagy in patient-derived hepatocellular carcinoma and TNBC cells (Haggag et al. 2021; Hamamura et al. 2014). Additional pharmacological agents, including the microtubule-disrupting compound CYT997 and the antiretroviral drug nelfinavir, have been shown to suppress tumour growth through ISR-dependent apoptotic mechanisms in vivo and in preclinical settings (Z. Wang et al. 2019; Brüning et al. 2009; Lines et al. 2023).

Targeting the ISR through pharmacological inhibition has emerged as a promising strategy to counteract cancer cell adaptation and resistance. Inhibition can be achieved at multiple levels, either by directly blocking the eIF2α kinases that initiate ISR signalling or by preventing the downstream translational repression mediated by phosphorylated

eIF2α. PERK inhibitors such as GSK2606414, GSK2656157, LY-4, and AMG44 have demonstrated potent antitumor activity in preclinical models, including pancreatic cancer, BRAF-mutant melanoma, and MYC-driven lymphomas, although some early compounds were limited by pancreatic toxicity (Axten et al. 2013; Mohamed et al. 2020; Pytel et al. 2016; Tameire et al. 2019; C. Zhang et al. 2026). Similarly, inhibitors of PKR (e.g., 2-aminopurine and C16), HRI (e.g., Aminopyrazolindane), and GCN2 (e.g., GCN2iB, GZD824, 6D, and 6E) have shown efficacy in reducing ISR-mediated survival mechanisms, sensitizing cancer cells to nutrient deprivation, chemotherapy, or targeted therapies in vitro and in xenograft models (Watanabe et al. 2020; Rosen et al. 2009; Kato et al. 2020; Fujimoto et al. 2019; Lines et al. 2023). ISRIB and its derivatives represent a complementary approach by acting downstream of all four eIF2α kinases, maintaining eIF2B activity even in the presence of phosphorylated eIF2α, thereby restoring global translation and impairing the adaptive response of tumour cells. In preclinical models of prostate cancer, BC, and chronic myeloid leukemia, ISRIB has successfully reduced metastatic potential, blocked therapy-induced plasticity, and enhanced the cytotoxicity of conventional treatments such as bortezomib and imatinib. (Zyryanova et al. 2021; H. G. Nguyen et al. 2018; Dudka et al. 2022; D. M. Lee et al. 2022; Jewer et al. 2020)

Collectively, these studies highlight the ISR as a versatile therapeutic target in cancer, as both its pharmacological reinforcement and inhibition can disrupt tumour cell homeostasis. By shifting the stress response from an adaptive to a maladaptive state or by preventing adaptive resistance mechanisms, modulation of ISR signalling, particularly when combined with conventional therapies, can ultimately promote cancer cell death and enhance therapeutic efficacy across multiple cancer types.

However, while ISR activation can exert cytotoxic effects, particularly in highly proliferative tumours and in combination with conventional therapies, its pleiotropic nature may also promote pro-survival programs such as migration, drug resistance, and immune evasion. Instead, ISR inhibition can impair tumour growth and display cytostatic, anti-angiogenic, and anti-metastatic effects. These apparently paradoxical outcomes suggest that the therapeutic efficacy of targeting the ISR is highly context-dependent and influenced by factors such as tumour type, stage of progression, and intratumoral heterogeneity, indicating that neither sustained activation nor inhibition alone is universally effective (Licari et al. 2021). (**Figure 3**)

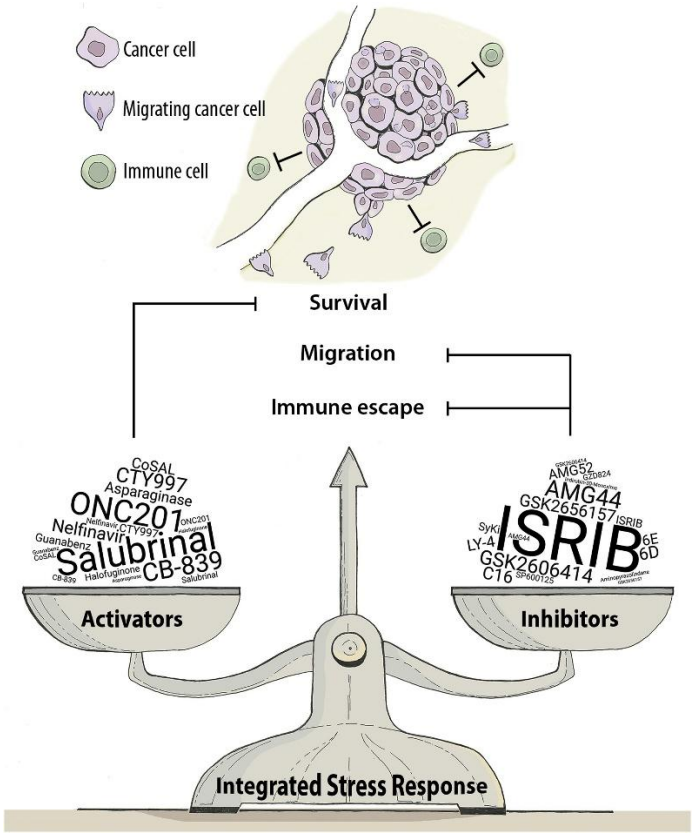

Figure 3. Therapeutic targeting of the Integrated Stress Response (ISR) in oncology. *This image illustrates that ISR modulation, either through direct inhibition or over-activation, disrupts the cancer cell's equilibrium. Image from Licari et al. 2021*

4. Lipid metabolic reprogramming in breast cancer

Among the major risk factors associated with BC incidence and prognosis, systemic metabolic alterations, such as obesity and dyslipidaemia, have emerged as particularly relevant (Abe et al. 1976; Protani et al. 2010; Maiti et al. 2010). Excess adipose tissue has been correlated with more aggressive tumour phenotypes, higher recurrence rates, and reduced survival following chemotherapy, with epidemiological data linking higher Body Mass Index (BMI) and waist circumference specifically to luminal B and TNBC subtypes (Pajares et al. 2013; Dignam 2003; Agresti et al. 2016). Beyond these systemic effects, altered lipid metabolism plays a central role in breast tumour biology: BC cells undergo profound lipid metabolic reprogramming encompassing enhanced uptake, de novo synthesis, oxidation, and storage, a metabolic flexibility that enables tumour cells to maintain proliferation, viability and metastatic capability under hypoxic and nutrient-limited conditions (Bensaad et al. 2014; Pascual et al. 2017) (**Figure 4**). Lipids sustain tumour growth through multiple complementary

mechanisms, providing structural components for membrane biogenesis, serving as long-term energy reservoirs, functioning as bioactive signalling molecules, and contributing to the regulation of oxidative stress and cellular homeostasis (Siniossoglou 2009; Voelker 2009; Burkhalter et al. 2015; X. Wu et al. 2020; S. Li et al. 2025). Furthermore, lipids profoundly influence immune cell function within the TME, modulating the activity of tumour-associated macrophages and tumour-infiltrating dendritic cells, thereby linking lipid metabolic reprogramming to immune evasion and disease aggressiveness (Wan et al. 2025; Yorek et al. 2024). In this sense, lipid metabolism should be viewed not as an isolated anabolic module, but as a broader adaptive platform that influences membrane composition, mitochondrial function, redox balance, and ultimately the susceptibility of BC cells to stress-induced cell death.

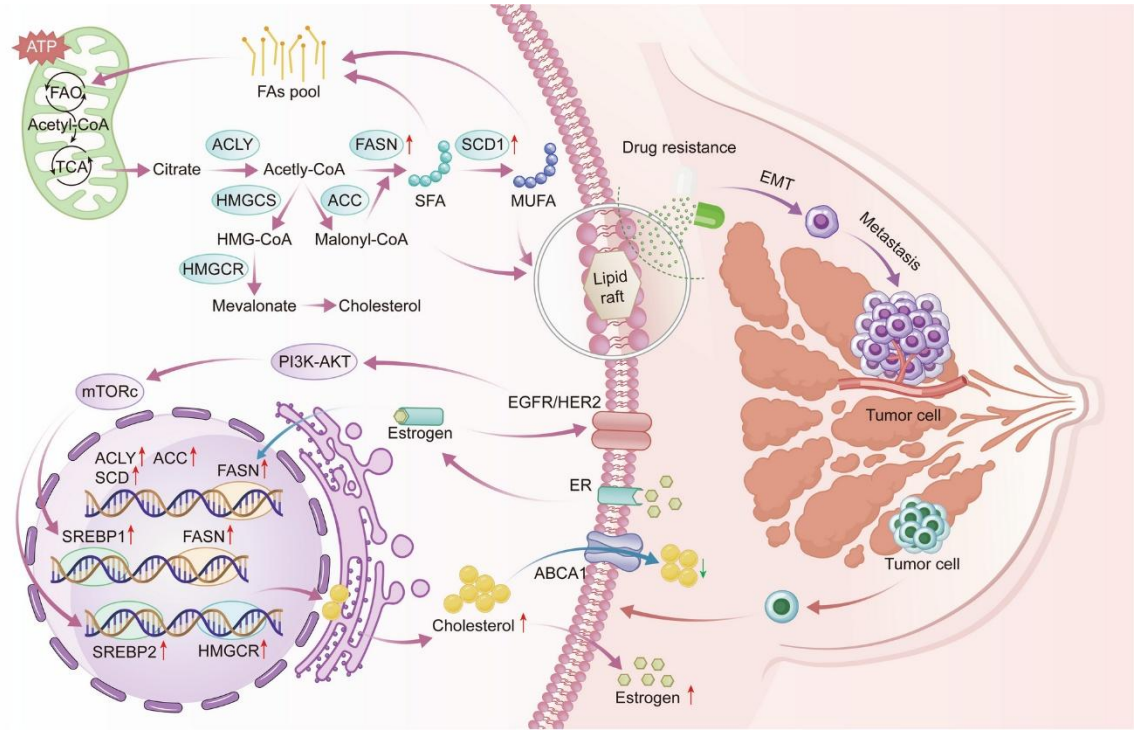

Figure 4. Dysregulation of lipid metabolism and oncogenic signaling in breast cancer (BC). *This image details the lipid metabolism reprogramming of BC cells, showing the interplay between lipid biosynthetic pathways and signaling pathways in BC progression. Image from Wan et al. 2025*

4.1 Lipid acquisition and de novo fatty acid synthesis

Lipids are structurally diverse molecules classifiable into eight major subclasses based on their chemical backbone: fatty acids, glycerolipids, glycerophospholipids, sphingolipids, sterol lipids, prenol lipids, saccharolipids, and polyketides (Fahy et al.

2005). Structural distinctions underpin the broad functional versatility of lipid subclasses that serve fundamental and multifaceted roles in cellular biology: as the primary constituents of biological membranes, as energy storage molecules, as signalling mediators, and as modulators of protein function and organelle identity.

BC cells acquire fatty acids through two principal routes: uptake of extracellular lipids, mediated by membrane transporters and de novo fatty acid synthesis. A key hallmark of cancer cell metabolism is the persistent activation of de novo lipogenesis: whereas normal cells restrict fatty acid synthesis to specialized tissues, tumour cells markedly upregulate the expression and activity of lipogenic enzymes, which can account for up to 90% of total lipid production (J. Zhang et al. 2021). This enhanced lipogenic capacity is sustained by the increased availability of glycolytic intermediates resulting from the Warburg effect (Mathew et al. 2024). Lipid biosynthesis is initiated by the conversion of citrate, exported from the TCA cycle into the cytoplasm, into acetyl-CoA by ATP-citrate lyase (ACLY). Acetyl-CoA is then carboxylated by acetyl-CoA carboxylase (ACC), the rate-limiting enzyme of the pathway, to generate malonyl-CoA, which serves as the building block for the sequential condensation reactions catalysed by fatty acid synthase (FASN), yielding long-chain saturated fatty acids (SFAs) (Wan et al. 2025). In BC, ACLY, ACC, and FASN are frequently overexpressed and hyperactivated, correlating with tumour aggressiveness, metastatic potential, and poor prognosis (Shuo Xu et al. 2020; Pizato et al. 2021; M. Jin et al. 2023; Szutowvicz et al., n.d.; D. Wang et al. 2017), and their activity is reinforced by oncogenic signalling through PI3K/AKT/mTOR, MAPK, HER2, and Sterol regulatory element-binding protein 1 (SREBP-1).

In TNBC specifically, FASN overexpression is further amplified through SREBP-mediated transcriptional programs and mTORC1 signalling (Ricoult et al. 2016), while exogenous lipid acquisition relies on LPL-mediated hydrolysis of circulating triglycerides followed by CD36-dependent uptake (Kuemmerle et al. 2011; DeFilippis et al. 2012), with Fatty Acid Binding Protein 5 and 7 (FABP5 and FABP7) facilitating intracellular lipid trafficking and correlating with poor clinical outcomes (Powell et al. 2015; Kwong et al. 2019).

The newly synthesized fatty acids can undergo further modification through elongases (elongation of very long-chain fatty acids (ELOVL) family) and desaturases (fatty acid desaturases (FADS)), generating the full spectrum of long-chain saturated and unsaturated

fatty acids required for cellular processes, a diversification that is centrally governed by the activity of stearoyl-CoA desaturase 1 (SCD1), which controls the balance between SFAs and monounsaturated fatty acids (MUFAs) within the cell and thereby shapes membrane composition, lipid signalling, and stress responsiveness.

4.2 Stearoyl-CoA desaturase 1 (SCD1) and the regulation of fatty acid desaturation

SCD1 is a key enzyme that catalyses the rate-limiting step in the biosynthesis of MUFAs, including palmitoleic (C16:1) and oleic acid (C18:1), from their corresponding SFAs. Also referred to as Δ9-desaturase, SCD1 mediates an oxidative desaturation reaction that introduces a *cis* double bond at the 9,10 positions of the carbon chain in both palmitoyl-CoA (C16:0) and stearoyl-CoA (C18:0) (ALJohani et al. 2017; Ying Zou et al. 2020). This reaction represents the first desaturation event in the fatty acyl chain, a crucial modification that significantly influences membrane fluidity, lipid signalling, and metabolic regulation.

SCD1 is an integral membrane protein localized to the ER, where it is ubiquitously expressed and constitutes the predominant isoform in humans (Dobrzyn et al. 2010). In addition to SCD1, a second human isoform, SCD5, has been identified. Unlike SCD1, SCD5 exhibits a more restricted, tissue-specific expression pattern, being mainly localized in the brain and pancreas. In murine models, four SCD isoforms have been characterized, each displaying distinct tissue distribution and regulatory properties (Miyazaki et al. 2006).

Transcription of SCD1 is tightly regulated by nutritional, hormonal, developmental and environmental factors. Glucose, SFAs, insulin, SREBP-1c, peroxisome proliferator-activated receptor α (PPARα), liver X receptor (LXR), PI3K, MAPK, carbohydrate-response element-binding protein (ChREBP), and ER stress signalling positively regulate its expression. In contrast, leptin, via Signal transducer and activator of transcription 3 (STAT3)-driven SREBP1c suppression, polyunsaturated fatty acids (PUFAs), via the extracellular signal-regulated kinase/mitogen-activated protein kinase (ERK/MAPK) signalling pathway, and estrogen negatively regulate SCD1 gene expression. (Sen et al. 2023)

Through its enzymatic activity, SCD1 governs the critical balance between SFAs and MUFAs, thereby modulating lipid composition, biosynthetic pathways, and overall cellular metabolism. SCD1 has emerged as a central metabolic regulator, integrating

signals across glycolipid metabolism, inflammatory pathways, and autophagic processes. Disruptions in SCD1 expression or activity have been implicated in diverse metabolic disorders, underscoring its central role in lipid homeostasis and metabolic health. (Q. Sun et al. 2024)

SCD1 has emerged as a central metabolic regulator in cancer, where it contributes to tumorigenesis, progression, invasion, and metastasis by shaping the lipid metabolic landscape of malignant cells. Its expression is markedly elevated in multiple tumour types, including ovarian, gastric, colorectal, pancreatic, lung, and BCs, in which high SCD1 levels frequently correlate with poor prognosis (Holder et al. 2013). By catalysing the conversion of SFAs into MUFAs, SCD1 protects cancer cells from SFA-induced lipotoxicity (Sammarco et al. 2024), sustains membrane biosynthesis, and promotes proliferation, migration, and tumour regrowth (Tracz-Gaszewska and Dobrzyn 2019). Consistent with this, MUFA supplementation rescues the apoptosis and growth arrest induced by SCD1 inhibition (Z. Guo et al. 2023). Beyond its metabolic functions, SCD1 engages stress-response and survival pathways: it suppresses autophagy-induced cell death in hepatocellular carcinoma through inhibition of the AMP-activated protein kinase (AMPK) axis (G.-M. Huang et al. 2015), and it confers resistance to ferroptosis via PI3K/AKT/mTOR signalling (Yi et al. 2020), thereby promoting cancer recurrence, protecting cancer cells from cell death. Increasing evidence show that elevated SCD1 levels reduce the accumulation of lipid peroxides, increasing MUFAs, which are less susceptible to lipid peroxidation (Carbone and Melino 2019; G.-M. Huang et al. 2015). Pharmacological inhibition of SCD1 was shown to prime tumour cells for ferroptosis, especially when combined with ferroptosis inducers, pointing to a promising therapeutic strategy (Wohlhieter et al. 2020).

SCD1 also modulates ER homeostasis; its inhibition elicits a robust UPR, characterized by X-box binding protein 1 (XBP1) splicing, eIF2α phosphorylation, and CHOP upregulation, ultimately triggering apoptosis. Oleic acid, a major SCD1 product, appears to mediate this protective effect by dampening ER stress and counteracting palmitate-induced cytotoxicity. (Juwon Lee et al. 2024)

Collectively, aberrant SCD1 activation not only sustains the metabolic demands of cancer cells but also enhances their adaptability to cellular stress, enabling tumour growth, metastasis, immune evasion, and therapy resistance.

4.3 From fatty acids to complex lipids

SFAs, MUFAs and PUFAs serve as precursors for the biosynthesis of complex lipids, including glycerophospholipids, sphingolipids, and eicosanoids. Glycerophospholipids are synthesized through two major routes: the Kennedy pathway, which generates phosphatidylcholine (PC) and phosphatidylethanolamine (PE), and the CDP-DAG pathway, responsible for phosphatidylserine (PS), phosphatidylinositol (PI), and phosphatidylglycerol (PG), used as mitochondrial precursor for cardiolipin biosynthesis (Farese and Walther 2023). The fatty acid composition of these phospholipids, determined by the balance between SFAs, MUFAs and PUFAs, critically shapes membrane biophysical properties, organelle function, and susceptibility to oxidative damage, and is therefore tightly regulated by the activity of enzymes such as SCD1 and the acyl-CoA synthetase long-chain family member (ACSL) family. By connecting fatty acid availability to membrane architecture and organelle identity, this layer of lipid remodelling provides a mechanistic bridge between metabolic rewiring, mitochondrial adaptation, and ferroptotic vulnerability.

4.3.1 Ether-linked phospholipids: biosynthesis, function, and cancer relevance

Among the complex lipid species generated through these biosynthetic pathways, a structurally and functionally distinct subclass has attracted growing attention in the context of cancer biology: ether-linked phospholipids (ePLs), whose unique chemical properties confer specialized roles in membrane organization, signalling, iron metabolism, and oxidative stress regulation that cannot be fulfilled by their ester-linked counterparts (S. Li et al. 2025).

Ether lipids are characterized by an ether bond at the sn-1 position of the glycerol backbone. Their biosynthesis follows a specialized pathway that is initiated in peroxisomes and completed in the ER. The process begins with dihydroxyacetone phosphate (DHAP), a glycolytic intermediate derived from fructose-1,6-bisphosphate and glyceraldehyde-3-phosphate. Within the peroxisomal matrix, DHAP is acylated at the sn-1 position by glyceronephosphate O-acyltransferase (GNPAT), using a long-chain acyl-CoA as the donor. This initial step is followed by the action of alkylglycerone phosphate synthase (AGPS), which replaces the acyl group with an alkyl chain, thereby establishing the characteristic ether linkage. The fatty alcohol required for this exchange is produced by peroxisomal fatty acyl-CoA reductases (FAR1 or FAR2), which catalyse the rate-

limiting reaction in ether lipid synthesis. Subsequently, the peroxisomal acyl/alkyl-dihydroxyacetone phosphate reductase (AADHAP-R) reduces the ketone group at the sn-2 position, enabling the addition of a second fatty acyl chain. Once these early steps are completed, the intermediates are transferred to the ER, where subsequential reactions of acylation and dephosphorylation take place. The final step involves cytidine diphosphate (CDP)–activated ethanolamine or choline, generating ether analogues of phosphatidylethanolamine and phosphatidylcholine. (Dean and Lodhi 2018; Brites et al. 2004; Z. Hu et al. 2025)

Through this coordinated peroxisomal–ER biosynthetic pathway, cells produce ether lipids that play essential roles in membrane architecture, oxidative stress protection, and cellular signalling. Ether lipids play fundamental structural and functional roles within cellular membranes. By promoting tighter phospholipid packing, they decrease membrane fluidity and increase membrane rigidity, thereby contributing to the stability of higher-order membrane architectures, including lipid raft microdomains (Lohner 1996; Pike et al. 2002; Rodemer et al. 2003; Tulodziecka et al. 2016; Vani Raju et al. 2026). Through these effects on membrane organization, ether lipids also influence membrane trafficking, as changes in membrane flexibility, curvature, and fusion capacity can modulate vesicle formation, endocytosis, and intracellular transport (Komljenovic et al. 2009). Recent studies have also revealed that are implicated in the regulation of iron uptake through their impact on the biophysical properties of the plasma membrane (Mansell et al. 2024). This mechanism adds an additional layer of relevance, as altered iron handling directly affects the cell's susceptibility to ferroptosis, an iron-dependent form of regulated cell death driven by lipid peroxidation. Ether lipids, particularly plasmalogens, a subclass that carries a vinyl-ether bond at the sn-1 position, also play a key biochemical role in ferroptosis regulation because polyunsaturated ether phospholipids (PUFA-ePLs) represent primary substrates for lipid peroxidation (C. Liu et al. 2026). Plasmalogens typically contain higher levels of PUFAs compared to their diacyl counterparts, suggesting that they may function as storage depots for PUFAs, thereby shaping the cellular pool of peroxidation-prone lipids. Due to the unique vinyl-ether bond at the sn-1 position, plasmalogens have also been proposed to exert antioxidant properties, protecting other membrane lipids from oxidative damage (Cui et al. 2021; Yilong Zou, Henry, et al. 2020).

Elevated levels of ether lipids have been reported in several aggressive tumours, including BC, and are associated with tumour growth, invasion, and metabolic reprogramming. In particular, the peroxisomal enzyme AGPS, a key enzyme in ether lipid biosynthesis, is frequently upregulated in malignant cells, and its inhibition reduces cancer cell migration, survival, and tumorigenicity (Benjamin et al. 2013; Z. Hu et al. 2025). In BC models, lipidomic analyses have also revealed increased levels of ether phospholipids compared with normal cells, suggesting that alterations in ether lipid metabolism contribute to tumour development (Hahnefeld et al. 2020). More recently, ether lipids have been implicated in the regulation of tumour aggressiveness by modulating signalling pathways and ion channels that control calcium entry, cell migration, and invasion (Z. Hu et al. 2025). Together, these findings indicate that ether lipid metabolism represents an emerging metabolic vulnerability in cancer and may be particularly relevant in aggressive subtypes such as TNBC.

4.4 ISR as a coordinator of lipid metabolic reprogramming

The ISR intersects lipid metabolism at multiple levels, functioning as a broad coordinator of lipid homeostasis under conditions of nutrient deprivation and cellular stress. At the level of de novo lipogenesis, ATF4 promotes fatty acid synthesis through direct upregulation of ACC and through transcriptional regulation of FASN via cooperation with C/EBPδ and PPARγ, collectively sustaining the lipogenic demands of cancer cells under stress conditions (Yan and Liu 2025). Consistently, ATF4 deficiency has been shown to reduce the expression of upstream lipogenic regulators ChREBP and SREBP-1c alongside their downstream targets (Hu Chen et al. 2016), underscoring its role as a positive modulator of the lipogenic program. However, selective ISR activation experiments using synthetic tools have revealed a more nuanced picture: while ATF4 promotes specific lipogenic outputs, it simultaneously redirects carbon utilization away from fatty acid synthesis and toward amino acid production, while driving an ATF4-independent reorganization of the lipidome characterized by Diacylglycerol O-acyltransferase (DGAT)-dependent triglyceride synthesis and lipid droplet accumulation, a pro-survival response that sequesters free fatty acids to mitigate lipotoxicity and preserve ER integrity under stress (Labbé et al. 2024). The ISR also broadly remodels the cell lipidome in an ATF4-independent manner, with selective ISR activation altering the abundance of multiple phospholipid classes.

The relationship between the ISR and SCD1 adds a further layer of complexity to this regulatory network. In melanoma, loss of SCD1 activity leads to accumulation of SFAs, which directly activates the ISR through eIF2α phosphorylation, establishing a bidirectional feedback loop: reduced SCD1 activity triggers ISR activation, while ISR-driven ATF4 induction represses Microphthalmia-associated transcription factor (MITF), the principal transcriptional activator of SCD1, further suppressing SCD1 expression and stabilizing a mesenchymal, stress-resistant cellular state (Vivas-García et al. 2020). This axis illustrates how the stress response can reshape the balance between SFAs and MUFAs, with direct consequences for membrane composition, ferroptosis susceptibility, and cellular plasticity.

Together, these findings position the ISR as a central integrator of lipid metabolic reprogramming, coordinating de novo synthesis, desaturation, storage, and oxidation in a stress- and context-dependent manner. The convergence of ISR-driven lipid remodelling on membrane phospholipid composition, MUFA/PUFA balance, and mitochondrial fatty acid utilization establishes a direct mechanistic link between stress adaptation and the regulation of oxidative cell death. In this way, the ISR provides a conceptual hinge between the lipid-centered adaptations described above and the mitochondrial rewiring discussed in the next section.

5. Mitochondria dynamics and bioenergetics in cancer

The extensive remodelling of lipid metabolism described above does not occur in isolation but is intimately coupled to mitochondrial structure and function: mitochondria are not only the primary site of FAO, but also key determinants of membrane lipid composition, redox balance, and cellular stress signalling. Alterations in mitochondrial dynamics and bioenergetics therefore represent both a consequence and an amplifier of the metabolic rewiring that underlies TNBC aggressiveness, linking lipid metabolic plasticity to the signalling capacity that ultimately shapes cell fate decisions between survival and death.

5.1 Mitochondrial structure and compartmentalization

Mitochondria are multifunctional organelles whose structure is tightly linked to their metabolic and signalling roles. Beyond their classical function as the main site of ATP production through OXPHOS, mitochondria coordinate key cellular processes

including metabolic signalling, calcium handling, redox balance, and the regulation of programmed cell death (Spinelli and Haigis 2018; Riley et al. 2018; Sinha et al. 2013; J. X. Tan and Finkel 2020; Y. Zhu et al. 2023). This functional plasticity relies on a highly compartmentalized and dynamic structure, which enables mitochondria to adapt their activity to changing metabolic demands and stress conditions, promoting cellular adaptation and survival (Eisner et al. 2018; Elhage et al. 2024).

Structurally, mitochondria are delimited by two distinct membranes, the outer mitochondrial membrane (OMM) and the inner mitochondrial membrane (IMM), that define two functionally specialized compartments: the intermembrane space (IMS) and the matrix. The OMM provides a selective interface with the cytosol and is permeable to small metabolites through porin channels such as voltage-dependent anion channels (VDACs), thereby supporting substrate exchange and metabolic communication (Kuwana et al. 2002; Camara et al. 2017; Amsalem et al. 2020). In addition to transport, the outer membrane hosts signalling platforms that regulate apoptosis, lipid metabolism, and mitochondrial dynamics, underscoring its role in coordinating mitochondrial behaviour with cellular cues (Yin et al. 2023). The IMM represents the functional core of the organelle, since it represents the primary site of ATP production. Its low permeability is essential for maintaining the proton gradient that drives ATP synthesis (Meinecke et al. 2006; Wagner et al. 2009; Szabò et al. 2012). The extensive folding into cristae increases surface area and optimizes the spatial organization of the protein complexes (complexes I-IV) which compose the electron transport chain (ETC) and of ATP synthase (Paumard et al. 2002). Cristae morphology is not static but reflects differences in metabolic demand and is closely associated with changes in mitochondrial efficiency and respiratory output (Stephan et al. 2020). Proteins involved in mitochondrial protein import, such as components of the TIM machinery, further contribute to sustaining mitochondrial function and integrity (Lutz 2003).

The electrochemical gradient established across the IMM, the mitochondrial membrane potential ($\Delta\Psi m$), provides the driving force for ATP synthesis and supports essential mitochondrial functions including ion homeostasis, protein import via the TIM machinery, and the regulation of mitochondrial dynamics (Martínez-Reyes et al. 2016). Loss of membrane potential is a hallmark of irreversible mitochondrial damage and activates quality control mechanisms including stress response pathways and selective

mitochondrial clearance (Thayer et al. 2025; Martínez-Rojas et al. 2024). The IMS serves as a specialized signalling compartment, contributing to proton storage during respiration (Ľupták and Hroudová 2019) and harbouring key apoptotic factors, including cytochrome c and Smac/DIABLO, whose regulated release links mitochondrial dysfunction to cell death pathways (Desagher and Martinou 2000). Enclosed by the inner membrane, the mitochondrial matrix hosts the enzymatic machinery of the TCA cycle, contains mitochondrial DNA, and harbours proteolytic systems including LON and ClpXP that ensure protein quality control (Nouri et al. 2020; Cole et al. 2015; Chatre 2024), as well as ion- and redox-sensitive regulators that influence mitochondrial morphology and performance (Cobine et al. 2006), integrating metabolic fluxes with structural and functional adaptations of the organelle.

In cancer cells, including aggressive subtypes, the expression and activity of compartment-specific mitochondrial proteins are frequently altered, reflecting adaptive responses to metabolic stress (H. Du et al. 2025). These changes affect membrane organization, redox homeostasis, and bioenergetic output, reinforcing the concept that mitochondrial architecture constitutes a functional platform integrating structure, metabolism, and survival signalling.

5.2 Mitochondria dynamics

Mitochondria are highly dynamic organelles that continuously undergo remodelling through coordinated cycles of fusion, fission, mitophagy, and intracellular transport. These processes collectively determine mitochondrial morphology, distribution, quality, and function, allowing cells to adapt mitochondrial activity to metabolic demands and stress conditions. Maintaining a proper balance between opposing fusion and fission events is essential for mitochondrial homeostasis, as disruption of either process leads to organelle dysfunction and impaired cellular physiology. (W. Chen et al. 2023)

Mitochondrial fusion promotes the mixing of mitochondrial contents, including proteins, metabolites, and mitochondrial DNA, thereby preserving functional integrity and buffering the effects of localized damage (S. Gao and Hu 2021; Hsiuchen Chen et al. 2010). In mammalian cells, fusion is a multistep process involving the sequential merging of the outer and inner mitochondrial membranes Outer membrane fusion is mediated by the GTPases Mitofusin 1 and 2 (MFN1 and MFN2), whereas inner membrane fusion and

cristae organization are controlled by Optic Atrophy Protein 1 (OPA1) (**Figure 5**). (Song et al. 2009; Weaver et al. 2014). Through these coordinated events, fusion supports mitochondrial bioenergetics, maintains membrane potential, and contributes to the stability of OXPHOS (Hsiuchen Chen et al. 2005).

Mitochondrial fission enables the division of mitochondria, a process required for organelle biogenesis, equal inheritance during cell division, and quality control (Twig et al. 2008; Lewis et al. 2016; Boldogh et al. 2003). Fission is primarily driven by the cytosolic GTPase Dynamin-related protein (DRP1), which is finely regulated through post translational modifications as phosphorylation, SUMOylation, ubiquitination and S-nitrosylation (Smirnova et al. 2001; Chang and Blackstone 2010; Adaniya et al. 2019). Upon activation, through phosphorylation at Ser616, cytoplasmatic Drp1 is recruited to the pre-constricted sites on the OMM, often defined by contacts with the ER, where it assembles into oligomeric structures that constrict the mitochondrial tubule and promote division, through adaptor proteins such as Fis1, MFF and MiD49/51 (Friedman et al. 2011; Losón et al. 2013) (**Figure 5**). By segregating damaged or dysfunctional mitochondrial segments, fission facilitates their selective removal through mitophagy.

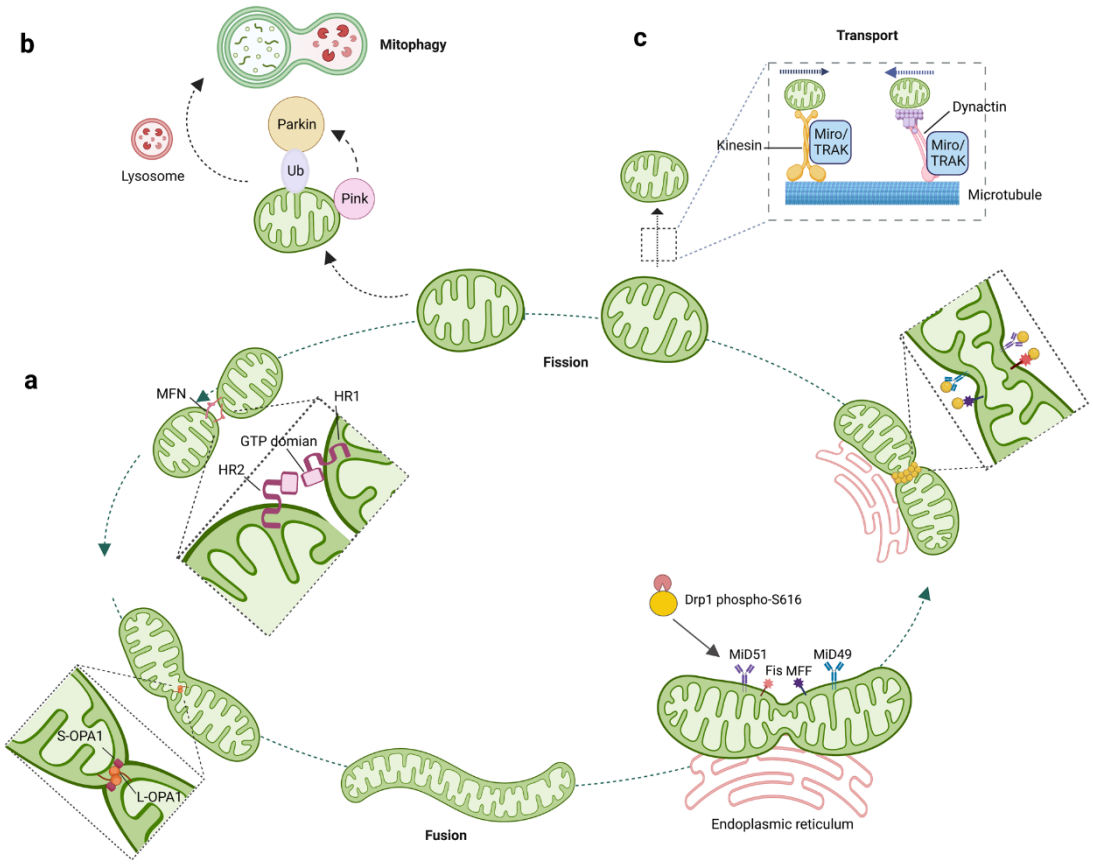

Figure 5. Overview of mitochondrial dynamics. a. *Mitochondrial fission and fusion cycles: fusion is mediated by the coordinated action of Mitofusins 1 and 2 (MFN1/2) on the outer mitochondrial membrane (OMM) and Optic Atrophy Protein 1 (Opa1) on the inner mitochondrial membrane (IMM); fission is driven by the recruitment of Dynamin-related protein 1 (Drp1) to the OMM, where it assembles into a contractile ring-like structure to mediate organelle scission.* ***b.*** *Mitophagy: degradation of dysfunctional or damaged mitochondria is executed through the PINK1/Parkin signaling axis.* ***c.*** *Intracellular Trafficking: the movement of mitochondria along the microtubule network is regulated by the TRAK/Miro motor adapter complex, ensuring proper organelle distribution according to cellular energy demands. Figure from Chen et al., 2023.*

Together, these dynamic processes allow mitochondria to continuously adjust their structure and function in response to environmental cues. Fusion supports metabolic efficiency and resilience, whereas fission enables adaptation, quality control, and, under severe stress, the initiation of apoptotic pathways. The tight coupling between mitochondrial morphology and function underscores the importance of mitochondrial dynamics as regulators of cell fate, stress responses, and metabolic flexibility.

5.2.1 Mitochondria dynamics in the regulation of cancer progression

Mitochondrial dynamics have emerged as critical regulators of cancer cell behaviour, influencing invasion, metastasis, metabolism, and cell fate decisions. An

imbalance in these processes is now recognized as a driving force in tumour progression, as changes in mitochondrial morphology are tightly linked to metabolic adaptation and stress responses. (Hsiuchen Chen and Chan 2017; Tufail et al. 2024)

In BC, increased mitochondrial fragmentation, often associated with elevated levels of the fission mediator DRP1 and reduced expression of fusion proteins such as MFNs, correlates with enhanced metastatic potential, while promoting mitochondrial fusion or inhibiting fission has been shown to restrain cell migration and invasion (J. Zhao et al. 2013; Yufeng Li et al. 2018; Tufail et al. 2024).

This relationship is particularly pronounced in TNBC. Clinical TNBC samples display a marked increase in mitochondrial fission, accompanied by upregulation of DRP1 and downregulation of fusion factors such as MFN1 (J. Zhao et al. 2013; P. Zou et al. 2016). Notably, DRP1 expression is selectively induced by hypoxia in TNBC cells but not in hormone receptor–positive BC models, suggesting that mitochondrial fragmentation represents a stress-adaptive feature of this subtype (X.-J. Han et al. 2015; Cruz-Gregorio 2026).

Functionally, fragmented mitochondria preferentially localize to regions of high energy demand at the leading edge of migrating cells, supporting lamellipodia formation and directing invasion, processes that are impaired by genetic or pharmacological inhibition of fission (Hsiuchen Chen and Chan 2017; J. Zhao et al. 2013). While mitochondrial fission is generally required for cytochrome c release and apoptotic execution, in TNBC it often supports survival by limiting apoptotic sensitivity under moderate stress (L. Chen et al. 2018).

Together, these findings support the view that mitochondrial fission represents a preferred adaptive state in TNBC, enabling metabolic flexibility, stress tolerance, and aggressive behaviour.

5.3 Mitochondrial oxidative metabolism: OXPHOS and TCA cycle

Mitochondria are the primary site of oxidative energy metabolism, integrating three interconnected processes, OXPHOS, TCA cycle activity, and FAO, that collectively sustain ATP production, redox balance, and biosynthetic capacity. The efficiency of these processes is not fixed but is dynamically regulated by mitochondrial structural integrity, cristae organization, and the balance between fusion and fission, establishing a tight

coupling between mitochondrial morphology and metabolic output that is frequently disrupted in cancer cells to support stress adaptation and disease progression.

Mitochondria serve as the primary site of cellular energy production, housing the enzymatic systems responsible for the complete oxidation of metabolic substrates to ATP. Central to this process is the TCA cycle, which takes place in the mitochondrial matrix and represents the converging pathway for the oxidation of sugars, fatty acids, and amino acids: each of these substrates is catabolized to acetyl-CoA, which enters the cycle by condensing with oxaloacetate to form citrate. Through a series of enzymatic reactions, citrate is progressively oxidized back to oxaloacetate, releasing carbon dioxide and transferring electrons to the cofactors NADH and $FADH_2$. Beyond its catabolic role, the TCA cycle also functions as a biosynthetic hub, providing intermediates that exit the cycle to serve as precursors for the synthesis of lipids, amino acids, nucleotides, and other macromolecules, with their continuous replenishment ensured by anaplerotic reactions (Martínez-Reyes and Chandel 2020; Spinelli and Haigis 2018). The reducing equivalents generated by the TCA cycle are subsequently shuttled to the ETC, a series of multisubunit protein complexes embedded in the inner mitochondrial membrane. Here, electrons donated by NADH and $FADH_2$ are passed sequentially through complexes I–IV, driving the pumping of protons from the matrix into the intermembrane space and generating an electrochemical gradient across the inner membrane. This proton motive force is then harnessed by ATP synthase to phosphorylate ADP to ATP, completing the process of OXPHOS. Electron leakage from the ETC, primarily at complexes I and III, can result in the partial reduction of oxygen to superoxide, the precursor of ROS, thereby linking mitochondrial respiratory activity to cellular redox balance and oxidative stress. (Nolfi-Donegan et al. 2020)

Mitochondrial dynamics and cellular energy metabolism are bidirectionally coupled. Mitochondrial dynamics directly orchestrate metabolic output: fission induced by MFN deficiency or reduced GTPase activity results in suppressed OXPHOS, decreased ATP synthesis, mtDNA depletion, and elevated ROS, while fusion counteracts these metabolic insults primarily by enhancing OXPHOS and ATP generation and by protecting mitochondria from mitophagy (J. Li et al. 2022; Kawalec et al. 2015; Pich et al. 2005). At the molecular level, inner membrane fusion mediated by OPA1 is itself tuned by OXPHOS activity through a proteolytic feedback mechanism: under high OXPHOS

conditions, the inner membrane protease YME1L cleaves OPA1 more efficiently (Mishra et al. 2014), stimulating inner membrane fusion and thereby dynamically coupling mitochondrial morphology to respiratory state. In the context of cancer, MFF overexpression in MCF7 BC cells reduces mitochondrial mass and activity and impairs both OXPHOS and glycolysis, as assessed by Seahorse metabolic flux analysis, demonstrating that enhanced mitochondrial fission can directly compromise the bioenergetic competence of tumour cells (Sánchez-Alvarez et al. 2020).

This fine regulation can be determined by the bioenergetic state of the cell. Under nutrient-rich conditions, mitochondria tend to adopt a fragmented morphology whereas nutrient deprivation promotes mitochondrial elongation (Liesa and Shirihai 2013; Wai and Langer 2016; Rambold et al. 2011; Guedouari et al. 2017).

5.3.1 Mitochondrial oxidative metabolism in TNBC

Despite the apparent reliance on glycolysis respect to OXPHOS, TNBC tumours display heterogeneous mitochondrial activity, with evidence supporting both reduced and elevated OXPHOS depending on cellular context. OXPHOS activity has been associated to mtDNA mutations and reduced content of mtDNA encoding for respiratory chain subunits (Ashton et al. 2018). TNBC tumours display a higher frequency of mitochondrial defects respect to other subtypes (Guha et al. 2018), in addition it shows high levels of mitochondrial fragmentation, which coexist with a predominantly glycolytic phenotype in clinical samples (L. Chen et al. 2018; Lim et al. 2016; Reda et al. 2019a). These features suggest that impaired mitochondrial respiration represents a common characteristic of TNBC. Nevertheless, in metastatic TNBC cells, high OXPHOS activity has been reported alongside elevated glycolysis, indicating that these metabolic programs are not mutually exclusive (Dupuy et al. 2015). Enhanced OXPHOS in TNBC is also associated with chemoresistant phenotype (K. Lee et al. 2017).

Notably, under hypoxic conditions TNBC cells increase glucose uptake and glycolytic rate while reducing TCA cycle-coupled OXPHOS activity, yet under bioenergetic stress, activated AMPK and MYC pathways induce mitochondrial biogenesis and upregulate glutaminolysis and FAO to sustain OXPHOS. Fission has been implicated in limiting OXPHOS and controlling ROS production under metabolic stress, and by reducing mitochondrial fusion TNBC cells can dampen ROS accumulation and enhance survival in nutrient-deprived or oxidative environments. (H. Du et al. 2025)

Together, these findings establish that mitochondrial oxidative metabolism in TNBC is not a fixed function but a dynamically regulated capacity that is continuously shaped by morphological state, oncogenomic context, and therapeutic pressure and whose dysregulation at multiple interconnected levels creates both the metabolic vulnerabilities and the adaptive flexibility that define the aggressive behaviour of this tumour subtype.

5.4 Lipids catabolism: fatty acid oxidation and CPT1A

Lipid catabolism through FAO represents a complementary metabolic adaptation that sustains energy production and redox homeostasis. Through FAO, long-chain fatty acids are degraded within mitochondria to generate acetyl-CoA, which enters the TCA cycle, and the reducing equivalents NADH and $FADH_2$ that drive OXPHOS and ATP synthesis. Very-long-chain fatty acids that cannot be directly oxidized in mitochondria are first shortened within peroxisomes before entering this pathway. The import of fatty acids into the mitochondrial matrix is governed by the carnitine transport system: on the outer mitochondrial membrane, carnitine palmitoyltransferase 1 (CPT1) catalyses the conversion of fatty acyl-CoA to fatty acylcarnitine. This intermediate is translocated across the inner membrane by the carnitine/acylcarnitine translocase and subsequently reconverted to acyl-CoA by CPT2, located on the matrix side (Indiveri et al. 2011; Ceccarelli et al. 2011). Inside the mitochondria, FAO proceeds through sequential enzymatic reactions generating acetyl-CoA molecules that fuel the TCA cycle and drive ATP generation (Houten et al. 2016). Beyond its energetic contribution, FAO provides metabolic intermediates such as citrate, that, exported into the cytoplasm, allows the production of NADPH, essential for maintaining biosynthetic capacity and counteracting oxidative stress (Hatzivassiliou et al. 2005). By controlling whether fatty acids are stored, incorporated into membranes, or oxidized, FAO also influences the availability of lipid species that may later shape ferroptotic vulnerability (Kim et al. 2023).

CPT1 comprises three isoforms (CPT1A, CPT1B, and CPT1C) which differ in tissue distribution and sequence features. CPT1A is broadly expressed in liver, kidney, pancreas, adipose tissue, lymphocytes, and fibroblasts, exhibits the greatest affinity for carnitine among the isoforms, and has emerged as the predominant regulator of mitochondrial fatty acid import in cancer contexts (Ceccarelli et al. 2011; Ramsay et al. 2001; Bonnefont 2004).

CPT1A expression is regulated at multiple levels. At the transcriptional level, this regulation is primarily mediated by PPARα, which cooperates with PPARγ coactivator-1α (PGC-1α) (S. Song et al. 2010), which can interact with CCAAT/enhancer-binding protein β (CEBPB), to enhance CPT1A transcription and FAO (Du et al., 2019). Additional regulatory mechanisms involve leucine-rich repeat kinase 2 (LRRK2)-dependent activation of AMPK and PPARα (C.-W. Lin et al. 2020), as well as the PPARα-FGF21 axis, which modulates CPT1A expression through AMPK–ACC and PPARδ/γ signalling pathways (T. Xie et al. 2019). At the post-transcriptional level, specific microRNAs modulate CPT1A translation , while its enzymatic activity responds to hormonal cues including insulin, adiponectin, ERRα, and thyroxine . Long-chain fatty acids serve not only as substrates but also as positive regulators of CPT1A, promoting its expression through PPARα activation (Chatelain et al. 1996). Conversely, malonyl-CoA, generated by ACC2 during fatty acid synthesis, acts as a concentration-dependent allosteric inhibitor of CPT1A, creating a feedback loop that coordinates FAO with lipogenic activity and ensures metabolic balance (Akkaoui et al. 2009; E. A. Park et al. 1995).

Mitochondrial dynamics and FAO are intimately interconnected through a mechanistic link at the level of CPT1A. Mitochondrial fragmentation reduces the sensitivity of CPT1A to its allosteric inhibitor malonyl-CoA, thereby relieving the brake on long-chain FAO and selectively enhancing FAO, whereas mitochondrial elongation increases CPT1A sensitivity to malonyl-CoA inhibition, reducing FAO accordingly. This bidirectional coupling between mitochondrial shape and CPT1A activity establishes mitochondrial morphology as a direct post-translational regulator of FAO, independently of transcriptional changes in CPT1A expression (Ngo et al. 2023). In cancer, however, this relationship acquires additional complexity. In hepatocellular carcinoma, enhanced mitochondrial fission paradoxically suppresses FAO by downregulating CPT1A and ACOX1 through impairment of the NAD^+/SIRT1 axis and consequent reduction of PGC-1α/PPARα transcriptional activity, while simultaneously promoting lipogenesis through SREBP1 activation (D. Wu et al. 2022). Adding further complexity, CPT1A itself regulates mitochondrial dynamics through a non-enzymatic mechanism: in ovarian cancer cells, CPT1A promotes mitochondrial fission, mediating succinylation of the mitochondrial fission factor MFF at K302 and protecting it from Parkin-dependent

degradation, independently of its canonical CPT1 activity (Y. Zhu et al. 2023). Together, these findings reveal a bidirectional regulatory loop between mitochondrial dynamics and FAO in which morphological state shapes metabolic capacity and, reciprocally, metabolic enzymes feedback to regulate organelle structure, a crosstalk with important implications for the metabolic plasticity and adaptive capacity of cancer cells.

5.4.1 FAO and CPT1A in sustaining cancer progression

FAO is a central metabolic pathway supporting BC progression, particularly in therapy resistance and metastasis. Endocrine-resistant ER^+ tumours and TNBC cells show increased reliance on FAO to sustain mitochondrial energy production, driven by transcriptional regulation of key enzymes such as CPT1A and CPT1B, and contributing to chemo- and radio resistance (Ahn et al. 2024). Beyond treatment resistance, FAO promotes metastatic dissemination by enabling tumour cell survival in lipid-rich environments, such as the brain and lymph nodes (S.-S. Li et al. 2025), and by supporting EMT through energy supply and acetyl-CoA dependent epigenetic regulation (Pakhira and Roy 2025). In BC patients, elevated CPT1A expression is associated with significantly worse overall survival and correlates with disease stage (Das et al. 2022). Genetic or pharmacological suppression of CPT1A impairs BC cells invasion and lymphangiogenesis, underscoring its role in tumour aggressiveness (Y. Xiong et al. 2018) and aberrant activation of CPT1A-dependent FAO is increasingly recognized as a metabolic hallmark of therapy resistant tumour cells (Nandi et al. 2024; S. Han et al. 2019). In basal-like TNBC, CPT1A expression correlates with Src activation, which in turn phosphorylates mitochondrial electron transport chain proteins to sustain the bioenergetic demands of invasive cells (J. H. Park et al. 2016). This FAO-Src axis is further amplified in MYC-overexpressing TNBC, where CPT1A is strongly upregulated and its pharmacological or genetic inhibition effectively curtails mitochondrial energy production (Camarda et al. 2016).

Together, these findings identify FAO as a metabolic hub that fuels BC aggressiveness highlighting CPT1A as a promising metabolic vulnerability in this aggressive tumour subtype.

5.5 Mitochondrial Ca^{2+} homeostasis

Among the many functions that mitochondria perform beyond energy production, the regulation of intracellular calcium homeostasis stands out as a critical determinant of both cellular signalling and cell fate. In the present context, this topic follows directly from the bioenergetic sections above, because mitochondrial Ca^{2+} flux regulates metabolic pathways and signalling cascades (Denton 2009; Massimo Bonora et al. 2012).

Mitochondrial Ca^{2+} homeostasis is tightly controlled by a coordinated network of channels, transporters, and regulatory proteins that finely balance Ca^{2+} influx and efflux across mitochondrial membranes. Mitochondrial Ca^{2+} entry into the matrix is primarily mediated by the mitochondrial calcium uniporter (MCU) complex, a multi-protein assembly embedded in the inner mitochondrial membrane (Marchi and Pinton 2014). The Ca^{2+}-permeant pore is formed by MCU together with its paralog MCUb and the essential regulator EMRE, while channel activity is finely tuned by a set of associated modulators, including MICU1 and other members of the MICU family (Baughman et al. 2011; Sancak et al. 2013; Perocchi et al. 2010; Mallilankaraman et al. 2012). Importantly, MCU displays positive cooperativity and becomes highly active only at elevated local Ca^{2+} concentrations, ensuring that mitochondrial Ca^{2+} uptake occurs selectively under conditions of stimulated Ca^{2+} signalling (Csordás et al. 2013).

Because cytosolic Ca^{2+} levels are generally maintained in the nanomolar range , rapid and efficient mitochondrial Ca^{2+} uptake relies on the spatial organization of Ca^{2+} signalling. Tight contact sites between mitochondria and intracellular Ca^{2+} stores, known as mitochondria-associated membranes (MAMs), create localized Ca^{2+} microdomains in which Ca^{2+} concentrations reach the micromolar range required for MCU activation (Rizzuto et al. 2009; Missiroli et al. 2017; Giorgi, Missiroli, et al. 2015). At these sites, Ca^{2+} released from the ER through IP_3 receptors is efficiently transferred to mitochondria, via VDAC on the OMM (Schmitz et al. 2022; Colombini 2016). Ca^{2+} efflux from mitochondria is mainly mediated by the Na^+–Ca^{2+}–Li^+ exchanger NCLX, which exploits the mitochondrial membrane potential and the cytosolic Na^+ gradient to drive Ca^{2+} export, preventing mitochondrial Ca^{2+} overload while sustaining Ca^{2+}-dependent metabolic signalling (Palty et al. 2010; Garbincius and Elrod 2022).

Mitochondrial calcium signalling represents a central mechanism through which mitochondria integrate cellular activity with metabolic output. Fluctuations in cytosolic

Ca^{2+} levels, are rapidly sensed by mitochondria: a rise in mitochondria matrix Ca^{2+} concentration stimulates key rate-limiting dehydrogenases of the TCA cycle, enhancing NADH production, respiratory chain activity, and ultimately ATP synthesis, thereby coupling energy supply to cellular demand. In parallel, calcium-dependent activation of inner membrane transporters further supports substrate availability independently of mitochondrial bioenergetic status. (Duszyński et al. 2006; Gherardi et al. 2020)

Beyond metabolic control, mitochondria act as dynamic buffers of intracellular Ca^{2+}, preventing cytosolic overload, shaping spatially restricted calcium microdomains at contact sites with the ER, critical not only for physiological signalling but also for determining cell fate: excessive or prolonged mitochondrial Ca^{2+} accumulation promotes opening of the mitochondrial permeability transition pore (mPTP), leading to loss of membrane potential, cytochrome c release, and apoptosis (Baumgartner et al. 2009; M Bonora et al. 2015; Bernardi et al. 2023).

Calcium signalling also intersects with mitochondrial dynamics by modulating the balance between fusion and fission. Alterations in intracellular Ca^{2+} levels influence the activity and recruitment of core fission and fusion machinery. Mitochondrial Ca^{2+} is fundamental for the positive regulation of fission machinery, so that calcium overload can promote fission with sensitization to mitophagic or apoptotic pathways (Shangcheng Xu et al. 2016; Patra et al. 2021; Fonseca et al. 2019), whereas balanced Ca^{2+} homeostasis supports mitochondrial fusion, network connectivity, and functional resilience (Golic et al. 2014; Gatti et al. 2025).

5.5.1 Mitochondrial calcium signalling in cancer

In cancer cells, mitochondrial Ca^{2+} signalling emerges as a critical regulatory hub linking metabolic reprogramming with cell fate decisions. Basal mitochondrial Ca^{2+} uptake supports tumour growth by stimulating TCA cycle dehydrogenases and sustaining ATP production, while excessive ER-to-mitochondria Ca^{2+} transfer can trigger apoptosis through mPTP opening and cytochrome c release, highlighting the dual role of Ca^{2+} as both a pro-survival and pro-death signal (Massimo Bonora et al. 2012; Denton 2009; Baumgartner et al. 2009; M Bonora et al. 2015). Cancer cells exploit this balance by fine-tuning ER–mitochondria Ca^{2+} fluxes through alterations at MAMs: tumour suppressors like anti-apoptotic protein BCL-2 and oncogene AKT reduces ER Ca^{2+} release preventing apoptosis, an effect exacerbated by loss of PTEN, and absence or mutation of TP53 and

PML (Rimessi et al. 2014; Giorgi, Bonora, et al. 2015; Giorgi et al. 2010; A Bononi et al. 2013; Angela Bononi et al. 2017), highlighting how deregulated Ca^{2+} signalling at mitochondria contributes to cancer cell survival and therapy resistance.

Alterations in the expression or function of Ca^{2+} transport systems have been detected in several cancers, including TNBC. Central to the regulation of calcium influx is the mitochondrial calcium uniporter (MCU) complex. Enhanced MCU-dependent Ca^{2+} uptake has been associated with increased TCA cycle activity, invasion, and poor prognosis, whereas reduced mitochondrial Ca^{2+} accumulation favours a metabolic shift toward glycolysis and resistance to Ca^{2+}-dependent apoptosis (H. Zhao et al. 2019; Tosatto et al. 2016; Ren et al. 2017).

In TNBC cells specifically, sustained IP3-dependent Ca^{2+} oscillations are efficiently sensed by mitochondria and reinforced by mitochondrial Ca^{2+} uptake through the MCU complex. This Ca^{2+} signalling pathway supports metabolic rewiring associated with TNBC progression by promoting CPT1A-dependent mitochondrial fatty acid uptake and FAO, essential for cell migration and invasiveness (Filadi et al. 2023). At advanced stages of disease, increased MCU expression and reduced MCUb levels enhance mitochondrial Ca^{2+} transients, conferring a selective advantage to TNBC cells (Hall et al. 2014). MCU depletion impairs migration, invasion and metastatic spread in vivo and is associated with reduced mitochondrial NAD(P)H levels, altered redox balance and decreased mitochondrial ROS production with consequent suppression of HIF-1α transcriptional activity, resulting in downregulation of pro-migratory and pro-metastatic gene programs (Tosatto et al. 2016).

Overall, sustained mitochondrial Ca^{2+} uptake emerges as a key driver of TNBC progression by integrating metabolic, redox and transcriptional signalling pathways.

5.6 The ISR as a regulator of mitochondrial structure and function

A growing body of evidence indicates that the ISR is tightly interconnected with mitochondrial function. In recent years, this pathway has emerged as a central mediator of mitochondrial stress signalling across multiple cellular models. Indeed, perturbation of mitochondrial membrane potential activates the OMA1–DELE1–HRI signalling axis, mitochondrial uncoupling or inhibition of ATP synthase activates the ISR through cytosolic accumulation and oligomerization of the mitochondrial protein DELE1, which in turn engages the HRI kinase (Fessler et al. 2020). Similarly, inhibition of respiratory

complex I triggers ISR activation downstream of GCN2 (Mick et al. 2020), while CRISPRi-mediated depletion of mitochondrial proteostatic factors preferentially induces ISR signalling over other stress-response pathways (Madrazo et al. 2024). Findings in mammalian cells identify, despite stressor-specific differences, the ISR as a major retrograde pathway responding to a wide spectrum of mitochondrial perturbations.

ISR-mediated regulation of mitochondrial homeostasis can have opposite outcomes depending on cellular context and stress duration. In corneal endothelial cells subjected to chronic ER stress, ATF4 induction contributes to mitochondrial dysfunction, fragmentation, impaired mitophagy, and apoptosis. In this system, ATF4 knockdown attenuates both ER and mitochondrial stress responses, restores mitochondrial membrane potential, and prevents cell death, underscoring the dual adaptive or pro-apoptotic roles of ISR–mitochondria crosstalk (Qureshi et al. 2026).

Beyond stress signalling, the ISR also plays an active role in regulating mitochondrial morphology: ER stress, activating PERK, promotes adaptive mitochondrial elongation through phosphatidic acid accumulation at the OMM and subsequent inhibition of DRP1, preserving respiratory chain function and limiting mitophagy (Perea et al. 2023), while GCN2 pharmacological activation similarly promotes elongation, highlighting a broader role for ISR signalling in mitochondrial structural adaptation (Baron et al. 2025).

The functional interplay between ISR activation and mitochondrial dynamics is further exemplified in disease-relevant models. In acute myeloid leukemia (AML), pharmacological inhibition of the inner mitochondrial membrane fusion protein OPA1 induces apoptotic cristae remodelling and cytochrome c release, rendering cells dependent on glutamine metabolism and sensitizing them to ferroptosis through activation of ATF4-dependent ISR signalling (Vecchia et al. 2025). In skeletal muscle cells, OPA1 deficiency induces mitochondrial and ER stress and reveals a novel role for ATF4 in regulating mitochondria–ER contact sites (MERCs), calcium homeostasis, and compensatory remodelling of mitochondrial function (Hinton et al. 2024).

The ISR actively remodels the physical interface between the ER and mitochondria, known as mitochondria-associated membranes (MAMs). This process is primarily mediated by the PERK kinase, physically localized and highly enriched at the MAMs. During acute or chronic stress, ISR activation induces a structural tightening of MAMs

and increases contact density by modulating tethering proteins like Mitofusin-2 (MFN2). (Tao et al. 2025; Carreras-Sureda et al. 2022, 2017)

This architectural shift severely disrupts ER-mitochondria calcium transfer. In pathologic conditions the ISR-mediated tightening facilitates an uncontrolled, massive influx of Ca^{2+} from the ER into the mitochondria via the IP3R-GRP75-VDAC1 channel complex, causing mitochondrial calcium overload, depolarization, and subsequent cell death. Conversely, silencing PERK normalizes the MAM distance and restores calcium homeostasis. (Tao et al. 2025; Zhao and Sheng 2025; Loncke et al. 2021) In endocrine-resistant breast cancer cells, PERK localizes directly to ER-mitochondrial contact sites, where it modulates Ca^{2+} transfer and induces apoptotic sensitivity under sustained estrogen signaling. Breast cancer cells also manipulate other MAM-resident proteins to balance proliferation and evade cell death. (Pandey 2026)

MAMs are critical platforms for non-vesicular lipid shuttling, enabling the direct transfer of phosphatidylserine from the ER to the mitochondria for conversion into phosphatidylethanolamine. Alteration of the precise intermembrane spacing directly impairs localized lipid exchange. Consequently, the physical dysregulation of MAMs mediated by the ISR could compromise this vital lipid transfer, but no evidence are present in the literature. (Carreras-Sureda et al. 2022; Bui et al. 2026; Loncke et al. 2021)

Extending this regulatory network to lipid metabolism, ISR modulates FAO through ATF4-dependent transcriptional control of CPT1A. Under glutamine deprivation, ATF4 upregulates the E3 ubiquitin ligase TRIM2, which enhances CPT1A enzymatic activity independently of its ligase function, facilitating mitochondrial fatty acid import and FAO to sustain energy production (Liao et al. 2025), positioning the ISR as a regulator of the metabolic switch between lipid anabolism and catabolism when biosynthetic substrates are limiting.

Together, these findings reveal that the ISR is not only a sensor of cytosolic and ER stress, but also a key regulator of mitochondrial structure, calcium homeostasis, and mitochondria-ER communication, positioning it as a central coordinator of the adaptive mitochondrial rewiring that sustains cancer cell survival under adverse conditions. Given the prominent role of mitochondrial calcium signalling in supporting the bioenergetic and metastatic demands of TNBC cells, and the capacity of the ISR to reshape mitochondrial function at multiple interconnected levels, the intersection of these two pathways emerges

as a particularly relevant axis in the context of TNBC biology, one that may contribute to the metabolic plasticity and stress resilience that define the aggressive behaviour of this tumour subtype. This mitochondrial arm of the ISR is especially important for the transition to ferroptosis, because it links stress sensing to ROS generation, redox buffering, and the availability of oxidizable membrane lipids.

6. Ferroptotic cell death as a metabolic vulnerability

The capacity to evade cell death represents a fundamental requirement for tumour initiation, progression, and metastatic dissemination, and is now firmly established as a hallmark of cancer (Hanahan 2022). However, cancer cells are not unconditionally resistant to cell death, a fact of critical therapeutic importance, since the efficacy of the majority of anticancer strategies ultimately depends on their ability to eliminate malignant cells. Crucially, the susceptibility of tumour cells to distinct forms of regulated cell death is not fixed but is dynamically shaped by their metabolic state: the same metabolic reprogramming that sustains proliferation and stress adaptation also determines the threshold for activation of cell death pathways, including apoptosis, necroptosis, pyroptosis, and ferroptosis. This intimate crosstalk between metabolism and cell death is particularly relevant in TNBC, where the extensive remodelling of lipid metabolism, mitochondria function, FAO and redox homeostasis collectively reconfigures the cellular landscape in ways that directly impact ferroptotic vulnerability (F. Yang et al. 2023; Verma et al. 2020). Among these forms of regulated cell death, ferroptosis occupies a unique position as an inherently metabolic process, whose initiation and execution are inseparable from the lipid, iron, and redox metabolic state of the cell (Stockwell 2022).

6.1 Mechanism governing ferroptosis and principal hallmarks

Ferroptosis is a regulated, non-apoptotic form of cell death whose execution depends on the balance between cellular oxidative injury and compensatory antioxidant defence. The term “ferroptosis” was introduced in 2012 to describe a distinct iron-dependent cell death mechanism driven by the abnormal accumulation of lipid peroxides on cellular membranes (Dixon et al. 2012). Unlike apoptosis or other forms of regulated cell death, ferroptosis cannot be prevented by inhibitors of caspase-dependent pathways, while it is effectively blocked by iron chelators and lipophilic antioxidants (Dolma et al. 2003; Yagoda et al. 2007; W. S. Yang and Stockwell 2008).

At its core, ferroptosis lies at the intersection of iron metabolism, ROS biology, and lipid metabolism. Ferroptosis arises when lipid peroxidation–driving metabolic processes overwhelm the cellular defence systems responsible for maintaining redox balance, normally restricting lipid peroxidation, leading to uncontrolled oxidative damage of membrane phospholipids and ultimately to loss of membrane integrity and cell death. (X. Jiang et al. 2021) Disruptions in iron utilization, iron accumulation, and altered expression of iron-related genes further sensitize cells to ferroptosis (Q. Zhou et al. 2024). These metabolic and biochemical alterations are accompanied by characteristic morphological alterations, different from the ones regarding other cell death mechanisms: ferroptotic cells show mitochondrial shrinkage, increased mitochondrial membrane density, and loss or reduction of mitochondrial cristae, with nuclear morphology largely intact and limited chromatin condensation, while loss of plasma membrane integrity and swelling of cytoplasmic organelles may occur at later stages. Genetically, ferroptosis is regulated by multiple genes involved in iron homeostasis and lipid metabolism, and the altered expression of specific genes and proteins has been proposed as a hallmark of this cell death pathway. (Dolma et al. 2003; Yagoda et al. 2007; W. S. Yang and Stockwell 2008; Dixon et al. 2012; Friedmann Angeli et al. 2014)

Together, these features define ferroptosis as a distinct, metabolism-driven form of regulated cell death caused by a profound imbalance between oxidative damage and antioxidant defence, with lipid peroxidation acting as the central event for the determination of cell fate.

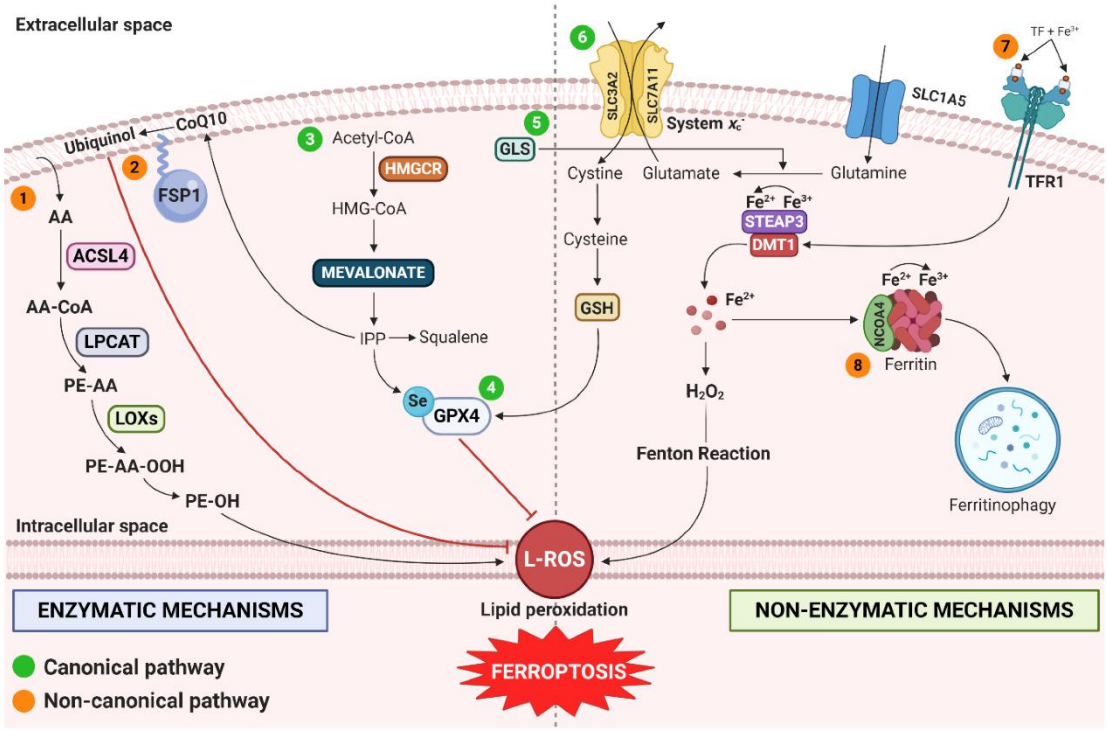

Figure 6. Metabolic pathways which regulate ferroptosis. *1) Lipid metabolism pathway (2) FSP1-CoQ10-NADPH pathway; 3) Mevalonate pathway; 4) GPX4 pathway; 5) Glutaminolysis pathway; 6) Cystine import by amino acid antiporter system x_c^- (SLC3A2 and SLC7A11 subunits) and GSH production; 7) Iron metabolism pathway; 8) Ferritinophagy. Figure from Battaglia et al., 2020*

6.1.1 Iron metabolism and ferroptotic vulnerability

Ferroptosis relies on iron, whose central role extends beyond driving the molecular events underlying lipid peroxidation. Iron is indispensable for the Fenton reaction, which initiates and propagates phospholipid peroxidation (Conrad and Pratt 2019). In addition to its role in non-enzymatic reactions, iron also serves as an essential cofactor for multiple enzymes involved in lipid oxidation, including lipoxygenases (LOXs) and cytochrome P450 oxidoreductase (POR), further reinforcing its contribution to ferroptosis execution (W. S. Yang et al. 2016; Yilong Zou, Li, et al. 2020).

Given the dual role of iron as both a catalyst and an enzymatic cofactor, cellular iron homeostasis is tightly regulated through coordinated mechanisms controlling iron uptake, storage, utilization, and export. Iron enters cells primarily through transferrin/transferrin receptor 1 (TF/TFR-1) mediated endocytosis, where ferric iron (Fe3+) is reduced to its ferrous form (Fe2+) by six transmembrane epithelial antigen of the prostate 3 (STEAP3) and released through dimetal transporter-1 (DMT1) into the cytosol, contributing to the

intracellular labile iron pool (LIP) (Bogdan et al. 2016; Pei et al. 2022; Philpott et al. 2020). This pool represents a highly reactive fraction of iron that directly influences cellular sensitivity to ferroptosis, participating in Fenton Reaction. Excess iron is sequestered in ferritin complexes composed of ferritin light chain (FTL) and ferritin heavy chain 1 (FTH1), whereas selective autophagic degradation of ferritin through NCOA4-mediated ferritinophagy liberates stored iron and enhances ferroptotic susceptibility (Hou et al. 2016; M. Gao et al. 2016). (**Figure 6**)

Perturbations in any of these regulatory nodes, including altered TFR1 expression, dysregulated ferritin turnover, or imbalances in the LIP, can therefore profoundly modulate ferroptosis sensitivity (M. Gao et al. 2016; Kwon et al. 2015; Gammella et al. 2015). Additional layers of regulation involve iron-regulatory proteins that fine-tune the expression of genes associated with iron storage and transport, as well as iron chaperones that coordinate intracellular iron trafficking (Hentze et al. 2010; Philpott et al. 2020).

Collectively, these mechanisms highlight iron metabolism as a critical determinant of ferroptosis, positioning iron not only as a biochemical trigger of lipid peroxidation but also as a tightly regulated cellular factor whose dysregulation can decisively influence cell fate in pathological contexts such as cancer.

6.1.2 Lipid peroxidation and its intersection with lipid metabolism

Ferroptosis is driven by iron-dependent lipid peroxidation of polyunsaturated fatty acid–containing phospholipids (PUFA-PLs), which accumulate as oxidized species within cellular membranes until they compromise membrane integrity and trigger cell death (Dixon et al. 2012). This process is initiated by the abstraction of a bis-allylic hydrogen atom from polyunsaturated fatty acyl chains, generating lipid radicals that react with molecular oxygen to form lipid peroxyl radicals and hydroperoxides (Conrad and Pratt 2019). In the presence of labile iron and ROS such as hydroxyl radicals, Fenton chemistry amplifies this chain reaction, and if lipid hydroperoxides are not detoxified, they propagate further oxidative damage and generate toxic secondary products that ultimately cause cell death (Rochette et al. 2022; Pope and Dixon 2023; Dixon et al. 2012). Although peroxidation of PUFA-containing phospholipids is primarily initiated by nonenzymatic iron-catalyzed reactions, enzymatic pathways can also contribute to lipid oxidation: rachidonate lipoxygenases (LOXs) and cytochrome P450 oxidoreductase

(POR) have been implicated in promoting lipid peroxidation under specific conditions (W. S. Yang et al. 2016; Yilong Zou, Li, et al. 2020).

As a result, membranes enriched in PUFA-containing phospholipids are particularly vulnerable to peroxidation, placing lipid composition at the core of ferroptosis susceptibility. The membrane incorporation of peroxidation-prone fatty acids is tightly regulated by lipid remodeling enzymes that constitute critical determinants of ferroptotic sensitivity. PUFAs, particularly arachidonic acid (AA) and adrenic acid (AdA), which contain multiple bis-allylic moieties, are highly susceptible to oxidative damage and represent essential substrates for ferroptotic lipid peroxidation, when esterified into membrane phospholipids rather than free fatty acids (Kagan et al. 2017). The coordinated activity of ACSL4 and lysophosphatidylcholine acyltransferase 3 (LPCAT3) promotes the conversion of free PUFAs into PUFA-CoAs and their subsequent incorporation into membrane phospholipids, thereby expanding the pool of oxidizable substrates and sensitizing cells to ferroptosis (Kang et al. 1997; Hishikawa et al. 2008) (**Figure 6**). Conversely, genetic or pharmacological inhibition of ACSL4, LPCAT3, or upstream enzymes involved in PUFA biosynthesis and elongation suppresses PUFA-containing phospholipid formation and confers resistance to ferroptosis (Doll et al. 2017; Kagan et al. 2017).

In contrast to PUFAs, MUFAs, which lack bis-allylic bonds, and are less prone to peroxidation and protect cellular membranes by displacing PUFAs from phospholipid species. The synthesis of MUFAs protects cells from ferroptosis, as these lipids are relatively resistant to peroxidation (Magtanong et al. 2019). Accordingly, enzymes involved in MUFA metabolism, such as SCD1 and ACSL3, contribute to ferroptosis resistance, whereas their inhibition sensitizes cells to lipid peroxidation. Additional lipid remodeling pathways further modulate this balance: membrane-bound O-acyltransferase domain-containing proteins MBOAT1 and MBOAT2 have been shown to transfer MUFAs to lyso-phosphatidylethanolamine, increasing MUFA-containing PE species while concomitantly reducing PUFA-PE levels. (Liang et al. 2023; Tesfay et al. 2019; Magtanong et al. 2019; Ubellacker et al. 2020)

More broadly, additional metabolic processes, including de novo fatty acid synthesis, exogenous lipid uptake, lipid droplet dynamics for lipid storage, FAO, and cholesterol metabolism through the mevalonate pathway, further modulate ferroptosis sensitivity by

shaping the intracellular availability of peroxidation-prone substrates, antioxidant cofactors, and membrane lipid composition, integrating systemic metabolic cues with the local redox state of the cell (Pope and Dixon 2023). In particular, FAO further modulates ferroptosis: catabolizing fatty acids, FAO reduces the pool of free PUFAs available for lipid peroxidation. Inhibition of FAO leads to PUFA accumulation and sensitizes cancer cells to ferroptotic cell death, highlighting the importance of metabolic flux between lipid synthesis and degradation (Z. Zhou et al. 2025).

These findings highlight ferroptosis as the outcome of a finely tuned interplay between iron-dependent oxidative reactions and lipid metabolic programs that dictate membrane composition, positioning lipid metabolism as a central regulator of ferroptotic cell fate.

6.1.3 Ether-linked phospholipids as determinants of ferroptotic susceptibility

Recent studies have expanded the classical view of ferroptosis beyond diacyl phospholipids, identifying ether-linked phospholipids as key modulators of ferroptotic vulnerability. In particular, PUFA-ePLs, synthesized through the peroxisomal pathway described above, have emerged as critical contributors to ferroptosis by shaping the cellular pool of oxidizable membrane lipids (Cui et al. 2021; Yilong Zou, Henry, et al. 2020). Genome-wide genetic screens have revealed that disruption of peroxisome biogenesis or ether lipid biosynthetic enzymes, such as PEX3, PEX10, GNPAT, FAR1, AGPS, and AGPAT3, markedly reduces PUFA-ePL, primarily ether-phosphatidylethanolamine (ePE) and ether-phosphatidylcholine (ePC), levels and confer resistance to ferroptosis, highlighting the functional importance of this lipid class (Cui et al. 2021; Yilong Zou, Henry, et al. 2020). Mechanistically, PUFA-ePLs act as substrates for lipid peroxidation during ferroptotic stress, facilitating the propagation of membrane damage. Importantly, their pro-ferroptotic role does not reflect intrinsic susceptibility conferred by the ether linkage itself, but rather their contribution to the overall abundance of polyunsaturated phospholipids available for peroxidation. Remodeling pathways that selectively enrich ether phospholipids with arachidonic acid further enhance ferroptotic sensitivity: TMEM164 facilitates the direct transfer of arachidonic acid from phosphatidylcholines to lyso-ether-phosphatidylethanolamines, generating AA-containing ePE species that are highly oxidizable, whereas shifts toward monounsaturated ether phospholipids have been associated with ferroptosis resistance in specific cellular contexts (Reed et al. 2023; J.-Y. Lee et al. 2023).

Beyond lipid peroxidation, ether phospholipids influence ferroptosis through interactions with iron metabolism. Loss of ether lipid synthesis through AGPS knockout reduces intracellular iron levels by impairing CD44-mediated endocytosis of iron-bound hyaluronates, thereby limiting the availability of redox-active iron required to sustain lipid peroxidation cascades (Mansell et al. 2024).

Together, these findings support a model in which ether phospholipids regulate ferroptosis through multiple interconnected mechanisms, controlling polyunsaturated phospholipid availability, modulating lipid peroxidation dynamics, and regulating intracellular iron homeostasis, actively shaping the biochemical landscape that determines ferroptotic susceptibility in a manner strongly influenced by cellular context, fatty acid composition, and metabolic state.

6.2 Regulation of ferroptosis: GPX4 and the antioxidant surveillance systems

Ferroptosis is tightly regulated by a complex redox surveillance network whose core function is the detoxification of phospholipid hydroperoxides (PLOOHs). Among the glutathione peroxidase family members, GPX4 plays a pivotal role as the central executor of ferroptosis suppression: it catalyses the conversion of reduced glutathione (GSH) into oxidized glutathione (GSSG), reducing toxic lipid hydroperoxides to their corresponding non-toxic alcohols, thereby preventing the accumulation of lipid radicals (Fulvio Ursini et al. 1985; F. Ursini et al. 1982) (**Figure 6**). Pharmacological or genetic inhibition of GPX4 results in rapid PLOOH accumulation and induction of ferroptosis, as demonstrated by the increased sensitivity of cells with reduced GPX4 expression and by the activity of ferroptosis inducers such as RSL3, DPI7, and DPI10, which directly inhibit GPX4 (Seiler et al. 2008; W. S. Yang et al. 2014; W. S. Yang and Stockwell 2008).

GPX4 is regulated at multiple levels. Its activity critically depends on the availability of selenocysteine, incorporated into GPX4 catalytic site via a specialized tRNA whose maturation is regulated by the mevalonate (MVA) pathway (Warner et al. 2000; W. S. Yang et al. 2014). The availability of cysteine, supplied through cystine import via system Xc^- (composed of SLC7A11 and SLC3A2), is essential for GSH biosynthesis, thus for GPX4 function, and it is responsible for mTORC1 activation, to stimulate GPX4 protein synthesis (Fulvio Ursini and Maiorino 2020; Y. Zhang et al. 2021). GPX4 phosphorylation mediated by creatine kinase B (CKB) stabilizes GPX4 and enhances its ferroptosis-suppressive activity (K. Wu et al. 2023). (**Figure 6**)

Although the cyst(e)ine–GSH–GPX4 axis constitutes the primary antiferroptotic defence, several GPX4-independent surveillance pathways provide additional protection. The best characterized is the pathway mediated by ferroptosis suppressor protein 1 (FSP1, also known as AIFM2), an NAD(P)H-dependent oxidoreductase that suppresses ferroptosis independently of GPX4 through a mechanistically distinct route (Bersuker et al. 2019; Doll et al. 2019) (**Figure 6**). Upon myristoylation-dependent targeting to the plasma membrane, FSP1 catalyses the reduction of coenzyme Q (CoQ) to its active form $CoQH_2$, a potent lipophilic radical-trapping antioxidant that intercepts lipid peroxyl radicals and prevents their propagation through membrane phospholipids (Doll et al. 2019). Loss of FSP1 markedly sensitizes cells to ferroptosis even under conditions of GPX4 inhibition or deletion, establishing it as a component of the antiferroptotic surveillance network. FSP1 expression is transcriptionally regulated by NRF2, CRBP, and PPARα, integrating ferroptosis resistance with broader antioxidant and lipid metabolic programs, a regulatory architecture of particular relevance in cancer contexts where these pathways are frequently dysregulated (Chorley et al. 2012; H. P. Nguyen et al. 2020; Venkatesh et al. 2020). Additional GPX4-independent mechanisms include mitochondrial $CoQH_2$ regeneration by DHODH, GCH1-derived tetrahydrobiopterin (BH_4) as a radical-trapping antioxidant, and vitamin K reduction by VKORC1L1, together constituting a broader, compartmentalized defence network that buffers ferroptotic stress across distinct subcellular compartments (Mao et al. 2021; Bersuker et al. 2019; Kraft et al. 2020; Mishima et al. 2022).

Taken together, GPX4-dependent and GPX4-independent mechanisms form a multilayered antioxidant network that tightly controls the initiation and propagation of lipid peroxidation. This intricate regulatory architecture reflects the high vulnerability of cellular membranes to oxidative damage and underscores how perturbations in any of these pathways can profoundly alter cellular sensitivity to ferroptosis, with important implications for physiology and disease, including cancer.

6.3 Ferroptosis as a regulator of cancer cell fate

Ferroptosis has emerged as a fundamental regulator of cancer biology, acting both as an intrinsic tumour-suppressive mechanism and as a process that cancer cells must actively evade during progression. Multiple tumour suppressors exert part of their anticancer function by promoting ferroptosis, supporting the idea that it represents an

innate barrier to tumorigenesis. A paradigmatic example is TP53, which induces ferroptosis by transcriptionally repressing the cystine transporter SLC7A11, thereby limiting glutathione synthesis and increasing vulnerability to lipid peroxidation; notably, specific acetylation-defective TP53 mutants retain tumour-suppressive activity through ferroptosis despite losing canonical functions such as apoptosis induction (Yufei Wang et al. 2019; Chu et al. 2019; L. Jiang et al. 2015). Similarly, BAP1, fumarate hydratase (FH), KEAP1, and the epigenetic regulator MLL4 promote ferroptosis through distinct mechanisms, including epigenetic repression of SLC7A11, modulation of mitochondrial oxidative metabolism, and regulation of lipid peroxidation enzymes (Y. Zhang et al. 2018; Koppula et al. 2022; Fan et al. 2017; Egolf et al. 2021).

Conversely, cancer-associated mutations and oncogenic signalling pathways frequently suppress ferroptosis to support tumour growth. Oncogenic KRAS activation and PI3K–mTORC1 signalling enhance ferroptosis resistance by upregulating antioxidant defences, while NRF2 induces expression of key anti-ferroptotic factors such as SLC7A11 (Q. Zhou et al. 2024; K. Hu et al. 2020; G. Lei et al. 2021). During tumour progression, cancer cells further evade ferroptosis by rewiring lipid and iron metabolism, reducing peroxidation-prone PUFA-containing phospholipids or limiting the labile iron pool through export or sequestration mechanisms. Importantly, specific cancer cell states, including mesenchymal, dedifferentiated, or therapy-resistant persister cells, exhibit heightened sensitivity to ferroptosis due to their dependence on GPX4-mediated detoxification of lipid peroxides, revealing exploitable vulnerabilities that are directly coupled to the aggressive features of these states.

Beyond its role in primary tumour biology, ferroptosis functions as a critical checkpoint during metastatic dissemination, where circulating and newly extravasated tumour cells are exposed to intense oxidative, lipid, and iron-dependent stresses (Wahida and Conrad 2023; Jaewang Lee and Roh 2023). EMT profoundly reshapes lipid metabolism, iron handling, and antioxidant defences, with mesenchymal and EMT-high cancer cells displaying increased PUFA-containing phospholipid incorporation through modulation of factors such as ACSL4 and FADS2 (Schwab et al. 2024; Viswanathan et al. 2017). To survive this intrinsic pro-ferroptotic pressure, these cells become strongly dependent on GPX4-centered detoxification pathways, a phenomenon described as "GPX4 addiction". Therapy-tolerant or stem-like EMT states across multiple tumour

types undergo rapid ferroptotic death upon GPX4 inhibition, whereas reinforcement of GPX4 stability or glutathione metabolism supports metastatic competence. Thus, EMT does not simply confer ferroptosis resistance, but instead positions cancer cells in a precarious state in which enhanced invasive capacity is coupled to a latent vulnerability to ferroptotic collapse when protective circuits fail. The most aggressive, mesenchymal, and therapy-resistant cell states are paradoxically the most vulnerable to ferroptotic collapse when protective circuits are disrupted (Viswanathan et al. 2017). In this sense, ferroptotic susceptibility represents the biological cost of aggressiveness, and the activation of protective mechanisms is the means by which cells pay that cost and survive.

This vulnerability is further shaped by the route of metastatic transit. The bloodstream represents a highly pro-ferroptotic environment, enriched in ROS and labile iron, which amplifies lipid peroxidation and eliminates poorly equipped circulating tumor cells (Merteroglu and Santoro 2024). In the meantime, in the blood intrinsic adaptations, such as coordinated lipogenic and iron-regulatory programs, and extrinsic protection via platelet-derived extracellular vesicles suppress lipid peroxidation and promote survival, thereby facilitating distant seeding (Merteroglu and Santoro 2024; F. Li et al. 2022). In contrast, the lymphatic system provides a comparatively antioxidant- and lipid-rich environment that buffers ferroptotic stress and favours survival (Ubellacker et al. 2020).

Upon extravasation and early colonization, enrichment of polyunsaturated phospholipids, frequently driven by ACSL4, enhances membrane fluidity and invasive capacity but simultaneously increases vulnerability to lipid peroxidation, creating a strong dependency on GPX4-centered detoxification (Yuqi Wang et al. 2025; Kalkavan et al. 2022). Across multiple metastatic niches, including lung, liver, and bone, successful colonization therefore requires rapid membrane stabilization, preservation of NADPH, and engagement of sterol- and quinone-based radical-trapping pathways (F. Guo et al. 2026). Together, these observations identify ferroptosis not as a passive byproduct of dissemination, but as an active biochemical gatekeeper that shapes metastatic efficiency and route preference and highlight its potential as a therapeutic target across the metastatic cascade.

6.3.1 Ferroptosis susceptibility in TNBC

Among BC subtypes, TNBC has emerged as particularly susceptible to ferroptosis. Within the heterogeneous landscape of TNBC, ferroptosis susceptibility is not

uniform: the luminal androgen receptor (LAR) subtype has been identified as particularly vulnerable, in part through androgen receptor-dependent regulation of GPX4, while immunomodulatory (IM) and basal-like immune-suppressed (BLIS) subtypes show less convincing ferroptotic vulnerability (F. Yang et al. 2023).

TNBC cell vulnerability to ferroptosis lies in both its distinctive molecular landscape and its profound metabolic reprogramming, which together generate a characteristic imbalance between pro- and anti-ferroptotic factors. Iron uptake is enhanced through elevated transferrin receptor 1 (TFR1) expression, while the iron exporter ferroportin (FPN) is markedly downregulated, collectively expanding the labile iron pool and priming cells for iron-dependent lipid peroxidation (Feng et al. 2020; S. Ma et al. 2017). Simultaneously, antioxidant defences are weakened: TNBC cells exhibit reduced intracellular GSH content and lower glutathione synthetase activity (Verma et al. 2020; Beatty et al. 2018). Central to this vulnerability is the cystine/glutamate transporter System Xc- (xCT/SLC7A11), whose suppression, whether through pharmacological inhibition, or p53-mediated transcriptional repression, triggers ferroptotic cell death (Timmerman et al. 2013; Wei et al. 2022). Marked dependency on glutamine, which characterizes TNBC cells, further reinforces ferroptosis susceptibility: glutamine fuels both the TCA cycle and GSH synthesis through glutaminolysis (Timmerman et al. 2013; Bhutia and Ganapathy 2016). Accordingly, SLC1A5-mediated glutamine uptake is elevated in basal-like TNBC relative to luminal subtypes (H.-C. Chen et al. 2022). The lipid composition of TNBC further amplifies this vulnerability: high expression of ACSL4 promotes the incorporation of PUFAs into membrane phospholipids, increasing the substrate available for peroxidation (Doll et al. 2017). Importantly, this intrinsic ferroptotic susceptibility is not incidental but is mechanistically coupled to the aggressive features that define TNBC. The same molecular programs that confer invasive and metastatic capacity require extensive membrane remodelling driven by high PUFA-containing phospholipid biosynthesis, which simultaneously renders membranes highly susceptible to lipid peroxidation.

However, TNBC cells simultaneously activate robust evasion mechanisms that counteract this intrinsic vulnerability, and this balance between susceptibility and resistance is itself a driver of disease progression. At the molecular level, PGRMC1, which is more expressed in TNBC than in other BC subtypes, functions as an iron-binding

protein that reduces intracellular iron availability, suppressing ferroptosis and sustaining tumor malignancy (Y. Zhao et al. 2023). Methylenetetrahydrofolate dehydrogenase 2 (MTHFD2), a mitochondrial enzyme whose expression correlates negatively with patient prognosis, protects cells from ferroptosis: MTHFD2 knockdown determines ferroptosis, up-regulation of ROS and lipid peroxidation (H. Zhang et al. 2023). At the epitranscriptomic level, WTAP-mediated m6A modification of NUPR1 leading to upregulation of lipocalin2 (LCN2), which suppresses ferroptosis and sustains proliferative and invasive capacity (M. Tan et al. 2024). Oncogenic signalling through Gankyrin further facilitates MDM2-mediated degradation of p53, resulting in elevated SLC7A11 and GPX4 expression (M. Lei et al. 2023); notably, the high frequency of p53 mutations in TNBC introduces an additional layer of complexity, as mutant p53 can either repress or upregulate SLC7A11 (S.-J. Wang et al. 2016; Y. Liu and Gu 2022).

These molecular evasion mechanisms are complemented by metabolic adaptation: enzymes such as SCD1 and FADS2 produce MUFAs that compete with PUFAs for membrane incorporation, reducing the peroxidation-prone lipid substrate, while the mevalonate pathway sustains production of CoQ and GPX4 through the FSP1 and GPX4 axes, respectively. FSP1 overexpression has been observed across most TNBC cell lines, identifying the CoQ/FSP1 axis as a particularly important resistance mechanism (Doll et al. 2019). The TME further reinforces this protective state through mammary adipocyte-derived oleic acid (Y. Xie et al. 2022). Notably, this interplay between susceptibility and resistance has direct clinical implications: tumours that acquire resistance to conventional therapies or display high metastatic propensity have been shown to exhibit increased sensitivity to ferroptosis induction, suggesting that therapeutic resistance and ferroptotic vulnerability are two faces of the same metabolic reprogramming. Collectively, these findings reveal that ferroptosis in TNBC is not a binary state of sensitivity or resistance, but rather a dynamic equilibrium in which the aggressive features of the tumour are intrinsically coupled to a latent ferroptotic vulnerability that can be therapeutically exploited when protective circuits are dismantled.

6.4 The ISR as a regulator of ferroptotic cell death

The ISR has emerged as a critical regulatory node connecting cellular metabolic stress to ferroptosis, with ATF4 serving as the pivotal effector of this crosstalk. Upon ISR activation, selective ATF4 synthesis orchestrates a broad adaptive gene expression

program that intersects with ferroptosis regulation at multiple levels, with the net outcome depending on the nature, intensity, and duration of the upstream stress. On one hand, ATF4 promotes ferroptosis resistance through multiple converging mechanisms: it stabilizes GPX4 regulating the chaperone HSPA5 (S. Zhu et al. 2017); it drives SLC7A11 expression to sustain cystine import and GSH synthesis, both directly and through cooperation with YAP/TAZ-TEAD transcriptional complexes and through NFE2L2 induction (He et al. 2023; R. Gao et al. 2021; Kreß et al. 2023); and it activates NUPR1, which upregulates lipocalin 2 (LCN2) to restrict intracellular iron availability (J. Liu et al. 2021). The anti-ferroptotic function of the ATF4-SLC7A11 axis has been demonstrated across multiple cancer contexts, where its suppression consistently sensitizes tumour cells to ferroptosis (H. Tang et al. 2024). Additionally, a lysosome-nucleus signalling axis, operating independently of canonical ISR, couples lysosomal cystine depletion to ATF4 transcription through activation of the aryl hydrocarbon receptor (AHR) and the kynurenine pathway, providing a further adaptive layer of ferroptosis resistance (Swanda et al. 2023). At the epigenetic level, LSD1 regulates this axis by controlling histone methylation at the ATF4 promoter: LSD1 inhibition increases H3K9me2 at the ATF4 promoter, repressing ATF4 transcription and consequently reducing SLC7A11 expression, while simultaneously upregulating TFRC and ACSL4 through H3K4me2 modifications, collectively promoting ferroptosis (L. Du et al. 2023).

On the other hand, ATF4 can promote ferroptosis under conditions of severe or prolonged stress, primarily through induction of CHAC1, which degrades GSH by cleaving its γ-glutamyl bond, and of DDIT3, which downregulates GPX4 and promotes ferritinophagy-dependent iron release, amplifying lipid peroxidation in a positive feedback loop (M.-S. Chen et al. 2017). Mitochondria further integrate into this regulatory network: mitochondrial stress through Oma1-DELE1 axis activates an ATF4-mediated ISR that supports the trans-sulfuration pathway for GSH synthesis as a compensatory survival response against oxidative stress, revealing the mitochondria as a dual sensor and executor within this signalling network (Ahola et al. 2022).

The net outcome of ATF4 activation in ferroptosis is therefore context-dependent: moderate or transient ISR engagement tends to be cytoprotective, whereas intense or sustained activation tips the balance toward ferroptotic cell death.

6.4.1 ISR- ferroptosis crosstalk in TNBC

In TNBC, the ISR-ferroptosis axis acquires particular biological significance given the marked dependency of these cells on extracellular cystine for survival. Unlike most normal tissues, which can synthesize cysteine through the trans-sulfuration pathway, TNBC cells rely heavily on cystine import via System Xc- to sustain GSH production and redox homeostasis (Timmerman et al. 2013); accordingly, cystine starvation represents one of the most potent ferroptotic stimuli in this tumor subtype. Mechanistically, cystine deprivation in TNBC cells activates GCN2 leading to eIF2α phosphorylation, ATF4 induction, and upregulation of the ATF4 target gene CHAC1, which degrades intracellular GSH and amplifies oxidative stress beyond the threshold compatible with cell survival (M.-S. Chen et al. 2017). This ISR activation is positioned downstream of RIP1/RIP3/MLKL-dependent necroptotic signalling, triggered by mitochondrial damage and ROS accumulation consequent to cystine deprivation, integrating necroptosis and ferroptosis in a unified cell death program. The dual depletion of GSH, through blocked cystine import and active CHAC1-mediated degradation, creates a catastrophic collapse of antioxidant defences, rendering TNBC cells exquisitely sensitive to lipid peroxidation-driven ferroptosis. Importantly, this mechanism has direct therapeutic implications: the previously discussed adaptive ATF4 response activated by lysosomal cystine depletion, mediated through the AHR-kynurenine axis, represents a resistance mechanism that limits the *in vivo* efficacy of cystine-depleting strategies, suggesting that co-targeting the adaptive ISR response alongside cystine deprivation may be necessary to maximize ferroptotic induction in TNBC (Swanda et al. 2023). Together, these findings position the GCN2-eIF2α-ATF4-CHAC1 axis as a mechanistic bridge between the metabolic vulnerabilities of TNBC and ferroptotic cell death and identify its components as rational therapeutic targets in this aggressive tumour subtype.

7. Conceptual framework and rationale of the study

Taken together, the literature supports a unifying view in which TNBC aggressiveness emerges from the ability of tumour cells to survive chronic microenvironmental stress through coordinated translational and metabolic adaptation. Within this framework, the ISR occupies a central position because it links nutrient limitation, oxidative stress, ER stress, and mitochondrial dysfunction to changes in amino acid metabolism, lipid remodelling, redox control, and cell-fate determination. Lipid metabolism and

mitochondrial function are not ancillary branches of this response, but major effectors through which TNBC cells preserve membrane integrity, sustain bioenergetic flexibility, and regulate susceptibility to ferroptosis. The logic of the preceding sections therefore converges on a single axis: stress-adaptive signalling reshapes lipid and mitochondrial biology, and these changes in turn define whether aggressive TNBC cells remain viable or undergo ferroptotic collapse.

Despite the growing evidence connecting the ISR with cancer adaptation, important questions remain unresolved regarding how ISR-driven remodelling of lipid metabolism and mitochondrial homeostasis shapes ferroptotic vulnerability in aggressive TNBC. Clarifying this relationship is biologically relevant because it may explain how the same stress-response pathway can either protect tumour cells from oxidative damage or, under specific conditions, push them toward ferroptotic collapse. On this basis, the present thesis is framed around the hypothesis that the ISR is a key integrator of metabolic adaptation in TNBC and that its control over lipid and mitochondrial programs has direct consequences for ferroptosis susceptibility and therapeutic vulnerability.

AIM OF THE THESIS

The identification of novel targetable vulnerabilities is an urgent unmet therapeutic need for metastatic Triple-negative Breast Cancer.

A promising therapeutic strategy lies in targeting the stress-adaptive programs that TNBC cells exploit to survive hostile microenvironments and sustain aggressive behaviour. Among these pathways, the Integrated Stress Response has emerged as a central driver of TNBC aggressiveness. However, its dual nature, which can drive either pro-survival or pro-apoptotic signalling depending on context, renders direct pharmacological targeting clinically challenging.

We therefore propose to identify the downstream mechanisms through which the ISR drives its pro-tumorigenic effect, to uncover novel actionable vulnerabilities in metastatic TNBC.

In this framework, the present thesis addresses two main aims:

AIM 1. Define ISR-driven metabolic reprogramming in TNBC

This section investigates how ISR activation reshapes TNBC metabolism through two interconnected axes: mitochondrial function and lipid metabolism.

AIM 2. Determine the functional role of ISR in TNBC aggressive behaviour

This section investigates the mechanism by which ISR-driven metabolic reprogramming leads to the acquisition of functionally relevant aggressive traits in TNBC, with particular focus on invasiveness and susceptibility to ferroptotic cell death.

Together, these aims are designed to establish how ISR reprograms TNBC metabolism, and how this reprograming functionally contributes to tumour aggressiveness. Defining this axis is essential to understand the mechanistic basis through which the ISR sustains metastatic and stress-adaptive traits.

RESULTS

1. Elevated ISR activity defines TNBC and promotes an adaptive, pro-invasive phenotype

Breast Cancer is the primary cause of death for cancer for women worldwide, therefore presenting an unmet therapeutic need, underscoring the urgency for identification of novel molecular vulnerabilities that could be exploited to improve patient outcomes (Bray et al. 2024). In this context, we investigated whether the Integrated Stress Response may represent a clinically relevant adaptive program in BC, and whether its activation correlates with disease aggressiveness. Kaplan-Meier survival analysis of BC patient cohorts from TCGA-BRCA dataset revealed that high expression of a metabolic stress signature, originally generated in melanoma upon glutamine starvation (Falletta et al. 2017), is significantly associated with reduced overall survival compared to patients with low signature expression (**Figure 7A**), suggesting that ISR activation carries prognostic relevance in BC. To further characterize the distribution of ISR activity across breast cancer subtypes, we interrogated the TCGA breast cancer transcriptomic dataset, stratifying patient samples according to molecular subtype. This analysis revealed that Triple-negative Breast Cancer, the most aggressive and metastasising BC subtype, displays the highest levels of ISR activation, as reflected by elevated expression of ATF4 and its transcriptional target ASNS, as well as by enrichment of both the metabolic stress signature and a chemical stress signature induced by Salubrinal, a potent and specific ISR activator (**Figure 7B**). Collectively, these observations identify TNBC as the subtype with the highest intrinsic ISR activity, providing a strong clinical and molecular rationale for investigating the functional role of this pathway in TNBC biology and its potential as a therapeutic target in this aggressive disease.

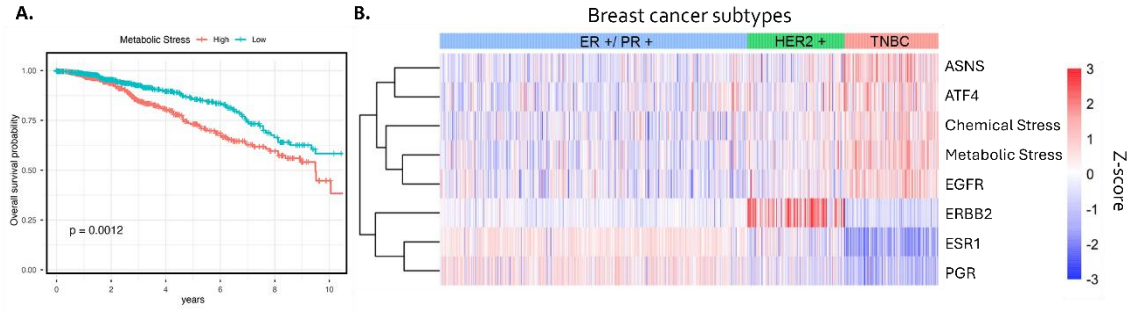

Figure 7. ISR predicts poor prognosis in BC patients and is enriched in TNBC. A. *Kaplan-Meier Overall Survival Analysis of Breast Cancer patients from TCGA-BRCA dataset, divided by low and high Metabolic Stress Signature.* ***B.*** *Heatmap representing hierarchical clustering of ISR-related genes and signatures in TCGA breast cancer dataset grouped by subtypes.*

To address this question experimentally, we first characterized the broad phenotypic consequences of ISR activation in TNBC cells, investigating how ISR affects cell cycle and viability of MDA-MB-231 TNBC cell line, since proliferation and survival are principal hallmarks of tumours. MDA-MB-231 is an epithelial cell line derived from a pleural effusion of a patient with metastatic breast adenocarcinoma (Cailleau et al. 1978). Molecularly, MDA-MB-231 belongs to the claudin-low subtype, defined by downregulation of cell-cell adhesion genes, enrichment for epithelial-to-mesenchymal transition markers (EMT), and a $CD44^{+}/CD24^{-}$ stem cell-like phenotype associated with increased invasive and metastatic potential. Mutated TP53 and KRAS contribute to the aggressive mesenchymal transcriptional program that makes MDA-MB-231 one of the most widely used preclinical models for TNBC research. (Chavez et al. 2011)

Cell cycle analysis following 48 hours of Salubrinal revealed a modest but significant delay in G1 phase, accompanied by a corresponding reduction in the fraction of cells in S and G2 phase (**Figure 8A**). This pattern is consistent with a canonical stress checkpoint response, in which cells subordinate proliferation to stress resolution and resource reallocation, a well-established outcome of ISR activation that reflects the prioritization of adaptive programs over cell division (Ryoo 2024; Falletta et al. 2017). To assess apoptotic cell death, we employed the CellEvent Caspase-3/7 assay following 48 hours of Salubrinal treatment. This analysis revealed only a marginal increase in caspase-3/7 activity compared to untreated cells, around 4-5% (**Figure 8B**), indicating that most MDA-MB-231 cells successfully activate pro-survival programs sufficient to evade stress-induced apoptosis. The negligible extent of apoptosis under these conditions indicates that Salubrinal treatment does not exert significant cytotoxic effects in this

model and at this timepoint, and that the observed G1 delay reflects a reversible adaptive checkpoint rather than a prelude to cell death.

Given that ISR activation imposed a proliferative brake without triggering significant cell death, we next asked whether this adaptive state was associated with changes in the aggressiveness of TNBC cells, particularly in invasive behaviour, property that is central to the metastatic potential of this tumour subtype and has been linked to stress-driven transcriptional reprogramming. Invasion was assessed using a Transwell assays, which revealed a significant enhancement of invasive capacity following Salubrinal treatment (**Figure 8C**). This observation indicates that ISR activation does not only support survival but actively reshapes the aggressive potential of TNBC cells, promoting a more invasive phenotype. Rather than contradicting the G1 delay, this finding is consistent with a model in which cells that successfully resolve stress emerge with enhanced migratory and invasive properties, a phenomenon linked to the metabolic and transcriptional rewiring driven by ISR (Nagelkerke et al. 2013; García-Jiménez and Goding 2019; Avivar-Valderas et al. 2011), whose molecular underpinnings in lipid metabolism, mitochondrial function, and ferroptosis susceptibility are investigated in the sections that follow.

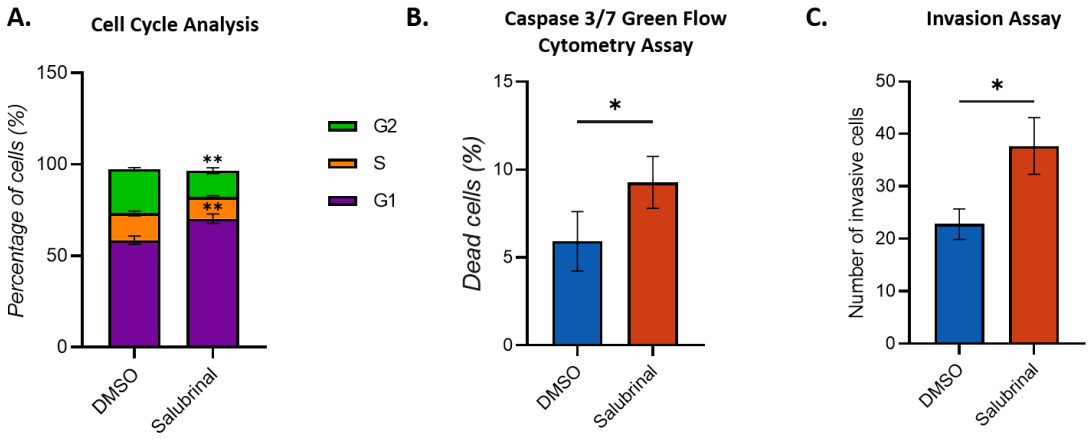

Figure 8. ISR confers negligible cell death, delay in G1 and increased invasive potential. *MDA-MB-231 cells treated for 48h with vehicle (DMSO) or Salubrinal:* ***A.*** *percentage of cells in G1, S or G2 phase, detected by flow cytometric analysis of DNA content stained with propidium iodide (PI), n=3 biological replicates;* ***B.*** *percentage of apoptotic cells detected by Cell Event caspase 3/7 Green Flow Cytometry Assay, n=4 biological replicates;* ***C.*** *number of cells that migrated across the membrane of a Transwell Chamber, n= 3 biological replicates. Statistical analyses (A., B.): means +/- SD, (Mann-Whitney test) (C.) mean +/- SEM. (Student's T-test) *P < 0.05, **P < 0.01*

2. ISR shapes TNBC Cells Mitochondrial architecture, signalling and metabolism

2.1 ISR regulates mitochondria bioenergetics remodelling

To define the earliest phases of ISR-dependent translation reprogramming in an unbiased manner, we combined Ribosome Profiling (Ribo-sequencing) with matched RNA-sequencing in MDA-MB-231 TNBC cells upon ISR induction. Cells were treated overnight (16 hours) with Salubrinal, a well-established pharmacological inhibitor of eIF2α dephosphorylation which targets the GADD34- and CReP-associated phosphatase machinery, in comparison to vehicle control (DMSO). This dual-omics approach enabled us to quantify ribosome-protected fragments (RPFs) abundance, representing active ribosome occupancy and therefore ongoing protein synthesis (Clamer et al. 2018), in parallel with total transcript levels, to identify the primary and specific translational events induced by ISR activation (**Figure 9A**). The 16-hour time point was selected to specifically capture the early translational events driven by eIF2α phosphorylation, while minimizing the contribution of the downstream transcriptional response mediated by ATF4 and the possible secondary compensatory modulation of protein synthesis. This strategy allowed us to obtain a snapshot of the combined transcriptional and translational modulation occurring in MDA-MB-231 cells upon early and specific ISR activation. The comparison of RNA-seq and Ribo-seq $\log_2$ Fold Changes showed that most transcripts clusters around the origin, indicating that most mRNAs remain largely unchanged, representing a limited global response consistent with the relatively early time point analysed. This landscape, therefore, most likely allowed us to capture the initial phase of ISR-dependent translational remodelling and in particular: 1) changes restricted to mRNA abundance (blue dots), representing transcription-dominant regulation, are relatively scarce; 2) none of the mRNAs showing altered transcription and translation reach statistical significance, probably due to a strong uncoupling of the two events in this phase of ISR activation; and 3) a more evident subset of transcripts displays modulated RPFs amount in absence of mRNA alterations (red dots), representing translation-dominant regulation (**Figure 9B**). The upregulated fraction of this group constitutes the main focus of our analysis, as it is the most likely to represent an early ISR-induced set of translational targets.

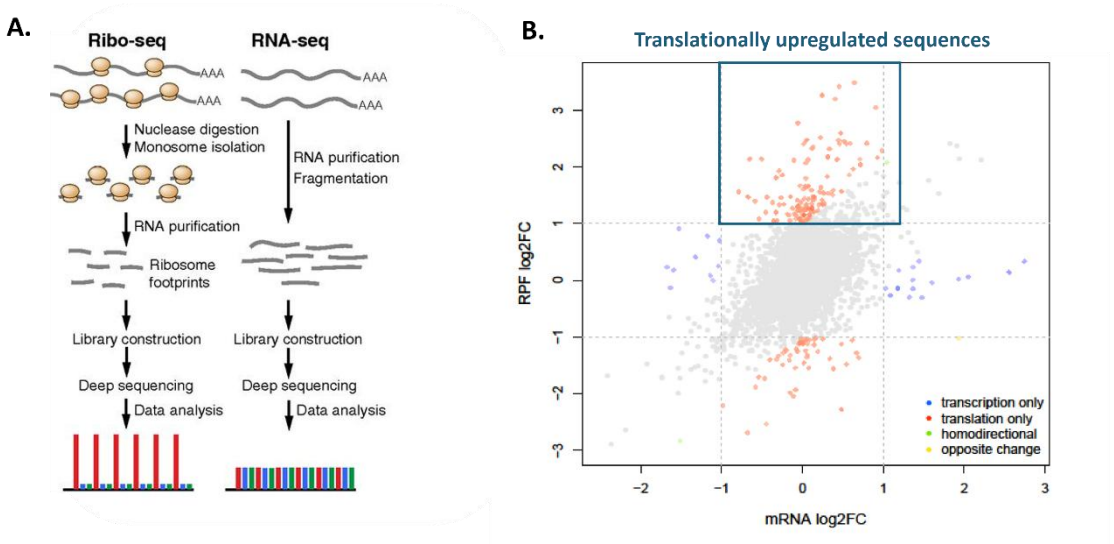

Figure 9. ISR-dependent transcriptional and translational landscape in TNBC. *Ribo-seq/RNA-seq analysis on MDA-MB-231 cells after 16h of treatment with Salubrinal or vehicle (DMSO): **A.** schematic representation of the technique (adapted from NT Ingolia et al., 2009); **B.** scatter plot showing the correlation between Ribosome Protected mRNA Fragments (RPF) and mRNA fold change.*

To identify the biological programs preferentially engaged at the translational level by ISR activation, we performed an over-representation analysis of the translationally upregulated transcripts using the Reactome database. As expected, pathways associated with the translational machinery itself, including ribosomal proteins, translation, and translation initiation, were enriched, validating the efficacy of our method to capture canonical ISR-mediated translational outputs. Strikingly, the analysis uncovered a parallel, wide, and highly coherent enrichment in mitochondrial pathways which can be summarised in two main categories, the first being bioenergetic functions and respiration (e.g., oxidative phosphorylation, mitochondrial ATP synthesis coupled to proton transport, electron transport, and respiratory chain complex I activity); while the second representing structural mitochondria features (mitochondria inner membrane, matrix components, cristae formation), indicating that this response could be involved in the regulation of mitochondria architecture (**Figure 10**). Finally, over-representation analysis also revealed enrichment for calcium-dependent processes, such as protein and phospholipids binding (**Figure 10**). Although this last set of categories at first glance might appear less directly connected to mitochondria, it may nevertheless converge on mitochondria signalling. Indeed, mitochondria are central regulators on intracellular calcium homeostasis, serving as one of the major intracellular calcium storages and

working in coordination with the endoplasmic reticulum (ER) (Angela Bononi et al. 2012). In this functional interplay, calcium fluxes between the ER and the mitochondrion affect mitochondria metabolism and adaptation to stress (Duszyński et al. 2006). Thus, the enrichment of calcium-related signatures may support the hypothesis that ISR engages a broad adaptive program regulating mitochondria function, directly through metabolic components and architectural determinants and indirectly through calcium signalling and homeostasis.

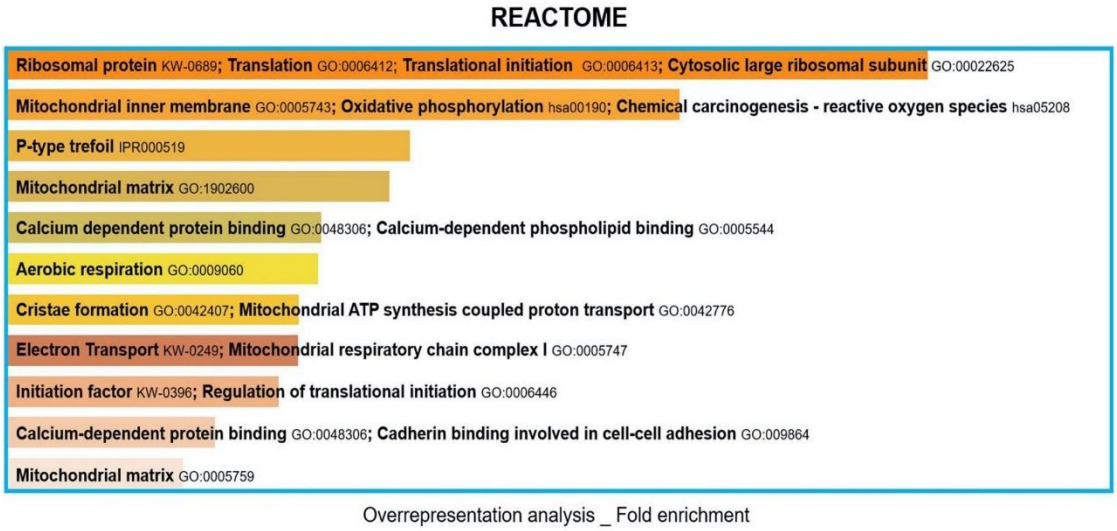

Figure 10. ISR upregulates the mitochondrial translatome. *Reactome pathway overrepresentation analysis of translationally upregulated mRNAs identified by Ribo-seq/RNA-seq in MDA-MB-231 cells treated with Salubrinal for 16 hours relative to vehicle (DMSO) treated cells.*

In conclusion, these results highlight mitochondria as a major target of the early ISR-dependent translational remodelling program: selective ISR activation rapidly promotes a translational response centred on mitochondria bioenergetics, architecture and signalling, providing us with a rationale for the subsequent structural and functional analysis of mitochondria in this system.

On these bases, we next first asked whether the translational enrichment of mitochondria architectural determinants was accompanied by measurable morphological alterations and dynamics.

2.2 ISR-dependent translation reprogramming drives reversible mitochondria fragmentation and cristae disorganization in TNBC

Mitochondria morphology is tightly connected to organelle function, including respiration, bioenergetics, stress adaptation and inter-organelle signalling. Therefore, the assessment of mitochondria architecture represents a logical step forward to determine whether the translation remodelling previously identified can be translated into a distinguished structural phenotype.

To this aim, we employed complementary high-resolution advanced imaging techniques in TNBC cell lines, combining three-dimensional (3D) confocal reconstruction of the mitochondrial network with ultrastructural analysis via electron microscopy (EM), to qualitatively and quantitatively assess ISR-induced mitochondrial alterations. To strengthen the robustness of our observations and exclude findings exclusively dependent on the genetic background of a single cell line, the BT549 cell line was employed in parallel as a second TNBC model. BT549 is an epithelial cell line derived from a papillary invasive ductal carcinoma that had metastasized to regional lymph nodes (Cailleau et al. 1978). Molecularly, BT549 belongs to the mesenchymal (M) TNBC subtype according to the Lehmann classification (Lehmann et al. 2011), a subtype defined by activation of epithelial-to-mesenchymal transition programs, enhanced invasiveness, and therapy resistance. Its mutational landscape is characterized by mutations in TP53 and loss of function of RB1, a combination frequently observed in aggressive mesenchymal TNBC and associated with deregulated cell cycle progression and EMT (Chavez et al. 2011). Together, MDA-MB-231 and BT549 represent two molecularly distinct TNBC subtypes that share the defining TNBC features while differing in key genetic alterations, providing a complementary experimental framework to identify observations of broader biological relevance beyond cell line-specific effects.

Live-cell 3D confocal microscopy was performed on TNBC cells transiently expressing mitochondrial-targeted GFP (mtGFP) and treated with either vehicle (DMSO) or Salubrinal for 48 hours, thereby allowing visualization of the downstream structural effects of sustained ISR activation. Representative confocal images clearly show that, following Salubrinal treatment, the mitochondrial network is shifted towards a more fragmented phenotype, with most mitochondria appearing shorter and more punctate compared to the elongated and connected structures observed in the DMSO vehicle

control cells (**Figure 11A**). To enable a robust quantitative assessment, a mitochondrial 3D mask was generated from the mtGFP signal and used for segmentation (**Figure 11B**). This approach allowed the measurement of key morphometric parameters via ImageJ and Hyugenes software, including mitochondrial number, single mitochondrial volume and total mitochondrial volume per cell. The marked increase in the number of mitochondria, accompanied by a concomitant reduction in their average volume, and in the absence of change in the total mitochondrial volume per cell (**Figure 8C**), is indicative of mitochondria fragmentation rather than a change in overall mitochondrial mass, leading us to exclude mitochondria biogenesis or mitophagy as the possible ISR-dependent programs leading to the altered phenotype.

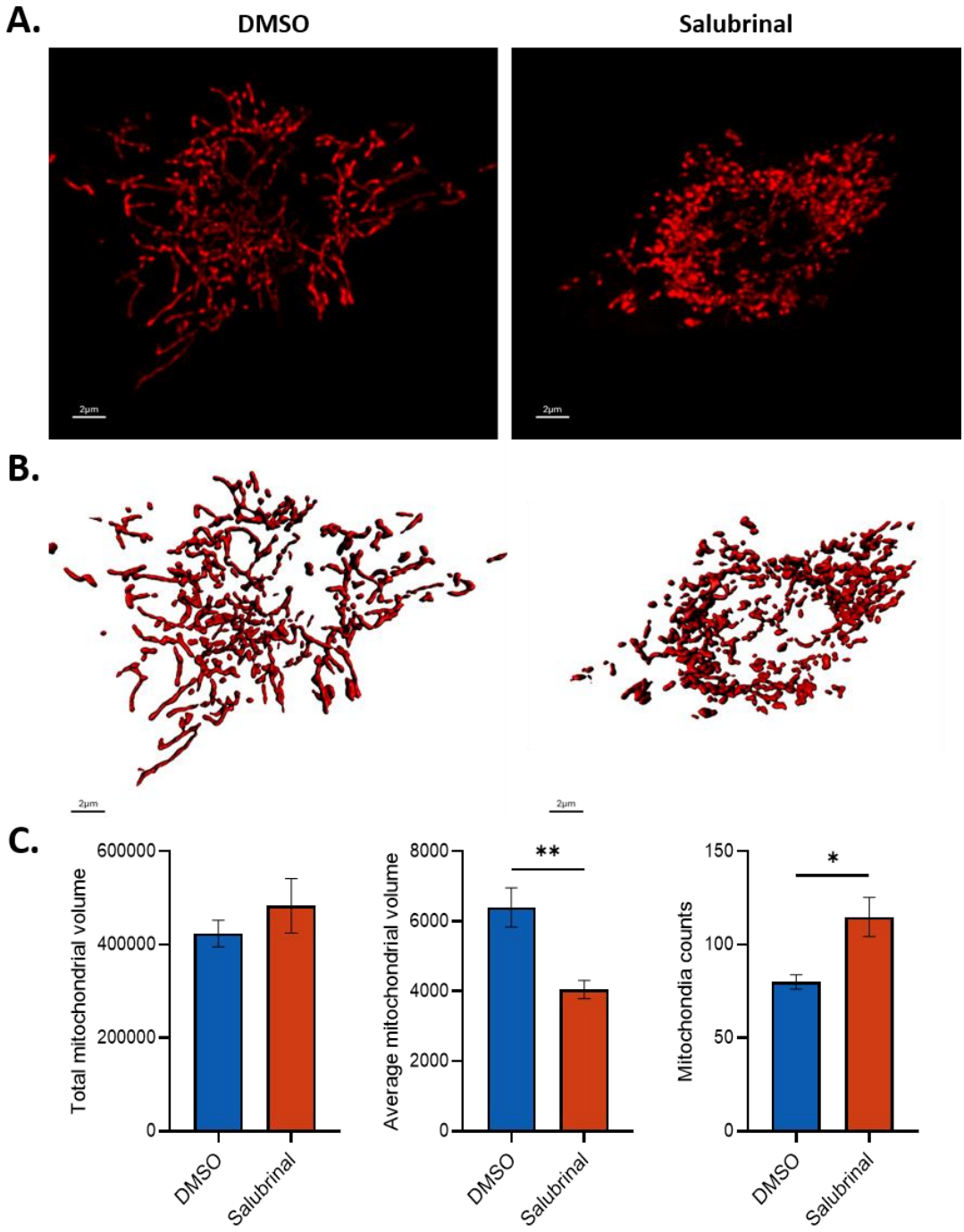

Figure 11. ISR induces mitochondria fragmentation. ***A.*** *Representative confocal microscopy images and* ***B.*** *3D reconstruction of the mitochondrial network (scale bar: 2 µm) and* ***C.*** *total and average mitochondrial volume (voxels) and mitochondria counts, in BT549 cells transiently expressing mitochondrial-targeted GFP (mtGFP), treated with vehicle (DMSO) or Salubrinal for 48 h, n=2 biological replicates. Statistical analyses (C.): means +/- SEM. *P < 0.05, **P < 0.01 (Mann-Whitney test).*

Taken together, these observations and measures demonstrated that prolonged ISR activation is associated with a marked remodelling of the mitochondrial network towards a fragmented phenotype. Intriguingly, increased mitochondrial fragmentation is often associated with enhanced metastatic potential. For instance, promoting mitochondrial fusion or inhibiting fission has been shown to restrain cell migration and invasion, highlighting mitochondrial morphology as a determinant of breast cancer aggressiveness (L. Chen et al. 2018).

To extend the architectural characterization by direct examination of the mitochondrial ultrastructure, we next performed transmission electron microscopy. This allowed us to determine whether the fragmented phenotype observed in the 3D confocal reconstruction was paralleled by sub-mitochondrial structural modification. To this end, we analysed MDA-MB-231 cells after 48 hours of Salubrinal treatment. Cells showed extensive mitochondrial fragmentation, characterised by reduced mitochondrial volume and increased circularity, thereby confirming the confocal microscopy findings at ultrastructural resolution (**Figure 12A**). Quantification of both parameters displayed a robust statistical significance (**Figure 12B**). Moreover, the fragmentation was accompanied by a pronounced disorganization of the cristae architecture, which appeared irregular, swollen, with loss of the normal shelf-like pattern. With the analysis of the solidity parameter, we obtained a quantification of shape regularity, which allowed to measure the disorganization of cristae upon ISR induction compared to control (**Figure 12A, B**). This set of data indicates that ISR affects not only the global morphology of the mitochondrial network, but also the internal ultrastructural integrity of the organelle. Importantly, both the fragmentated phenotype and the cristae alterations were completely reversed three days after Salubrinal washout, indicating that these changes are dynamic and reversible.

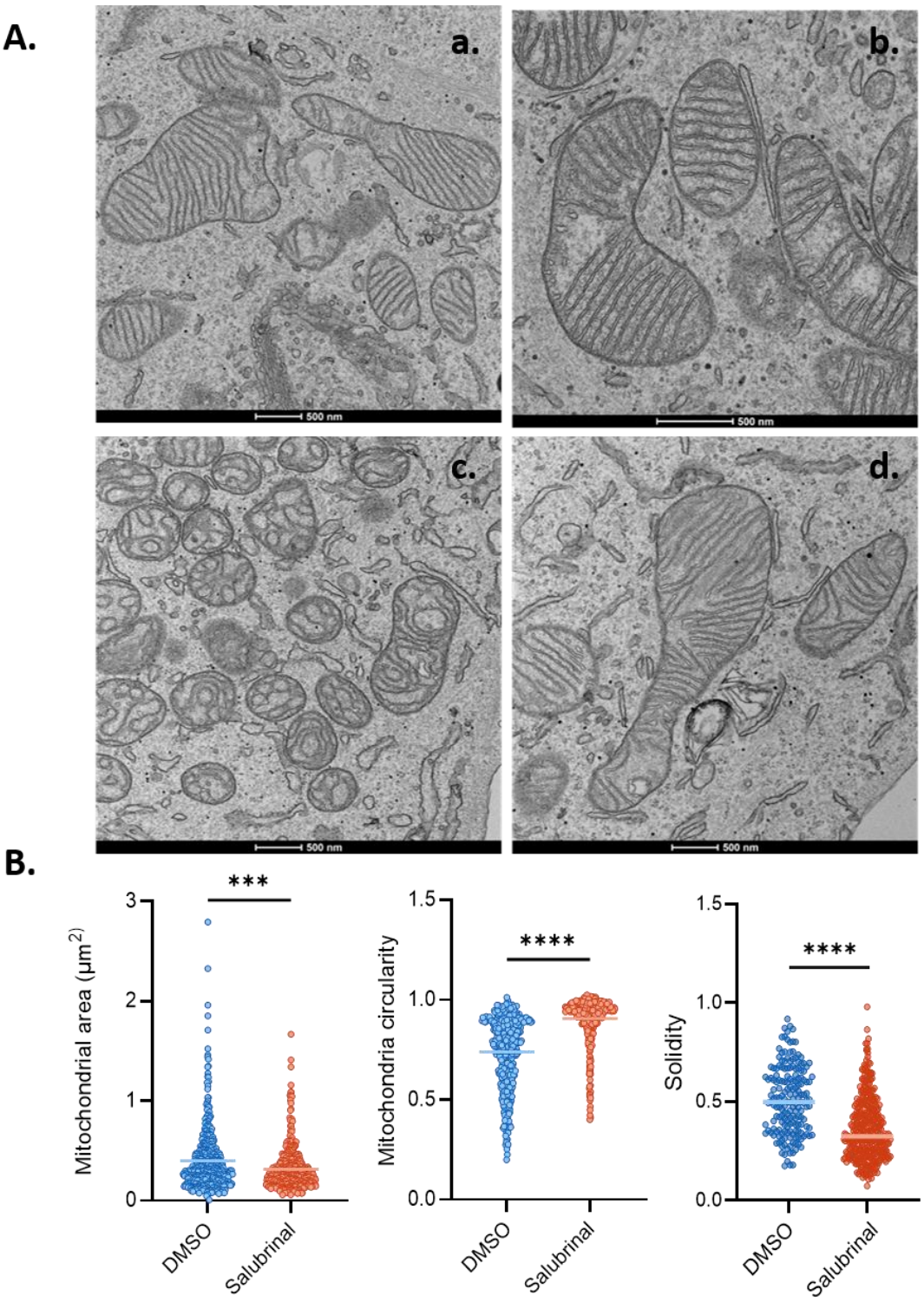

Figure 12. ISR induces mitochondria fragmentation and cristae alterations. A. *Representative electron micrographs of MDA-MB-231 cells untreated (a.), or after 72h treatment with vehicle (DMSO) (b.), Salubrinal without (c.) and with (d.) washout (scale bar: 500 nm).* ***B.*** *Quantification of mitochondria morphologic alterations in Salubrinal vs vehicle treated cells: area (µm²), circularity ((4π*p)/A), cristae solidity (Area/Convex Area). Statistical analyses (B.): means +/- SD. ***P < 0.001, ****P < 0.0001 (Student's T-test).*

Taken together, these results show that ISR activation drives a profound yet reversible remodelling of mitochondrial architecture, characterised by enhanced fragmentation and disruption of cristae organization. Notably, this structural phenotype is consistent with our Ribo-seq findings, which identified selective translational upregulation of mitochondrial and mitochondrial-associated proteins. Collectively, these observations support a model by which ISR activation orchestrates a coordinated rewiring of mitochondrial structure and function through early translational reprogramming. Interestingly, the increased translation of a mitochondria architecture subset of mRNA resulted in the disruption of fusion and cristae organisation rather than an enhancement of their morphological organisation.

2.3 ISR rewires mitochondrial function and metabolism

2.3.1 ISR activation suppresses mitochondrial Ca^{2+} Uptake

After establishing that ISR activation induces an important remodelling of mitochondrial architecture, we next investigated whether these structural modifications were accompanied by measurable modulation of mitochondrial function. Emerging from the coupled Ribo-seq/RNA-seq results previously described, and tightly linked to mitochondrial phenotype, is the role of calcium signalling. Mitochondrial calcium flux plays an essential role in the regulation of oxidative metabolism, ATP production, intracellular signalling, mitochondrial dynamics, and cell fate decisions. Its precise regulation ensures that mitochondria respond appropriately to cellular demand, whereas even subtle perturbations in mitochondria calcium homeostasis can severely impair organelle functionality and contribute to a wide range of pathological conditions, including, neurodegeneration, metabolic disease and cancer (Denton 2009; Massimo Bonora et al. 2012).

To assess the functional consequence of ISR activation on intracellular calcium dynamics, we measured calcium fluxes in mitochondria, cytosol, and endoplasmic reticulum (ER) using recombinant compartment-specific aequorins.

MDA-MB-231 and BT549 TNBC cells were transiently transfected with the appropriate bioluminescent probes (mtAEQ, cytAEQ and erAEQ) and pre-treated for 48 hours with vehicle (DMSO) or Salubrinal before luminescence recording. To determine

calcium mobilization, cells were stimulated with Ca^{2+} -perturbing agents. The choice of calcium-perturbing agent was guided by a careful review of the literature, considering the specific cell line employed (Massimo Bonora et al. 2013; Filadi et al. 2023). Indeed, the type, expression level and coupling efficiency of the receptors capable of initiating intracellular Ca^{2+} waves vary substantially across cellular models and may critically determine the amplitude and dynamics of the evoked calcium response. This experimental strategy allowed a direct measure of calcium handling across intracellular compartments under sustained ISR activation.

Mitochondria Ca^{2+} uptake was markedly reduced (almost completely abrogated) in both MDA-MB-231 and BT549 cells upon Salubrinal treatment, as shown peak amplitude and kinetic traces (**Figure 13A, B**). This effect indicates that ISR impairs the ability of mitochondria to efficiently uptake Ca^{2+} in response to stimulus, suggesting a substantial functional alteration fully consistent with the observed structural remodelling. Moreover, given the importance of mitochondrial Ca^{2+} transfer for metabolic processes, these findings suggest that ISR-dependent mitochondrial reprogramming extends beyond morphology and directly influences the organelle functionality.

To determine whether this phenotype depends on the canonical ISR transcriptional program, we next tested the contribution of ATF4. Notably, ATF4 silencing partially restored mitochondrial Ca^{2+} uptake in Salubrinal-treated cells and further improved the Ca^{2+} uptake in vehicle-treated conditions (**Figure 13C**). This functional analysis indicates that the negative effect of ATF4 on mitochondrial calcium handling is not restricted to conditions of acute pharmacological ISR activation but reflects a constitutive role in setting the basal threshold of mitochondrial calcium uptake, as evidenced by the ability of ATF4 depletion alone to enhance mitochondrial Ca^{2+} uptake even in the absence of Salubrinal. Therefore, these data place ATF4 as a critical mediator linking ISR signalling to mitochondrial function adaptation and suggests that modulation of the ATF4 downstream signalling may be sufficient to reshape mitochondrial calcium flux even independently from acute ISR activation.

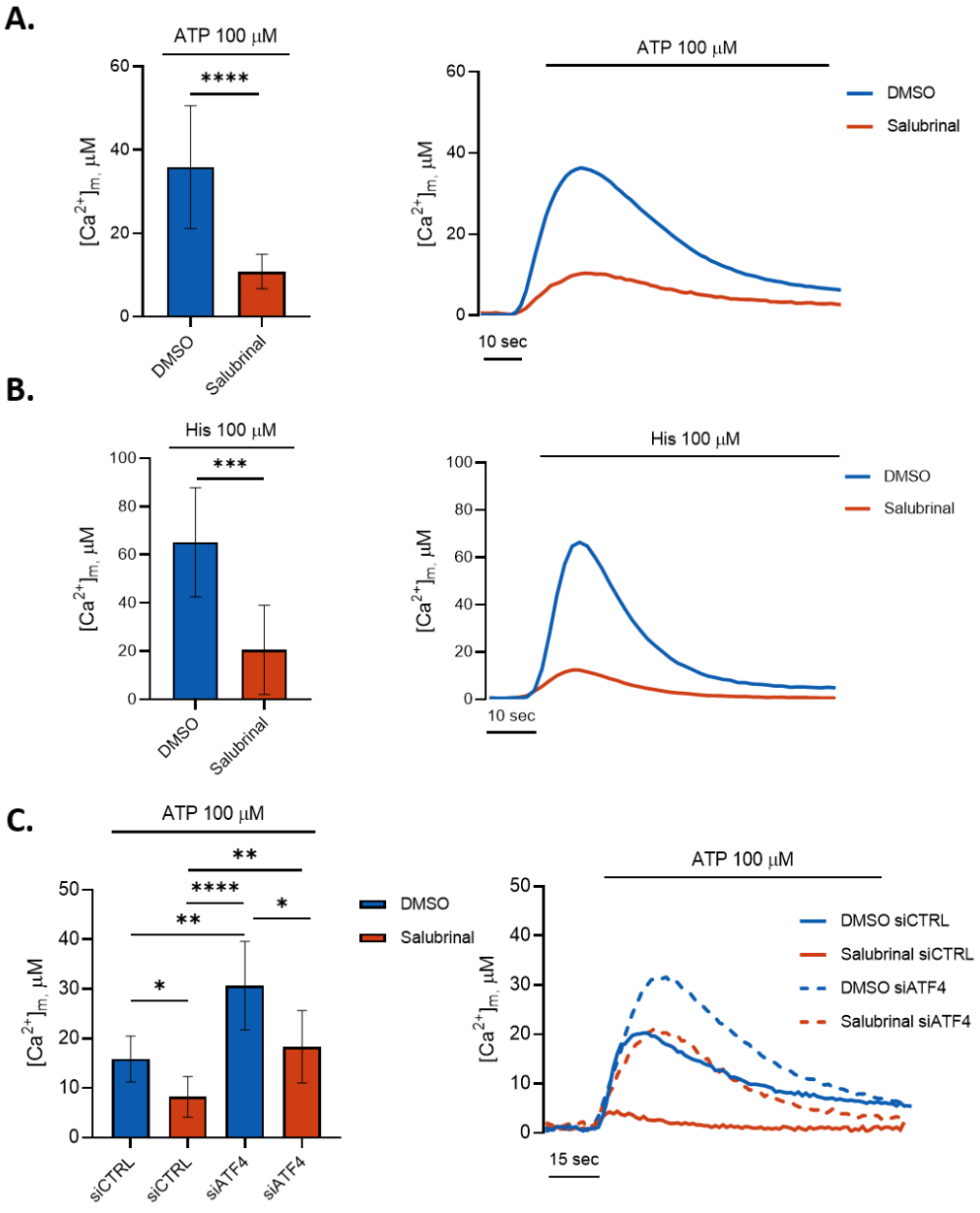

Figure 13. ISR induces mitochondrial Calcium fluxes alterations via ATF4. *Representative mitochondrial Ca^{2+}measurements in* ***A.*** *MDA-MB-231 cells challenged with 100 µM ATP,* ***B.*** *BT549 cells challenged with 100 µM Histamine (His) and C. MDA-MB-231 cells transfected with siRNA Silencer Control (siCTRL) or siRNA ATF4 (siATF4) and challenged with 100 µM ATP, n=3 biological replicates. Cells were treated for 48h with Salubrinal or vehicle (DMSO). Statistical analyses (A.-C.): means +/- SD. ***P < 0.001, ****P < 0.0001 (Mann-Whitney test).*

We then investigated whether the strong impairment od mitochondrial Ca^{2+} uptake could be elucidated by broader alterations in cellular Ca^{2+} dynamics. Cytosolic calcium responses were differentially affected in the two TNBC models: they remained substantially unchanged in MDA-MB-231 cells, whereas they were significantly reduced in BT549 cells (**Figure 14A, B**). This divergent behaviour suggests that the impaired mitochondrial Ca^{2+} uptake observed in MDA-MB-231 cells may not result simply from a reduced total amount of Ca^{2+}, or an impaired global Ca^{2+} signalling, buy may in contrast reflect a direct and specific defect in mitochondrial Ca^{2+} transfer or uptake efficiency. By contrast, in BT549 cells, the concomitant reduction in cytosolic Ca^{2+} suggests a broader perturbating effect of ISR in the intracellular calcium homeostasis.

To further dissect the origin of these discrepancies, we measured ER Ca^{2+} dynamics using the bioluminescent reporter erAEQ. Following complete depletion of ER Ca^{2+} stores and reconstitution of the aequorin probe, cells were perfused with Ca^{2+}-containing buffer to allow store reloading, detected as a luminescence peak whose amplitude reflects ER Ca^{2+} concentration and whose kinetics report the refilling rate. After that, agonist-evoked Ca^{2+} release was triggered by perfusion with the Ca^{2+} - perturbing agent ATP (MDA-MB-231) or histamine (BT549), with the resulting luminescence decay reporting the rate and extent of Ca^{2+} release from the ER. In MDA-MB-231, ER Ca^{2+} storage and release were largely preserved, and only the refilling rate was reduced (**Figure 14C**). This pattern is consistent with the unaltered cytosolic calcium dynamics and suggests that, in this cellular context, ISR activation does not widely impair ER calcium content, but may affect the efficiency of calcium cycling between intracellular compartments. In contrast, in BT549 cells, ISR activation caused marked defects in ER calcium accumulation, release, and refilling kinetics, indicating a global disruption of ER calcium homeostasis (**Figure 14D**).

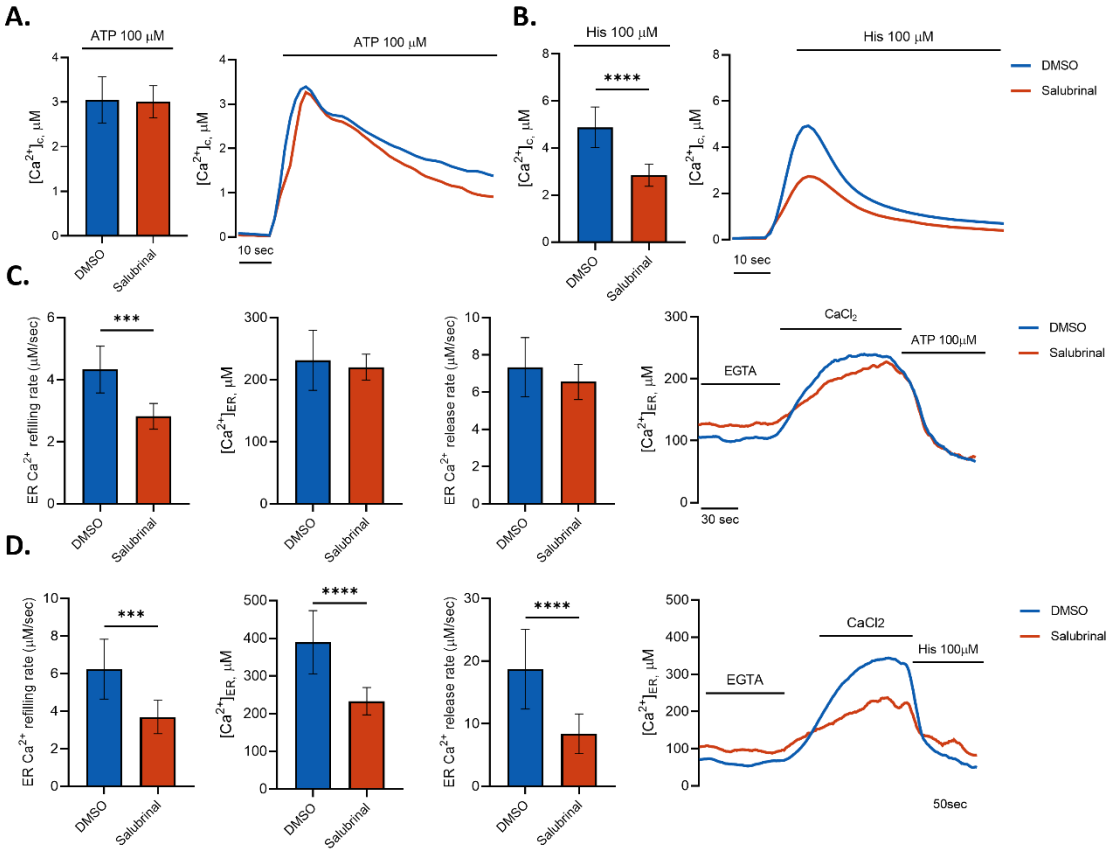

Figure 14. ISR-dependent total Calcium fluxes alteration is cell type specific. A.-B. *Representative cytosolic Ca^{2+} measurements in **A.** MDA-MB-231 cells challenged with 100 µM ATP, **B.** BT549 cells challenged with 100 µM Histamine (His), n=3 biological replicates. **C.-D.** Representative ER Ca^{2+} refilling rate, content and release rate in **C.** MDA-MB-231 and **D.** BT549. EGTA was used to chelate calcium, 1mM $CaCl_2$ to induce Ca^{2+} accumulation in the ER, 100 µM ATP or Histamine (His) to induce Ca^{2+} release from the ER. Cells were treated for 48h with Salubrinal or vehicle (DMSO), n=2 biological replicates, A. n samples=10 DMSO, 11 Salubrinal, B. n samples=9 DMSO, 10 Salubrinal. Statistical analyses (A.-D.): means +/- SD. ***P < 0.001, ****P < 0.0001 (Mann-Whitney test).*

Overall, our results show that ISR activation impairs mitochondrial calcium uptake in TNBC cells, possibly revealing a direct functional consequence of the mitochondrial remodelling program induced as an early consequence of the ISR-dependent translation rewiring we discovered. At the same time, the distinct profiles observed in the two TNBC cells indicate that the mechanisms underlying this phenotype may differ across models. One possibility is that these differences reflect the magnitude of ISR activation, with a comparatively milder response in MDA-MB-231 cells and a stronger and more pervasive response in BT549. Alternatively, BT549 may harbour pre-existing genetic or signalling unbalances that exacerbate the disruption of calcium homeostasis upon ISR activation. In this context, the broader alteration of ER-to-mitochondria calcium crosstalk observed in

BT549 may represent either a quantitative amplification of the same ISR-induced program or the consequence of additional cell line-specific vulnerabilities. To assess this possibility, it will be crucial to identify a direct molecular effector which modulation is sufficient to recapitulate the calcium dynamics in both cell lines. Given that ATF4 knock-down strongly affects mitochondria Ca2+ uptake in MDA-MB-231 not only upon acute ISR induction by Salubrinal, but also at basal conditions, a particularly suitable candidate would be a direct ATF4 transcriptional target. The identification of such an effector remains an important objective for future investigations.

Overall, these findings identify mitochondria calcium homeostasis as a major functional target of ISR activation and further support the evidence of an ISR-driven transcriptional and translational remodelling of mitochondria physiology.

2.3.2 ISR suppresses mitochondrial respiratory capacity and carbon metabolism

The reduction in mitochondrial Ca^{2+} uptake capacity observed upon ISR activation, combined with the structural remodelling of mitochondria, raised the hypothesis that ISR activation may be associated with a broader and functionally significant impairment of mitochondrial metabolic functions. It is documented that mitochondrial calcium uptake plays a central role in the regulation of oxidative metabolism: Ca^{2+} accumulation within the mitochondrial matrix directly stimulates key rate-limiting dehydrogenases of the TCA cycle, enhances electron transport chain activity, and ultimately drives ATP synthesis, thereby coupling cellular energy supply to demand (Gherardi et al. 2020). Moreover, cristae remodelling has been shown to directly affect the assembly and stability of respiratory supercomplexes, rendering the electron transport chain less efficient and reducing the overall oxidative capacity of the organelle.

To test our hypothesis and characterize the metabolic consequences of ISR activation at the mitochondrial level, we assessed mitochondrial respiratory activity in MDA-MB-231 cells were treated with Salubrinal or vehicle (DMSO) for 48 hours. Results from Seahorse Extracellular Flux Analyser, that enables real-time quantification of oxygen consumption rate (OCR), providing a readout of key mitochondrial bioenergetic parameters (basal respiration, ATP-linked respiration, and maximal respiratory capacity), shows that Salubrinal treated cells display a significant reduction in oxygen consumption rate (OCR) compared to control cells. Notably, ISR affects not only the maximal

respiratory capacity but also the basal OCR, indicating that ISR activation suppresses mitochondrial respiration already under resting conditions (**Figure 15A**). To further characterize the metabolic consequences of ISR activation at the level of central carbon metabolism, TCA cycle intermediates were profiled by metabolomics analysis. Salubrinal treatment resulted in a broad and coordinated reduction in the abundance of TCA cycle intermediates, suggesting a global impairment of oxidative metabolism and mitochondrial substrate utilization. (**Figure 15B**) An exception is represented by malate, whose abundance was increased upon ISR activation. This may reflect compensatory replenishment from alternative pathways, such as malic enzyme-mediated conversion of pyruvate or aspartate-malate shuttle activity, rather than an increase in canonical TCA cycle flux.

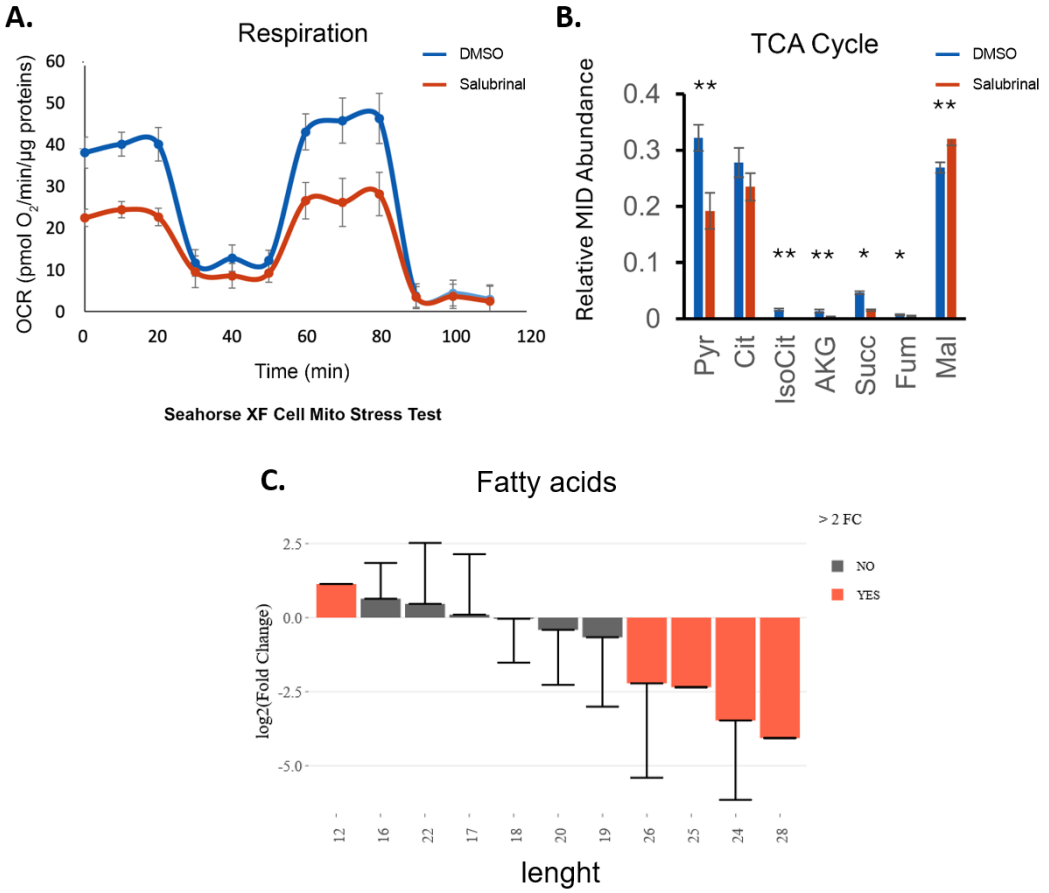

Figure 15. ISR suppresses mitochondrial respiratory capacity and carbon metabolism while promoting a reduction in long-chain Fatty Acids. A. *Mitochondrial respiratory profile assessed by Seahorse XF Cell Mito Stress Test, which shows oxygen consumption rate (OCR) among time.* ***B.*** *TCA cycle intermediates abundance, assessed by untargeted metabolomics. Pyr: pyruvate, Cit: citrate, IsoCit: isocitrate, AKG: α-ketoglutarate, Succ: succinate, Fum: fumarate, and Mal: malate.* ***C.*** *Lenght of fatty acids in Salubrinal treated cells vs vehicle (DMSO) measured by univariate lipidomic analysis. NO: < 2 FC SI: > 2 FC. Cells were treated for 48h with Salubrinal or vehicle (DMSO). Analyses were performed on MDA-MB-231 cells treated for 48h with Salubrinal or vehicle (DMSO).*

Collectively, these data indicate that ISR activation is associated with a significant suppression of mitochondrial oxidative metabolism, reflected in a reduction of basal and maximal respiratory capacity and a broad depletion of TCA cycle intermediates. These findings suggest that the structural alterations induced by ISR activation are not merely morphological features but translate into a functionally relevant impairment of mitochondrial bioenergetic output. Notably, the translational upregulation of mitochondrial respiratory proteins observed at 16 hours may reflect an early compensatory response to this emerging bioenergetic deficit, which nevertheless proved insufficient to prevent the functional impairment detected at 48 hours. These observations delineate a coherent picture in which ISR activation in TNBC cells reconfigures

mitochondrial function at multiple interconnected levels, from calcium-dependent metabolic stimulation to oxidative substrate utilization, ultimately reducing the overall capacity of the organelle to sustain energy production through oxidative phosphorylation.

2.3.3 ISR engages a metabolic reprogramming through the induction of CPT1A and increased fatty acid oxidation

Despite the evident ISR-driven alteration of mitochondrial architecture and impairment of mitochondria functions, these profound alterations do not translate into a global loss of cell fitness. On the opposite side, the activation of ISR induces a mild delay in the G1 phase of the cell cycle, a negligible apoptosis-mediated cell death, and an enhancement in migratory and invasive capacity in TNBC cells, as shown in **Figure 8**. All together, these observations indicate that the mitochondrial phenotype described above is compatible with, or may even support, a more aggressive tumour cell phenotype. This apparent paradox suggests that ISR does not simply impair mitochondrial function but rather may promote its adaptive rewiring. In this context, the mitochondrial structural and functional alterations described so far may reflect a transition towards a mitochondrial phenotype less optimized for canonical respiratory activity and oxidative signalling but better suited to sustain stress adaptation and metastatic behaviour. Indeed, in cancer remodelled mitochondria can preserve fitness and sustain plasticity and invasion (J. Zhao et al. 2013; Yufeng Li et al. 2018). Importantly, metastatic tumours often rely on lipid metabolism, particularly fatty acid oxidation (FAO), which can provide an alternative source of energy under adverse conditions (S.-S. Li et al. 2025). This possibility is especially relevant in TNBC cells, where lipid metabolism has been linked to migratory and invasive traits, and where FAO has emerged as a major determinant of metastatic potential (Y. Xiong et al. 2018).

Supporting this hypothesis, lipidomic profiling revealed a marked reduction in long-chain fatty acids upon 48 hours of Salubrinal treatment in MDA-MB-231 cells (**Figure 15C**). While this observation may reflect multiple metabolic processes, including reduced *de novo* synthesis or altered membrane incorporation, the concomitant suppression of canonical mitochondrial respiration and TCA cycle activity raises the possibility that long-chain fatty acids are being preferentially channelled toward β-oxidation as an alternative bioenergetic route, rather than accumulating as free lipid species. This interpretation is consistent with the known capacity of ISR-activated cancer cells to shift

metabolic reliance toward oxidative lipid catabolism under conditions of biosynthetic stress (Liao et al. 2025), and led us to hypothesize that the ISR-driven mitochondrial phenotype is paralleled by a broader metabolic rewiring, which results in a distinct functional state in which fatty acids catabolism may play a central bioenergetic role. Therefore, we consequently investigated whether ISR may promote a shift towards fatty acid consumption as a fuel to support TNBC aggressiveness.

To start addressing the possibility that ISR activation promotes a metabolic rewiring towards lipids consumption, we focused on carnitine palmitoyltransferase 1 (CPT1A), the rate limiting enzyme for mitochondrial fatty acid import and FAO. Among its several isoforms, CPT1A is the major form expressed in breast cancer, and is frequently associated with tumour metabolic adaptation (Das et al. 2022; J. H. Park et al. 2016). MDA-MB 231 and BT549 were subjected for 48 hours to pharmacological ISR-activation (Salubrinal) and glutamine starvation, commonly used as microenvironmental metabolic stress which triggers ISR activation (Falletta et al. 2017). WB analysis showed that ISR activation driven by both the chemical and metabolic stimuli resulted in an increase in CPT1A protein levels (**Figure 16A**), supporting the hypothesis that ISR may engage a lipid-fuelled mitochondrial program. Notably, glutamine deprivation induced a more pronounced upregulation of CPT1A compared to Salubrinal treatment, despite both conditions converged on ISR activation. This quantitative difference may reflect the broader metabolic impact of glutamine starvation, which simultaneously perturbs multiple interconnected metabolic pathways, including TCA cycle, nucleotide biosynthesis, and redox homeostasis, thereby generating a more extensive metabolic stress that may amplify the transcriptional and post-translational signals driving to CPT1A upregulation.

To confirm that this effect was directly linked to ISR signalling rather than off-target consequences of the potential metabolic alterations led by glutamine starvation, or of the off-target effect of Salubrinal, we created a genetically engineered MDA-MB-231 model in which expression of a phosphomimetic eIF2α mutant (eIF2α Dmut) can be induced upon doxycycline treatment. This model genetically recapitulated the ISR activation independently of metabolic or pharmacological stressors. Validation of the system is shown in **Figure 16B**, whereby a dose-course of doxycycline for the induction of eIF2α Dmut expression resulted in ISR activation, as evidenced by a dose-dependent increase

in ATF4 protein levels. The robust ISR activation in the inducible system, indicated by the expected modulation of the canonical ISR markers ATF4 and GADD34, was sufficient to reproduce the increase in CPT1A protein levels observed with Salubrinal and glutamine starvation (**Figure 16C**). This evidence strengthens the conclusion that CPT1A upregulation is a *bona fide* downstream effect of ISR activation.

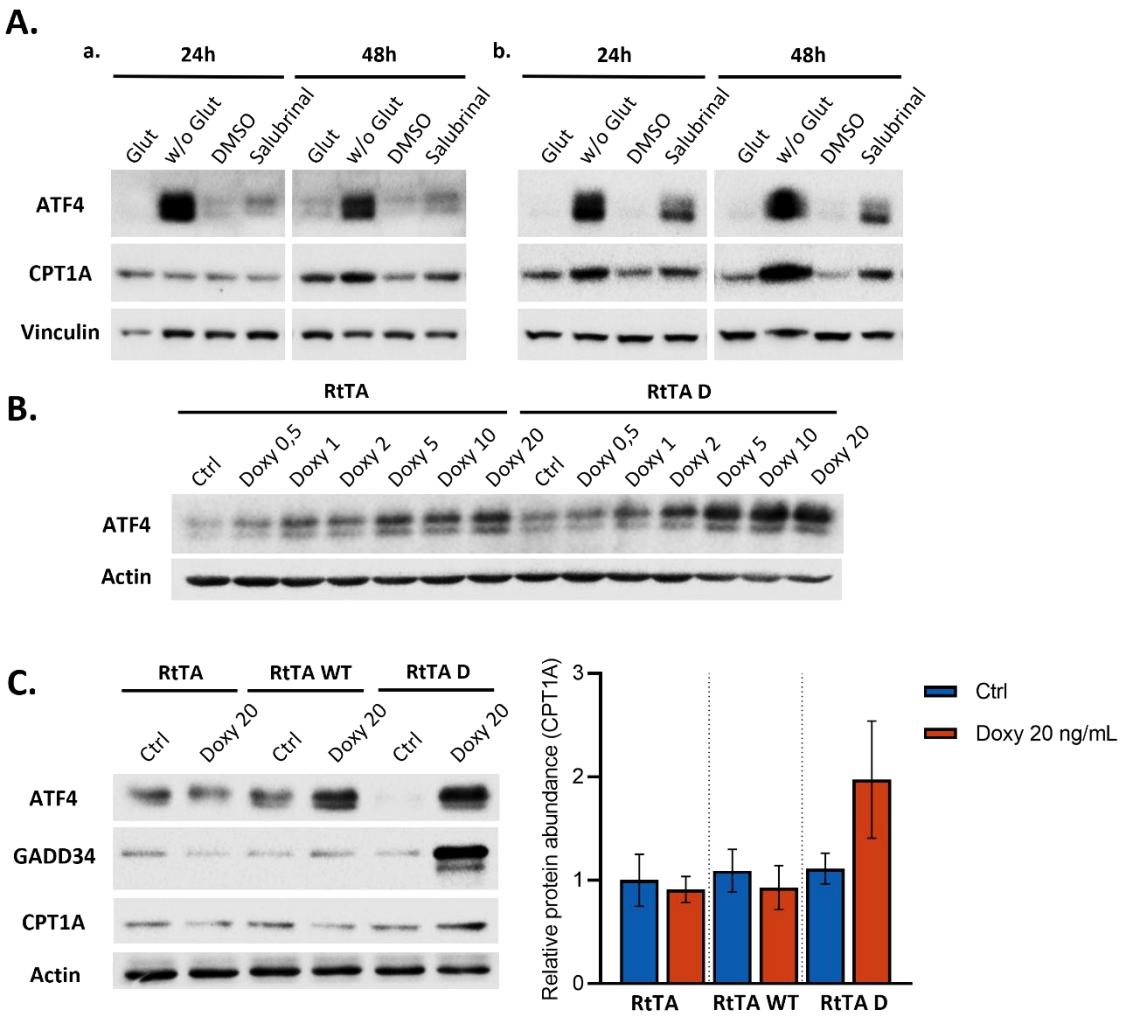

Figure 16. ISR determines an increase of CPT1A protein levels in TNBC cells. ***A.*** *Representative immunoblot* ***showing protein abundance*** *of ATF4 and Carnitine Palmytoil Transferase 1A (CPT1A) after 24h and 48h of glutamine starvation (w/o Glut) vs complete medium (Glut), and treatment with Salubrinal vs vehicle (DMSO) in MBA-MB 231 (a.) and BT549 (b.) cells, n=3 biological replicates.* ***B.-C.*** *Representative immunoblot of genetically engineered MDA-MB-231 (Dmut) cells showing:* ***B.*** *ATF4 protein abundance upon induction of phosphomimetic eIF2α mutant with increasing dose of Doxycycline (0,5-1-2-5-10-20 ng/mL);* ***C.*** *ATF4, GADD34 and CPT1A protein abundance in genetically engineered MDA-MB-231 (Dmut) cells upon induction of phosphomimetic eIF2α mutant with 20 ng/mL Doxycycline; n=3 biological replicates. RtTA: empty plasmid, RtTA WT: eIF2α wt, RtTA D: eIF2α D (phosphomimetic). Statistical analyses: means +/- SEM. (Student's t-test), not significant.*

We next addressed the question of a potential ATF4-dependent CPT1A upregulation. Indeed, ATF4 knock-down reduced CPT1A protein accumulation upon Salubrinal-induced ISR activation, indicating that ATF4 is required for this regulation (**Figure 17A**). However, despite the established role of ATF4 as transcription factor, qPCR analysis did not show significant changes in CPT1A mRNA levels at either 24 or 48 hours (**Figure 17B**). Together, these observations indicate that CPT1A is regulated downstream of ISR in an ATF4-dependent but transcriptionally independent manner, consistent with a possible post-transcriptional control.

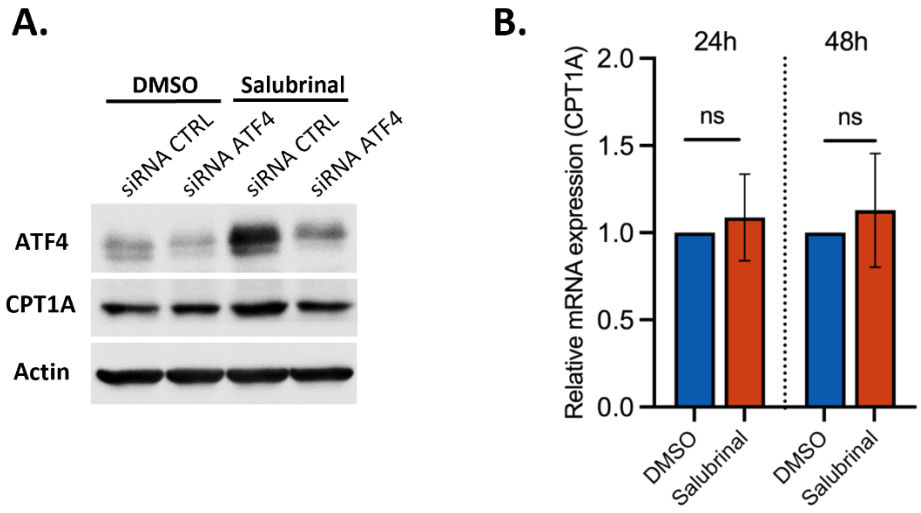

Figure 17. ISR-driven CPT1A increase is not dependent on ATF4 transcriptional regulation. A. *Representative immunoblot of ATF4 and CPT1A in MDA-MB-231 transfected with siRNA Silencer Control (siCTRL) or siRNA ATF4 (siATF4) and treated for 48h with Salubrinal or vehicle (DMSO).* ***B.*** *Relative mRNA expression of CPT1A from qPCR analysis after 24h and 48h of treatment with Salubrinal or vehicle (DMSO), n=3 biological replicates. Statistical analyses: means +/- SEM. (Student's t-test), ns: not significant.*

Overall, the previously demonstrated identification of CPT1A as a novel ISR target may provide a mechanistic link between stress signaling and mitochondrial metabolic adaptation in breast cancer. Indeed, in this context, CPT1A increased expression suggests that ISR may redirect mitochondrial outputs toward a distinct bioenergetic status characterised by fatty acids consumption. This interpretation could offer a potential explanation for the coexistence of altered mitochondria architecture and calcium signalling with a stress-coping mechanism and enhanced metastatic behaviour.

A future step forward would be to determine whether the increase in CPT1A is functionally relevant to the ISR-induced migratory phenotype. For example, genetic or

pharmacologic CPT1A inhibition could be tested to assess its potential impairment of the migratory advantage provided by ISR activation. At the same time, it would be crucial to dissect the mechanisms leading to increased CPT1A protein levels, ad underpin the role of ATF4 or ATF4-dependent effectors in regulating protein translation, stability, or degradation. Collectively, these results evidence CPT1A as a novel potential effector if ISR-driven metabolic rewiring and support the hypothesis that FAO may contribute to the adaptive mitochondrial phenotype in stressed TNBC cells.

The clinical relevance of CPT1A upregulation in breast cancer is supported by survival data from the publicly available TCGA-BRCA patients' dataset. Kaplan-Meier analysis revealed that elevated CPT1A expression is associated with significantly reduced overall survival in breast cancer patients (**Figure 18**), consistent with the notion that increased reliance on fatty acid oxidation confers a survival and proliferative advantage to tumour cells operating under metabolic stress. Taken together, the ISR-dependent upregulation of CPT1A observed in TNBC cells, combined with its negative prognostic value in breast cancer patients, supports the hypothesis that ISR activation promotes a metabolic shift toward fatty acid oxidation as a bioenergetic and adaptive strategy that may ultimately contribute to disease aggressiveness and poor clinical outcome.

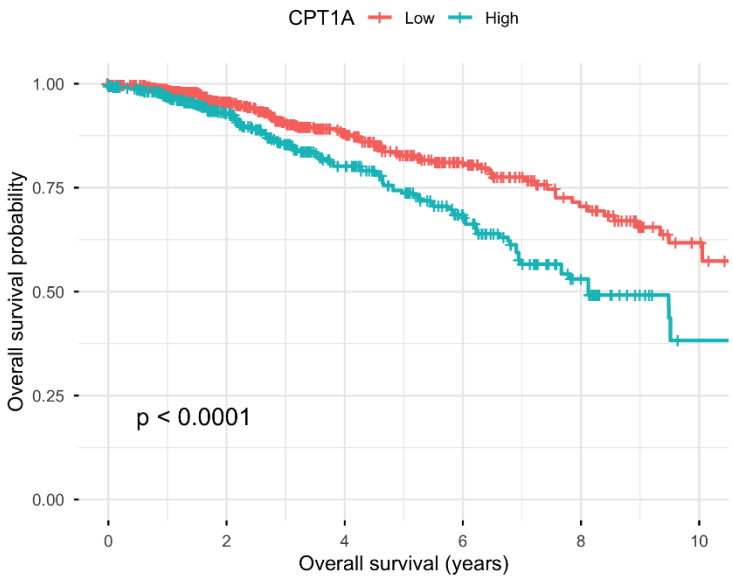

Figure 18. CPT1A overexpression is predictive of poor prognosis in BC patients. *Kaplan-Meier Survival Analysis of BC patients from TCGA-BRCA dataset, divided by low and high CPT1A gene expression.*

3. ISR Promotes TNBC Cell Aggressiveness Through Lipid Metabolism Modulation

3.1 ISR Promotes Invasiveness Through Lipid Landscape Remodelling

3.1.1 ISR remodels fatty acid composition and unsaturation

The results presented in Chapter 2 indicate that ISR activation promotes an adaptive mitochondrial rewiring affecting organelle architecture, calcium homeostasis and metabolic reprogramming. This evidence suggests that ISR activation does not merely impair mitochondrial function but may redirect it towards a distinct and functional metabolic state. Furthermore, the impaired respiration and the increase in CPT1A protein levels concomitant with the decrease in the total amount of long chain fatty acids provides a rationale to explore whether lipid metabolism is engaged as part of the ISR-driven adaptive response in TNBC cells. To address this question, we performed a comprehensive mass-spectrometry-based untargeted lipidomic analysis on lipid extracts obtained from MDA-MB-231 cells treated with either vehicle (DMSO) or Salubrinal for 48 hours.

In line with current lipidomic workflows, lipid extracts were generated by organic solvent extraction and analysed by chromatographic separation coupled to high-resolution mass spectrometry, to obtain a robust profiling of fatty acid composition and lipid saturation features (Merciai et al. 2024). The analysis revealed a clear alteration in the fatty acid saturation profile upon ISR activation. In particular, Salubrinal treatment caused a significant increase in the ratio between saturated fatty acids (SFAs) and monounsaturated fatty acids (MUFAs), indicating a global shift towards a more saturated lipid state (**Figure 19A**). When the different lipid saturation classes were analysed separately, the overall abundance of SFAs remained largely unchanged, while both MUFAs and PUFAs levels were significantly reduced, suggesting that ISR activation does not simply alters the balance between SFAs and MUFAs, but more broadly reshapes the overall FAs composition of TNBC cells (**Figure 19B**).

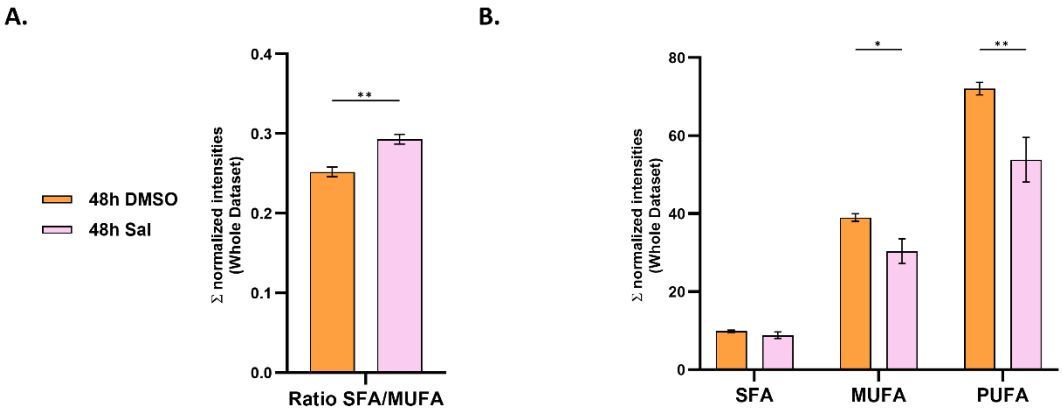

Figure 19. ISR alters Fatty Acids saturation degree of TNBC cells. A.-B. *Univariate **l**ipidomic analysis showing: **A.** ratio and **B.** intensities of fatty acids saturation after 48h of Salubrinal or vehicle (DMSO) treatment; n=3 biological replicates. SFA: Saturated Fatty Acids, MUFA: Monounsaturated Fatty Acids, PUFA: Polyunsaturated Fatty Acids**.** Statistical analyses (C.): means +/- SD. *P < 0.05, **P < 0.01 (Mann-Whitney test).*

Since MUFAs and PUFAs are major determinants of membrane fluidity (Maulucci et al. 2016; Baccouch et al. 2023), their reduction is fully consistent with the structural phenotype described in the previous chapter, where ISR activation induced mitochondria fragmentation and cristae disruption. PUFAs reduction may plausibly result from two concomitant mechanisms: on the one hand, the decrease in MUFAs may create a bottleneck for the downstream desaturation steps required for PUFAs synthesis; on the other hand, a CPT1A-driven increase in FAO may further reduce the net availability of PUFAs by diverging fatty acids towards mitochondrial utilization. In either case, the reduction of PUFAs is of particular interest from a functional point of view: PUFAs are involved in signalling, oxidative vulnerability, and adaptive stress response (Catalá 2009; Gruber et al. 2015), suggesting that their depletion may have broad consequences for organelle homeostasis and stress adaptation.

In this framework, the depletion of unsaturated fatty acids may suggest an ISR-driven wide functional rewiring of lipids metabolism.

3.1.2 ISR-driven downregulation of SCD1 provides a rationale for MUFA depletion

The striking reduction in MUFAs observed upon ISR activation led us to investigate the mechanisms that possibly underlie this shift in FAs composition. The balance between SFAs and MUFAs is primarily regulated by the first and rate-limiting step of fatty acid desaturation, catalysed by Stearoyl-CoA Desaturase 1 (SCD1) (ALJohani et al. 2017; Ying Zou et al. 2020). By converting SFAs into their MUFAs counterpart, SCD1 plays a central role in maintaining lipids desaturation and membrane lipid homeostasis (Q. Sun et al. 2024). On these premises, we next investigated whether SCD1 expression might be modulated by ISR signalling.

To explore this possibility in a clinically relevant setting, we analysed the TCGA breast cancer transcriptomic dataset, stratifying patients' samples according to breast cancer subtype. This analysis showed that SCD mRNA expression was significantly lower in TNBC samples compared with the other breast cancer subtypes (**Figure 20A**). Notably, this reduction was accompanied by increased expression of canonical ISR-associated genes, including ATF4, its transcriptional target ASNS, and transcripts belonging to ISR-related signatures associated with metabolic and chemical stress (**Figure 20B**). Although correlative, these findings suggest that in patients TNBC may be characterised by ISR activation associated with reduced SCD1 expression, raising the possibility that stress signalling contributes to the reduction of MUFAs biosynthesis and a reshaping of the lipid landscape.

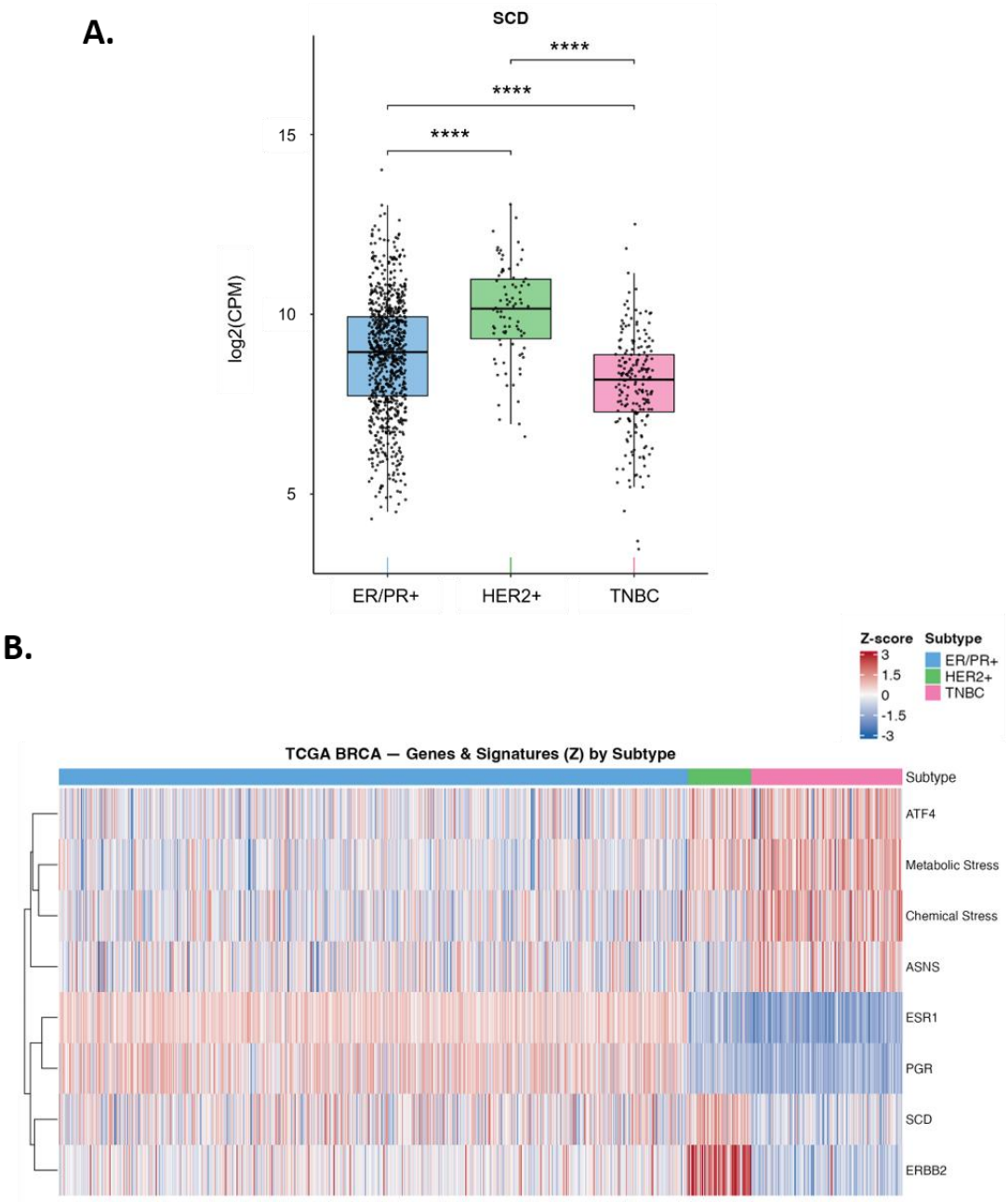

Figure 20. SCD expression is significantly lower in TNBC samples compared with the other breast cancer subtypes. ***A.*** *Box plot representing SCD gene expression and* ***B.*** *heatmap representing hierarchical clustering of SCD and ISR-related genes and signatures expression, in patients' samples from TCGA-BRCA dataset grouped by BC subtypes.*

To test the hypothesis of a causal relationship between ISR activation and the reduction of SCD1 levels, we next performed *in vitro* experiments in two TNBC cell lines, MDA-MB-231 and BT549. Western blot analyses showed that pharmacological or metabolic activation of ISR led to a consistent reduction of SCD1 protein levels in both models. In detail, treatment with Salubrinal (pharmacological activation) and glutamine depletion (metabolic stressor) led to a progressive decrease in SCD1 protein levels accompanied by

the expected increase of ISR markers: phosphorylated eIF2α and ATF4, at both 24 and 48 hours (**Figure 21A**). These results demonstrate that SCD1 downregulation is a reproducible event downstream ISR activation across distinct TNBC cell models and under different stress-inducing conditions.

The dependence of this mechanism on ISR signalling was further demonstrated using two complementary genetic approaches. First, we silenced GADD34, the stress-inducible phosphatase specific subunit responsible for the eIF2α dephosphorylation and ISR resolution. As expected, its depletion, which leads to accumulation of the eIF2α phosphorylated form and sustains ISR signalling, resulted in a reproducible decrease in SCD1 protein levels 72 hours after silencing (**Figure 21B**). Second, we employed the previously described (**Chapter 2.3.3, Figure 16**) genetically engineered MDA-MB-231 model (eIF2α Dmut). Induction of eIF2α Dmut for 48 hours caused a marked reduction in SCD1 protein levels (**Figure 21C**), which progressively decreased in a doxycycline dose dependent manner (**Figure 21D**). Together, these complementary models demonstrate that sustained ISR activation is sufficient to downregulate SCD1 expression.

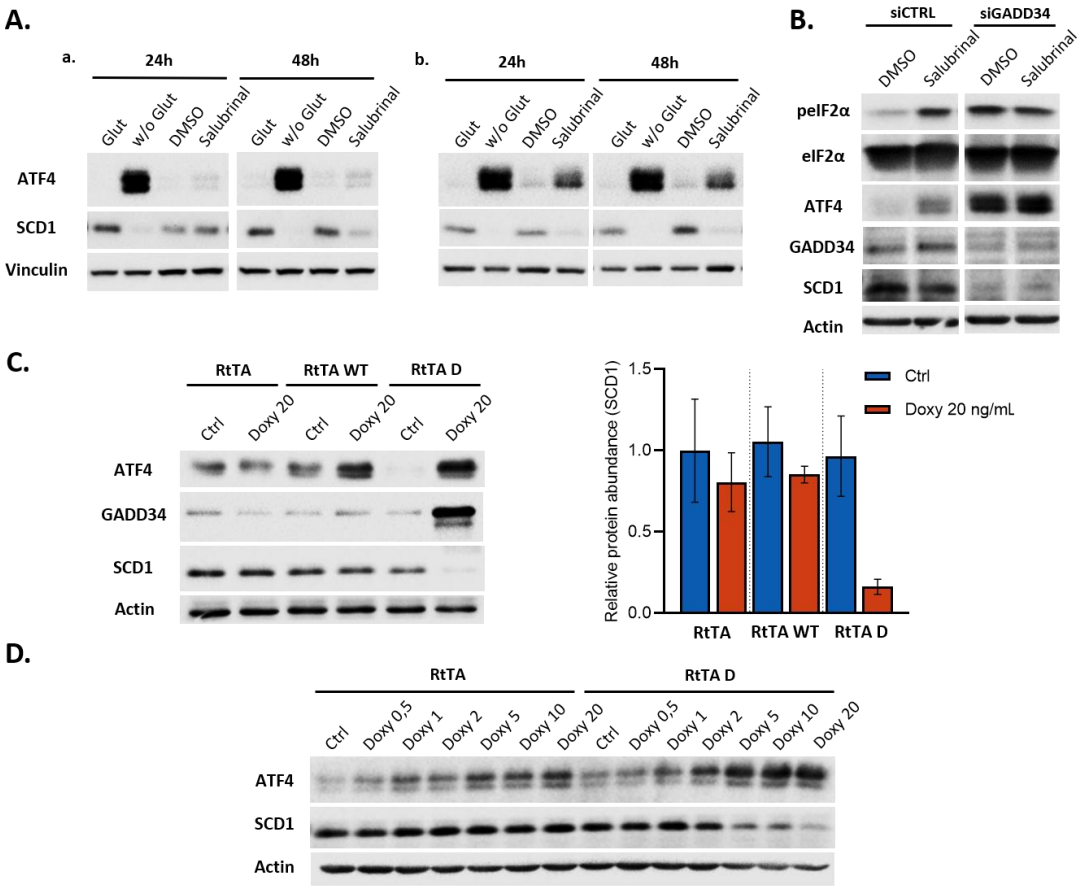

Figure 21. ISR drives SCD1 downregulation in TNBC cells. A.-B. *Representative immunoblot showing:* ***A.*** *ATF4 and Steaoryl-CoA Desaturase 1 (SCD1) after 24h and 48h of glutamine starvation (w/o Glut) vs complete medium (Glut), or treatment with Salubrinal vs vehicle (DMSO) in MBA-MB 231 (a.) and BT549 (b.) cells, n=3 biological replicates;* ***B.*** *peIF2α, eIF2α, ATF4, GADD34 and SCD1 in MDA-MB-231 transfected with Stealth™ RNAi siRNA Negative Control (siCTRL) or siRNA SCD (siSCD) and treated for 48h with Salubrinal or vehicle (DMSO), n=3 biological replicates.* ***C.-D.*** *Representative immunoblot of genetically engineered MDA-MB-231 (Dmut) cells showing:* ***C.*** *ATF4, GADD34 and SCD1 protein abundance upon induction of phosphomimetic eIF2α mutant with 20 ng/mL Doxycycline, n=3 biological replicates;* ***D.*** *ATF4 and SCD1 protein abundance upon induction of phosphomimetic eIF2α mutant with increasing dose of Doxycycline (0,5-1-2-5-10-20 ng/mL). RtTA: empty plasmid, RtTA WT: eIF2α wt, RtTA D: eIF2α D (phosphomimetic). Statistical analyses: means +/- SEM. (Student's t-test), not significant.*

Overall, these findings may provide a mechanistic explanation for the lipid landscape depicted above. ISR-driven downregulation of SCD1 emerges as a plausible molecular determinant of the reduced MUFAs content and altered lipid saturation profiles observed in stressed TNBC cells. More broadly, ISR activation may coordinately reprogram both the saturation state and the metabolic fate of fatty acids.

3.1.3 Reciprocal regulation between ISR signalling and SCD1

To better elucidate the functional relationship between ISR signalling and SCD1, we asked whether loss of SCD1 activity could feed back on ISR activation. For this purpose, since we observed an ISR-dependent SCD1 decrease, we hypothesize that its desaturase activity decreases in parallel to the protein amount. Therefore, we treated TNBC cell lines with a pharmacological SCD1 inhibitor (A939572). Western blot analysis carried out at 24, 48, and 72 hours after treatment revealed a clear time-dependent increase in the key ISR markers ATF4 and phosphorylated eIF2α (peIF2α), relative to vehicle-treated cells (**Figure 22A**).

To more closely reproduce the ISR-dependent decrease in SCD1 expression, we next used a genetic approach by silencing SCD1 in MDA-MB-231 TNBC cells. The downstream effects of SCD1 knockdown were evaluated by Western blot analysis 72 hours after silencing. Under these conditions, we observed a reproducible increase in ATF4 and peIF2α levels, compared to control cells (**Figure 22B**). Thus, both pharmacological inhibition and genetic depletion of SCD1 were sufficient to activate ISR, supporting the notion that SCD1 downregulation is not solely a downstream consequence of stress signalling, but is sufficient to act as a trigger of ISR activation in TNBC cells.

Considering that an imbalance between SFAs and MUFAs is known to promote ER stress (Volmer et al. 2013), thereby triggering the ISR, we then asked whether the ISR induced by SCD1 inhibition is functionally linked to the loss of MUFAs. Based on this rationale, TNBC cells were supplemented with exogenous oleic acid (OA), the major MUFA generated downstream of SCD1 enzymatic activity. Specifically, cells were treated with OA in combination with SCD1 inhibitor for 24 and 48 hours. In both MDA-MB-231 and BT549 cells, western blot analyses showed that the increase in ATF4 protein expression induced by SCD1 inhibitor was completely reversed upon OA supplementation after 48 hours of combined treatment, but not when OA was supplemented to Salubrinal treated cells (**Figure 22C**). A possible explanation for these observations is that SCD1 inhibition and OA act upstream of eIF2α phosphorylation. By restoring the balance between saturated and monounsaturated fatty acids altered upon SCD1 reduction, OA may prevent activation of stress-sensing kinases that phosphorylate eIF2α. Consistently, this effect was not observed when eIF2α phosphorylation was

stabilized by the specific pharmacological treatment with Salubrinal, which acts directly on eIF2α bypassing the kinases.

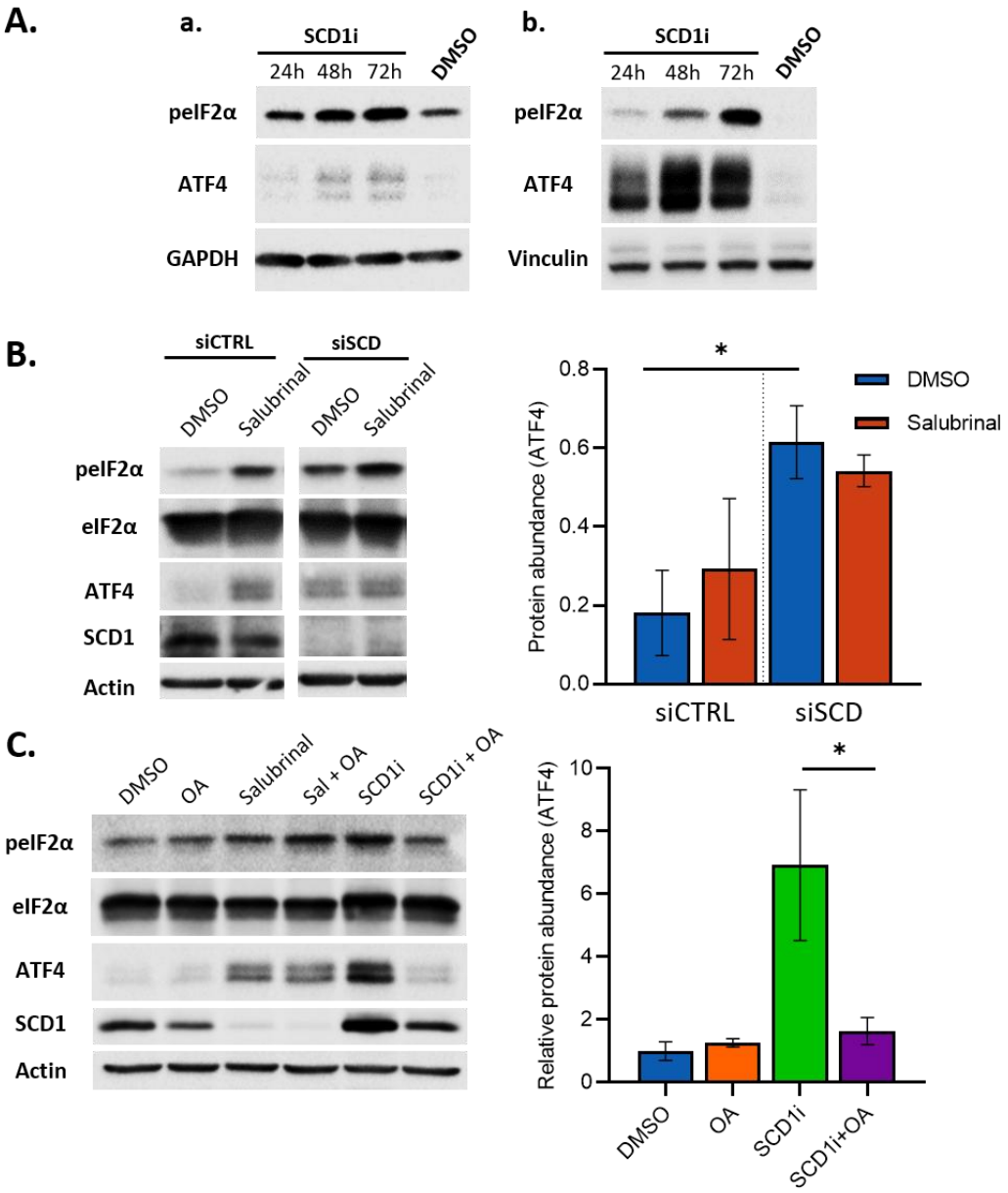

Figure 22. SCD1 modulation downstream effects regulate ISR through a feedback loop. A.-B. *Representative immunoblot showing:* ***A.*** *peIF2α and ATF4 in MDA-MB-231 (a.) and BT549 (b.) cells upon SCD1 inhibition with A939572 (SCD1i) for 24, 48, and 72h or vehicle (DMSO) for 72h, n=3 biological replicates;* ***B.*** *peIF2α, eIF2α, ATF4 and SCD1 in MDA-MB-231 cells transfected with Stealth™ RNAi siRNA Negative Control (siCTRL) or siRNA SCD (siSCD) and treated for 48h with Salubrinal or vehicle (DMSO), n=3 biological replicates;* ***C.*** *peIF2α, eIF2α, ATF4 and SCD1 in BT549 cells upon treatment with vehicle (DMSO), OA, Salubrinal and SCD1i alone or in combination with OA (Sal+OA, SCD1i+OA) for 48h, n=3 biological replicates. Statistical analyses: means +/- SEM. *P < 0.05, (Student's t-test).*

Altogether, these results indicate that restoration of MUFAs availability is sufficient to suppress ISR activation even when the extent of the response is sharp and sustained. These observations reveal that the remodelling of the lipid saturation profile induced by SCD1 downregulation is not only a net result of ISR activation but represents a functionally relevant mechanism that contributes to the maintenance of the stress status and signalling. We can therefore propose a model by which ISR-driven SCD1 downregulation reduces MUFAs availability creating a lipid unbalance that feeds back to sustain ISR activation. Indeed, these results identify SCD1 as a central hub at the interface between lipid metabolism and stress signalling.

3.1.4 ISR-driven SCD1 downregulation enhances the invasive potential of TNBC cells

After obtaining the evidence that ISR activation curbs SCD1 expression, and that loss of either SCD1 expression or activity is sufficient to activate and sustain the ISR, we next investigated whether this lipid desaturation remodelling could functionally contribute to the ISR-induced aggressive phenotype. To address this question, we assessed MDA-MB-231 invasive potential through the employment of a standardized microfluidic chip-based invasion assay (Identx3). MDA-MB-231 cells were cultured adjacent to a 3D collagen type I matrix under a controlled serum gradient, enabling highly reproducible, real-time, single-cell resolution tracking of directional invasion within a physiologically relevant extracellular matrix context (**Figure 23A**). TNBC cells were treated either with the SCD1 inhibitor (A939572), to mimic the downregulation of SCD1 observed upon ISR activation, or with Salubrinal, to pharmacologically activate ISR and provide a positive control for the SCD1i invasive potential. Analyses were performed on high-resolution z-stack confocal microscopy images taken after 48 hours of treatment. Quantitative analysis revealed a significant increase in invasive behaviour under both experimental conditions compared to control cells. In particular, both ISR activation and SCD1 inhibition increased the number of cells entering the collagen matrix and enhanced the distance travelled within the matrix. Interestingly, SCD1 inhibition produced a more pronounced effect compared to Salubrinal (**Figure 23B, C**), in line with the remarkable activation of ISR observed via WB (**Figure 22C**). These results indicate that reduction of SCD1 activity is sufficient to enhance the invasive potential of TNBC cells, and suggests that

SCD1 may represent a crucial downstream effector of the pro-invasive program triggered by ISR.

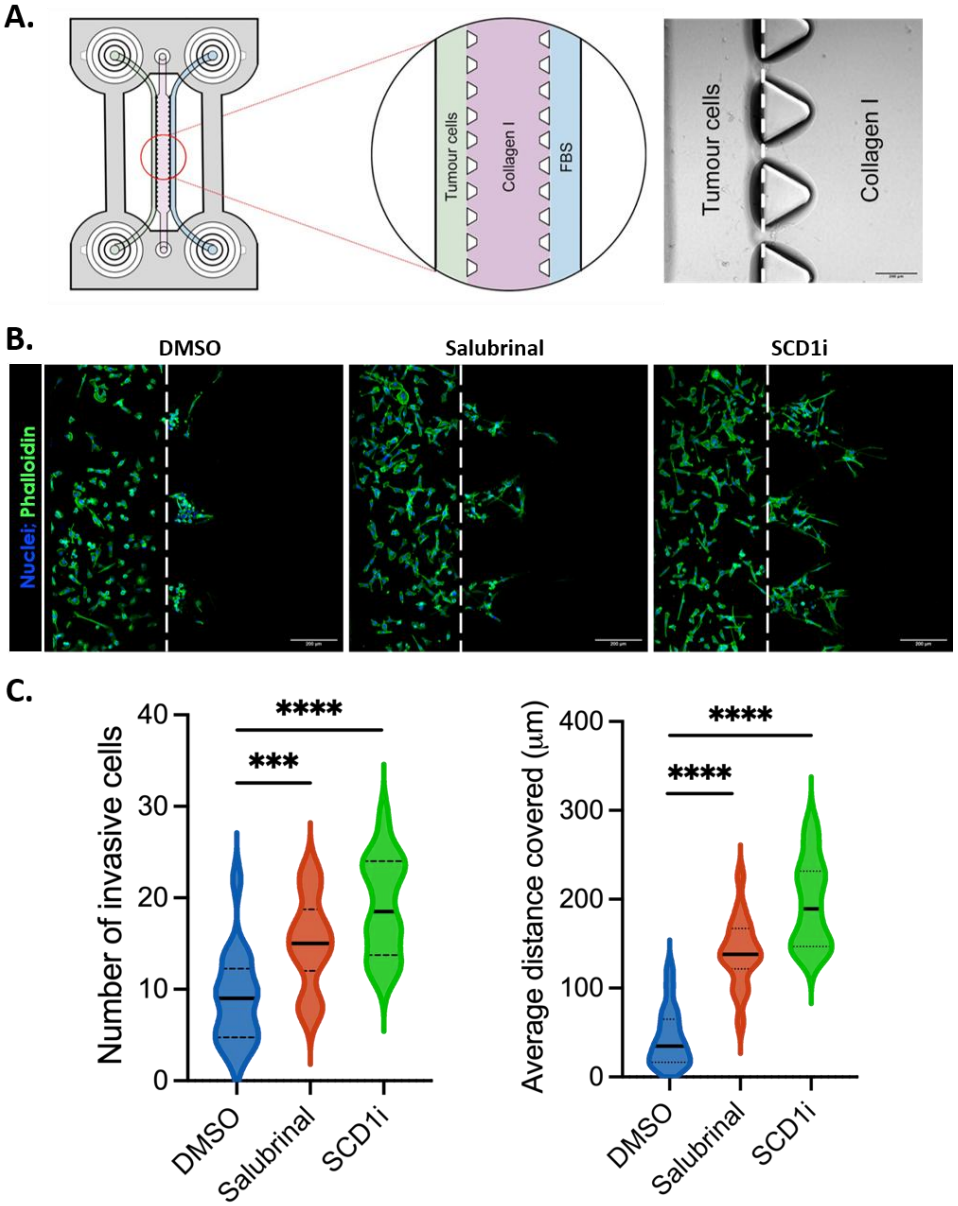

Figure 23. SCD1 inhibition enhances the invasive potential of TNBC cells. A. *Schematic of the invasion assay in the IdenTx 3 microfluidic device: MDA-MB-231 cells were seeded in the left chamber (green) and induced to migrate toward 20% FBS-containing medium in the right chamber (light blue) across a central collagen I channel (3 mg/ml; pink). Representative brightfield image showing the collagen I channel edge (white dashed line).* ***B.*** *Representative maximum intensity projection of Z-stacked confocal images of MDA-MB-231 cells invading the central channel, upon 48h treatment with Salubrinal, SCD1 inhibitor (SCD1i) or vehicle (DMSO). Green=F-actin, Blue=nuclei.* ***C.*** *Quantification of the number of invading cells and the average distance covered (µm). n=1 biological replicate, 6 technical replicates. Statistical analyses (C.): means +/- SD. ***P < 0.001, ****P < 0.0001 (Mann-Whitney test).*

Altogether, our results identify SCD1 downregulation as a functionally relevant component of the ISR-driven metabolic reprogramming.

3.2 ISR Promotes TNBC Cells Survival by modulating the susceptibility to ferroptotic cell death

The metastatic cascade requires tumour cells to simultaneously acquire and maintain two complementary capabilities: the capacity to invade surrounding tissues and disseminate to distant sites, and the ability to survive the hostile conditions encountered during this process. On the one hand the data presented above suggest that ISR activation in TNBC cells supports the invasive and migratory capability; on the other hand, the marked reduction in long-chain PUFAs, observed in the lipidomic profile of Salubrinal treated MDA-MB-231 cells (**Figure 15C**), raises a parallel and equally relevant question regarding survival. Given the well-established role of PUFAs as the primary substrates for lipid peroxidation (Doll et al. 2017; Kagan et al. 2017), their depletion from the cellular lipid landscape may reflect not only a shift in metabolic fuel utilization but also a remodelling of membrane composition with direct consequences for ferroptotic susceptibility. Ferroptosis is a form of programmed cell death driven by iron accumulation and iron-dependent lipid peroxidation (Dixon et al. 2012). This process has recently been shown to play a dual role in cancer, acting either as a tumour-suppressive mechanism or, conversely, as a selective pressure that promotes the survival of resistant, more aggressive populations of cells (Q. Zhou et al. 2024; K. Hu et al. 2020; G. Lei et al. 2021; Wahida and Conrad 2023; Jaewang Lee and Roh 2023). In this context, the ISR-driven reduction in PUFAs availability prompted us to investigate whether ISR activation confers protection from ferroptosis as a complementary survival mechanism that, alongside the pro-invasive metabolic rewiring described above, may collectively sustain the aggressive phenotype of TNBC cells.

3.2.1 ISR correlates with the principal actors of ferroptosis

We firstly investigated the relationship between ISR signalling and ferroptosis in BC. We measured the association between ISR-related signatures and ferroptosis driver or ferroptosis suppressor genes signatures, in patients' samples from TCGA-BRCA dataset.

Correlation analyses revealed a strong and defined relationships between ISR-related signatures and ferroptosis programs. Interestingly, ISR programs displayed a significant

correlation with both ferroptosis drivers and suppressor genes, suggesting the presence of a complex and dynamic intertwining of the ISR with the ferroptotic mechanisms. In particular, the metabolic stress signature, derived from the analysis of a broad ISR-inducing metabolic challenge such as glutamine starvation, showed a stronger positive association with ferroptosis driver genes compared to the ferroptosis suppressor genes, suggesting engagement of a broad ferroptosis-related stress-adaptive state rather than terminal ferroptotic cell death. In contrast, the chemical stress signature, derived from the more specific and direct ISR-activation using Salubrinal, correlated more strongly with ferroptosis suppressors, providing a negative net ferroptosis score, consistent with a ferroptosis-protective adaptive program (**Figure 24**).

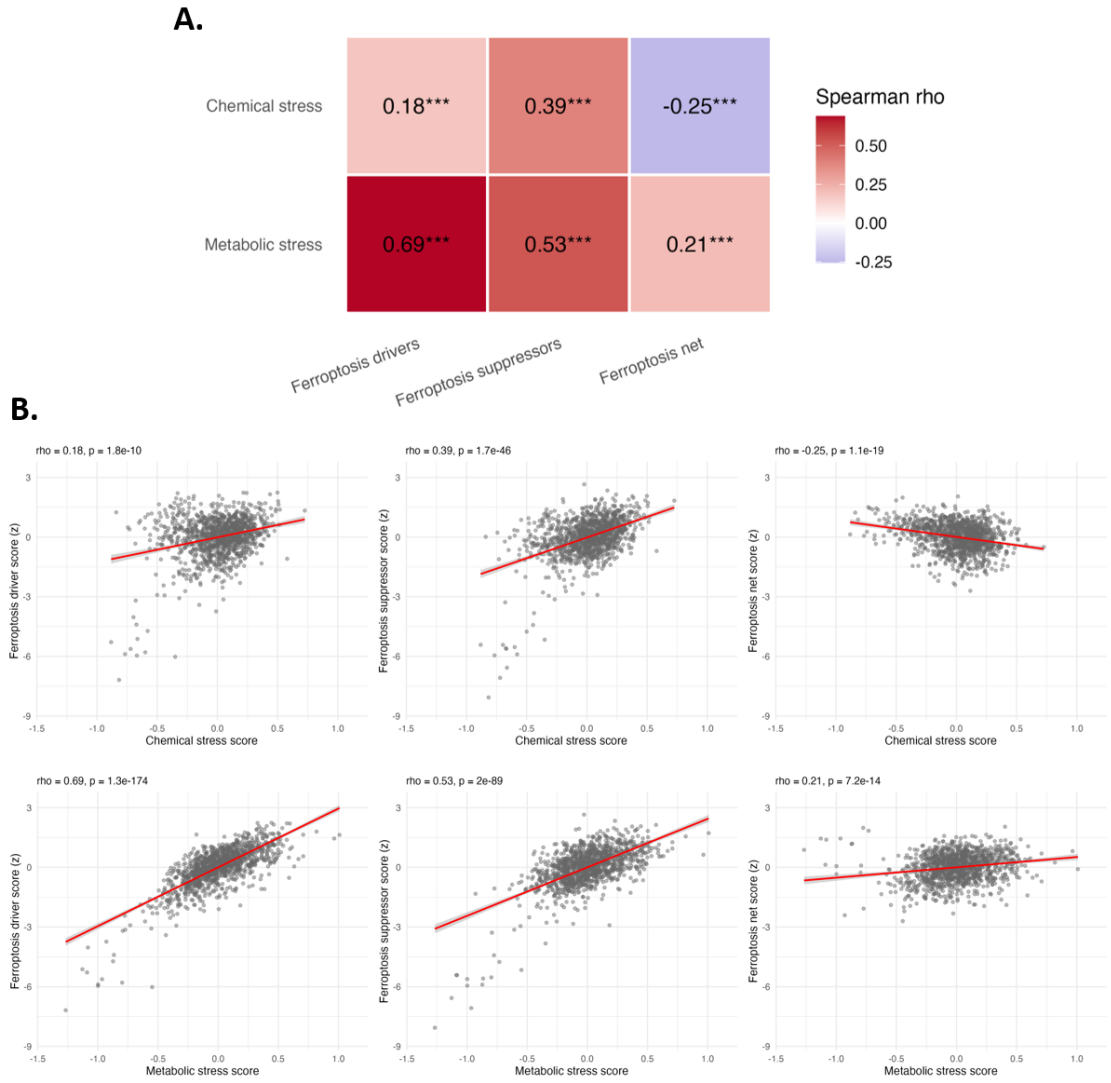

Figure 24. ISR program correlates with ferroptosis in BC patients. A.-B. *Correlation between ISR Stress signatures and ferroptosis pregrams. Heatmap (**A.**) and dot plot (**B.**) of Spearman correlation analyses between Chemical or Metabolic Stress Signature and ferroptosis drivers, suppressors or net genes signatures from FerrDB_v2 database, performed on patients' samples from TCGA-BRCA dataset.*

Having established this possible association between ISR activation and protection from ferroptosis, we next investigated the clinical relevance of ferroptosis-related pathways in breast cancer and determined their relationship with ISR signalling in TNBC by analysing the patient-derived gene expression data from the TCGA-BRCA dataset.

The analysis included genes implicated in distinct regulatory nodes of ferroptosis, including cystine import and glutathione metabolism (SLC7A11, SLC3A2), lipid remodelling and peroxidation (ACSL4, LPCAT3, PTGS2), antioxidant defence systems (GPX4, AIFM2/FSP1, FTH1), stress-responsive transcriptional regulation (NFE2L2),

and ferroptosis execution markers (CHAC1). Although multiple ferroptosis markers were initially analysed, only a subset displayed consistent subtype-specific regulation together with significant associations with ATF4 expression and clinical outcome; therefore, subsequent analyses focus on these key determinants.

Among the anti-ferroptosis factors, SLC7A11 and SLC3A2, which together form the system Xc^- cystine/glutamate antiporter (Fulvio Ursini and Maiorino 2020; Y. Zhang et al. 2021), emerged as relevantly modulated. Increased expression of these genes was associated with reduced overall survival in breast cancer patients (**Figure 25**), reaching statistical significance for SLC3A2, while SLC7A11 showed the same trend without achieving statistical significance.

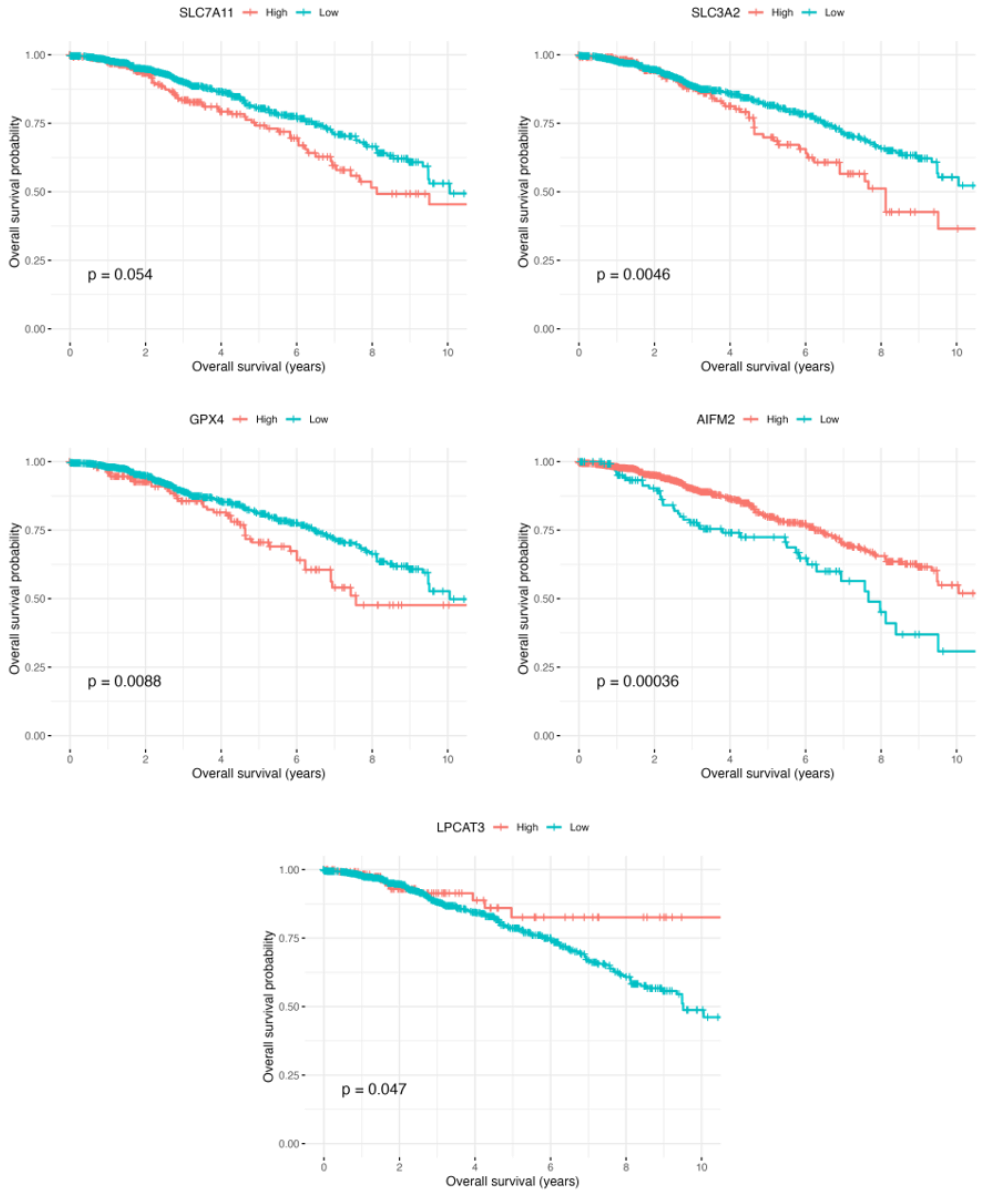

Figure 25. Expression of key ferroptosis effectors predicts clinical outcome in breast cancer patients. *Kaplan-Meier Survival Analysis of BC patients from TCGA-BRCA dataset, divided by low and high gene expression of the reported gene.*

When breast cancer patient's samples were clustered according to molecular subtypes, both SLC7A11 and SLC3A2 were significantly upregulated in TNBC relative to other breast cancer subtypes (**Figure 26**), indicating an enrichment of ferroptosis-protective redox programs in this aggressive subtype.

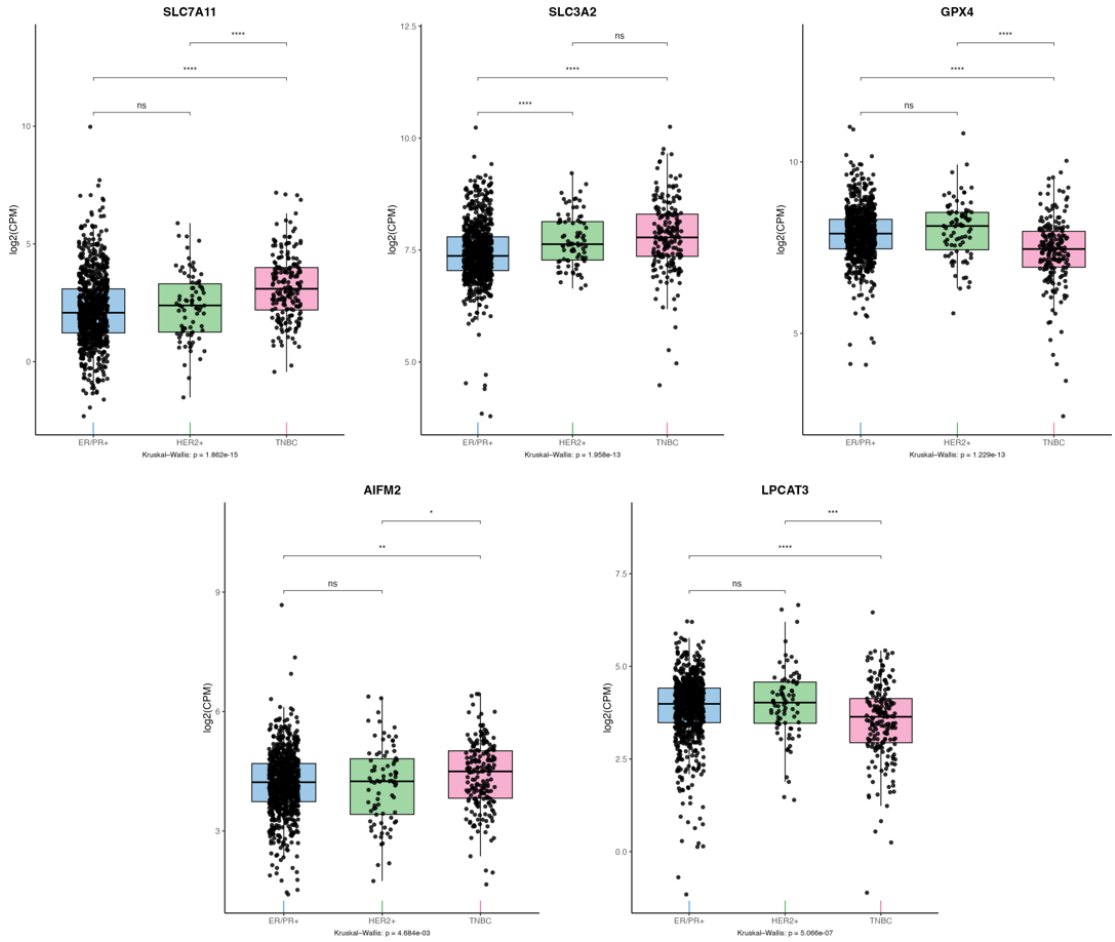

Figure 26. Ferroptosis effectors display subtype-specific expression profiles in human breast tumors. *Box plot representing gene expression of the reported gene in patients' samples from TCGA breast cancer dataset grouped in BC subtypes. Statistical analysis: Kruskal-Wallis test. SLC7A11 p=1.862e-15, SLC3A2 p=1.958e-13, GPX4 p=1.229e-13, AIFM2 p=4.684E-03, LPCAT3 p=5.066e-07.*

Moreover, to explore their relationship with ISR signalling, we ranked TCGA patient samples by ATF4 expression level and plotted the moving average of each indicated gene across the ranked patients, to assess their co-variation across the patient cohort. This analysis revealed a positive correlation between ATF4 expression and both system Xc^- components, with a moderate correlation for SLC7A11 (r = 0.423) and a very strong correlation for SLC3A2 (r = 0.875) (**Figure 27**). These data suggest a particularly tight association between ISR engagement and SLC3A2 expression across breast cancer samples.

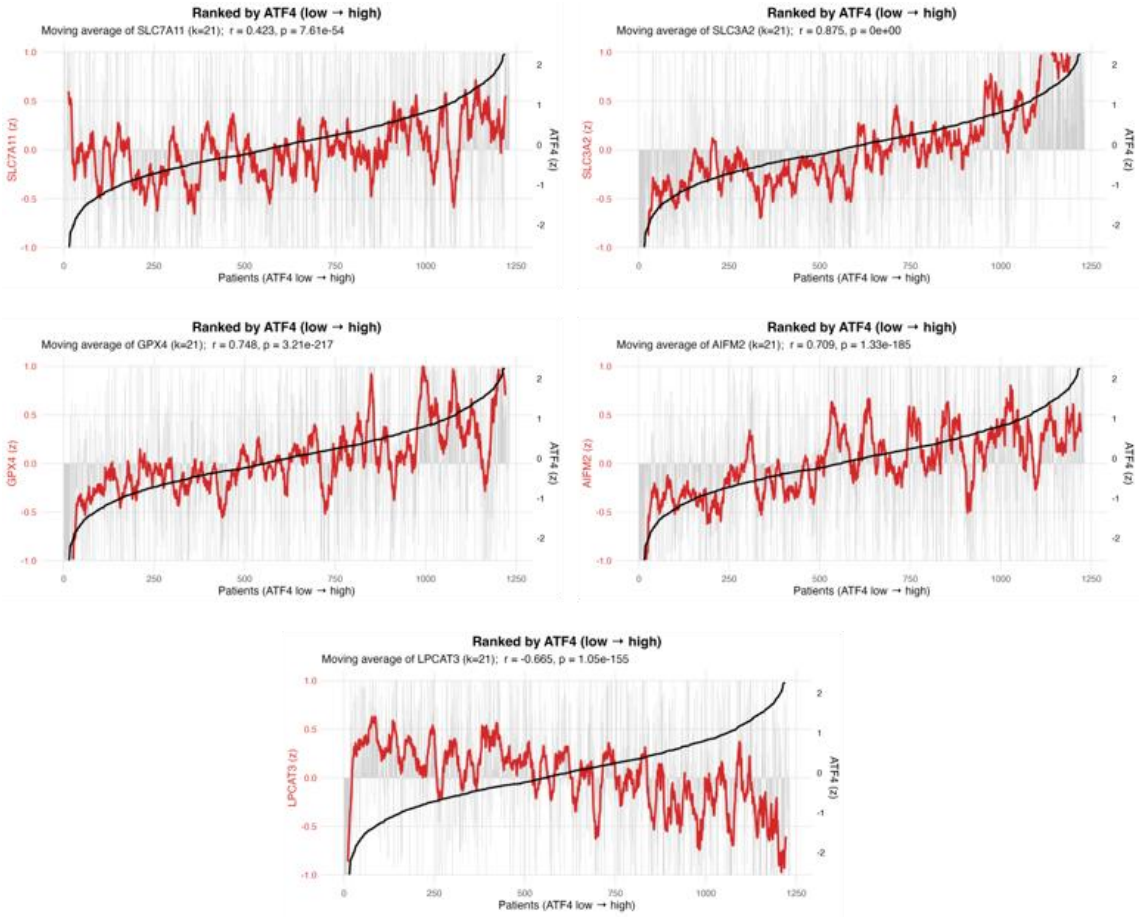

Figure 27. ISR correlates with the key effectors of ferroptotic cell death. *Co-variation of the reported gene and ATF4 gene expression in TCGA-BRCA dataset. The plot shows the moving average of the selected gene expression (red line) across TCGA-BRCA patients' samples ranked by ATF4 average gene expression, from low to high (black line). Vertical gray lines indicate expression of the ATF4 in each sample.*

In addition to system Xc^- components, other key negative regulators of ferroptosis were revealed by our analyses: GPX4, which suppresses ferroptosis by detoxifying lipid peroxides (Fulvio Ursini et al. 1985; F. Ursini et al. 1982), was positively correlated with ATF4 expression (r = 0.748) and associated with reduced overall survival, although its expression was lower in TNBC than in other breast cancer subtypes (**Figure 25, 26, 27**). Contrarily, AIFM2 (also known as FSP1) which inhibits ferroptosis by suppressing lipid peroxidation through a GPX4-independent and complementary antioxidant mechanisms (Bersuker et al. 2019; Doll et al. 2019), was both positively correlated with ATF4 (r = 0.709) and upregulated in TNBC samples, while being associated with improved overall survival. These findings point to a broad engagement of ferroptosis-protective pathways (**Figure 25, 26, 27**).

Among pro-ferroptotic factors, LPCAT3, an enzyme involved in phospholipid remodelling (Kang et al. 1997; Hishikawa et al. 2008), displayed a strong negative correlation with ATF4 ($r = -0.665$). Moreover, LPCAT3 was downregulated in TNBC relative to other breast cancer subtypes, and its lower expression was associated with reduced patient survival (**Figure 25, 26, 27**).

These results suggest a complex and context-dependent downregulation of ferroptosis sensitivity in TNBC. Multiple ferroptosis-inhibitory pathways are differentially engaged in breast cancer and TNBC, suggesting that TNBC cells may rely on a selective subset of ferroptosis-protective pathways to sustain survival.

3.2.2 ISR reshapes lipid and iron metabolism

To support the bioinformatic correlation with direct biochemical evidence, we next examined whether ISR activation alters lipid and iron-dependent mechanisms of ferroptosis in TNBC cells. Univariate lipidomic analysis performed in MDA-MB-231 cells after 48 hours of Salubrinal treatment showed a significant reduction in glycerophospholipid levels, with a pronounced decrease in the subclass of ether-linked phosphatidylcholines (PC-Os) relative to vehicle-treated cells (**Figure 28A**). The PC-O classes mostly affected by this decrease are characterized by polyunsaturation of the fatty acyl chain. (**Figure 28B**). PC-Os represent major substrates for lipid peroxidation, one of the key initiating events of ferroptotic cell death, in particular for their contribution to the overall abundance of polyunsaturated phospholipids available for peroxidation (Cui et al. 2021; Yilong Zou, Henry, et al. 2020). The reduction in the pool of polyunsaturated PC-Os indicates that ISR activation alters the susceptibility of TNBC cells to ferroptosis by remodelling the peroxidation-prone lipids pool. This observation is in line with the brad lipidomic alterations described in the previous section and supports the hypothesis that ISR signalling can modify the cellular lipid environment resulting in the regulation of ferroptosis vulnerability.

Proteomic profiling further revealed a reduction in transferrin receptor 1 (TFR1) levels following 48 hours of Salubrinal treatment (**Figure 28C**). Given that TFR1 mediates cellular iron uptake, this finding suggests that ISR activation may also modulate iron homeostasis, another core determinant of ferroptosis.

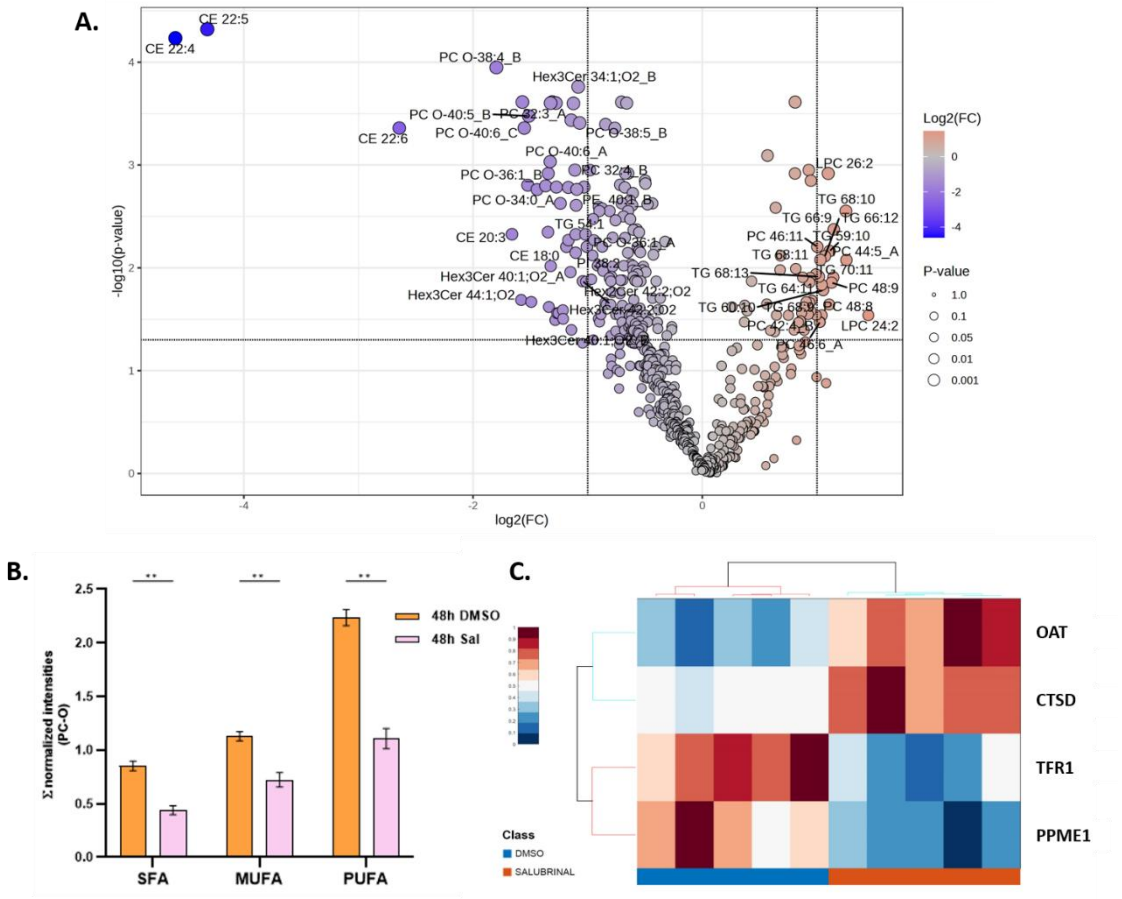

Figure 28. ISR reshapes lipid landscape and affects iron uptake. ***A.*** *Volcano plot representing lipid classes abundance in Salubrinal vs vehicle (DMSO) treated cells from univariate lipidomic analysis.* ***B.*** *Fatty acids saturation levels in ether-linked phosphatidylcholines (PC-Os). SFA: Saturated Fatty Acids, MUFA: Monounsaturated Fatty Acids, PUFA: Polyunsaturated Fatty Acids. Statistical analyses (C.): means +/- SD. *P < 0.05, **P < 0.01 (Mann-Whitney test).* ***C.*** *Heatmap representing hierarchical clustering of proteins from univariate proteomic analysis, OAT: Ornitine amino, CTSD: Cathepsin D, TFR1: Transferrin Receptor 1, PPME1: Protein phosphatase methylesterase 1. Analyses were performed on MDA-MB-231 cells treated for 48h with Salubrinal or vehicle (DMSO), n=3 biological replicates.*

To validate these observations, we examined TFR1 expression in the MDA-MB-231 cell line genetically engineered for doxycycline-inducible expression of phosphomimetic eIF2α (eIF2α Dmut). Western blot analyses did not reveal a consistent reduction in TFR1 protein levels after 48 hours induction, only showing a trend in reduction (**Figure 29A**). These results may be explained by the lower sensitivity of the technique relative to proteomic analysis, and by the rapid endocytic recycling and high basal expression that characterize TFR1, which may render subtle differences in its expression difficult to detect by Western blot (Gammella et al. 2015).

Notably, a much stronger reduction of TFR1 expression was observed upon 72 hours of SCD1 silencing, in parallel with a robust increase of ATF4 and phosphorylated eIF2α (**Figure 29B**). In addition, *in silico* analyses of the TCGA-BRCA dataset revealed a strong positive correlation between TfR1 and SCD expression (r = 0.774) (**Figure 29C**). Together, these results suggest that the effect of ISR activation on iron uptake may be mediated, at least in part, through the lipid desaturation machinery governed by SCD1. This points to a coordinated regulation of lipid desaturation and iron uptake by the ISR, potentially contributing to the modulation of ferroptosis sensitivity in TNBC cells. This provides a strong mechanistic ground to test whether ISR activation functionally affects the susceptibility of TNBC cells to ferroptotic stress.

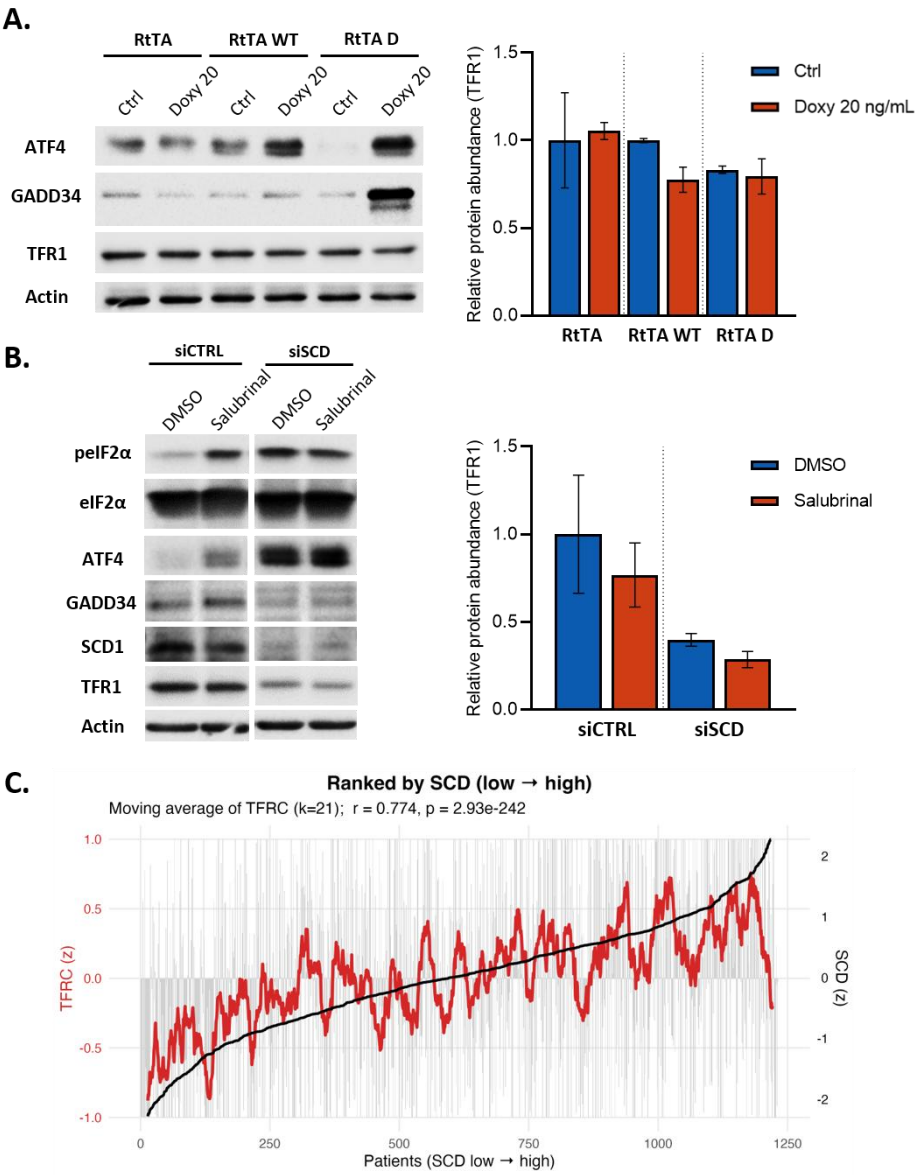

Figure 29. ISR-driven TFR1 downregulation may be mediated by SCD1. ***A.*** *Representative immunoblot showing protein abundance of ATF4, GADD34 and TFR1 upon induction of phosphomimetic eIF2α mutant with 20 ng/mL Doxycycline in genetically engineered MDA-MB-231 (Dmut), n=2 biological replicates. RtTA: empty plasmid, RtTA WT: eIF2α wt, RtTA D: eIF2α D (phosphomimetic).* ***B.*** *Representative immunoblot of eIF2α, peIF2α, ATF4, GADD34, TFR1 and SCD1 in MDA-MB-231 cells transfected with Stealth™ RNAi siRNA Negative Control (siCTRL) or siRNA SCD (siSCD) or siRNA GADD34 (siGADD34) and treated for 48h with Salubrinal or vehicle (DMSO), n=3 biological replicates. Statistical analyses: means +/- SEM. (Student's t-test), not significant.* ***C.*** *Co-variation of TFRC and SCD gene expression in TCGA-BRCA dataset. The plot shows the moving average of TFRC gene expression (red line) across TCGA-BRCA patients' samples ranked by SCD average gene expression, from low to high (black line). Vertical gray lines indicate expression of the SCD in each sample.*

3.2.3 ISR reduced the susceptibility of TNBC cells to ferroptosis

Based on the molecular changes described above, we next directly assessed whether ISR activation modulates lipid peroxidation and ferroptosis sensitivity. Lipid peroxidation was quantified by flow cytometry, using BODIPY™ 581/591 C11 undecanoic acid (Lipid Peroxidation Sensor), a membrane-localizing fluorescent probe that shifts its emission peak from red (~590 nm) to green (~510 nm) upon binding to peroxidized lipids in live cells. MDA-MB-231 cells were treated with Salubrinal for 24, 48, and 72 hours and challenged with RAS-selective lethal 3 (RSL3), a potent GPX4 inhibitor that triggers ferroptosis by inducing lipid peroxidation (Dolma et al. 2003; W. S. Yang and Stockwell 2008). Quantitative analysis revealed that acute ISR activation significantly reduced the proportion of cells positive for lipids peroxidation compared to vehicle control, with the most pronounced effect observed after 72 hours of treatment (**Figure 30A**). Collectively, these findings indicate that ISR activation establishes a protective state that limits the accumulation of lipid peroxides.

Finally, to determine whether this biochemical protection translated into improved cell survival under ferroptotic challenge, we performed a clonogenic survival assay. MDA-MB-231 cells were pretreated with Salubrinal for 72 hours to induce sustained ISR activation and were subsequently exposed to the pharmacological inducer of ferroptosis Erastin, an inhibitor of the cystine/glutamate antiporter xCT that triggers ferroptosis by inducing lipid peroxidation (Dolma et al. 2003; W. S. Yang and Stockwell 2008), either alone or in combination with and the ferroptosis inhibitor Ferrostatin-1 (Dixon et al. 2012). As expected, treatment with Erastin markedly reduced clonogenic survival after 5 days, confirming efficient induction of ferroptotic cell death. Co-treatment with Ferrostatin-1 fully rescued this effect, confirming the specificity of ferroptosis induction. Importantly, TNBC cells pretreated with Salubrinal displayed a significantly increased long-term survival upon exposure to Erastin, demonstrating that prior ISR activation confers resistance to ferroptotic death. Although Salubrinal treatment alone resulted in a mildly decreased clonogenic efficiency, likely reflecting the cytostatic effects of prolonged ISR activation, this reduction was not rescued by Ferrostatin-1, indicating that Salubrinal does not itself induce ferroptotic cell death (**Figure 30B**).

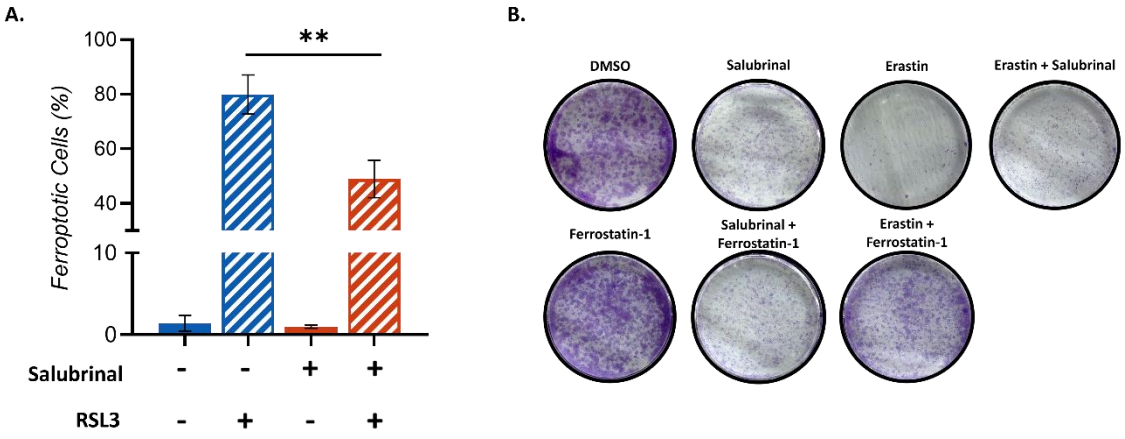

Figure 30. ISR reduces lipid peroxidation and protects TNBC cells from ferroptosis. A. *Percentage of cells undergoing lipid peroxidation, measured by flow cytometry analysis with BODIPY 581/591 C11 undecanoic acid (Lipid Peroxidation Sensor), n=3 biological replicates.* ***B.*** *Clonogenic assay of MDA-MB-231 cells pretreated with Salubrinal or vehicle (DMSO) for 72h, then treated as indicated for additional 72h, n=3 biological replicates. Statistical analyses (A.): means +/- SD. **P < 0.01 (Student's t-test).*

Collectively, these data demonstrate that sustained ISR activation elicits a protective program that limits ferroptosis and promotes long-term survival of TNBC cells. This adaptive response may enhance cellular fitness under stressful conditions and support the persistence of invasive tumour cells.

DISCUSSION

The present work was designed with the aim of dissecting the downstream consequences of Integrated Stress Response activation in Triple-negative Breast Cancer, a tumour subtype characterized by high intrinsic ISR activity and poor clinical outcome, to discover novel targetable vulnerabilities. The findings reported here support a model in which the ISR functions not as a passive survival mechanism but as an active coordinator of a broad adaptive reprogramming that simultaneously reshapes mitochondrial architecture and function, lipid metabolic homeostasis, and susceptibility to ferroptotic cell death. Collectively, these three axes converge on a unified functional outcome: the generation of a metabolically remodelled cellular state that is simultaneously more invasive and more resistant to oxidative stress-driven cell death, therefore more prone to metastatic dissemination.

A central finding of the present work is that ISR activation drives a profound and coordinated remodelling of mitochondrial architecture and function in TNBC cells. While it is well established in the literature that mitochondrial damage and dysfunction can activate the ISR through retrograde signalling, most notably via the OMA1–DELE1–HRI axis and GCN2-dependent sensing of respiratory chain impairment (Fessler et al. 2020; Mick et al. 2020), the present data support the converse relationship: that the ISR itself can actively determine the onset of a mitochondrial remodelling program. This directionality represents a conceptual advance, repositioning the ISR not only as a downstream responder to mitochondrial stress but as an upstream orchestrator of mitochondrial adaptation.

Importantly, this rewiring is not a destructive or degenerative process. The small fraction of cells undergoing apoptosis, approximately 4–5% as measured, suggests that most ISR-activated cells successfully tolerate this stress condition. In this context, the observed suppression of mitochondrial calcium uptake provides a potential mechanistic explanation for the low apoptotic rate. Reduced mitochondrial Ca^{2+} accumulation is known to limit calcium-dependent apoptosis by preventing mitochondrial permeability transition pore (mPTP) opening and cytochrome c release (Massimo Bonora et al. 2012; Denton 2009; Baumgartner et al. 2009; M Bonora et al. 2015). Thus, ISR-driven modulation of calcium handling may actively increase the threshold to reach in order to

trigger the apoptotic cascade, allowing cells to survive despite mitochondrial perturbations.

The mitochondrial phenotype induced by ISR is therefore better interpreted as an adaptive configuration that supports a more aggressive cellular state, rather than a sign of irreversible organelle damage. The observed ISR-driven mitochondrial fragmentation is consistent with previously reported observations in BC, where fragmented mitochondria have been associated with enhanced metastatic potential. Specifically, in TNBC, clinical samples display marked mitochondrial fission accompanied by DRP1 upregulation and MFN1 downregulation (J. Zhao et al. 2013; P. Zou et al. 2016). The present work adds a novel layer to this picture by demonstrating that ISR activation is sufficient to induce this fragmented phenotype, providing a mechanistic link between stress signalling and the mitochondrial morphological state associated with invasiveness. The molecular effector(s) through which ISR drives fragmentation remain to be identified, whether through ATF4-dependent transcriptional regulation of fission or fusion machinery, or through indirect effects mediated by changes in mitochondrial membrane potential and calcium dynamics.

A particularly interesting aspect of this structural remodelling is its relationship with the early translational response detected by Ribo-seq/RNA-seq at 16 hours. mRNAs encoding proteins involved in oxidative phosphorylation, mitochondrial ATP synthesis, electron transport, and respiratory chain complex I are upregulated. However, rather than enhancing mitochondrial organization or bioenergetic capacity, this response is followed at later timepoints by fragmentation, cristae disorganization, and suppression of respiratory function. This apparent paradox may be interpreted as either a compensatory response to maintain oxidative function that fails to prevent functional deterioration at 48 hours, or an imbalance in mitochondrial protein stoichiometry that disrupts supercomplexes assembly and cristae architecture. Futhermore, these possibilities are not mutually exclusive and highlight that increased protein synthesis could itself destabilize mitochondrial homeostasis.

The functional consequences of mitochondrial remodelling are multiple and interconnected, impacting both metabolism and survival. The suppression of mitochondrial calcium uptake observed upon ISR activation, in addition to raising the

apoptotic threshold, reveals a direct link between ISR-driven transcriptional reprogramming and the regulation of TCA cycle activity. Mitochondrial calcium is a key activator of several TCA cycle dehydrogenases (Duszyński et al. 2006; Gherardi et al. 2020), and its reduction is therefore expected to impair oxidative flux, consistent with the depletion of TCA cycle intermediates and the reduction in both basal and maximal respiratory capacity observed at 48 hours. Impaired mitochondrial respiration, accompanied by a shift toward glycolysis, is a common feature of TNBC, relative to other breast cancer subtypes (Reda et al. 2019b), and previous studies report that reduced MCU-mediated calcium uptake favours this metabolic shift (H. Zhao et al. 2019; Tosatto et al. 2016; Ren et al. 2017). The ISR-driven suppression of oxidative metabolism may therefore represent an amplification of a pre-existing metabolic configuration in TNBC, reinforcing the glycolytic shift that sustains rapid ATP generation and anabolic precursor supply under stress.

An additional layer of complexity emerges from the differential regulation of intracellular calcium dynamics across TNBC models. The divergent effects of ISR activation on calcium homeostasis between MDA-MB-231 and BT549 cells may reflect intrinsic differences in ER–mitochondria coupling and basal calcium handling across TNBC subtypes. In MDA-MB-231 cells, the preservation of cytosolic and ER Ca^{2+} levels suggests that ISR primarily targets mitochondrial Ca^{2+} uptake, potentially through modulation of mitochondria-associated membranes (MAMs) or components of the mitochondrial calcium uniporter complex, without broadly disrupting calcium release or storage. In contrast, the global impairment of cytosolic and ER Ca^{2+} dynamics observed in BT549 cells points to a more upstream effect of ISR on ER function, possibly involving altered activity of SERCA pumps, IP_3 receptors, or ER stress–dependent remodelling of calcium stores. These differences may arise from distinct basal metabolic states or degrees of ER stress sensitivity, ultimately dictating whether ISR engagement results in selective mitochondrial rewiring or widespread disruption of intracellular calcium homeostasis. To better characterize this phenotype, it would be highly compelling to explore how the ISR modulates ER-mitochondria contact sites, given their critical importance in regulating Ca^{2+} flux. Furthermore, it is equally important to expand this focus to investigate how the ISR regulates the broader inter-organelle network responsible for coordinating membrane composition, metabolite exchange, and stress survival.

In parallel, ISR activation promotes a metabolic shift toward fatty acid oxidation through upregulation of CPT1A. The upregulation of CPT1A downstream of ISR signalling provides a critical metabolic counterpoint to the suppression of oxidative phosphorylation. Despite the impairment of glucose-driven mitochondrial metabolism, ISR-activated TNBC cells upregulate the rate-limiting enzyme of mitochondrial fatty acid import, suggesting a switch from carbon metabolism to fatty acid oxidation as the primary mitochondrial fuel source, a transition supported by the reduction in long-chain fatty acids observed in lipidomic profiling, consistent with their increased channelling toward β-oxidation. This metabolic switch is particularly relevant in the context of TNBC biology, where FAO has been established as a major determinant of metastatic potential (Y. Xiong et al. 2018). The clinical relevance of this finding is supported by the negative prognostic value of elevated CPT1A expression in BC patients in the TCGA-BRCA cohort, suggesting that ISR-driven FAO upregulation may contribute to aggressive disease *in vivo*. Whether CPT1A upregulation is causally required for the ISR-induced migratory advantage remains to be directly established: genetic or pharmacological CPT1A inhibition in the context of ISR activation would determine whether FAO contributes to enhanced invasiveness. In parallel, the effective promotion of FAO and the mechanisms underlying ISR-driven CPT1A upregulation need further dissection. Our data indicate an ATF4-dependent regulation, but it remains unclear whether ATF4 directly regulates CPT1A transcription, acts through intermediate effectors, or influences CPT1A protein stability and turnover.

Beyond mitochondrial metabolism, ISR activation profoundly reshapes lipid homeostasis. The lipidomic profiling of ISR-activated TNBC cells revealed a broad depletion of monounsaturated fatty acids, suggesting a shift in the cellular lipid landscape that extends beyond individual metabolic reactions. The identification of SCD1 downregulation as the mechanistic driver of this MUFA depletion is consistent with the central role of this enzyme as the rate-limiting step in monounsaturated fatty acid biosynthesis and as a major determinant of membrane phospholipid composition (ALJohani et al. 2017; Ying Zou et al. 2020). The ISR-SCD1 axis therefore emerges as a key node through which stress signalling directly reshapes the biophysical properties of cellular membranes, with consequences that extend from membrane fluidity and organelle function to ferroptosis susceptibility, as discussed below.

Importantly, SCD1 and the ISR show a bidirectional relationship, mutually regulating each other in a feedback loop: ISR, once activated, suppresses SCD1 expression and the resulting lipid species unbalance activates the ISR, so that MUFA supplementation is sufficient to suppress ISR activation even in the context of a robust stress response. This loop creates a self-sustaining cycle that stabilizes the stress-adapted cellular state. This mechanism has been previously described in melanoma by Vivas-García et al. 2020 where SCD1 loss drives ISR activation through ATF4-mediated MITF repression, stabilizing a dedifferentiated cellular state, a parallel that suggests this axis may represent a broader mechanism of stress-driven phenotypic plasticity across tumour types characterized by mesenchymal identity. In the TNBC context, however, the absence of MITF as a mediator of this feedback loop suggests that alternative transcriptional effectors may fulfil a similar role downstream of ATF4. Identifying these factors will be important to understand how ISR–SCD1 coupling is maintained in TNBC and may reveal context-specific regulators of stress-driven phenotypic plasticity.

Beyond its role in establishing and maintaining the ISR-activated state, SCD1 downregulation has direct and immediate functional consequences for TNBC cell behaviour. The enhancement of invasive capacity upon SCD1 loss is consistent with the established role of the SFA/MUFA balance in regulating membrane rigidity, focal adhesion dynamics, and EMT-associated signalling depletion of MUFAs reduces membrane fluidity and may activate mechanosensitive pathways that promote cytoskeletal remodelling and invasive behaviour (Maulucci et al. 2016; Baccouch et al. 2023, Z. Chen et al. 2025; Basilico et al. 2022). Interestingly, SCD1 inhibition has been shown to cause cell cycle arrest in G1 phase through modulation of cyclin D1 and CDK6 (Hess et al. 2010; P. Li et al. 2022), an observation that aligns with the G1 delay we report upon ISR activation, suggesting that ISR-driven SCD1 downregulation may contribute not only to the invasive phenotype but also to the proliferative brake observed in our system.

The relationship between SCD1 and invasiveness in MDA-MB-231 cells is, however, more complex than a simple loss-of-function effect. In this cellular model, oleic acid supplementation mimicking SCD1 over-activity has similarly been shown to promote migration through an OA-PLD-mTOR signalling axis (Lingrand et al. 2020), indicating that perturbation of SCD1 activity in either direction enhances invasive capacity through

distinct mechanisms. This bidirectional pro-migratory effect suggests that MDA-MB-231 cells are poised to exploit changes in SCD1 activity, as signals that promote aggressive behaviour, likely reflecting the high metabolic plasticity and constitutively elevated stress-adaptive tone of this mesenchymal TNBC model. In this context, pharmacological SCD1 inhibition in our system is accompanied by ISR activation, raising the possibility that the compensatory stress response may itself contribute to the pro-migratory phenotype observed upon SCD1 inhibition.

This interpretation is directly supported by the parallel observations in melanoma reported by Vivas-García et al. 2020, where SCD1 loss similarly activates the ISR through ATF4-mediated MITF repression, stabilizing a dedifferentiated, invasive cellular state rather than inducing lipotoxicity. The convergence of findings between TNBC and melanoma in this context may reflect deeper shared biological features: both tumour types are characterized by high phenotypic plasticity and a mesenchymal, dedifferentiated identity associated with invasiveness, therapy resistance, and constitutively elevated oxidative pressure. This shared stress-adaptive architecture, supported by single-cell transcriptomic analyses identifying a conserved stress-like transcriptional program as a consistent feature of aggressive, poorly differentiated tumours including TNBC, melanoma, pancreatic cancer, and oligodendroglioma, may explain why cells of this biological identity are pre-adapted to convert SCD1 suppression into an adaptive advantage rather than succumbing to its metabolic consequences. These observations also raise the possibility that extending this analysis to other tumour types sharing this stress-adaptive architecture may uncover conserved ISR-dependent programs that represent a targetable vulnerability across a broader spectrum of aggressive cancers.

Together, these observations position SCD1 as a functional pivot point in the ISR-driven adaptive program, connecting stress signalling to membrane remodelling, cell cycle regulation, and invasiveness. At the same time, this lipid remodelling is expected to profoundly influence ferroptotic vulnerability.

In previous studies, SCD1 downregulation increases ferroptotic vulnerability by depleting the MUFA pool that normally displaces PUFAs from membrane phospholipids (Carbone and Melino 2019; G.-M. Huang et al. 2015). In the present work, however, ISR activation confers protection from ferroptotic cell death in TNBC cells. This result

represents perhaps the most therapeutically significant outcome of the present work, as it reveals a previously unappreciated functional link between stress-adaptive signalling and the regulation of oxidative cell death in this tumour subtype.

The apparent paradox between SCD downregulation and the activation of mechanism that promote evasion from ferroptosis becomes more intelligible when considered in the broader context of epithelial-to-mesenchymal transition (EMT) and metastatic selection. EMT-driven membrane remodelling, renders mesenchymal cancer cells intrinsically more susceptible to lipid peroxidation (Schwab et al. 2024; Viswanathan et al. 2017), establishing a selective pressure whereby cells that acquire invasive traits must simultaneously develop mechanisms to withstand ferroptotic stress.

TNBC cells are intrinsically primed for ferroptosis, but they simultaneously activate robust evasion mechanisms that counteract this vulnerability (F. Yang et al. 2023, H. Zhang et al. 2023; M. Tan et al. 2024; M. Lei et al. 2023). Within this framework, the ISR emerges as a key regulator of ferroptotic balance. While SCD1 downregulation is expected to promote a pro-ferroptotic lipid composition, ISR activation simultaneously induces a coordinated antioxidant program that counteracts this vulnerability at multiple levels, including downregulation of polyunsaturated PC-Os and restriction of intracellular iron availability, collectively restricting lipid peroxide accumulation. In addition, our data raise the possibility that ISR activation may impose broader constraints on lipid remodelling, potentially limiting the effective incorporation of PUFAs into membrane phospholipids, given the decrease in PUFAs observed at 48h in lipidomic analyses. While this effect alone is unlikely to account for the ferroptosis-resistant phenotype, it may contribute to shaping the lipid context in which antioxidant defences operate.

The net outcome is therefore not dictated by lipid composition alone, but by the hierarchical dominance of ISR-driven redox buffering systems, which allow cells to sustain a mesenchymal and invasive phenotype without undergoing ferroptotic collapse.

In this context, ISR activation acts as a selective pressure that favours cells capable of mounting an effective adaptive response. Cells that withstand this stress are not only survivors but are functionally reprogrammed toward increased invasiveness and metabolic plasticity. Tumour aggressiveness thus emerges as a state with an intrinsic biochemical cost, in this case increased susceptibility to ferroptotic damage, and the ISR

provides the adaptive framework that allows cancer cells to sustain this otherwise detrimental condition.

Clinical and functional data further support this model. In the TCGA-BRCA dataset, high ISR activity correlates with increased expression of key ferroptosis regulators, including SLC7A11, GPX4, FSP1, and SLC3A2, and with reduced LPCAT3 expression. This pattern suggests that ISR-high TNBC tumours engage a coordinated transcriptional program that strengthens antioxidant defences while limiting the incorporation of peroxidation-prone PUFAs. Notably, therapy-resistant TNBC cells display increased ferroptosis sensitivity (Doll et al. 2019), individuating ISR-driven resistance as a potential contributor to the poor response to conventional therapies that characterizes this tumour subtype.

Clonogenic assays provide direct functional support for this model, showing that ISR pre-activation with Salubrinal protects TNBC cells from Erastin-induced ferroptotic stress and enhances long-term survival. However, this protection is partial rather than absolute, indicating that ISR primarily shifts the ferroptotic threshold rather than conferring complete resistance. This protective state is therefore likely context-dependent and potentially fragile: disruption of ATF4-dependent antioxidant pathways, such as through SLC7A11 or GPX4 inhibition, may unmask the pro-ferroptotic effects of SCD1 suppression and sensitize ISR-activated cells to ferroptosis. These findings provide a strong rationale for combining ferroptosis inducers with inhibitors of the ISR antioxidant program in ISR-high TNBC.

Taken together, this work defines the Integrated Stress Response not simply as a survival pathway, but as a central adaptive system that enables cancer cells to tolerate the intrinsic biochemical constraints of aggressive behaviour. By coordinating metabolic rewiring, mitochondrial adaptation, and ferroptosis resistance, the ISR sustains highly invasive states that would otherwise be incompatible with survival. In this perspective, tumour aggressiveness is not a cost-free trait, but a state that requires continuous buffering of metabolic and oxidative stress, a dependency that exposes a unique therapeutic vulnerability in ISR-high TNBC.

MATERIALS AND METHODS

1. Cell lines and Culture Conditions

Human MDA-MB-231 (ATCC HTB-26, RRID:CVCL_0062) and BT-549 (ATCC HTB-122, RRID:CVCL_1092) cell lines were purchased from ATCC and authenticated by the vendor. Both cell lines were maintained in RPMI 1640 medium, GlutaMAX™ Supplement (Thermo Fisher Scientific, 61870044) supplemented with 10% heat-inactivated fetal bovine serum (FBS; Thermo Fisher Scientific, A5256701) and 1% penicillin-streptomycin (5,000 U/mL; Thermo Fisher Scientific, 15070063), hereafter referred to as complete RPMI medium, at 37°C in a humidified atmosphere with 5% CO_2. For regular maintenance, cells were passaged every 3–4 days by trypsinization and seeded into 75 cm^2 flasks or 100 mm Petri dishes. Cells were routinely tested for mycoplasma contamination every two weeks using a PCR-based assay. All experiments were performed using cells within 20 passages after thawing, and cells were not cultured continuously for longer than three months.

2. Generation of doxycycline inducible phosphomimetic eIF2α S52D cell lines

To obtain inducible expression of a phosphomimetic eIF2α S52D mutant, and relative controls, MDA-MB-231 cells were engineered using a tetracycline-responsive Tet-On system based on the reverse tetracycline-controlled transactivator (rtTA). Cells were transduced with a 3rd generation lentiviral reverse tetracycline-controlled transactivator 3 (rtTA3) expression vector, under a CMV promoter (Addgene, 26429) and selected with 5 µg/mL blasticidine (Thermo Fisher Scientific, A1113903) to obtain a population expressing the rtTA inducible system. A second round of infection was performed to express eIF2α S52D mutant and relative control eIF2α wild type, cloned into a pMA3211 lentiviral vector for Tet-induced expression (Addgene, 46879, (Ochoa et al. 2012)), through NotI and BamH1 restriction sites. Double selection with 1,5 µg/mL puromycin (Thermo Fisher Scientific, A1113803) and 5 µg/mL blasticidine was performed to select double positive cells.

To induce eIF2α wild type or S52D expression, for ISR activation, cells were treated for 48 hours with 20 ng/mL Doxycycline (Sigma-Aldrich, D9891).

3. RNA interference

For reverse transfection, siRNA–Lipofectamine RNAiMAX complexes were prepared by mixing the selected siRNA (*Silencer*™ Negative Control No. 1 siRNA, AM4635; Stealth RNAi™ siRNA Negative Control, 12935200; siRNA SCD, 1299001, siRNA ID: HSS109498; siRNA ATF4, AM16704, siRNA ID: 122372; siRNA GADD34, 1299001, siRNA ID: HSS119113, Thermo Fisher Scientific) with Lipofectamine RNAiMAX (Thermo Fisher Scientific, 13778150) in Opti-MEM (Thermo Fisher Scientific, 31985070) as follows: for 60 mm dishes 80 pmol of siRNA were mixed to 10 µL of Lipofectamine, in 1 mL of Opti-MEM; for 24-well plates 6 pmol of siRNA were mixed to 1 µL of Lipofectamine, in 100 µL of Opti-MEM. After 20 minutes incubation at RT for complex formation, cells were added directly to the transfection mixture, once resuspended in complete RPMI medium without antibiotics at a density such that the indicated volume (5 mL for 60 mm dishes and 500 µL for 24-well plates) contained the appropriate number of cells to reach 70–80% confluence the following day. Cells were incubated overnight at 37 °C in a humidified atmosphere with 5% CO_2.

For Western Blot Assay, the next day each 60 mm Petri dish was split into two 100 mm Petri dishes. Once cells had adhered, they were treated with vehicle (DMSO, 1:1000, Merck, D8418) or Salubrinal (Merck, SML0951) at a final concentration of 20 µM. For Aequorin-based calcium measurements, the next day the medium was changed with fresh one, the procedure was followed as described in *Aequorin based calcium measurements* section.

4. Proteins extraction and Western Blot Assay

Cells were cultured in 100-mm petri dishes until approximately 80% confluency. At the indicated experimental time points, cells were washed with 1X PBS (Thermo Fisher Scientific, AM9625) and lysed in 120 µL of RIPA buffer RIPA buffer (25 mM Tris HCl pH 7.6, 150 mM NaCl, 1% Sodium deoxycholate, 1% Triton X-100, 2 mM EDTA dihydrate) supplemented with protease and phosphatase inhibitors (Halt™ Protease and Phosphatase Inhibitor Cocktail, 100X, Thermo Fisher Scientific, 78441). Cells were collected using a cell scraper, and lysates were incubated for 15 min at 4 °C under constant rotation. Samples were then centrifuged at 12,000 × g for 15 min at 4 °C, and the supernatants were collected while the pellets were discarded.

Protein concentration was determined using the Pierce™ BCA Protein Assay Kit (Thermo Fisher Scientific, 23225). Samples were prepared to load equal amounts of protein (35–45 µg) adjusting the volume with RIPA buffer and adding 4X sample buffer (Biorad, 1610747, supplemented with 10% of β-mercaptoethanol) to a final 1X concentration. Samples were denatured at 95 °C for 5 min and loaded onto 10% SDS–polyacrylamide gels (Lower gel: 3.45 mL H2O, 2.5 mL Resolving Buffer, 3.3 mL 30% Acrylamide/Bis Solution (Biorad, 1610159), 100 µL 10% ammonium persulfate, 25 µL TEMED; Upper gel: 2.225 mL H2O, 1 mL Stacking Buffer, 500 µL 30% Acrylamide/Bis Solution, 15 µL ammonium persulfate, 15 µL TEMED). Electrophoresis was performed at a constant voltage of 100 V in 1X running buffer (25 mM Tris, 192 mM glycine**,** 0,1% w/v SDS) for approximately 2 h.

Proteins were transferred onto nitrocellulose membranes (Amersham, GE10600003). using cold 1X transfer buffer (25 mM Tris, 192 mM glycine, 20% methanol) at 100 V for 2 h at 4 °C, or alternatively overnight at 15 V. Membranes were stained with Ponceau S solution (Merck, P7170) to verify transfer efficiency, cut at the appropriate molecular weight, and washed with PBS-T (1X PBS supplemented with 0.1% Tween-20 (Merck, P2287)). Blocking was performed with 5% BSA (Thermo Fisher Scientific, A7906) in PBS-T for 1 h at room temperature under gentle oscillation. Membranes were then incubated overnight at 4 °C with the following primary antibodies appropriately diluted in 5% BSA in PBS-T: ATF4 (1:800; Cell Signaling, 97038); p-eIF2α (Ser51; 1:800; Cell Signaling, 3398); eIF2α (1:1000; Sigma Aldrich, E0157); GADD34 (1:1000; Proteintech, 10449-1-AP); SCD1 (1:800; Abcam, ab19862); CPT1A (1:1000; Cell Signaling, BK12252S); TFR1 (1:1000; Abcam, AB214039); β-actin (1:60000; Sigma Aldrich, A5441); GAPDH (1:10000; Thermo Fisher Scientific, MA5-15738-HRP); Vinculin (1:10000; Thermo Fisher Scientific, MA511690).

Following primary antibody incubation, membranes were washed three times for 5 min each with PBS-T and incubated for 45 min at room temperature with the appropriate HRP-conjugated secondary antibody (anti-mouse IgG, Cell Signalling, 7076 or anti-rabbit IgG, Cell Signalling, 7074) diluted 1:3000 in 5% BSA in PBS-T. Membranes were subsequently washed three times for 5 min each with PBS-T and incubated for 5 min with ECL detection kit (Bio-Rad, 1705061). Chemiluminescent signals were acquired using a

ChemiDoc imaging system (Bio-Rad) in signal accumulation mode. Band intensity was quantified via ImageLab software.

5. RNA extraction and RT-qPCR

Total RNA was extracted using the RNeasy Mini Kit (Qiagen, 74106), from MDA-MB-231 cells cultured on 60 mm Petri dishes up to 80 % of confluency. Total RNA was quantified and tested for purity by NanoDrop fluorometer (Thermo-Fisher). Reverse transcription of 1 μg of RNA was performed according to the manufacturer's instructions using the QuantiTect Reverse Transcription Kit (Qiagen, 205314). Real-time qPCR analysis was then performed to assess the expression of target genes. Primers for human CPT1A (F:5'-ATCAATCGGACTCTG -3'; R: 5'-TCAGGGAGTAGCGCA -3') were designed using the Primer Blast application from NCBI Reactions were performed using SYBR Green PCR Master Mix (ThermoFisher Scientific, 4334973) and analysed using a ViiA 7 Real-Time PCR System (ThermoFisher Scientific). Melting curve analyses were performed to ensure product specificity, and the data were analysed using the $2-\Delta\Delta Ct$ method. Relative mRNA expression levels were normalised to glyceraldehyde 3′ phosphate dehydrogenase (GAPDH).

6. Microscopy techniques

6.1 Live Confocal microscopy and analysis

BT549 cells were seeded onto circular glass coverslips (24 mm diameter) placed in 6-well plates in complete RPMI medium, at a density calculated to reach approximately 80% confluence at the experimental endpoint, with three technical replicates per experimental condition. The following day, cells were treated with vehicle (DMSO, 1:1000) or Salubrinal at a final concentration of 20 μM. After 24h from seeding, cells were infected with viruses for the expression of mt-GFP. Following infection, cells were incubated for an additional 36h maintaining the adequate treatment. Z-stack images on live cells were acquired using an Olympus FluoView FV3000RS confocal microscope with a 60x objective and a 0,36 μm z-step, at controlled temperature of 37°C and 5% CO_2.

Imaris software was used for analysing morphology parameters, using custom settings. To improve image resolution, Z-series acquisitions were deconvolved using Huygens Essential software. At least 10 cells per technical replicate were analysed.

6.2 Electron microscopy

Cells were cultured in 6-well plates up to 80 % of confluency in complete RPMI medium and treated with vehicle (DMSO, 1:1000) or 20 μM Salubrinal for 48 hours prior to the analyses. To prepare the samples for Transmission Electron Microscopy (TEM) analysis, they were fixed using a solution containing 2.5% glutaraldehyde in 0.1 M cacodylate buffer at pH 7.3 for 1 hour and subsequently washed three times with 0.1 M cacodylate buffer. Cells were then post-fixed in 1% osmium tetroxide and 1.5% potassium ferricyanide in 100 mM sodium cacodylate buffer for 1 hour on ice. After rinsing in sodium cacodylate buffer, the samples were washed five times with distilled water and stained with 0.5% uranyl acetate in distilled water overnight at 4°C, protected from light. Lastly, the specimens were rinsed again five times in distilled water, gradually dehydrated using increasing concentrations of ethanol, and embedded in Epon before curing at 60°C in an oven for 48 hours. Ultrathin sections (70 nm) were collected, stained with uranyl acetate and Sato's lead solution, and observed with a TALOS L120C Transmission Electron Microscope (Thermo Fisher Scientific). Images were acquired with a CETA 4×4k CMOS camera (Thermo Fisher Scientific). Microscopy Image Browser (MIB) was used to analyze mitochondria.

7. Aequorin-based calcium measurements

MDA-MB-231 or BT549 cells were seeded onto 13 mm circular glass coverslips in 24-well plates, with multiple technical replicates per experimental condition. The following day, cells were treated with vehicle (DMSO, 1:1000) or Salubrinal at a final concentration of 20 μM and simultaneously transduced with adenoviral vectors encoding the bioluminescent calcium reporters mitochondria-targeted aequorin (mt-AEQmut), cytosolic aequorin (cyt-AEQ), or endoplasmic reticulum-targeted aequorin (er-AEQ). Cells were incubated for an additional 36 hours under the respective treatment conditions prior to calcium measurement.

For cytosolic and mitochondrial calcium measurements, cells were washed twice with modified Krebs-Ringer buffer (KRB: 135 mM NaCl, 5 mM KCl, 0.4 mM KH_2PO_4, 1 mM $MgSO_4$, 20 mM HEPES, 5.5 mM glucose, 1 mM $CaCl_2$, pH 7.4) and incubated with 5 μM coelenterazine (Sigma-Aldrich) in KRB for 1.5 hours at 37°C to allow aequorin reconstitution, under reduced light conditions. Following two additional washes, each

coverslip was placed in a temperature-controlled perfusion chamber at 37°C and continuously perfused with KRB at 2.5 mL/min. Luminescence was recorded by a low-noise photomultiplier tube positioned at 2-3 mm from the cell monolayer. After baseline acquisition, calcium signaling was stimulated by switching perfusion to calcium-mobilizing solution (KRB supplemented with 100 μM ATP (Sigma-Aldrich, 20-306) for MDA-MB-231 cells or 100 μM histamine (Sigma-Aldrich, H7250) for BT549 cells) at increased flow rate (5 mL/min). At the end of each recording, cells were lysed with Triton X-100 (1:1000, 648463) in 10 mM $CaCl_2$ to discharge residual aequorin and quantify total aequorin content.

For ER calcium measurements using erAEQ, ER stores were first depleted by incubating cells in Ca^{2+}-free buffer (CFB: KRB supplemented with 100 μM EGTA) containing 50 μM ionomycin for 2 minutes. Aequorin reconstitution was then performed by incubating cells with 5 μM coelenterazine N in CFB at 4°C for 45 minutes, followed by three washes with 2% BSA to remove residual ionomycin. After baseline acquisition in CFB, ER stores were reloaded by perfusing cells with Ca^{2+}-containing KRB, detected as a luminescence peak. Agonist-evoked Ca^{2+} release was subsequently triggered by switching perfusion to calcium-mobilizing solution, resulting in a rapid decrease in luminescence signal reflecting Ca^{2+} release from ER stores.

Luminescence values were background-corrected and converted to $[Ca^{2+}]$ using calibration constants as described in Bonora et al., 2013. Refilling and release rate were calculated using Origin 2025b to smooth and derive $[Ca^{2+}]$ tracks.

8. Invasion assays

8.1 Invasion assay in Transwell

Matrigel invasion assays were performed using the Corning® BioCoat™ Matrigel® invasion chamber (Merck, CLS354483)**.** MDA-MB-231 were seeded at 2 × 105 cells per insert in triplicate and cultured overnight in complete RPMI medium before treatment with vehicle (DMSO 1:1000) or Salubrinal at a final concentration of 20 μM. After 48 h of incubation, cells remaining above the insert membrane were removed by gentle scraping with a sterile cotton swab. Cells that invaded through the Matrigel to the bottom of the insert were fixed in ethanol for 10 min, washed in 1X phosphate-buffered saline

(PBS), and stained with Methylene blue. The insert was then washed in 1X PBS and air-dried. Invading cells were counted, considering 3-4 random fields per insert.

8.2 3D invasion assay in a microfluidic chip

MDA-MB-231 cell invasion was assessed using the idenTX 3microfluidic device (Aim Biotech), according to manufacturer's instructions. The central gel channel was filled with Collagen I (3mg/ml; SIAL, 354249) and allowed to polymerize for 30 minutes at 37°C. MDA-MB-231 cells (50000 cells/device) were seeded in one lateral channel, whereas the opposite channel was filled with complete culture medium supplemented with additional 10% FBS as chemoattractant. After 8 hours to allow cell adhesion, cells were treated in the seeding channel with vehicle (DMSO) or 20 μM Salubrinal or 1 μM SCD1 inhibitor (A939572; Abcam, ab142089). Fixation in 4% paraformaldehyde (Thermo Fisher Scientific, 043368.9M) was performed 48 hours after treatment, and nuclei were stained with propidium iodide (0,3 μg/ml; Merck, P4170), to avoid interference from device autofluorescence in the 405 nm channel, and with Phalloidin Alexa Fluor 488 (Thermo Fisher Scientific, A12379) diluted 1:1000, to visualize the actin cytoskeleton. Following immunofluorescence staining, z-stack images were acquired using an Olympus FluoView FV3000RS confocal microscope with a 10x objective and a 4 μm z-step. For each device, three independent fields spanning the cell and gel channels were imaged.

Images were analysed using a custom Fiji macro. Briefly, nuclei z-stacks were projected into a single plane using the maximum Z projection command and adjusted for brightness and contrast. Before image binarization, a Gaussian blur filter was applied to define cell outlines, and the watershed function was used to separate closely apposed nuclei. Three regions of interest (ROI) per image were defined on the brightfield channel, extending from the base of the triangular post to the maximum distance reached by invading cells within the collagen channel. These ROIs were then transferred to the nuclei channel, and invading cells were quantified using the Analyze Particles function. Invasion was expressed as both the number of invaded cells and the distance travelled from the edge of the gel channel.

9. Clonogenic assay

MDA-MB-231 cells were seeded in four wells of a 12-well plate using serial 1:2 dilutions, with the highest seeding density corresponding to 5,000 cells per well, followed by three consecutive 1:2 dilutions resulting in progressively lower cell densities across the remaining wells. Cells were allowed to adhere overnight in complete RPMI 1640 medium. The experimental design included seven treatment conditions: vehicle (DMSO 1:1000), 20 μM Salubrinal, 2.5 μM Erastin (MedChem Express, HY-15763), 1 μM Ferrostatin-1 (MedChem Express, HY-100579), Salubrinal + Erastin, Salubrinal + Ferrostatin-1 and Erastin + Ferrostatin-1. For all conditions involving Salubrinal, cells were pre-treated with Salubrinal alone for 72 hours prior to the addition of the second agent. Following this pre-treatment phase, the appropriate compounds were added according to the experimental condition, and colonies were allowed to form for additional 72 hours at 37°C in a humidified atmosphere with 5% CO_2. At the endpoint, medium was removed, cells were gently washed with phosphate-buffered saline (PBS) and stained with crystal violet (Merck, C6158) solution (glutaraldehyde 6.0% (vol/vol), crystal violet 0.5% (wt/vol) in H2O) for 30 minutes. Excess stain was removed by gentle washing with distilled water, and plates were air-dried before imaging.

10. Flow cytometric analysis

10.1 Flow cytometric analysis for lipid peroxidation

MDA-MB 231 cells were cultured in 6-well plates until reaching approximately 80% confluence before analyses. Cells were treated with vehicle (DMSO, 1:1000) or Salubrinal at a final concentration of 20 μM for 72 hours. In the last 5 hours, cells were treated or not with RSL3 (MedChem Express, HY-100218A) at a final concentration of 0,1 μM. Cells were stained with BODIPY™ 581/591 C11 Lipid Peroxidation Sensor (Thermo Fisher Scientific, D3861) at 10 μM final concentration in complete RPMI medium for 30 minutes at 37 °C. Following incubation, cells were washed twice with 1X PBS, harvested pelleted and resuspended in SS5 buffer (5% FBS in 1X PBS) for analysis. Samples were acquired on a BD FACSCanto flow cytometer (BD Biosciences). Fluorescence signals were acquired at two wavelengths: excitation/emission 581/591 nm (PE channel) to detect the reduced form of the dye, and excitation/emission 488/510 nm (Alexa Fluor 488 channel) to detect the oxidized form.

10.2 Flow cytometric analysis of cell cycle distribution

MDA-MB-231 cells were seeded in 6-well plates until reaching approximately 80% confluence before analyses. Cells were treated with vehicle (DMSO, 1:1000) or Salubrinal at a final concentration of 20 μM for 48 hours. Following treatment, cells were harvested, centrifuged, and fixed in 70% ethanol for 1 h in ice. Fixed cells were then pelleted and resuspended in staining solution containing propidium iodide (50 μg/ml; Merck, P4170), RNAse A (0,1 mg/ml; Thermo Fisher Scientific, EN0531) and 0,05% Triton X-100 for 40 min at 37°C. After staining, cells were resuspended in SS5 buffer prior to acquisition.

Samples were acquired on a BD FACSCanto flow cytometer (BD Biosciences), and DNA content was measured by detecting linear PE fluorescence intensity versus cell count. Cell cycle distribution was quantified using the univariate Cell Cycle modeling tool in FlowJo software (BD Biosciences).

10.3 Flow cytometric analysis of apoptosis

MDA-MB-231 cells were seeded in 6-well plates until reaching approximately 80% confluence before analyses. Cells were treated with vehicle (DMSO, 1:1000) or Salubrinal at a final concentration of 20 μM for 48 hours. After treatment, both suspended and adherent cells were harvested and processed for apoptotic cell detection using CellEvent Caspase-3/7 Green Flow Cytometry Assay Kit (Thermo Fisher Scientific, C10427), according to manufacturer's instructions. Briefly, cell pellets were resuspended in staining solution containing CellEvent Caspase 3/7 Green detection reagent at a final concentration of 500 nM, and incubated for 30 min at 37°C. After staining, cells were washed and resuspended in SS5 buffer prior to flow cytometry acquisition.

Samples were acquired on a BD FACSCanto flow cytometer (BD Biosciences). Fluorescence signals were acquired using 488-nm excitation, collecting fluorescence emission using a 530/30 bandpass filter or equivalent and the percentage of Caspase-3/7-positive cells was determined. Data were analysed using FlowJo software (BD Biosciences).

11. Seahorse XF Cell Mito Stress Test

Seahorse XF Cell Mito Stress Test was performed with Agilent Seahorse XF Cell Mito Stress Test Kit (103015-100), according to manufacturer's instructions. MDA-MB-231

cells were seeded in Seahorse XF24-well plates in complete RPMI medium and treated with vehicle (DMSO, 1:1000) or 20 μM Salubrinal for 48 hours prior to the assay.

For the Agilent Seahorse XF Cell Mito Stress Test, culture medium was replaced with Agilent Seahorse XF Base Medium (Agilent, 103335-100) supplemented with 25 mM glucose and 2 mM pyruvate, adjusted to pH 7.4, and cells were equilibrated for 1 hour at 37°C in a non-CO_2 incubator prior to measurement. Following instrument calibration, basal oxygen consumption rate (OCR) was recorded, followed by sequential injection of oligomycin (ATP synthase inhibitor), FCCP (mitochondrial uncoupler), and a combination of rotenone and antimycin A (complex I and III inhibitors), allowing the determination of basal respiration, ATP-linked respiration, maximal respiratory capacity, and non-mitochondrial oxygen consumption.

Each experiment included at least three biological replicates. At the end of each assay, cells were lysed and protein concentration was determined by BCA assay. OCR values were normalized to 100 μg of total protein per well.

12. Statistical analyses

Results will be tested for statistical significance using GraphPad Prism 8.0 (GraphPad Software, Boston, MA, USA, www.graphpad.com) with the Mann-Whitney test to compare two sets of data or the Kruskal-Wallis test to compare data sets with more than two groups or using Excel performing Student's t-test, employing non-parametric methods that do not assume a normal distribution of residuals. Differences were considered significant for $p < 0.05$ (*), $p < 0.01$ (**), $p < 0.001$ (***) and $p < 0.0001$ (****). Results are presented as mean standard deviation (SD) or mean standard median error (SEM) as indicated in the figures.

13. Bioinformatic analyses

TCGA-BRCA bulk tumour RNA-sequencing data were obtained from the Genomic Data Commons using TCGAbiolinks. Harmonized STAR-Counts files were processed from the unstranded assay, normalized by TMM in edgeR, and converted to log2 CPM values. Clinical annotations were retrieved from matched TCGA metadata, and overall survival was defined from days_to_death or days_to_last_follow_up, as appropriate. Molecular subtypes were derived from PAM50/paper-subtype annotations and collapsed

into a 3-class framework comprising ER/PR+ (Luminal A, Luminal B, and Normal-like), HER2+ (HER2-enriched), and TNBC (Basal-like) tumours.

Curated metabolic stress (Falletta 2017) and chemical stress (Supplementary table 1) gene sets were used to quantify ISR-related transcriptional programs at the sample level, using either the mean log2 CPM expression for single genes or the mean of gene-wise z-scored expression values for signatures. Heatmaps were generated from per-gene z-scored expression values and signature mean z-scores. Survival analyses were performed after median stratification of tumours into high- and low.score groups, using Kaplan-Meier estimates and Cox proportional hazards models. For pathway analysis, genes were ranked by Pearson correlation with the indicated signature scores and subjected to pre-ranked GSEA against MSigDB Hallmark gene sets. Ranked moving-average plots were generated using a 10-sample sliding window.

All analyses were performed in R (version 4.5.0) using RStudio (version 2024.12.1+563; Posit Software, PBC).

14. RNA-seq and Ribo-seq analysis

To investigate the effects of ISR activation on transcriptional and translational regulation, MDA-MB-231 cells were treated with 20 μM Salubrinal or DMSO vehicle for 16 h. For each condition, three biological replicates were collected and processed in parallel for transcriptomic and translatomic profiling. For Ribo-seq experiments, cells were pre-treated with cycloheximide (CHX) prior to lysis to stabilize translating ribosomes and preserve ribosome-protected fragments.

14.1 RNA-sequencing

RNA extraction, library preparation, and sequencing

Total RNA was extracted from cells using the RNeasy Mini Kit (74106, Qiagen). RNA concentration was quantified by Qubit fluorometric assay, RNA purity was assessed spectrophotometrically using an Epoch microplate reader, and RNA integrity was evaluated using a Fragment Analyzer prior to library preparation. Poly(A)-selected mRNA libraries were prepared using the Standard Input mRNA library preparation protocol for NovaSeq 6000 and sequenced on an Illumina NovaSeq 6000 platform using paired-end 2 × 150-bp reads.

RNA-seq preprocessing and differential expression analysis

Raw RNA-seq read quality was evaluated using FastQC, and quality control reports were aggregated with MultiQC. Reads were aligned to the human reference genome GRCh38 using STAR, and gene-level counts were generated with FeatureCounts. Sample distribution and clustering were initially evaluated by principal component analysis (PCA) to assess grouping according to treatment condition.

Differential gene expression analysis was performed using the DESeq2 package. Genes with low counts were filtered prior to statistical testing. Differential RNA abundance between Salubrinal-treated and DMSO-treated cells was assessed using treatment as the main experimental factor. Genes were considered differentially expressed when the adjusted P value was < 0.05 and the absolute log2 fold change was ≥ 0.58, corresponding to a fold change of at least 1.5 in either direction.

14.2 Ribo-sequencing

Ribo-seq library preparation and sequencing

For translatome profiling, ribosome-protected fragments (RPFs) were generated using the RiboLace workflow (IMMAGINA BioTechnology), which enriches RNA fragments associated with actively translating ribosomes, accrding to manufacturer's instructions. Briefly, after CHX pre-treatment, cells were lysed under ribosome-preserving conditions and lysates were subjected to nuclease digestion to degrade unprotected RNA. Active ribosome complexes were then isolated using the RiboLace affinity-based purification system, and the associated ribosome-protected fragments were recovered and converted into sequencing libraries. Libraries were subsequently sequenced on an Illumina platform.

Ribo-seq preprocessing and differential ribosome occupancy analysis

Raw Ribo-seq reads were processed by adapter trimming and quality filtering prior to alignment. To minimize contamination from abundant non-coding RNAs, reads mapping to rRNA, tRNA, snRNA, and snoRNA were removed before genome alignment. The remaining reads were aligned to the human reference genome GRCh38, and only uniquely mapped reads were retained for downstream analyses.

Gene-level Ribo-seq quantification was restricted to reads mapping to annotated coding sequences (CDS). Differential ribosome occupancy between Salubrinal-treated and DMSO-treated cells was assessed using DESeq2 following the same count-based

framework used for RNA-seq. Adjusted p values were calculated using the Benjamini-Hochberg method, and genes with adjusted P value < 0.05 were considered significantly altered at the level of ribosome occupancy.

Ribo-seq quality control

Ribo-seq library quality was assessed using standard footprint-specific metrics, including fragment length distribution, enrichment of reads mapping to coding sequences, 3-nucleotide periodicity, and metagene profiles around translation initiation and termination sites. These analyses were used to confirm the presence of bona fide ribosome-protected fragments and the overall quality of the translatome dataset.

14.3 Integrated RNA-seq and Ribo-seq analysis

To distinguish transcriptional from translational regulation, RNA-seq and Ribo-seq datasets were analyzed jointly. For each gene, changes in transcript abundance were compared with changes in ribosome occupancy across treatment conditions. Translational efficiency (TE) was defined as the relative Ribo-seq signal normalized to RNA-seq abundance. Differential TE was assessed in DESeq2 using an interaction model including assay type (RNA-seq versus Ribo-seq), treatment (DMSO versus Salubrinal), and the assay × treatment interaction term. In this framework, a significant interaction term identified genes whose translational response could not be explained solely by changes in mRNA abundance and were therefore considered translationally regulated.

Based on the combined analysis, genes were classified as transcriptionally regulated when significant changes were detected at the RNA level only, translationally regulated when the interaction term indicated a significant change in TE, concordantly regulated when RNA abundance and ribosome occupancy changed in the same direction, or discordantly regulated when ribosome occupancy changed disproportionately relative to transcript abundance.

Sample relationships and replicate concordance were evaluated by PCA and correlation analysis on normalized count matrices. Differential analysis results were visualized using and scatter plot comparing RNA-seq and Ribo-seq log2 fold changes. Genes identified as significantly altered at the transcriptional, translational, or TE level were subsequently used for downstream functional enrichment analyses.

14.4 Statistical analysis

All analyses were performed in R. For both RNA-seq and Ribo-seq, count normalization and differential analysis were carried out using DESeq2. Multiple-testing correction was performed using the Benjamini-Hochberg false discovery rate method. Unless otherwise specified, genes with an adjusted P value < 0.05 were considered statistically significant.

15. Metabolomic, Lipidomic and Proteomic analyses

Sample collection and combined extraction for proteins, metabolites and lipids

For univariate metabolomic, lipidomic and proteomic profiling, MDA-MB-231 cells were seeded in 100 mm Petri dishes in complete RPMI medium supplemented with 10% FBS and 1% penicillin/streptomycin, at a density calculated to reach approximately 80% confluence at the experimental endpoint. Three technical replicates were prepared for each biological replicate. Cells were allowed to adhere overnight before treatment initiation and were subsequently incubated for 48 hours at 37 °C in a humidified atmosphere with 5% CO_2 prior to sample collection.

Prior to sample collection, 0.9% saline solution and labelled collection tubes were prepared and kept on ice; cell scrapers and cell extraction solution (MeOH/H_2O, 80:20 v/v) were pre-chilled at -80 °C until use to ensure effective metabolic quenching. At the experimental endpoint, medium was aspirated and cells were rinsed twice with 6 mL ice-cold 0.9% saline, performed rapidly to minimize metabolic alterations. Following aspiration of the saline, 600 µL of ice-cold cell extraction solution was added to each dish and cells were immediately scraped and transferred into pre-chilled, labelled 1.5 mL Eppendorf tubes kept on ice. Samples were snap-frozen in liquid nitrogen and stored at -80 °C until further processing.

Cell pellets were ice thawed, and ice-cold MeOH plus a mix of deuterated standards (225 µL) was added and vortexed. Next, cold MTBE (750 µL) was added, and the solution was stirred for 10 min, 300 rpm at 4 °C in a thermomixer. After, of H_2O (188 µL) was added, samples were vortexed for 20 s, and spun at 14680 rpm for 10 min at 4 °C for phase separation. The lower MeOH/ H_2O and the upper MTBE layer were collected separately, concentrated using a vacuum concentrator, and solubilized before injection in UHPLC-HRMS. The protein pellet was alkylated, reduced and trypsin digested.

15.1 Metabolomic analysis by UHPLC-HRMS

Instrumentation and LC setup

Metabolome analyses were performed on a Thermo Vanquish Flex UHPLC coupled online to hybrid quadrupole-Orbitrap Exploris 120 mass spectrometer (Thermo Fisher Scientific) equipped with HESI II (heated electrospray ionization probe). For targeted metabolomics analyses, separation was performed with an Acquity UPLC BEH Amide™ (100 × 2.1 mm × 1.7 µm, 130 Å) protected with a VanGuard BEH Amide™ precolumn (5.0 × 2.1 mm; 1.7 µm, 130 Å) (Waters, Milford). The mobile phases were composed of (A): H2O/ACN (95:5 v/v%) and (B): H2O/ACN (5:95 v/v%), both with 0.1% HCOOH (v/v %) + 10 mM HCOONH4 were employed of H-ESI (+), while the mobile phases were composed of (A): H2O/ACN (95:5 v/v%) and (B): H2O/ACN (5:95 v/v%), both with 0.1% NH4OH (v/v %) + 10 mM CH3OONH4 for H-ESI (-), were employed for H-ESI (-). The following gradient was used: 0-1 min, 99%B, 7-8 min 30% B, 8.1-11.5 min 99% B. The column temperature was set at 45 °C and a flow rate of 0.4 mL per min was used. Injection volume: 2 µL.

HRMS parameters

Acquisition of MS data was obtained in full scan-data dependent acquisition (FS-DDA) in the m/z range 70–800. MS1 scans were acquired in the Orbitrap at resolution of 60,000; with AGC set to auto and a maximum injection time of 100 ms. The S-Lens RF level was set to 70. Data-dependent MS/MS scans were acquired in the Orbitrap at resolution of 15,000, using a isolation window of 1.5 Da, dynamic exclusion of 10 s, AGC set to auto and maximum injection time of 22 ms. The acquisition method was run in TopN=4 mode. HCD fragmentationwas performed using normalized collision energies (NCE): 20, 40, 60.

For the HESI source, the sheath gas was set to 40 a.u. in positive ionization mode and 50 a.u. in negative ionization mode, while the auxiliary gas and sweep gas were set to 15 a.u. and 0 a.u., respectively. Spray voltage was set to 3.3 kV for ESI (+) and 3.0 kV ESI (−). The ion transfer tube and vaporizer temperatures were set to 300 °C and 320 °C, respectively. The same MS and MS/MS acquisition settings and calibration procedures described above were applied through the folloging steps.

Data processing and statistical analysis

RAW files were first visualized with FreeStyle (Thermo Fisher Scientific) and then imported into Compound Discoverer v.3.3 (Thermo Fisher Scientific) for detection, normalization, alignment, and identification of compounds. Features were extracted over the 0-10 min and 0-11 min retention time windows for HILIC and RP runs respectively, within an m/z range of 70–800. Alignments were performed using an adaptive curve alignment model. Compound detection was carried out using 5 ppm mass tolerance and 0.2 min retention time tolerance. The minimum peak intensity was set to 100,000 AU, the signal to noise threshold to 5, and the peak rating filter to 3. Blank subtraction was applied maintaining a max sample-to-max blank ratio > 5. For statistical comparisons, signal intensities were normalized by using the Constant Sum algorithm.

Elemental compositions prediction was performed using isotope pattern matching with relative intensity tolerance of 30%. Compound annnotatin was based on database matching with a 5 ppm mass tolerance for mzCloud precursor and fragment ions, ChemSpider structural search, and Metabolika pathway searches. The database used included BioCyc, the Human Metabolome Database (HMDB), and KEGG. Compound identities were assigned according to this priority order: (1) mzCloud; (2) Predicted Compositions; (3) MassList search; (4) ChemSpider Search; (5) Metabolika search.

Principal component analysis (PCA) was performed using MetaboAnalyst 6.0 after log transformation and autoscaling of the data. All other graphical representations were generated using GraphPad Prism 8.0 (GraphPad Software).

15.2 Lipidomic analysis by HT-4D-UHPLC-TIMS

Instrument setup

Instrument configuration was set as previously described (Merciai et al. 2022). Lipidomic analyses were performed on an Ultimate RS3000 UHPLC (Thermo Fisher Scientific) coupled to a TimsTOF Pro Q-TOF (Bruker Daltonics) equipped with an Apollo II ESI source. Lipid separation was achieved using an acquity UPLC CSH™ C18 column (50×2.1 mm; 1.7 µm, 130 Å) fitted with a VanGuard CSH™ precolumn (5.0×2.1 mm; 1.7 µm, 130 Å) (Waters, Milford). The column oven was maintained at 65 °C and the flow rate was set to 0.55 mL/min.

The mobile phases consisted of A: ACN/H2O (60:40 v/v) and B: IPA/ACN (90:10 v/v), both supplemented with 10 mM HCOONH4 and 0.1% HCOOH (v/v). The gradient was programmed as follows: 0 min, 40% B; 0.4 min, 43% B; 0.425 min, 50% B; 0.9 min, 57% B; 2.0 min, 70% B; 2.950 min, 99% B; 3.3 min, 99% B; 3.31, 40% B followed by 0.7 min of column re-equilibration. At the start of each run, mass accuracy and ion mobility were recalibrated by injecting 1:1 (v/v) mixture of 10 mM sodium formate calibrant solution and ESI-L Low Concentration Tuning Mix. Data were acquired in data-dependent parallel accumulation-serial fragmentation (DDA-PASEF). Analyses were performed in both positive and negative ESI mode in separate runs. Each sample was analyzed in triplicate, and 2 µL was injected per run.

Source conditions were set as follows: nebulizer gas (N2), 4.0 bar; dry gas (N2), 10 L/min; dry temperature, 280 °C. Mass spectra were acquired over an m/z range of 50–1500, with 100 ms accumulation time and 100 ms ramp time. The ion mobility range was scanned from 0.55 to 1.80 Vs/cm^2. Precursors were isolated within ±2 m/z and fragmented using ion mobility-dependent collision energies ranging from 20 to 40 eV. The total acquisition cycle was 0.32 s and consisted of one full TIMS-MS scan followed by two PASEF MS/MS scans. Exclusion time was set to 0.1 min, and ion charge control (ICC) was set to 7.5 million. In addition, separate experiments were performed using TIMS-stepping with alternative collision energy settings of 20–40 eV and 35–50 eV.

HT-4D-UHPLC-TIMS data processing and lipid annotation

Raw data were processed and annotated using MetaboScape 2023b (Bruker). Feature detection thresholds were set to 500 counts in positive mode and 250 counts in negative mode. The minimum number of data points was set to 100, and recursive feature extraction was enabled with a threshold of 75 points. Lipid annotation was initially performed using a rule-based workflow based on class-specific diagnostic fragment ions and their relative intensities in the corresponding MS/MS spectra. An additional annotation step was then carried out using the LipidBlast spectral library (http://prime.psc.riken.jp/compms/msdial/main.html). For library matching, the following parameters were applied: mass accuracy window, 2 ppm (narrow) and 10 ppm (wide); mSigma, 30 (narrow) and 250 (wide); MS/MS score, 800 (narrow) and 150 (wide); and collision cross section (CCS) tolerance, 1% (narrow) and 3.5% (wide).

In ESI positive mode, the following adducts were considered: [M+H]+, [M+Na]+, [M+K]+, [M+H–H2O]+, and [M+NH4]+. In ESI negative mode, the following adducts were considered: [M–H]−, [M+Cl]−, [M+HCOO]−, and [M–H2O]−. Experimental CCS values were compared with those predicted by the CCSbase platform (https://ccsbase.net/) and the CCS-Predict tool implemented in MetaboScape. Smart Formula™ was used for molecular formula assignment. All lipid annotations were manually curated according to Lipidomics Standard Initiative (LSI) (https://lipidomics-standards-initiative.org/guidelines/lipid-species-identifcation/general-rules) guidelines. In addotion to the presence of diagnosticMS/MS ions, annotation confidence was evaluated by considering the expected electrospray ionization adduct forms and the retention behaviour of each lipid class, including assessment according to the equivalent carbon number (ECN) model in RPLC. Where necessary, the LipidCreator extension in Skyline (https://skyline.ms/project/home/begin.view) was used for in silico comparison of specific product ions.

HT-4D-UHPLC-TIMS method validation

Quality control (QC) sampes spiked with six to eight concentration levels of a mixture of labeled internal standards (IS) were injected at regular intervals throughout the anaytica batch to monitor instrument linearity and evalutate dynamic range. A mixture of authentic lipid standards was analyzed in parallel, and blanks were included to assess potential carryover. Study samples were anayzed in randomized order.

Method repeatability was evaluated by measuring internal standard signal intensities, retention times, and collision cross section values across five LC runs acquired on the same day and over two consecutive days. Repeatability was expressed as coefficient of variation (CV %).

Method accuracy was determined for each internal standard by calculating the percentage deviation between the measured and theoretical concentrations at low, medium, and high spike levels. Acceptance criteria were set at ±20% for low-level spike and ±15% for medium- and high-level spikes. The limits of detection (LOD) and limits of quantification (LOQ) were calculated from the analytical calibarion curves as 3 x SD/slope and 10 x SD/slope, respectively, where SD represents the standard deviation of response and slope the slope of the calibration curve.

Recovery was calculated as the ratio of the average internal standard signal intensity measured before and after extraction. Selectivity was assessed by verifying the absence of interfering peaks at the retention time of each internal standard.

Normalization, quantification and statistical analysis

Data normalization and quantification by single-point calibration were performed in Microsoft Excel. Multivariate analyses were carried out with MetaboAnalyst 5.0, after log transformation of the data prior to statistical testing. Figures were generated using MATLAB, RAWgraph 2.0 and GraphPad Prism 8.0 (GraphPad Software).

15.3 Proteomics analysis by nLC-HRMS/MSA

Proteomic profiling was performed using a label-free quantification (LFQ) approach. After extraction, samples were resuspended in 100 µL of a solution containing 95% LC–MS grade water, 5% LC–MS grade acetonitrile, and 0.1% trifluoroacetic acid (TFA). Samples were analyzed on a Thermo Scientific Ultimate 3000 nano-LC system coupled to an Orbitrap Fusion Lumos mass spectrometer (Thermo Scientific) equipped with a nano-electrospray ionization source (EasySpray, Thermo).

Chromatographic separation was carried out using solvent A consisting of LC–MS grade water with 0.1% formic acid and solvent B consisting of 80% acetonitrile, 20% water, and 0.08% formic acid. Peptides were first concentrated on a trap column and subsequently separated in a PepMap C18 analytical column (75 µm × 150 mm, 2 µm particle size, 100 Å pore size, Thermo Scientific) at a flow rate of 0.3 µL/min over a 60-min gradient. The percentage of solvent B was increased from 4% to 35% over 40 min, then ramped to 99% in 2 min, reduced back to 4% over 5 min, and held at that composition until the end of the run.

Data were acquired in data-dedependent acquisition (DDA) mode. Full MS scans were recorded over an m/z range of 375–1500 at a resolution of 120,000. AGC target and ion injection time were maintained at default settings using quadrupole isolation. MS/MS spectra were acquired in the Orbitrap at a resolution of 15,000. Singly charged ions and ions with undetermined charge state were excluded from fragmentation. A 1.6 Da isolation window was used, and peptide fragmentation was performed by HCD with a normalized collision energy of 30. The maximum injection time for MS/MS scans was

set to 50 ms, with a standard AGC settings. Dynamic exclusion was enabled with a duration of 30 s.

Proteomics data analysis

Raw proteomics data were processed in Proteome Discoverer v2.5.0.400, using a 1%. false discovery rate (FDR) threshold. Database search was performed against the Homo Sapiens FASTA database, using trypsin as the proteolytic enzyme. Carbamidomethylation of cysteine was set as a fixed modification, while methionine oxidation was included as a variable modification.

The data processing workflow included MS PepSearch followed by Sequest HT. Search parameters allowed up to 2 missing cleavages, with a minimum peptide length of 7 amino acids and a maximum length of 30 amino acids. Quantitative data were median-normalized, log-transformed, and autoscaled prior to statistical analysis.Identified proteins were subsequently, subjected to functional enrichment analysis using STRING and ShinyGO to identify enriched biological processes and signalling pathways.

REFERENCES

Abe, Rikiya, Nobuo Kumagai, Michio Kimura, Akio Hirosaki, and Takashi Nakamura. 1976. 'Biological Characteristics of Breast Cancer in Obesity'. *The Tohoku Journal of Experimental Medicine* 120 (4): 351–59. https://doi.org/10.1620/tjem.120.351.

Adaniya, Stephanie M., Jin O-Uchi, Michael W. Cypress, Yoichiro Kusakari, and Bong Sook Jhun. 2019. 'Posttranslational Modifications of Mitochondrial Fission and Fusion Proteins in Cardiac Physiology and Pathophysiology'. *American Journal of Physiology-Cell Physiology* 316 (5): C583–604. https://doi.org/10.1152/ajpcell.00523.2018.

Adomavicius, Tomas, Margherita Guaita, Yu Zhou, et al. 2019. 'The Structural Basis of Translational Control by eIF2 Phosphorylation'. *Nature Communications* 10 (1): 2136. https://doi.org/10.1038/s41467-019-10167-3.

Agresti, Roberto, Elisabetta Meneghini, Paolo Baili, et al. 2016. 'Association of Adiposity, Dysmetabolisms, and Inflammation with Aggressive Breast Cancer Subtypes: A Cross-Sectional Study'. *Breast Cancer Research and Treatment* 157 (1): 179–89. https://doi.org/10.1007/s10549-016-3802-3.

Ahn, Songyeon, Jun Hyoung Park, Sandra L. Grimm, et al. 2024. 'Metabolomic Rewiring Promotes Endocrine Therapy Resistance in Breast Cancer'. *Cancer Research* 84 (2): 291–304. https://doi.org/10.1158/0008-5472.CAN-23-0184.

Ahola, Sofia, Pablo Rivera Mejías, Steffen Hermans, et al. 2022. 'OMA1-Mediated Integrated Stress Response Protects against Ferroptosis in Mitochondrial Cardiomyopathy'. *Cell Metabolism* 34 (11): 1875-1891.e7. https://doi.org/10.1016/j.cmet.2022.08.017.

Akkaoui, Marie, Isabelle Cohen, Catherine Esnous, et al. 2009. 'Modulation of the Hepatic Malonyl-CoA–Carnitine Palmitoyltransferase 1A Partnership Creates a Metabolic Switch Allowing Oxidation of *de Novo* Fatty Acids'. *Biochemical Journal* 420 (3): 429–38. https://doi.org/10.1042/BJ20081932.

ALJohani, Ahmed M., Deeba N. Syed, and James M. Ntambi. 2017. 'Insights into Stearoyl-CoA Desaturase-1 Regulation of Systemic Metabolism'. *Trends in Endocrinology & Metabolism* 28 (12): 831–42. https://doi.org/10.1016/j.tem.2017.10.003.

Amsalem, Zohar, Tasleem Arif, Anna Shteinfer-Kuzmine, Vered Chalifa-Caspi, and Varda Shoshan-Barmatz. 2020. 'The Mitochondrial Protein VDAC1 at the Crossroads of Cancer Cell Metabolism: The Epigenetic Link'. *Cancers* 12 (4): 1031. https://doi.org/10.3390/cancers12041031.

Anderson, Peter M., Matteo M. Trucco, Rohinton S. Tarapore, et al. 2022. 'Phase II Study of ONC201 in Neuroendocrine Tumors Including Pheochromocytoma-

Paraganglioma and Desmoplastic Small Round Cell Tumor'. *Clinical Cancer Research* 28 (9): 1773–82. https://doi.org/10.1158/1078-0432.CCR-21-4030.

Armstrong, Jane L., Ross Flockhart, Gareth J. Veal, Penny E. Lovat, and Christopher P. F. Redfern. 2010. 'Regulation of Endoplasmic Reticulum Stress-Induced Cell Death by ATF4 in Neuroectodermal Tumor Cells'. *Journal of Biological Chemistry* 285 (9): 6091–100. https://doi.org/10.1074/jbc.M109.014092.

Ashton, Thomas M., W. Gillies McKenna, Leoni A. Kunz-Schughart, and Geoff S. Higgins. 2018. 'Oxidative Phosphorylation as an Emerging Target in Cancer Therapy'. *Clinical Cancer Research* 24 (11): 2482–90. https://doi.org/10.1158/1078-0432.CCR-17-3070.

Avivar-Valderas, Alvaro, Eduardo Salas, Ekaterina Bobrovnikova-Marjon, et al. 2011. 'PERK Integrates Autophagy and Oxidative Stress Responses To Promote Survival during Extracellular Matrix Detachment'. *Molecular and Cellular Biology* 31 (17): 3616–29. https://doi.org/10.1128/mcb.05164-11.

Axten, Jeffrey M., Stuart P. Romeril, Arthur Shu, et al. 2013. 'Discovery of GSK2656157: An Optimized PERK Inhibitor Selected for Preclinical Development'. *ACS Medicinal Chemistry Letters* 4 (10): 964–68. https://doi.org/10.1021/ml400228e.

Baccouch, Rim, Yarong Shi, Emilie Vernay, et al. 2023. 'The Impact of Lipid Polyunsaturation on the Physical and Mechanical Properties of Lipid Membranes'. *Biochimica et Biophysica Acta (BBA) - Biomembranes* 1865 (2): 184084. https://doi.org/10.1016/j.bbamem.2022.184084.

Bai, Xupeng, Jie Ni, Julia Beretov, et al. 2021. 'Activation of the eIF2α/ATF4 Axis Drives Triple-Negative Breast Cancer Radioresistance by Promoting Glutathione Biosynthesis'. *Redox Biology* 43 (July): 101993. https://doi.org/10.1016/j.redox.2021.101993.

Bareche, Y., D. Venet, M. Ignatiadis, et al. 2018. 'Unravelling Triple-Negative Breast Cancer Molecular Heterogeneity Using an Integrative Multiomic Analysis'. *Annals of Oncology* 29 (4): 895–902. https://doi.org/10.1093/annonc/mdy024.

Baron, Kelsey R., Samantha Oviedo, Sophia Krasny, et al. 2025. 'Pharmacologic Activation of Integrated Stress Response Kinases Inhibits Pathologic Mitochondrial Fragmentation'. *eLife* 13 (February): RP100541. https://doi.org/10.7554/eLife.100541.

Basilico, Bernadette, Ilaria Elena Palamà, Stefania D'Amone, et al. 2022. 'Substrate Stiffness Effect on Molecular Crosstalk of Epithelial-Mesenchymal Transition Mediators of Human Glioblastoma Cells'. *Frontiers in Oncology* 12 (August): 983507. https://doi.org/10.3389/fonc.2022.983507.

Baughman, Joshua M., Fabiana Perocchi, Hany S. Girgis, et al. 2011. 'Integrative Genomics Identifies MCU as an Essential Component of the Mitochondrial

Calcium Uniporter'. *Nature* 476 (7360): 341–45. https://doi.org/10.1038/nature10234.

Baumgartner, Heidi K., Julia V. Gerasimenko, Christopher Thorne, et al. 2009. 'Calcium Elevation in Mitochondria Is the Main Ca2+ Requirement for Mitochondrial Permeability Transition Pore (mPTP) Opening'. *Journal of Biological Chemistry* 284 (31): 20796–803. https://doi.org/10.1074/jbc.M109.025353.

B'Chir, Wafa, Anne Catherine Maurin, Valérie Carraro, et al. 2013. 'The eIF2α/ATF4 Pathway Is Essential for Stress-Induced Autophagy Gene Expression'. *Nucleic Acids Research* 41 (16): 7683–99. https://doi.org/10.1093/nar/gkt563.

Beatty, Alexander, Lauren S. Fink, Tanu Singh, et al. 2018. 'Metabolite Profiling Reveals the Glutathione Biosynthetic Pathway as a Therapeutic Target in Triple-Negative Breast Cancer'. *Molecular Cancer Therapeutics* 17 (1): 264–75. https://doi.org/10.1158/1535-7163.MCT-17-0407.

Benjamin, Daniel I., Alyssa Cozzo, Xiaodan Ji, et al. 2013. 'Ether Lipid Generating Enzyme AGPS Alters the Balance of Structural and Signaling Lipids to Fuel Cancer Pathogenicity'. *Proceedings of the National Academy of Sciences* 110 (37): 14912–17. https://doi.org/10.1073/pnas.1310894110.

Bensaad, Karim, Elena Favaro, Caroline A. Lewis, et al. 2014. 'Fatty Acid Uptake and Lipid Storage Induced by HIF-1α Contribute to Cell Growth and Survival after Hypoxia-Reoxygenation'. *Cell Reports* 9 (1): 349–65. https://doi.org/10.1016/j.celrep.2014.08.056.

Bergers, Gabriele, and Sarah Maria Fendt. 2021. 'The Metabolism of Cancer Cells during Metastasis'. *Nature Reviews Cancer* 21 (3): 162–80. https://doi.org/10.1038/s41568-020-00320-2.

Bernardi, Paolo, Christoph Gerle, Andrew P. Halestrap, et al. 2023. 'Identity, Structure, and Function of the Mitochondrial Permeability Transition Pore: Controversies, Consensus, Recent Advances, and Future Directions'. *Cell Death & Differentiation* 30 (8): 1869–85. https://doi.org/10.1038/s41418-023-01187-0.

Bersuker, Kirill, Joseph M. Hendricks, Zhipeng Li, et al. 2019. 'The CoQ Oxidoreductase FSP1 Acts Parallel to GPX4 to Inhibit Ferroptosis'. *Nature* 575 (7784): 688–92. https://doi.org/10.1038/s41586-019-1705-2.

Bhutia, Yangzom D., and Vadivel Ganapathy. 2016. 'Glutamine Transporters in Mammalian Cells and Their Functions in Physiology and Cancer'. *Biochimica et Biophysica Acta (BBA) - Molecular Cell Research* 1863 (10): 2531–39. https://doi.org/10.1016/j.bbamcr.2015.12.017.

Bian, Xueli, Rui Liu, Ying Meng, Dongming Xing, Daqian Xu, and Zhimin Lu. 2021. 'Lipid Metabolism and Cancer'. *Journal of Experimental Medicine* 218 (1). https://doi.org/10.1084/JEM.20201606.

Bianchini, Giampaolo, Justin M. Balko, Ingrid A. Mayer, Melinda E. Sanders, and Luca Gianni. 2016. 'Triple-Negative Breast Cancer: Challenges and Opportunities of a Heterogeneous Disease'. *Nature Reviews Clinical Oncology* 13 (11): 674–90. https://doi.org/10.1038/nrclinonc.2016.66.

Bianchini, Giampaolo, Carmine De Angelis, Luca Licata, and Luca Gianni. 2022. 'Treatment Landscape of Triple-Negative Breast Cancer — Expanded Options, Evolving Needs'. *Nature Reviews Clinical Oncology* 19 (2): 91–113. https://doi.org/10.1038/s41571-021-00565-2.

Biswas, Swarajit Kumar, Saswati Banerjee, Ginger Wendolyn Baker, Chieh-Yin Kuo, and Indrajit Chowdhury. 2022. 'The Mammary Gland: Basic Structure and Molecular Signaling during Development'. *International Journal of Molecular Sciences* 23 (7): 3883. https://doi.org/10.3390/ijms23073883.

Blais, Jaime D., Christina L. Addison, Robert Edge, et al. 2006. 'Perk-Dependent Translational Regulation Promotes Tumor Cell Adaptation and Angiogenesis in Response to Hypoxic Stress'. *Molecular and Cellular Biology* 26 (24): 9517–32. https://doi.org/10.1128/MCB.01145-06.

Bobrovnikova-Marjon, E., C. Grigoriadou, D. Pytel, et al. 2010. 'PERK Promotes Cancer Cell Proliferation and Tumor Growth by Limiting Oxidative DNA Damage'. *Oncogene* 29 (27): 3881–95. https://doi.org/10.1038/onc.2010.153.

Bogdan, Alexander R., Masaki Miyazawa, Kazunori Hashimoto, and Yoshiaki Tsuji. 2016. 'Regulators of Iron Homeostasis: New Players in Metabolism, Cell Death, and Disease'. *Trends in Biochemical Sciences* 41 (3): 274–86. https://doi.org/10.1016/j.tibs.2015.11.012.

Boldogh, Istvan R., Dan W. Nowakowski, Hyeong-Cheol Yang, et al. 2003. 'A Protein Complex Containing Mdm10p, Mdm12p, and Mmm1p Links Mitochondrial Membranes and DNA to the Cytoskeleton-Based Segregation Machinery'. *Molecular Biology of the Cell* 14 (11): 4618–27. https://doi.org/10.1091/mbc.e03-04-0225.

Bonnefont, J. 2004. 'Carnitine Palmitoyltransferases 1 and 2: Biochemical, Molecular and Medical Aspects'. *Molecular Aspects of Medicine* 25 (5–6): 495–520. https://doi.org/10.1016/j.mam.2004.06.004.

Bononi, A, M. Bonora, S. Marchi, et al. 2013. 'Identification of PTEN at the ER and MAMs and Its Regulation of Ca2+ Signaling and Apoptosis in a Protein Phosphatase-Dependent Manner'. *Cell Death & Differentiation* 20 (12): 1631–43. https://doi.org/10.1038/cdd.2013.77.

Bononi, Angela, Carlotta Giorgi, Simone Patergnani, et al. 2017. 'BAP1 Regulates IP3R3-Mediated Ca2+ Flux to Mitochondria Suppressing Cell Transformation'. *Nature* 546 (7659): 549–53. https://doi.org/10.1038/nature22798.

Bononi, Angela, Sonia Missiroli, Federica Poletti, et al. 2012. 'Mitochondria-Associated Membranes (MAMs) as Hotspot Ca2+ Signaling Units'. In *Calcium Signaling*, edited by Md. Shahidul Islam, vol. 740. Advances in Experimental Medicine and Biology. Springer Netherlands. https://doi.org/10.1007/978-94-007-2888-2_17.

Bonora, M, M. R. Wieckowski, C. Chinopoulos, et al. 2015. 'Molecular Mechanisms of Cell Death: Central Implication of ATP Synthase in Mitochondrial Permeability Transition'. *Oncogene* 34 (12): 1475–86. https://doi.org/10.1038/onc.2014.96.

Bonora, Massimo, Carlotta Giorgi, Angela Bononi, et al. 2013. 'Subcellular Calcium Measurements in Mammalian Cells Using Jellyfish Photoprotein Aequorin-Based Probes'. *Nature Protocols* 8 (11): 2105–18. https://doi.org/10.1038/nprot.2013.127.

Bonora, Massimo, Simone Patergnani, Alessandro Rimessi, et al. 2012. 'ATP Synthesis and Storage'. *Purinergic Signalling* 8 (3): 343–57. https://doi.org/10.1007/s11302-012-9305-8.

Boone, Morgane, and Francesca Zappa. 2023. 'Signaling Plasticity in the Integrated Stress Response'. *Frontiers in Cell and Developmental Biology* 11 (December): 1271141. https://doi.org/10.3389/fcell.2023.1271141.

Boyce, Michael, Kevin F. Bryant, Céline Jousse, et al. 2005. 'A Selective Inhibitor of elF2α Dephosphorylation Protects Cells from ER Stress'. *Science* 307 (5711): 935–39. https://doi.org/10.1126/science.1101902.

Bray, Freddie, Mathieu Laversanne, Hyuna Sung, et al. 2024. 'Global Cancer Statistics 2022: GLOBOCAN Estimates of Incidence and Mortality Worldwide for 36 Cancers in 185 Countries'. *CA: A Cancer Journal for Clinicians* 74 (3): 229–63. https://doi.org/10.3322/caac.21834.

Brites, Pedro, Hans R. Waterham, and Ronald J. A. Wanders. 2004. 'Functions and Biosynthesis of Plasmalogens in Health and Disease'. *Biochimica et Biophysica Acta (BBA) - Molecular and Cell Biology of Lipids* 1636 (2–3): 219–31. https://doi.org/10.1016/j.bbalip.2003.12.010.

Brüning, Ansgar, Petra Burger, Marianne Vogel, et al. 2009. 'Nelfinavir Induces the Unfolded Protein Response in Ovarian Cancer Cells, Resulting in ER Vacuolization, Cell Cycle Retardation and Apoptosis'. *Cancer Biology & Therapy* 8 (3): 226–32. https://doi.org/10.4161/cbt.8.3.7339.

Bryant, Kevin F., Elizabeth R. Macari, Natasha Malik, Michael Boyce, Junying Yuan, and Donald M. Coen. 2008. 'ICP34.5-Dependent and -Independent Activities of Salubrinal in Herpes Simplex Virus-1 Infected Cells'. *Virology* 379 (2): 197–204. https://doi.org/10.1016/j.virol.2008.06.028.

Burns, Jorge, and Gina Manda. 2017. 'Metabolic Pathways of the Warburg Effect in Health and Disease: Perspectives of Choice, Chain or Chance'. *International*

Journal of Molecular Sciences 18 (12): 2755. https://doi.org/10.3390/ijms18122755.

Burstein, Matthew D., Anna Tsimelzon, Graham M. Poage, et al. 2015. 'Comprehensive Genomic Analysis Identifies Novel Subtypes and Targets of Triple-Negative Breast Cancer'. *Clinical Cancer Research* 21 (7): 1688–98. https://doi.org/10.1158/1078-0432.CCR-14-0432.

Cailleau, Relda, Matilde Olivé, and Quita V. J. Cruciger. 1978. 'Long-Term Human Breast Carcinoma Cell Lines of Metastatic Origin: Preliminary Characterization'. *In Vitro* 14 (11): 911–15. https://doi.org/10.1007/BF02616120.

Calvo, Veronica, Wei Zheng, Anna Adam-Artigues, et al. 2023. 'A PERK-Specific Inhibitor Blocks Metastatic Progression by Limiting Integrated Stress Response–Dependent Survival of Quiescent Cancer Cells'. *Clinical Cancer Research* 29 (24): 5155–72. https://doi.org/10.1158/1078-0432.CCR-23-1427.

Camara, Amadou K. S., YiFan Zhou, Po-Chao Wen, Emad Tajkhorshid, and Wai-Meng Kwok. 2017. 'Mitochondrial VDAC1: A Key Gatekeeper as Potential Therapeutic Target'. *Frontiers in Physiology* 8 (June): 460. https://doi.org/10.3389/fphys.2017.00460.

Camarda, Roman, Alicia Y. Zhou, Rebecca A. Kohnz, et al. 2016. 'Inhibition of Fatty Acid Oxidation as a Therapy for MYC-Overexpressing Triple-Negative Breast Cancer'. *Nature Medicine* 22 (4): 427–32. https://doi.org/10.1038/nm.4055.

Carbone, Michele, and Gerry Melino. 2019. 'Stearoyl CoA Desaturase Regulates Ferroptosis in Ovarian Cancer Offering New Therapeutic Perspectives'. *Cancer Research* 79 (20): 5149–50. https://doi.org/10.1158/0008-5472.CAN-19-2453.

Carracedo, Arkaitz, Lewis C. Cantley, and Pier Paolo Pandolfi. 2013. 'Cancer Metabolism: Fatty Acid Oxidation in the Limelight'. *Nature Reviews Cancer* 13 (4): 227–32. https://doi.org/10.1038/nrc3483.

Catalá, Angel. 2009. 'Lipid Peroxidation of Membrane Phospholipids Generates Hydroxy-Alkenals and Oxidized Phospholipids Active in Physiological and/or Pathological Conditions'. *Chemistry and Physics of Lipids* 157 (1): 1–11. https://doi.org/10.1016/j.chemphyslip.2008.09.004.

Ceccarelli, Simona M., Odile Chomienne, Marcel Gubler, and Arduino Arduini. 2011. 'Carnitine Palmitoyltransferase (CPT) Modulators: A Medicinal Chemistry Perspective on 35 Years of Research'. *Journal of Medicinal Chemistry* 54 (9): 3109–52. https://doi.org/10.1021/jm100809g.

Cerqua, Marina, Marco Foiani, Carla Boccaccio, Paolo M. Comoglio, and Dogus M. Altintas. 2025. 'The Integrated Stress Response Drives MET Oncogene Overexpression in Cancers'. *The EMBO Journal* 44 (4): 1107–30. https://doi.org/10.1038/s44318-024-00338-4.

Chang, Chuang-Rung, and Craig Blackstone. 2010. 'Dynamic Regulation of Mitochondrial Fission through Modification of the Dynamin-related Protein Drp1'. *Annals of the New York Academy of Sciences* 1201 (1): 34–39. https://doi.org/10.1111/j.1749-6632.2010.05629.x.

Chatre, Laurent. 2024. 'Mitochondria and the Reactive Species Interactome: Shaping the Future of Mitoredox Medicine'. *Journal of Mitochondria, Plastids and Endosymbiosis* 2 (1): 2304348. https://doi.org/10.1080/28347056.2024.2304348.

Chavez, Kathryn J., Sireesha V. Garimella, and Stanley Lipkowitz. 2011. 'Triple Negative Breast Cancer Cell Lines: One Tool in the Search for Better Treatment of Triple Negative Breast Cancer'. *Breast Disease* 32 (1–2): 35–48. https://doi.org/10.3233/BD-2010-0307.

Chen, Hsin-Chih, Han-Hsuan Tang, Wei-Hsiang Hsu, et al. 2022. 'Vulnerability of Triple-Negative Breast Cancer to Saponin Formosanin C-Induced Ferroptosis'. *Antioxidants* 11 (2): 298. https://doi.org/10.3390/antiox11020298.

Chen, Hsiuchen, and David C. Chan. 2017. 'Mitochondrial Dynamics in Regulating the Unique Phenotypes of Cancer and Stem Cells'. *Cell Metabolism* 26 (1): 39–48. https://doi.org/10.1016/j.cmet.2017.05.016.

Chen, Hsiuchen, Anne Chomyn, and David C. Chan. 2005. 'Disruption of Fusion Results in Mitochondrial Heterogeneity and Dysfunction'. *Journal of Biological Chemistry* 280 (28): 26185–92. https://doi.org/10.1074/jbc.M503062200.

Chen, Hsiuchen, Marc Vermulst, Yun E. Wang, et al. 2010. 'Mitochondrial Fusion Is Required for mtDNA Stability in Skeletal Muscle and Tolerance of mtDNA Mutations'. *Cell* 141 (2): 280–89. https://doi.org/10.1016/j.cell.2010.02.026.

Chen, Hu, Renqiang Yuan, Ying Zhang, et al. 2016. 'ATF4 Regulates SREBP1c Expression to Control Fatty Acids Synthesis in 3T3-L1 Adipocytes Differentiation'. *Biochimica et Biophysica Acta (BBA) - Gene Regulatory Mechanisms* 1859 (11): 1459–69. https://doi.org/10.1016/j.bbagrm.2016.07.010.

Chen, Jane Jane. 2007. 'Regulation of Protein Synthesis by the Heme-Regulated eIF2α Kinase: Relevance to Anemias'. *Blood* 109 (7): 2693–99. https://doi.org/10.1182/blood-2006-08-041830.

Chen, Li, Jing Zhang, Zhuomin Lyu, et al. 2018. 'Positive Feedback Loop between Mitochondrial Fission and Notch Signaling Promotes Survivin-Mediated Survival of TNBC Cells'. *Cell Death & Disease* 9 (11): 1050. https://doi.org/10.1038/s41419-018-1083-y.

Chen, Meng-Shian, Sheng-Fan Wang, Chih-Yi Hsu, et al. 2017. 'CHAC1 Degradation of Glutathione Enhances Cystine-Starvation-Induced Necroptosis and Ferroptosis in Human Triple Negative Breast Cancer Cells via the GCN2-eIF2α-ATF4 Pathway'. *Oncotarget* 8 (70): 114588–602. https://doi.org/10.18632/oncotarget.23055.

Chen, Wen, Huakan Zhao, and Yongsheng Li. 2023. 'Mitochondrial Dynamics in Health and Disease: Mechanisms and Potential Targets'. *Signal Transduction and Targeted Therapy* 8 (1): 333. https://doi.org/10.1038/s41392-023-01547-9.

Chen, Zhicong, Yanqing Gong, Fukai Chen, et al. 2025. 'Orchestrated Desaturation Reprogramming from stearoyl-CoA Desaturase to Fatty Acid Desaturase 2 in Cancer Epithelial-mesenchymal Transition and Metastasis'. *Cancer Communications* 45 (3): 245–80. https://doi.org/10.1002/cac2.12644.

Cheng, Chunming, Feng Geng, Xiang Cheng, and Deliang Guo. 2018. 'Lipid Metabolism Reprogramming and Its Potential Targets in Cancer'. *Cancer Communications* 38 (1): 27. https://doi.org/10.1186/s40880-018-0301-4.

Chorley, B. N., M. R. Campbell, X. Wang, et al. 2012. 'Identification of Novel NRF2-Regulated Genes by ChIP-Seq: Influence on Retinoid X Receptor Alpha'. *Nucleic Acids Research* 40 (15): 7416–29. https://doi.org/10.1093/nar/gks409.

Chu, Bo, Ning Kon, Delin Chen, et al. 2019. 'ALOX12 Is Required for P53-Mediated Tumour Suppression through a Distinct Ferroptosis Pathway'. *Nature Cell Biology* 21 (5): 579–91. https://doi.org/10.1038/s41556-019-0305-6.

Clamer, Massimiliano, Toma Tebaldi, Fabio Lauria, et al. 2018. 'Active Ribosome Profiling with RiboLace'. *Cell Reports* 25 (4): 1097-1108.e5. https://doi.org/10.1016/j.celrep.2018.09.084.

Cobine, Paul A., Fabien Pierrel, Megan L. Bestwick, and Dennis R. Winge. 2006. 'Mitochondrial Matrix Copper Complex Used in Metallation of Cytochrome Oxidase and Superoxide Dismutase'. *Journal of Biological Chemistry* 281 (48): 36552–59. https://doi.org/10.1074/jbc.M606839200.

Cole, Alicia, Zezhou Wang, Etienne Coyaud, et al. 2015. 'Inhibition of the Mitochondrial Protease ClpP as a Therapeutic Strategy for Human Acute Myeloid Leukemia'. *Cancer Cell* 27 (6): 864–76. https://doi.org/10.1016/j.ccell.2015.05.004.

Colombini, Marco. 2016. 'The VDAC Channel: Molecular Basis for Selectivity'. *Biochimica et Biophysica Acta (BBA) - Molecular Cell Research* 1863 (10): 2498–502. https://doi.org/10.1016/j.bbamcr.2016.01.019.

Conrad, Marcus, and Derek A. Pratt. 2019. 'The Chemical Basis of Ferroptosis'. *Nature Chemical Biology* 15 (12): 1137–47. https://doi.org/10.1038/s41589-019-0408-1.

Corazzari, M., F. Rapino, F. Ciccosanti, et al. 2015. 'Oncogenic BRAF Induces Chronic ER Stress Condition Resulting in Increased Basal Autophagy and Apoptotic Resistance of Cutaneous Melanoma'. *Cell Death & Differentiation* 22 (6): 946–58. https://doi.org/10.1038/cdd.2014.183.

Cordova, Ricardo A., Jagannath Misra, Parth H. Amin, et al. 2022. 'GCN2 eIF2 Kinase Promotes Prostate Cancer by Maintaining Amino Acid Homeostasis'. *eLife* 11 (September): e81083. https://doi.org/10.7554/eLife.81083.

Costa-Mattioli, Mauro, and Peter Walter. 2020. 'The Integrated Stress Response: From Mechanism to Disease'. *Science* 368 (6489): eaat5314. https://doi.org/10.1126/science.aat5314.

Couch, Fergus J., Steven N. Hart, Priyanka Sharma, et al. 2015. 'Inherited Mutations in 17 Breast Cancer Susceptibility Genes Among a Large Triple-Negative Breast Cancer Cohort Unselected for Family History of Breast Cancer'. *Journal of Clinical Oncology* 33 (4): 304–11. https://doi.org/10.1200/JCO.2014.57.1414.

Cruz-Gregorio, Alfredo. 2026. 'Mitochondrial Redox Vulnerabilities in Triple-Negative Breast Cancer: Integrative Perspectives and Emerging Therapeutic Strategies'. *Metabolites* 16 (1): 60. https://doi.org/10.3390/metabo16010060.

Csordás, György, Tünde Golenár, Erin L. Seifert, et al. 2013. 'MICU1 Controls Both the Threshold and Cooperative Activation of the Mitochondrial Ca2+ Uniporter'. *Cell Metabolism* 17 (6): 976–87. https://doi.org/10.1016/j.cmet.2013.04.020.

Cui, Weiwei, Dong Liu, Wei Gu, and Bo Chu. 2021. 'Peroxisome-Driven Ether-Linked Phospholipids Biosynthesis Is Essential for Ferroptosis'. *Cell Death & Differentiation* 28 (8): 2536–51. https://doi.org/10.1038/s41418-021-00769-0.

Darini, Cedric, Nour Ghaddar, Catherine Chabot, et al. 2019. 'An Integrated Stress Response via PKR Suppresses HER2+ Cancers and Improves Trastuzumab Therapy'. *Nature Communications* 10 (1): 2139. https://doi.org/10.1038/s41467-019-10138-8.

Das, Mitali, Athina Giannoudis, and Vijay Sharma. 2022. 'The Role of CPT1A as a Biomarker of Breast Cancer Progression: A Bioinformatic Approach'. *Scientific Reports* 12 (1): 16441. https://doi.org/10.1038/s41598-022-20585-x.

Dávalos, Alberto, Leigh Goedeke, Peter Smibert, et al. 2011. 'miR-33a/b Contribute to the Regulation of Fatty Acid Metabolism and Insulin Signaling'. *Proceedings of the National Academy of Sciences* 108 (22): 9232–37. https://doi.org/10.1073/pnas.1102281108.

De La Cruz-López, Karen G., Leonardo Josué Castro-Muñoz, Diego O. Reyes-Hernández, Alejandro García-Carrancá, and Joaquín Manzo-Merino. 2019. 'Lactate in the Regulation of Tumor Microenvironment and Therapeutic Approaches'. *Frontiers in Oncology* 9 (November): 1143. https://doi.org/10.3389/fonc.2019.01143.

Dean, John M., and Irfan J. Lodhi. 2018. 'Structural and Functional Roles of Ether Lipids'. *Protein & Cell* 9 (2): 196–206. https://doi.org/10.1007/s13238-017-0423-5.

DeFilippis, Rosa Anna, Hang Chang, Nancy Dumont, et al. 2012. 'CD36 Repression Activates a Multicellular Stromal Program Shared by High Mammographic Density and Tumor Tissues'. *Cancer Discovery* 2 (9): 826–39. https://doi.org/10.1158/2159-8290.CD-12-0107.

Denton, Richard M. 2009. 'Regulation of Mitochondrial Dehydrogenases by Calcium Ions'. *Biochimica et Biophysica Acta (BBA) - Bioenergetics* 1787 (11): 1309–16. https://doi.org/10.1016/j.bbabio.2009.01.005.

Derakhshan, Fatemeh, and Jorge S. Reis-Filho. 2022. 'Pathogenesis of Triple-Negative Breast Cancer'. *Annual Review of Pathology: Mechanisms of Disease* 17 (1): 181–204. https://doi.org/10.1146/annurev-pathol-042420-093238.

Desagher, Solange, and Jean-Claude Martinou. 2000. 'Mitochondria as the Central Control Point of Apoptosis'. *Trends in Cell Biology* 10 (9): 369–77. https://doi.org/10.1016/S0962-8924(00)01803-1.

Deval, Christiane, Cédric Chaveroux, Anne Catherine Maurin, et al. 2009. 'Amino Acid Limitation Regulates the Expression of Genes Involved in Several Specific Biological Processes through GCN2-Dependent and GCN2-Independent Pathways'. *FEBS Journal* 276 (3): 707–18. https://doi.org/10.1111/j.1742-4658.2008.06818.x.

Dietze, Eric C., Christopher Sistrunk, Gustavo Miranda-Carboni, Ruth O'Regan, and Victoria L. Seewaldt. 2015. 'Triple-Negative Breast Cancer in African-American Women: Disparities versus Biology'. *Nature Reviews Cancer* 15 (4): 248–54. https://doi.org/10.1038/nrc3896.

Dignam, J. J. 2003. 'Obesity, Tamoxifen Use, and Outcomes in Women With Estrogen Receptor-Positive Early-Stage Breast Cancer'. *CancerSpectrum Knowledge Environment* 95 (19): 1467–76. https://doi.org/10.1093/jnci/djg060.

Dikic, Ivan, and Zvulun Elazar. 2018. 'Mechanism and Medical Implications of Mammalian Autophagy'. *Nature Reviews Molecular Cell Biology* 19 (6): 349–64. https://doi.org/10.1038/s41580-018-0003-4.

Dixon, Scott J., Kathryn M. Lemberg, Michael R. Lamprecht, et al. 2012. 'Ferroptosis: An Iron-Dependent Form of Nonapoptotic Cell Death'. *Cell* 149 (5): 1060–72. https://doi.org/10.1016/j.cell.2012.03.042.

Dobrzyn, Pawel, Magdalena Jazurek, and Agnieszka Dobrzyn. 2010. 'Stearoyl-CoA Desaturase and Insulin Signaling — What Is the Molecular Switch?' *Biochimica et Biophysica Acta (BBA) - Bioenergetics* 1797 (6–7): 1189–94. https://doi.org/10.1016/j.bbabio.2010.02.007.

Doll, Sebastian, Florencio Porto Freitas, Ron Shah, et al. 2019. 'FSP1 Is a Glutathione-Independent Ferroptosis Suppressor'. *Nature* 575 (7784): 693–98. https://doi.org/10.1038/s41586-019-1707-0.

Doll, Sebastian, Bettina Proneth, Yulia Y. Tyurina, et al. 2017. 'ACSL4 Dictates Ferroptosis Sensitivity by Shaping Cellular Lipid Composition'. *Nature Chemical Biology* 13 (1): 91–98. https://doi.org/10.1038/nchembio.2239.

Dolma, Sonam, Stephen L. Lessnick, William C. Hahn, and Brent R. Stockwell. 2003. 'Identification of Genotype-Selective Antitumor Agents Using Synthetic Lethal

Chemical Screening in Engineered Human Tumor Cells'. *Cancer Cell* 3 (3): 285–96. https://doi.org/10.1016/S1535-6108(03)00050-3.

Du, Hongxiang, Tianhan Xu, Sihui Yu, Sufang Wu, and Jiawen Zhang. 2025. 'Mitochondrial Metabolism and Cancer Therapeutic Innovation'. *Signal Transduction and Targeted Therapy* 10 (1): 245. https://doi.org/10.1038/s41392-025-02311-x.

Du, Linna, Han Yang, Yufei Ren, et al. 2023. 'Inhibition of LSD1 Induces Ferroptosis through the ATF4-xCT Pathway and Shows Enhanced Anti-Tumor Effects with Ferroptosis Inducers in NSCLC'. *Cell Death & Disease* 14 (11): 716. https://doi.org/10.1038/s41419-023-06238-5.

Dudka, Wioleta, Grazyna Hoser, Shamba S. Mondal, et al. 2022. 'Targeting Integrated Stress Response with ISRIB Combined with Imatinib Treatment Attenuates RAS/RAF/MAPK and STAT5 Signaling and Eradicates Chronic Myeloid Leukemia Cells'. *BMC Cancer* 22 (1): 1254. https://doi.org/10.1186/s12885-022-10289-w.

Dupuy, Fanny, Sébastien Tabariès, Sylvia Andrzejewski, et al. 2015. 'PDK1-Dependent Metabolic Reprogramming Dictates Metastatic Potential in Breast Cancer'. *Cell Metabolism* 22 (4): 577–89. https://doi.org/10.1016/j.cmet.2015.08.007.

Duszyński, Jerzy, Rafał Kozieł, Wojciech Brutkowski, Joanna Szczepanowska, and Krzysztof Zabłocki. 2006. 'The Regulatory Role of Mitochondria in Capacitative Calcium Entry'. *Biochimica et Biophysica Acta (BBA) - Bioenergetics* 1757 (5–6): 380–87. https://doi.org/10.1016/j.bbabio.2006.04.017.

Echeverria, Gloria V., Zhongqi Ge, Sahil Seth, et al. 2019. 'Resistance to Neoadjuvant Chemotherapy in Triple-Negative Breast Cancer Mediated by a Reversible Drug-Tolerant State'. *Science Translational Medicine* 11 (488): eaav0936. https://doi.org/10.1126/scitranslmed.aav0936.

Egolf, Shaun, Jonathan Zou, Amy Anderson, et al. 2021. 'MLL4 Mediates Differentiation and Tumor Suppression through Ferroptosis'. *Science Advances* 7 (50): eabj9141. https://doi.org/10.1126/sciadv.abj9141.

Eisner, Verónica, Martin Picard, and György Hajnóczky. 2018. 'Mitochondrial Dynamics in Adaptive and Maladaptive Cellular Stress Responses'. *Nature Cell Biology* 20 (7): 755–65. https://doi.org/10.1038/s41556-018-0133-0.

Elhage, Rima, Mairead Kelly, Nicolas Goudin, et al. 2024. 'Mitochondrial Dynamics and Metabolic Regulation Control T Cell Fate in the Thymus'. *Frontiers in Immunology* 14 (January): 1270268. https://doi.org/10.3389/fimmu.2023.1270268.

Elia, Ilaria, and Marcia C. Haigis. 2021. 'Metabolites and the Tumour Microenvironment: From Cellular Mechanisms to Systemic Metabolism'. *Nature Metabolism* 3 (1): 21–32. https://doi.org/10.1038/s42255-020-00317-z.

Ellis, Matthew J., and Charles M. Perou. 2013. 'The Genomic Landscape of Breast Cancer as a Therapeutic Roadmap'. *Cancer Discovery* 3 (1): 27–34. https://doi.org/10.1158/2159-8290.CD-12-0462.

Fahy, Eoin, Shankar Subramaniam, H. Alex Brown, et al. 2005. 'A Comprehensive Classification System for Lipids'. *Journal of Lipid Research* 46 (5): 839–61. https://doi.org/10.1194/jlr.E400004-JLR200.

Falletta, Paola, Luis Sanchez-del-Campo, Jagat Chauhan, et al. 2017. 'Translation Reprogramming Is an Evolutionarily Conserved Driver of Phenotypic Plasticity and Therapeutic Resistance in Melanoma'. *Genes and Development* 31 (1): 18–33. https://doi.org/10.1101/gad.290940.116.

Fan, Z., A. K. Wirth, D. Chen, et al. 2017. 'Nrf2-Keap1 Pathway Promotes Cell Proliferation and Diminishes Ferroptosis'. *Oncogenesis* 6 (8): e371–e371. https://doi.org/10.1038/oncsis.2017.65.

Fang, Chunyao, Suiqing Zhou, Kai Yu, et al. 2026. 'Lactate Metabolism and Lactylation in Cancer: From Pathogenesis to Therapeutic Advances'. *Signal Transduction and Targeted Therapy* 11 (1): 190. https://doi.org/10.1038/s41392-026-02672-x.

Farese, Robert V., and Tobias C. Walther. 2023. 'Glycerolipid Synthesis and Lipid Droplet Formation in the Endoplasmic Reticulum'. *Cold Spring Harbor Perspectives in Biology* 15 (5): a041246. https://doi.org/10.1101/cshperspect.a041246.

Feitelson, Mark A., Alla Arzumanyan, Rob J. Kulathinal, et al. 2015. 'Sustained Proliferation in Cancer: Mechanisms and Novel Therapeutic Targets'. *Seminars in Cancer Biology* 35 (December): S25–54. https://doi.org/10.1016/j.semcancer.2015.02.006.

Feng, Huizhong, Kenji Schorpp, Jenny Jin, et al. 2020. 'Transferrin Receptor Is a Specific Ferroptosis Marker'. *Cell Reports* 30 (10): 3411-3423.e7. https://doi.org/10.1016/j.celrep.2020.02.049.

Fessler, Evelyn, Eva-Maria Eckl, Sabine Schmitt, et al. 2020. 'A Pathway Coordinated by DELE1 Relays Mitochondrial Stress to the Cytosol'. *Nature* 579 (7799): 433–37. https://doi.org/10.1038/s41586-020-2076-4.

Filadi, Riccardo, Agnese De Mario, Matteo Audano, et al. 2023. 'Sustained IP3-Linked Ca2+ Signaling Promotes Progression of Triple Negative Breast Cancer Cells by Regulating Fatty Acid Metabolism'. *Frontiers in Cell and Developmental Biology* 11 (March): 1071037. https://doi.org/10.3389/fcell.2023.1071037.

Fonseca, Tiago Branco, Ángela Sánchez-Guerrero, Ira Milosevic, and Nuno Raimundo. 2019. 'Mitochondrial Fission Requires DRP1 but Not Dynamins'. *Nature* 570 (7761): E34–42. https://doi.org/10.1038/s41586-019-1296-y.

Friedman, Jonathan R., Laura L. Lackner, Matthew West, Jared R. DiBenedetto, Jodi Nunnari, and Gia K. Voeltz. 2011. 'ER Tubules Mark Sites of Mitochondrial Division'. *Science* 334 (6054): 358–62. https://doi.org/10.1126/science.1207385.

Friedmann Angeli, Jose Pedro, Manuela Schneider, Bettina Proneth, et al. 2014. 'Inactivation of the Ferroptosis Regulator Gpx4 Triggers Acute Renal Failure in Mice'. *Nature Cell Biology* 16 (12): 1180–91. https://doi.org/10.1038/ncb3064.

Fujimoto, Jun, Osamu Kurasawa, Terufumi Takagi, et al. 2019. 'Identification of Novel, Potent, and Orally Available GCN2 Inhibitors with Type I Half Binding Mode'. *ACS Medicinal Chemistry Letters* 10 (10): 1498–503. https://doi.org/10.1021/acsmedchemlett.9b00400.

Galluzzi, Lorenzo, Catherine Brenner, Eugenia Morselli, Zahia Touat, and Guido Kroemer. 2008. 'Viral Control of Mitochondrial Apoptosis'. *PLoS Pathogens* 4 (5): e1000018. https://doi.org/10.1371/journal.ppat.1000018.

Gammella, Elena, Stefania Recalcati, Ilona Rybinska, Paolo Buratti, and Gaetano Cairo. 2015. 'Iron-Induced Damage in Cardiomyopathy: Oxidative-Dependent and Independent Mechanisms'. *Oxidative Medicine and Cellular Longevity* 2015: 1–10. https://doi.org/10.1155/2015/230182.

Gao, Minghui, Prashant Monian, Qiuhui Pan, Wei Zhang, Jenny Xiang, and Xuejun Jiang. 2016. 'Ferroptosis Is an Autophagic Cell Death Process'. *Cell Research* 26 (9): 1021–32. https://doi.org/10.1038/cr.2016.95.

Gao, Ruize, Ravi K. R. Kalathur, Mairene Coto-Llerena, et al. 2021. 'YAP/TAZ and ATF4 Drive Resistance to Sorafenib in Hepatocellular Carcinoma by Preventing Ferroptosis'. *EMBO Molecular Medicine* 13 (12): e14351. https://doi.org/10.15252/emmm.202114351.

Gao, Song, and Junjie Hu. 2021. 'Mitochondrial Fusion: The Machineries In and Out'. *Trends in Cell Biology* 31 (1): 62–74. https://doi.org/10.1016/j.tcb.2020.09.008.

Garbincius, Joanne F., and John W. Elrod. 2022. 'Mitochondrial Calcium Exchange in Physiology and Disease'. *Physiological Reviews* 102 (2): 893–992. https://doi.org/10.1152/physrev.00041.2020.

García-Jiménez, Custodia, and Colin R. Goding. 2019. 'Starvation and Pseudo-Starvation as Drivers of Cancer Metastasis through Translation Reprogramming'. *Cell Metabolism* 29 (2): 254–67. https://doi.org/10.1016/j.cmet.2018.11.018.

Gatti, Priya, Cara Schiavon, Julien Cicero, Uri Manor, and Marc Germain. 2025. 'Mitochondria- and ER-Associated Actin Are Required for Mitochondrial Fusion'. *Nature Communications* 16 (1): 451. https://doi.org/10.1038/s41467-024-55758-x.

Geng, Peizhen, Yuhua Chi, Yuan Yuan, et al. 2023. 'Novel Chimeric Antigen Receptor T Cell-Based Immunotherapy: A Perspective for Triple-Negative Breast Cancer'. *Frontiers in Cell and Developmental Biology* 11 (June): 1158539. https://doi.org/10.3389/fcell.2023.1158539.

Gherardi, Gaia, Halenya Monticelli, Rosario Rizzuto, and Cristina Mammucari. 2020. 'The Mitochondrial Ca2+ Uptake and the Fine-Tuning of Aerobic Metabolism'.

Frontiers in Physiology 11 (October): 554904. https://doi.org/10.3389/fphys.2020.554904.

Giorgi, Carlotta, Massimo Bonora, Giovanni Sorrentino, et al. 2015. 'P53 at the Endoplasmic Reticulum Regulates Apoptosis in a Ca^{2+} -Dependent Manner'. *Proceedings of the National Academy of Sciences* 112 (6): 1779–84. https://doi.org/10.1073/pnas.1410723112.

Giorgi, Carlotta, Keisuke Ito, Hui-Kuan Lin, et al. 2010. 'PML Regulates Apoptosis at Endoplasmic Reticulum by Modulating Calcium Release'. *Science* 330 (6008): 1247–51. https://doi.org/10.1126/science.1189157.

Giorgi, Carlotta, Sonia Missiroli, Simone Patergnani, Jerzy Duszynski, Mariusz R. Wieckowski, and Paolo Pinton. 2015. 'Mitochondria-Associated Membranes: Composition, Molecular Mechanisms, and Physiopathological Implications'. *Antioxidants & Redox Signaling* 22 (12): 995–1019. https://doi.org/10.1089/ars.2014.6223.

Giri, Pragatheiswar, Ignacio G. Camarillo, and Raji Sundararajan. 2023. 'Enhancement of Reactive Oxygen Species Production in Triple Negative Breast Cancer Cells Treated with Electric Pulses and Resveratrol'. *Exploration of Targeted Anti-Tumor Therapy*, February 28, 42–56. https://doi.org/10.37349/etat.2023.00122.

Giró-Perafita, Ariadna, Ariadna Sarrats, Ferran Pérez-Bueno, et al. 2017. 'Fatty Acid Synthase Expression and Its Association with Clinico-Histopathological Features in Triple-Negative Breast Cancer'. *Oncotarget* 8 (43): 74391–405. https://doi.org/10.18632/oncotarget.20152.

Golic, I., K. Velickovic, M. Markelic, et al. 2014. 'Calcium-Induced Alteration of Mitochondrial Morphology and Mitochondrial-Endoplasmic Reticulum Contacts in Rat Brown Adipocytes'. *European Journal of Histochemistry* 58 (3). https://doi.org/10.4081/ejh.2014.2377.

Gong, Yue, Peng Ji, Yun-Song Yang, et al. 2021. 'Metabolic-Pathway-Based Subtyping of Triple-Negative Breast Cancer Reveals Potential Therapeutic Targets'. *Cell Metabolism* 33 (1): 51-64.e9. https://doi.org/10.1016/j.cmet.2020.10.012.

Gruber, Florian, Cayo Mecking Ornelas, Susanne Karner, et al. 2015. 'Nrf2 Deficiency Causes Lipid Oxidation, Inflammation, and Matrix-Protease Expression in DHA-Supplemented and UVA-Irradiated Skin Fibroblasts'. *Free Radical Biology and Medicine* 88 (November): 439–51. https://doi.org/10.1016/j.freeradbiomed.2015.05.006.

Guedouari, Hala, Tanya Daigle, Luca Scorrano, and Etienne Hebert-Chatelain. 2017. 'Sirtuin 5 Protects Mitochondria from Fragmentation and Degradation during Starvation'. *Biochimica et Biophysica Acta (BBA) - Molecular Cell Research* 1864 (1): 169–76. https://doi.org/10.1016/j.bbamcr.2016.10.015.

Guha, Manti, Satish Srinivasan, Pichai Raman, et al. 2018. 'Aggressive Triple Negative Breast Cancers Have Unique Molecular Signature on the Basis of Mitochondrial Genetic and Functional Defects'. *Biochimica et Biophysica Acta (BBA) - Molecular Basis of Disease* 1864 (4): 1060–71. https://doi.org/10.1016/j.bbadis.2018.01.002.

Guo, Feng, Shi Zong, Xin Zhang, et al. 2026. 'Ferroptosis and Metastasis: Molecular Checkpoints, Microenvironmental Dynamics, and Therapeutic Opportunities'. *Molecular Cancer* 25 (1): 45. https://doi.org/10.1186/s12943-025-02544-y.

Guo, Zhiqiang, Karl-Frédérik Bergeron, Marine Lingrand, and Catherine Mounier. 2023. 'Unveiling the MUFA–Cancer Connection: Insights from Endogenous and Exogenous Perspectives'. *International Journal of Molecular Sciences* 24 (12): 9921. https://doi.org/10.3390/ijms24129921.

Gwinn, Dana M., Alex G. Lee, Marcela Briones-Martin-del-Campo, et al. 2018. 'Oncogenic KRAS Regulates Amino Acid Homeostasis and Asparagine Biosynthesis via ATF4 and Alters Sensitivity to L-Asparaginase'. *Cancer Cell* 33 (1): 91-107.e6. https://doi.org/10.1016/j.ccell.2017.12.003.

Haggag, Yusuf A., Mohamed Yasser, Murtaza M. Tambuwala, Suleiman S. El Tokhy, Mohammad Isreb, and Ahmed A. Donia. 2021. 'Repurposing of Guanabenz Acetate by Encapsulation into Long-Circulating Nanopolymersomes for Treatment of Triple-Negative Breast Cancer'. *International Journal of Pharmaceutics* 600 (May): 120532. https://doi.org/10.1016/j.ijpharm.2021.120532.

Hahnefeld, Lisa, Lisa Gruber, Nina Schömel, et al. 2020. 'Ether Lipid and Sphingolipid Expression Patterns Are Estrogen Receptor-Dependently Altered in Breast Cancer Cells'. *The International Journal of Biochemistry & Cell Biology* 127 (October): 105834. https://doi.org/10.1016/j.biocel.2020.105834.

Halbrook, Christopher J., Galloway Thurston, Seth Boyer, et al. 2022. 'Differential Integrated Stress Response and Asparagine Production Drive Symbiosis and Therapy Resistance of Pancreatic Adenocarcinoma Cells'. *Nature Cancer* 3 (11): 1386–403. https://doi.org/10.1038/s43018-022-00463-1.

Hall, Duane D., Yuejin Wu, Frederick E. Domann, Douglas R. Spitz, and Mark E. Anderson. 2014. 'Mitochondrial Calcium Uniporter Activity Is Dispensable for MDA-MB-231 Breast Carcinoma Cell Survival'. *PLoS ONE* 9 (5): e96866. https://doi.org/10.1371/journal.pone.0096866.

Hamamura, Kazunori, Kazumasa Minami, Nancy Tanjung, et al. 2014. 'Attenuation of Malignant Phenotypes of Breast Cancer Cells through eIF2α-Mediated Downregulation of Rac1 Signaling'. *International Journal of Oncology* 44 (6): 1980–88. https://doi.org/10.3892/ijo.2014.2366.

Han, Shujun, Ryan Wei, Xiaodi Zhang, et al. 2019. 'CPT1A/2-Mediated FAO Enhancement—A Metabolic Target in Radioresistant Breast Cancer'. *Frontiers in Oncology* 9 (November): 1201. https://doi.org/10.3389/fonc.2019.01201.

Han, Xiao-Jian, Zhang-Jian Yang, Li-Ping Jiang, et al. 2015. 'Mitochondrial Dynamics Regulates Hypoxia-Induced Migration and Antineoplastic Activity of Cisplatin in Breast Cancer Cells'. *International Journal of Oncology* 46 (2): 691–700. https://doi.org/10.3892/ijo.2014.2781.

Hanahan, Douglas. 2022. 'Hallmarks of Cancer: New Dimensions'. *Cancer Discovery* 12 (1): 31–46. https://doi.org/10.1158/2159-8290.CD-21-1059.

Harbeck, Nadia, Frédérique Penault-Llorca, Javier Cortes, et al. 2019. 'Breast Cancer'. *Nature Reviews Disease Primers* 5 (1): 66. https://doi.org/10.1038/s41572-019-0111-2.

Harding, Heather P., Isabel Novoa, Yuhong Zhang, et al. 2000. 'Regulated Translation Initiation Controls Stress-Induced Gene Expression in Mammalian Cells'. *Molecular Cell* 6 (5): 1099–108. https://doi.org/10.1016/S1097-2765(00)00108-8.

Hart, Lori S., John T. Cunningham, Tatini Datta, et al. 2012. 'ER Stress–Mediated Autophagy Promotes Myc-Dependent Transformation and Tumor Growth'. *Journal of Clinical Investigation* 122 (12): 4621–34. https://doi.org/10.1172/JCI62973.

Hartman, Anne-Renee, Rajesh R. Kaldate, Lisa M. Sailer, et al. 2012. 'Prevalence of *BRCA* Mutations in an Unselected Population of Triple-negative Breast Cancer'. *Cancer* 118 (11): 2787–95. https://doi.org/10.1002/cncr.26576.

Hatzivassiliou, Georgia, Fangping Zhao, Daniel E. Bauer, et al. 2005. 'ATP Citrate Lyase Inhibition Can Suppress Tumor Cell Growth'. *Cancer Cell* 8 (4): 311–21. https://doi.org/10.1016/j.ccr.2005.09.008.

He, Feng, Peng Zhang, Junlai Liu, et al. 2023. 'ATF4 Suppresses Hepatocarcinogenesis by Inducing SLC7A11 (xCT) to Block Stress-Related Ferroptosis'. *Journal of Hepatology* 79 (2): 362–77. https://doi.org/10.1016/j.jhep.2023.03.016.

Hentze, Matthias W., Martina U. Muckenthaler, Bruno Galy, and Clara Camaschella. 2010. 'Two to Tango: Regulation of Mammalian Iron Metabolism'. *Cell* 142 (1): 24–38. https://doi.org/10.1016/j.cell.2010.06.028.

Hess, Daniel, Jeffrey W. Chisholm, and R. Ariel Igal. 2010. 'Inhibition of StearoylCoA Desaturase Activity Blocks Cell Cycle Progression and Induces Programmed Cell Death in Lung Cancer Cells'. *PLoS ONE* 5 (6): e11394. https://doi.org/10.1371/journal.pone.0011394.

Hinton, Antentor, Prasanna Katti, Margaret Mungai, et al. 2024. 'ATF4-dependent Increase in Mitochondrial-endoplasmic Reticulum Tethering Following OPA1

Deletion in Skeletal Muscle'. *Journal of Cellular Physiology* 239 (4): e31204. https://doi.org/10.1002/jcp.31204.

Hiramatsu, Nobuhiko, Carissa Messah, Jaeseok Han, Matthew M. LaVail, Randal J. Kaufman, and Jonathan H. Lin. 2014. 'Translational and Posttranslational Regulation of XIAP by eIF2α and ATF4 Promotes ER Stress–Induced Cell Death during the Unfolded Protein Response'. *Molecular Biology of the Cell* 25 (9): 1411–20. https://doi.org/10.1091/mbc.e13-11-0664.

Hishikawa, Daisuke, Hideo Shindou, Saori Kobayashi, Hiroki Nakanishi, Ryo Taguchi, and Takao Shimizu. 2008. 'Discovery of a Lysophospholipid Acyltransferase Family Essential for Membrane Asymmetry and Diversity'. *Proceedings of the National Academy of Sciences* 105 (8): 2830–35. https://doi.org/10.1073/pnas.0712245105.

Holder, Ashley M., Ana M. Gonzalez-Angulo, Huiqin Chen, et al. 2013. 'High Stearoyl-CoA Desaturase 1 Expression Is Associated with Shorter Survival in Breast Cancer Patients'. *Breast Cancer Research and Treatment* 137 (1): 319–27. https://doi.org/10.1007/s10549-012-2354-4.

Hou, Wen, Yangchun Xie, Xinxin Song, et al. 2016. 'Autophagy Promotes Ferroptosis by Degradation of Ferritin'. *Autophagy* 12 (8): 1425–28. https://doi.org/10.1080/15548627.2016.1187366.

Houten, Sander M., Sara Violante, Fatima V. Ventura, and Ronald J. A. Wanders. 2016. 'The Biochemistry and Physiology of Mitochondrial Fatty Acid β-Oxidation and Its Genetic Disorders'. *Annual Review of Physiology* 78 (1): 23–44. https://doi.org/10.1146/annurev-physiol-021115-105045.

Hu, Jinsong, Nana Dang, Eline Menu, et al. 2012. 'Activation of ATF4 Mediates Unwanted Mcl-1 Accumulation by Proteasome Inhibition'. *Blood* 119 (3): 826–37. https://doi.org/10.1182/blood-2011-07-366492.

Hu, Kewen, Kun Li, Jing Lv, et al. 2020. 'Suppression of the SLC7A11/Glutathione Axis Causes Synthetic Lethality in KRAS-Mutant Lung Adenocarcinoma'. *Journal of Clinical Investigation* 130 (4): 1752–66. https://doi.org/10.1172/JCI124049.

Hu, Zhenghui, Yuwen Wang, Chuan Liu, Wei Wu, Hui Zeng, and Hong Zhou. 2025. 'From Biosynthesis to Function: The Roles of Ether Lipids in Cancer Development and Treatment'. *Lipids in Health and Disease* 24 (1): 377. https://doi.org/10.1186/s12944-025-02791-4.

Huang, Guang-Ming, Qing-Hu Jiang, Can Cai, Mei Qu, and Wei Shen. 2015. 'SCD1 Negatively Regulates Autophagy-Induced Cell Death in Human Hepatocellular Carcinoma through Inactivation of the AMPK Signaling Pathway'. *Cancer Letters* 358 (2): 180–90. https://doi.org/10.1016/j.canlet.2014.12.036.

Huang, Xiaojia, Xing Li, Xinhua Xie, et al. 2016. 'High Expressions of LDHA and AMPK as Prognostic Biomarkers for Breast Cancer'. *The Breast* 30 (December): 39–46. https://doi.org/10.1016/j.breast.2016.08.014.

Hurvitz, Sara Alsterlind, Nicholas P. McAndrew, Aditya Bardia, et al. 2021. 'A Careful Reassessment of Anthracycline Use in Curable Breast Cancer'. *Npj Breast Cancer* 7 (1): 134. https://doi.org/10.1038/s41523-021-00342-5.

Indiveri, Cesare, Vito Iacobazzi, Annamaria Tonazzi, et al. 2011. 'The Mitochondrial Carnitine/Acylcarnitine Carrier: Function, Structure and Physiopathology'. *Molecular Aspects of Medicine* 32 (4–6): 223–33. https://doi.org/10.1016/j.mam.2011.10.008.

Jackson, Richard J., Christopher U. T. Hellen, and Tatyana V. Pestova. 2010. 'The Mechanism of Eukaryotic Translation Initiation and Principles of Its Regulation'. *Nature Reviews Molecular Cell Biology* 11 (2): 113–27. https://doi.org/10.1038/nrm2838.

Jewer, Michael, Laura Lee, Matthew Leibovitch, et al. 2020. 'Translational Control of Breast Cancer Plasticity'. *Nature Communications* 11 (1): 2498. https://doi.org/10.1038/s41467-020-16352-z.

Jiang, Le, Ning Kon, Tongyuan Li, et al. 2015. 'Ferroptosis as a P53-Mediated Activity during Tumour Suppression'. *Nature* 520 (7545): 57–62. https://doi.org/10.1038/nature14344.

Jiang, Shuai, Ling-Fei Zhang, Hong-Wei Zhang, et al. 2012. 'A Novel miR-155/miR-143 Cascade Controls Glycolysis by Regulating Hexokinase 2 in Breast Cancer Cells'. *The EMBO Journal* 31 (8): 1985–98. https://doi.org/10.1038/emboj.2012.45.

Jiang, Xuejun, Brent R. Stockwell, and Marcus Conrad. 2021. 'Ferroptosis: Mechanisms, Biology and Role in Disease'. *Nature Reviews Molecular Cell Biology* 22 (4): 266–82. https://doi.org/10.1038/s41580-020-00324-8.

Jiang, Yi-Zhou, Ding Ma, Chen Suo, et al. 2019. 'Genomic and Transcriptomic Landscape of Triple-Negative Breast Cancers: Subtypes and Treatment Strategies'. *Cancer Cell* 35 (3): 428-440.e5. https://doi.org/10.1016/j.ccell.2019.02.001.

Jin, Hyeon-Ok, Sung-Keum Seo, Sang-Hyeok Woo, et al. 2009. 'Nuclear Protein 1 Induced by ATF4 in Response to Various Stressors Acts as a Positive Regulator on the Transcriptional Activation of ATF4'. *IUBMB Life* 61 (12): 1153–58. https://doi.org/10.1002/iub.271.

Jin, Mei, Chunlei Yuan, Sijia Duan, Bin Zeng, and Lingjuan Pan. 2023. 'Downregulation of ACC Expression Suppresses Cell Viability and Migration in the Malignant Progression of Breast Cancer'. *Experimental and Therapeutic Medicine* 26 (3): 445. https://doi.org/10.3892/etm.2023.12144.

Johnstone, Timothy G., Ariel A. Bazzini, and Antonio J. Giraldez. 2016. 'Upstream ORF s Are Prevalent Translational Repressors in Vertebrates'. *The EMBO Journal* 35 (7): 706–23. https://doi.org/10.15252/embj.201592759.

Jousse, Céline, Seiichi Oyadomari, Isabel Novoa, et al. 2003. 'Inhibition of a Constitutive Translation Initiation Factor 2α Phosphatase, *CReP* , Promotes Survival of Stressed Cells'. *The Journal of Cell Biology* 163 (4): 767–75. https://doi.org/10.1083/jcb.200308075.

Juárez, Patricia, Khalid S. Mohammad, Juan Juan Yin, et al. 2012. 'Halofuginone Inhibits the Establishment and Progression of Melanoma Bone Metastases'. *Cancer Research* 72 (23): 6247–56. https://doi.org/10.1158/0008-5472.CAN-12-1444.

Kagan, Valerian E., Gaowei Mao, Feng Qu, et al. 2017. 'Oxidized Arachidonic and Adrenic PEs Navigate Cells to Ferroptosis'. *Nature Chemical Biology* 13 (1): 81–90. https://doi.org/10.1038/nchembio.2238.

Kalkavan, Halime, Mark J. Chen, Jeremy C. Crawford, et al. 2022. 'Sublethal Cytochrome c Release Generates Drug-Tolerant Persister Cells'. *Cell* 185 (18): 3356-3374.e22. https://doi.org/10.1016/j.cell.2022.07.025.

Kang, Man-Jong, Takahiro Fujino, Hironobu Sasano, et al. 1997. 'A Novel Arachidonate-Preferring Acyl-CoA Synthetase Is Present in Steroidogenic Cells of the Rat Adrenal, Ovary, and Testis'. *Proceedings of the National Academy of Sciences* 94 (7): 2880–84. https://doi.org/10.1073/pnas.94.7.2880.

Kardos, Gregory R., Raghavendra Gowda, Saketh Sriram Dinavahi, Scot Kimball, and Gavin P. Robertson. 2020. 'Salubrinal in Combination With 4E1RCat Synergistically Impairs Melanoma Development by Disrupting the Protein Synthetic Machinery'. *Frontiers in Oncology* 10 (June): 834. https://doi.org/10.3389/fonc.2020.00834.

Karpinski, B. A., G. D. Morle, J. Huggenvik, M. D. Uhler, and J. M. Leiden. 1992. 'Molecular Cloning of Human CREB-2: An ATF/CREB Transcription Factor That Can Negatively Regulate Transcription from the cAMP Response Element.' *Proceedings of the National Academy of Sciences* 89 (11): 4820–24. https://doi.org/10.1073/pnas.89.11.4820.

Kato, Yu, Kazuhiro Kunimasa, Mizuki Takahashi, et al. 2020. 'GZD824 Inhibits GCN2 and Sensitizes Cancer Cells to Amino Acid Starvation Stress'. *Molecular Pharmacology* 98 (6): 669–76. https://doi.org/10.1124/molpharm.120.000070.

Kaufman, Randal J. 1999. *Stress Signaling from the Lumen of the Endoplasmic Reticulum: Coordination of Gene Transcriptional and Translational Controls*. www.genesdev.org.

Kawalec, Maria, Anna Boratyńska-Jasińska, Małgorzata Beręsewicz, Dorota Dymkowska, Krzysztof Zabłocki, and Barbara Zabłocka. 2015. 'Mitofusin 2 Deficiency Affects Energy Metabolism and Mitochondrial Biogenesis in MEF

Cells'. *PLOS ONE* 10 (7): e0134162. https://doi.org/10.1371/journal.pone.0134162.

Kazemi, Shirin, Zineb Mounir, Dionissios Baltzis, et al. n.d. *A Novel Function of eIF2 Kinases as Inducers of the Phosphoinositide-3 Kinase Signaling Pathway□D*.

Keller, Tracy L., Davide Zocco, Mark S. Sundrud, et al. 2012. 'Halofuginone and Other Febrifugine Derivatives Inhibit Prolyl-tRNA Synthetase'. *Nature Chemical Biology* 8 (3): 311–17. https://doi.org/10.1038/nchembio.790.

Keskinkilic, Merve, and Ruth Sacks. 2024. 'Antibody-Drug Conjugates in Triple Negative Breast Cancer'. *Clinical Breast Cancer* 24 (3): 163–74. https://doi.org/10.1016/j.clbc.2024.01.008.

Kim, Jong Woo, Ji-Yoon Lee, Mihee Oh, and Eun-Woo Lee. 2023. 'An Integrated View of Lipid Metabolism in Ferroptosis Revisited via Lipidomic Analysis'. *Experimental & Molecular Medicine* 55 (8): 1620–31. https://doi.org/10.1038/s12276-023-01077-y.

Komljenovic, Dorde, Roger Sandhoff, Andre Teigler, Hans Heid, Wilhelm W. Just, and Karin Gorgas. 2009. 'Disruption of Blood-Testis Barrier Dynamics in Ether-Lipid-Deficient Mice'. *Cell and Tissue Research* 337 (2): 281–99. https://doi.org/10.1007/s00441-009-0809-7.

Koppula, Pranavi, Guang Lei, Yilei Zhang, et al. 2022. 'A Targetable CoQ-FSP1 Axis Drives Ferroptosis- and Radiation-Resistance in KEAP1 Inactive Lung Cancers'. *Nature Communications* 13 (1): 2206. https://doi.org/10.1038/s41467-022-29905-1.

Kraft, Vanessa A. N., Carla T. Bezjian, Susanne Pfeiffer, et al. 2020. 'GTP Cyclohydrolase 1/Tetrahydrobiopterin Counteract Ferroptosis through Lipid Remodeling'. *ACS Central Science* 6 (1): 41–53. https://doi.org/10.1021/acscentsci.9b01063.

Kreß, Julia Katharina Charlotte, Christina Jessen, Anita Hufnagel, et al. 2023. 'The Integrated Stress Response Effector ATF4 Is an Obligatory Metabolic Activator of NRF2'. *Cell Reports* 42 (7): 112724–112724. https://doi.org/10.1016/j.celrep.2023.112724.

Kuemmerle, Nancy B., Evelien Rysman, Portia S. Lombardo, et al. 2011. 'Lipoprotein Lipase Links Dietary Fat to Solid Tumor Cell Proliferation'. *Molecular Cancer Therapeutics* 10 (3): 427–36. https://doi.org/10.1158/1535-7163.MCT-10-0802.

Kung, Hsiu-Ni, Jeffrey R. Marks, and Jen-Tsan Chi. 2011. 'Glutamine Synthetase Is a Genetic Determinant of Cell Type–Specific Glutamine Independence in Breast Epithelia'. *PLoS Genetics* 7 (8): e1002229. https://doi.org/10.1371/journal.pgen.1002229.

Kuwana, Tomomi, Mason R. Mackey, Guy Perkins, et al. 2002. 'Bid, Bax, and Lipids Cooperate to Form Supramolecular Openings in the Outer Mitochondrial

Membrane'. *Cell* 111 (3): 331–42. https://doi.org/10.1016/S0092-8674(02)01036-X.

Kwon, Min-Young, Eunhee Park, Seon-Jin Lee, and Su Wol Chung. 2015. 'Heme Oxygenase-1 Accelerates Erastin-Induced Ferroptotic Cell Death'. *Oncotarget* 6 (27): 24393–403. https://doi.org/10.18632/oncotarget.5162.

Kwong, Soke Chee, Amira Hajirah Abd Jamil, Anthony Rhodes, Nur Aishah Taib, and Ivy Chung. 2019. 'Metabolic Role of Fatty Acid Binding Protein 7 in Mediating Triple-Negative Breast Cancer Cell Death via PPAR-α Signaling'. *Journal of Lipid Research* 60 (11): 1807–17. https://doi.org/10.1194/jlr.M092379.

Labbé, Katherine, Lauren LeBon, Bryan King, et al. 2024. 'Specific Activation of the Integrated Stress Response Uncovers Regulation of Central Carbon Metabolism and Lipid Droplet Biogenesis'. *Nature Communications* 15 (1): 8301. https://doi.org/10.1038/s41467-024-52538-5.

Lampa, Michael, Heike Arlt, Timothy He, et al. 2017. 'Glutaminase Is Essential for the Growth of Triple-Negative Breast Cancer Cells with a Deregulated Glutamine Metabolism Pathway and Its Suppression Synergizes with mTOR Inhibition'. *PLOS ONE* 12 (9): e0185092. https://doi.org/10.1371/journal.pone.0185092.

Lee, Dong Min, Min Ji Seo, Hong Jae Lee, Hyo Joon Jin, and Kyeong Sook Choi. 2022. 'ISRIB plus Bortezomib Triggers Paraptosis in Breast Cancer Cells via Enhanced Translation and Subsequent Proteotoxic Stress'. *Biochemical and Biophysical Research Communications* 596 (March): 56–62. https://doi.org/10.1016/j.bbrc.2022.01.082.

Lee, Jaewang, and Jong-Lyel Roh. 2023. 'Epithelial-Mesenchymal Plasticity: Implications for Ferroptosis Vulnerability and Cancer Therapy'. *Critical Reviews in Oncology/Hematology* 185 (May): 103964. https://doi.org/10.1016/j.critrevonc.2023.103964.

Lee, Ji-Yoon, Jong Woo Kim, and Eun-Woo Lee. 2023. 'A New Way to Create Ether Lipids'. *Nature Chemical Biology* 19 (3): 259–60. https://doi.org/10.1038/s41589-023-01255-z.

Lee, Juwon, Suin Jang, Jihye Im, et al. 2024. 'Stearoyl-CoA Desaturase 1 Inhibition Induces ER Stress-Mediated Apoptosis in Ovarian Cancer Cells'. *Journal of Ovarian Research* 17 (1): 73. https://doi.org/10.1186/s13048-024-01389-1.

Lee, Kyung-min, Jennifer M. Giltnane, Justin M. Balko, et al. 2017. 'MYC and MCL1 Cooperatively Promote Chemotherapy-Resistant Breast Cancer Stem Cells via Regulation of Mitochondrial Oxidative Phosphorylation'. *Cell Metabolism* 26 (4): 633-647.e7. https://doi.org/10.1016/j.cmet.2017.09.009.

Lee, Sangjun, Syed K. Mohsin, Sufeng Mao, Susan G. Hilsenbeck, Dan Medina, and D. Craig Allred. 2005. 'Hormones, Receptors, and Growth in Hyperplastic Enlarged

Lobular Units: Early Potential Precursors of Breast Cancer'. *Breast Cancer Research* 8 (1): R6. https://doi.org/10.1186/bcr1367.

Lehmann, Brian D., Joshua A. Bauer, Xi Chen, et al. 2011. 'Identification of Human Triple-Negative Breast Cancer Subtypes and Preclinical Models for Selection of Targeted Therapies'. *Journal of Clinical Investigation* 121 (7): 2750–67. https://doi.org/10.1172/JCI45014.

Lehmann, Brian D., Antonio Colaprico, Tiago C. Silva, et al. 2021. 'Multi-Omics Analysis Identifies Therapeutic Vulnerabilities in Triple-Negative Breast Cancer Subtypes'. *Nature Communications* 12 (1): 6276. https://doi.org/10.1038/s41467-021-26502-6.

Lehmann, Brian D., Bojana Jovanović, Xi Chen, et al. 2016. 'Refinement of Triple-Negative Breast Cancer Molecular Subtypes: Implications for Neoadjuvant Chemotherapy Selection'. *PLOS ONE* 11 (6): e0157368. https://doi.org/10.1371/journal.pone.0157368.

Lei, Guang, Li Zhuang, and Boyi Gan. 2021. 'mTORC1 and Ferroptosis: Regulatory Mechanisms and Therapeutic Potential'. *BioEssays* 43 (8): 2100093. https://doi.org/10.1002/bies.202100093.

Lei, Ming, Yun-Long Zhang, Feng-Ying Huang, et al. 2023. 'Gankyrin Inhibits Ferroptosis through the P53/SLC7A11/GPX4 Axis in Triple-Negative Breast Cancer Cells'. *Scientific Reports* 13 (1): 21916. https://doi.org/10.1038/s41598-023-49136-8.

Lei, Yunpeng, Lirui He, Chang Yan, Yuchen Wang, and Guoqing Lv. 2021. 'PERK Activation by CCT020312 Chemosensitizes Colorectal Cancer through Inducing Apoptosis Regulated by ER Stress'. *Biochemical and Biophysical Research Communications* 557 (June): 316–22. https://doi.org/10.1016/j.bbrc.2021.03.041.

León-Annicchiarico, Clara Lucía, Silvia Ramírez-Peinado, Dídac Domínguez-Villanueva, Anika Gonsberg, Theodore J. Lampidis, and Cristina Muñoz-Pinedo. 2015. 'ATF 4 Mediates Necrosis Induced by Glucose Deprivation and Apoptosis Induced by 2-deoxyglucose in the Same Cells'. *The FEBS Journal* 282 (18): 3647–58. https://doi.org/10.1111/febs.13369.

Lewis, Samantha C., Lauren F. Uchiyama, and Jodi Nunnari. 2016. 'ER-Mitochondria Contacts Couple mtDNA Synthesis with Mitochondrial Division in Human Cells'. *Science* 353 (6296): aaf5549. https://doi.org/10.1126/science.aaf5549.

Li, Fei, Ting Xu, Peiling Chen, et al. 2022. 'Platelet-Derived Extracellular Vesicles Inhibit Ferroptosis and Promote Distant Metastasis of Nasopharyngeal Carcinoma by Upregulating ITGB3'. *International Journal of Biological Sciences* 18 (15): 5858–72. https://doi.org/10.7150/ijbs.76162.

Li, Jiajia, Xiawei Dang, Antonietta Franco, and Gerald W. Dorn. 2022. 'Reciprocal Regulation of Mitofusin 2-Mediated Mitophagy and Mitochondrial Fusion by

Different PINK1 Phosphorylation Events'. *Frontiers in Cell and Developmental Biology* 10 (May): 868465. https://doi.org/10.3389/fcell.2022.868465.

Li, Pengyun, Qiaohong Lin, Shiyang Sun, et al. 2022. 'Inhibition of Cannabinoid Receptor Type 1 Sensitizes Triple-Negative Breast Cancer Cells to Ferroptosis via Regulating Fatty Acid Metabolism'. *Cell Death & Disease* 13 (9): 808. https://doi.org/10.1038/s41419-022-05242-5.

Li, Shan-Shan, Baifeng Zhang, Cuicui Huang, et al. 2025. 'FAO-Fueled OXPHOS and NRF2-Mediated Stress Resilience in MICs Drive Lymph Node Metastasis'. *Proceedings of the National Academy of Sciences* 122 (15): e2411241122. https://doi.org/10.1073/pnas.2411241122.

Li, Siqi, Hang Yuan, Liang Li, Qin Li, Ping Lin, and Kai Li. 2025. 'Oxidative Stress and Reprogramming of Lipid Metabolism in Cancers'. *Antioxidants* 14 (2): 201. https://doi.org/10.3390/antiox14020201.

Li, Xiaoli, Xiaoping Yu, Duanfang Zhou, et al. 2020. 'CCT020312 Inhibits Triple-Negative Breast Cancer Through PERK Pathway-Mediated G1 Phase Cell Cycle Arrest and Apoptosis'. *Frontiers in Pharmacology* 11 (May): 737. https://doi.org/10.3389/fphar.2020.00737.

Li, Xinhui, Jian Zhou, Mingming Xiao, et al. 2021. 'Uncovering the Subtype-Specific Molecular Characteristics of Breast Cancer by Multiomics Analysis of Prognosis-Associated Genes, Driver Genes, Signaling Pathways, and Immune Activity'. *Frontiers in Cell and Developmental Biology* 9 (July): 689028. https://doi.org/10.3389/fcell.2021.689028.

Li, Yufeng, Wenyue Dong, Xijin Shan, et al. 2018. 'The Anti-Tumor Effects of Mfn2 in Breast Cancer Are Dependent on Promoter DNA Methylation, the P21Ras Motif and PKA Phosphorylation Site'. *Oncology Letters*, ahead of print, March 21. https://doi.org/10.3892/ol.2018.8314.

Li, Yun, Huajun Zhang, Yulia Merkher, et al. 2022. 'Recent Advances in Therapeutic Strategies for Triple-Negative Breast Cancer'. *Journal of Hematology & Oncology* 15 (1): 121. https://doi.org/10.1186/s13045-022-01341-0.

Liang, Deguang, Yan Feng, Fereshteh Zandkarimi, et al. 2023. 'Ferroptosis Surveillance Independent of GPX4 and Differentially Regulated by Sex Hormones'. *Cell* 186 (13): 2748-2764.e22. https://doi.org/10.1016/j.cell.2023.05.003.

Liao, Kaimin, Kaiyue Liu, Zhongyu Wang, Kailiang Zhao, and Yide Mei. 2025. 'TRIM 2 Promotes Metabolic Adaptation to Glutamine Deprivation via Enhancement of CPT 1 A Activity'. *The FEBS Journal* 292 (2): 275–93. https://doi.org/10.1111/febs.17218.

Licari, Eugenia, Luis Sánchez-del-Campo, and Paola Falletta. 2021. 'The Two Faces of the Integrated Stress Response in Cancer Progression and Therapeutic Strategies'.

The International Journal of Biochemistry & Cell Biology 139 (October): 106059. https://doi.org/10.1016/j.biocel.2021.106059.

Liesa, Marc, and Orian S. Shirihai. 2013. 'Mitochondrial Dynamics in the Regulation of Nutrient Utilization and Energy Expenditure'. *Cell Metabolism* 17 (4): 491–506. https://doi.org/10.1016/j.cmet.2013.03.002.

Lim, Seung-Oe, Chia-Wei Li, Weiya Xia, et al. 2016. 'EGFR Signaling Enhances Aerobic Glycolysis in Triple-Negative Breast Cancer Cells to Promote Tumor Growth and Immune Escape'. *Cancer Research* 76 (5): 1284–96. https://doi.org/10.1158/0008-5472.CAN-15-2478.

Lin, Chiao-Wei, Yu-Ju Peng, Yuan-Yu Lin, Harry John Mersmann, and Shih-Torng Ding. 2020. 'LRRK2 Regulates CPT1A to Promote β-Oxidation in HepG2 Cells'. *Molecules* 25 (18): 4122. https://doi.org/10.3390/molecules25184122.

Lin, Nancy U., Elizabeth Claus, Jessica Sohl, Abdul R. Razzak, Amal Arnaout, and Eric P. Winer. 2008. 'Sites of Distant Recurrence and Clinical Outcomes in Patients with Metastatic Triple-negative Breast Cancer: High Incidence of Central Nervous System Metastases'. *Cancer* 113 (10): 2638–45. https://doi.org/10.1002/cncr.23930.

Lin, Yuan-Hong, Phoebe Chidley, Lorenztino Admojo, et al. 2023. 'Pathologic Complete Response and Oncologic Outcomes in Locally Advanced Breast Cancers Treated With Neoadjuvant Radiation Therapy: An Australian Perspective'. *Practical Radiation Oncology* 13 (4): 301–13. https://doi.org/10.1016/j.prro.2022.12.004.

Lines, Caleb L., Morgan J. McGrath, Tanis Dorwart, and Crystal S. Conn. 2023. 'The Integrated Stress Response in Cancer Progression: A Force for Plasticity and Resistance'. *Frontiers in Oncology* 13 (August): 1206561. https://doi.org/10.3389/fonc.2023.1206561.

Lingrand, Marine, Simon Lalonde, Antoine Jutras-Carignan, Karl-F. Bergeron, Eric Rassart, and Catherine Mounier. 2020. 'SCD1 Activity Promotes Cell Migration via a PLD-mTOR Pathway in the MDA-MB-231 Triple-Negative Breast Cancer Cell Line'. *Breast Cancer* 27 (4): 594–606. https://doi.org/10.1007/s12282-020-01053-8.

Liu, Chuan, Chuan Hu, Jinlin Cheng, et al. 2026. 'AGPAT3 Reshapes Tumor Cell Vulnerability to IFNγ-Mediated Ferroptosis and Enhances Immunotherapy Efficacy through Lipid Remodeling'. *Journal for ImmunoTherapy of Cancer* 14 (3): e013305. https://doi.org/10.1136/jitc-2025-013305.

Liu, Chuan Yin, Martin Schröder, and Randal J. Kaufman. 2000. 'Ligand-Independent Dimerization Activates the Stress Response Kinases IRE1 and PERK in the Lumen of the Endoplasmic Reticulum'. *Journal of Biological Chemistry* 275 (32): 24881–85. https://doi.org/10.1074/jbc.M004454200.

Liu, Jiao, Xinxin Song, Feimei Kuang, et al. 2021. 'NUPR1 Is a Critical Repressor of Ferroptosis'. *Nature Communications* 12 (1): 647. https://doi.org/10.1038/s41467-021-20904-2.

Liu, Suling, Gabriela Dontu, and Max S. Wicha. 2005. 'Mammary Stem Cells, Self-Renewal Pathways, and Carcinogenesis'. *Breast Cancer Research* 7 (3): 86. https://doi.org/10.1186/bcr1021.

Liu, Yanqing, and Wei Gu. 2022. 'P53 in Ferroptosis Regulation: The New Weapon for the Old Guardian'. *Cell Death & Differentiation* 29 (5): 895–910. https://doi.org/10.1038/s41418-022-00943-y.

Lohner, Karl. 1996. 'Is the High Propensity of Ethanolamine Plasmalogens to Form Non-Lamellar Lipid Structures Manifested in the Properties of Biomembranes?' *Chemistry and Physics of Lipids* 81 (2): 167–84. https://doi.org/10.1016/0009-3084(96)02580-7.

Losón, Oliver C., Zhiyin Song, Hsiuchen Chen, and David C. Chan. 2013. 'Fis1, Mff, MiD49, and MiD51 Mediate Drp1 Recruitment in Mitochondrial Fission'. *Molecular Biology of the Cell* 24 (5): 659–67. https://doi.org/10.1091/mbc.e12-10-0721.

Luengo, Alba, Dan Y. Gui, and Matthew G. Vander Heiden. 2017. 'Targeting Metabolism for Cancer Therapy'. *Cell Chemical Biology* 24 (9): 1161–80. https://doi.org/10.1016/j.chembiol.2017.08.028.

Lunt, Sophia Y., and Matthew G. Vander Heiden. 2011. 'Aerobic Glycolysis: Meeting the Metabolic Requirements of Cell Proliferation'. *Annual Review of Cell and Developmental Biology* 27 (1): 441–64. https://doi.org/10.1146/annurev-cellbio-092910-154237.

Ľupták, M., and J. Hroudová. 2019. 'Important Role of Mitochondria and the Effect of Mood Stabilizers on Mitochondrial Function'. *Physiological Research*, October 31, S3–15. https://doi.org/10.33549/physiolres.934324.

Lutz, T. 2003. 'Import of Small Tim Proteins into the Mitochondrial Intermembrane Space'. *The EMBO Journal* 22 (17): 4400–4408. https://doi.org/10.1093/emboj/cdg421.

Ma, Chaobing, Xueyin Zu, Kangdong Liu, et al. n.d. *Knockdown of Pyruvate Kinase M Inhibits Cell Growth and Migration by Reducing NF-kB Activity in Triple-Negative Breast Cancer Cells*.

Ma, Shumei, Rebecca F. Dielschneider, Elizabeth S. Henson, et al. 2017. 'Ferroptosis and Autophagy Induced Cell Death Occur Independently after Siramesine and Lapatinib Treatment in Breast Cancer Cells'. *PLOS ONE* 12 (8): e0182921. https://doi.org/10.1371/journal.pone.0182921.

Madrazo, Nicole, Zinia Khattar, Evan T. Powers, Jessica D. Rosarda, and R. Luke Wiseman. 2024. 'Mapping Stress-Responsive Signaling Pathways Induced by

Mitochondrial Proteostasis Perturbations'. *Molecular Biology of the Cell* 35 (5): ar74. https://doi.org/10.1091/mbc.E24-01-0041.

Magtanong, Leslie, Pin-Joe Ko, Milton To, et al. 2019. 'Exogenous Monounsaturated Fatty Acids Promote a Ferroptosis-Resistant Cell State'. *Cell Chemical Biology* 26 (3): 420-432.e9. https://doi.org/10.1016/j.chembiol.2018.11.016.

Maiti, B., M. N. Kundranda, T. P. Spiro, and H. A. Daw. 2010. 'The Association of Metabolic Syndrome with Triple-Negative Breast Cancer'. *Breast Cancer Research and Treatment* 121 (2): 479–83. https://doi.org/10.1007/s10549-009-0591-y.

Mallilankaraman, Karthik, Patrick Doonan, César Cárdenas, et al. 2012. 'MICU1 Is an Essential Gatekeeper for MCU-Mediated Mitochondrial Ca2+ Uptake That Regulates Cell Survival'. *Cell* 151 (3): 630–44. https://doi.org/10.1016/j.cell.2012.10.011.

Mansell, Ryan P., Sebastian Müller, Jia-Shu Yang, et al. 2024. 'Ether Lipids Influence Cancer Cell Fate by Modulating Iron Uptake'. Preprint, Cancer Biology, March 21. https://doi.org/10.1101/2024.03.20.585922.

Mao, Chao, Xiaoguang Liu, Yilei Zhang, et al. 2021. 'DHODH-Mediated Ferroptosis Defence Is a Targetable Vulnerability in Cancer'. *Nature* 593 (7860): 586–90. https://doi.org/10.1038/s41586-021-03539-7.

Marchi, Saverio, and Paolo Pinton. 2014. 'The Mitochondrial Calcium Uniporter Complex: Molecular Components, Structure and Physiopathological Implications'. *The Journal of Physiology* 592 (5): 829–39. https://doi.org/10.1113/jphysiol.2013.268235.

Marciniak, Stefan J., Joseph E. Chambers, and David Ron. 2022. 'Pharmacological Targeting of Endoplasmic Reticulum Stress in Disease'. *Nature Reviews Drug Discovery* 21 (2): 115–40. https://doi.org/10.1038/s41573-021-00320-3.

Marciniak, Stefan J., Chi Y. Yun, Seiichi Oyadomari, et al. 2004. 'CHOP Induces Death by Promoting Protein Synthesis and Oxidation in the Stressed Endoplasmic Reticulum'. *Genes & Development* 18 (24): 3066–77. https://doi.org/10.1101/gad.1250704.

Mardamshina, Mariya, Shiri Karagach, Vishnu Mohan, et al. 2025. 'Integrated Spatial Proteomic Analysis of Breast Cancer Heterogeneity Unravels Cancer Cell Phenotypic Plasticity'. *Nature Communications* 16 (1): 10482. https://doi.org/10.1038/s41467-025-65477-6.

Margenthaler, Julie A., and David W. Ollila. 2016. 'Breast Conservation Therapy Versus Mastectomy: Shared Decision-Making Strategies and Overcoming Decisional Conflicts in Your Patients'. *Annals of Surgical Oncology* 23 (10): 3133–37. https://doi.org/10.1245/s10434-016-5369-y.

Martínez-Reyes, Inmaculada, and Navdeep S. Chandel. 2020. ‘Mitochondrial TCA Cycle Metabolites Control Physiology and Disease’. *Nature Communications* 11 (1): 102. https://doi.org/10.1038/s41467-019-13668-3.

Martínez-Reyes, Inmaculada, and Navdeep S. Chandel. 2021. ‘Cancer Metabolism: Looking Forward’. *Nature Reviews Cancer* 21 (10): 669–80. https://doi.org/10.1038/s41568-021-00378-6.

Martínez-Reyes, Inmaculada, Lauren P. Diebold, Hyewon Kong, et al. 2016. ‘TCA Cycle and Mitochondrial Membrane Potential Are Necessary for Diverse Biological Functions’. *Molecular Cell* 61 (2): 199–209. https://doi.org/10.1016/j.molcel.2015.12.002.

Martínez-Rojas, Miguel Ángel, Hiram Balcázar, Isaac González-Soria, et al. 2024. ‘Transient Inhibition of Sodium-Glucose Cotransporter 2 after Ischemia/Reperfusion Injury Ameliorates Chronic Kidney Disease’. *JCI Insight* 9 (6): e173675. https://doi.org/10.1172/jci.insight.173675.

Masuri, Sebastiano, Petr Vaňhara, Maria Grazia Cabiddu, et al. 2021. ‘Copper(II) Phenanthroline-Based Complexes as Potential AntiCancer Drugs: A Walkthrough on the Mechanisms of Action’. *Molecules* 27 (1): 49. https://doi.org/10.3390/molecules27010049.

Mathew, Marilyn, Nhi Nguyen, Yangzom Bhutia, Sathish Sivaprakasam, and Vadivel Ganapathy. 2024. ‘Metabolic Signature of Warburg Effect in Cancer: An Effective and Obligatory Interplay between Nutrient Transporters and Catabolic/Anabolic Pathways to Promote Tumor Growth’. *Cancers* 16 (3): 504. https://doi.org/10.3390/cancers16030504.

Maulucci, G., O. Cohen, B. Daniel, et al. 2016. ‘Fatty Acid-Related Modulations of Membrane Fluidity in Cells: Detection and Implications’. *Free Radical Research* 50 (sup1): S40–50. https://doi.org/10.1080/10715762.2016.1231403.

Meinecke, Michael, Richard Wagner, Peter Kovermann, et al. 2006. ‘Tim50 Maintains the Permeability Barrier of the Mitochondrial Inner Membrane’. *Science* 312 (5779): 1523–26. https://doi.org/10.1126/science.1127628.

Merciai, Fabrizio, Manuela Giovanna Basilicata, Danila La Gioia, et al. 2024. ‘Sub-5-Min RP-UHPLC-TIMS for High-Throughput Untargeted Lipidomics and Its Application to Multiple Matrices’. *Analytical and Bioanalytical Chemistry* 416 (4): 959–70. https://doi.org/10.1007/s00216-023-05084-w.

Merciai, Fabrizio, Simona Musella, Eduardo Sommella, Alessia Bertamino, Anna Maria D’Ursi, and Pietro Campiglia. 2022. ‘Development and Application of a Fast Ultra-High Performance Liquid Chromatography-Trapped Ion Mobility Mass Spectrometry Method for Untargeted Lipidomics’. *Journal of Chromatography A* 1673 (June): 463124. https://doi.org/10.1016/j.chroma.2022.463124.

Merteroglu, Munise, and Massimo M. Santoro. 2024. 'Exploiting the Metabolic Vulnerability of Circulating Tumour Cells'. *Trends in Cancer* 10 (6): 541–56. https://doi.org/10.1016/j.trecan.2024.03.004.

METABRIC Group, Christina Curtis, Sohrab P. Shah, et al. 2012. 'The Genomic and Transcriptomic Architecture of 2,000 Breast Tumours Reveals Novel Subgroups'. *Nature* 486 (7403): 346–52. https://doi.org/10.1038/nature10983.

Mick, Eran, Denis V. Titov, Owen S. Skinner, Rohit Sharma, Alexis A. Jourdain, and Vamsi K. Mootha. 2020. 'Distinct Mitochondrial Defects Trigger the Integrated Stress Response Depending on the Metabolic State of the Cell'. *eLife* 9 (May): e49178. https://doi.org/10.7554/eLife.49178.

Mishima, Eikan, Junya Ito, Zijun Wu, et al. 2022. 'A Non-Canonical Vitamin K Cycle Is a Potent Ferroptosis Suppressor'. *Nature* 608 (7924): 778–83. https://doi.org/10.1038/s41586-022-05022-3.

Mishra, Prashant, Valerio Carelli, Giovanni Manfredi, and David C. Chan. 2014. 'Proteolytic Cleavage of Opa1 Stimulates Mitochondrial Inner Membrane Fusion and Couples Fusion to Oxidative Phosphorylation'. *Cell Metabolism* 19 (4): 630–41. https://doi.org/10.1016/j.cmet.2014.03.011.

Missiroli, Sonia, Alberto Danese, Tommaso Iannitti, et al. 2017. 'Endoplasmic Reticulum-Mitochondria Ca2+ Crosstalk in the Control of the Tumor Cell Fate'. *Biochimica et Biophysica Acta (BBA) - Molecular Cell Research* 1864 (6): 858–64. https://doi.org/10.1016/j.bbamcr.2016.12.024.

Miyazaki, Makoto, Sean M. Bruggink, and James M. Ntambi. 2006. 'Identification of Mouse Palmitoyl-Coenzyme A Δ9-Desaturase'. *Journal of Lipid Research* 47 (4): 700–704. https://doi.org/10.1194/jlr.C500025-JLR200.

Mohamed, Eslam, Rosa A. Sierra, Jimena Trillo-Tinoco, et al. 2020. 'The Unfolded Protein Response Mediator PERK Governs Myeloid Cell-Driven Immunosuppression in Tumors through Inhibition of STING Signaling'. *Immunity* 52 (4): 668-682.e7. https://doi.org/10.1016/j.immuni.2020.03.004.

Morais-Santos, Filipa, Sara Granja, Vera Miranda-Gonçalves, et al. 2015. 'Targeting Lactate Transport Suppresses *in Vivo* Breast Tumour Growth'. *Oncotarget* 6 (22): 19177–89. https://doi.org/10.18632/oncotarget.3910.

Mustacchi, Giorgio, and Michelino De Laurentiis. 2015. 'The Role of Taxanes in Triple-Negative Breast Cancer: Literature Review'. *Drug Design, Development and Therapy*, August, 4303. https://doi.org/10.2147/DDDT.S86105.

Nagasawa, Ikuko, Masaru Koido, Yuri Tani, Satomi Tsukahara, Kazuhiro Kunimasa, and Akihiro Tomida. 2020. 'Disrupting ATF4 Expression Mechanisms Provides an Effective Strategy for BRAF-Targeted Melanoma Therapy'. *iScience* 23 (4). https://doi.org/10.1016/j.isci.2020.101028.

Nagelkerke, Anika, Johan Bussink, Hilda Mujcic, et al. 2013. 'Hypoxia Stimulates Migration of Breast Cancer Cells via the PERK/ATF4/LAMP3-Arm of the Unfolded Protein Response'. *Breast Cancer Research* 15 (1): R2. https://doi.org/10.1186/bcr3373.

Nakamura, Takahisa, Masato Furuhashi, Ping Li, et al. 2010. 'Double-Stranded RNA-Dependent Protein Kinase Links Pathogen Sensing with Stress and Metabolic Homeostasis'. *Cell* 140 (3): 338–48. https://doi.org/10.1016/j.cell.2010.01.001.

Nandi, Ipshita, Linjia Ji, Harvey W. Smith, et al. 2024. 'Targeting Fatty Acid Oxidation Enhances Response to HER2-Targeted Therapy'. *Nature Communications* 15 (1): 6587. https://doi.org/10.1038/s41467-024-50998-3.

Nedeljković, Milica, and Ana Damjanović. 2019. 'Mechanisms of Chemotherapy Resistance in Triple-Negative Breast Cancer-How We Can Rise to the Challenge'. *Cells* 8 (9). https://doi.org/10.3390/cells8090957.

Ngo, Jennifer, Dong Wook Choi, Illana A. Stanley, et al. 2023. 'Mitochondrial Morphology Controls Fatty Acid Utilization by Changing CPT1 Sensitivity to MALONYL-COA'. *The EMBO Journal* 42 (11): e111901. https://doi.org/10.15252/embj.2022111901.

Nguyen, Hai P., Danielle Yi, Frances Lin, et al. 2020. 'Aifm2, a NADH Oxidase, Supports Robust Glycolysis and Is Required for Cold- and Diet-Induced Thermogenesis'. *Molecular Cell* 77 (3): 600-617.e4. https://doi.org/10.1016/j.molcel.2019.12.002.

Nguyen, Hao G., Crystal S. Conn, Yae Kye, et al. 2018. 'Development of a Stress Response Therapy Targeting Aggressive Prostate Cancer'. *Science Translational Medicine* 10 (439): eaar2036. https://doi.org/10.1126/scitranslmed.aar2036.

Nicosia, Luca, Luciano Mariano, Giuseppe Pellegrino, et al. 2024. 'Atypical Ductal Hyperplasia and Lobular In Situ Neoplasm: High-Risk Lesions Challenging Breast Cancer Prevention'. *Cancers* 16 (4): 837. https://doi.org/10.3390/cancers16040837.

Nolfi-Donegan, Deirdre, Andrea Braganza, and Sruti Shiva. 2020. 'Mitochondrial Electron Transport Chain: Oxidative Phosphorylation, Oxidant Production, and Methods of Measurement'. *Redox Biology* 37 (October): 101674. https://doi.org/10.1016/j.redox.2020.101674.

Nouri, Kazem, Yue Feng, and Aaron D. Schimmer. 2020. 'Mitochondrial ClpP Serine Protease-Biological Function and Emerging Target for Cancer Therapy'. *Cell Death & Disease* 11 (10): 841. https://doi.org/10.1038/s41419-020-03062-z.

Novoa, Isabel, Huiqing Zeng, Heather P. Harding, and David Ron. 2001. *Feedback Inhibition of the Unfolded Protein Response by GADD34-Mediated Dephosphorylation of eIF2*.

Ochoa, Cristhiaan D., Mikhail Alexeyev, Viktoriya Pastukh, Ron Balczon, and Troy Stevens. 2012. 'Pseudomonas Aeruginosa Exotoxin Y Is a Promiscuous Cyclase

That Increases Endothelial Tau Phosphorylation and Permeability'. *Journal of Biological Chemistry* 287 (30): 25407–18. https://doi.org/10.1074/jbc.M111.301440.

Oh, Sunhwa, Hyungjoo Kim, KeeSoo Nam, and Incheol Shin. 2017. 'Glut1 Promotes Cell Proliferation, Migration and Invasion by Regulating Epidermal Growth Factor Receptor and Integrin Signaling in Triple-Negative Breast Cancer Cells'. *BMB Reports* 50 (3): 132–37. https://doi.org/10.5483/BMBRep.2017.50.3.189.

Ohoka, Nobumichi, Satoshi Yoshii, Takayuki Hattori, Kikuo Onozaki, and Hidetoshi Hayashi. 2005. 'TRB3, a Novel ER Stress-inducible Gene, Is Induced via ATF4–CHOP Pathway and Is Involved in Cell Death'. *The EMBO Journal* 24 (6): 1243–55. https://doi.org/10.1038/sj.emboj.7600596.

Oyama, Tetsunari, Kotaro Lijima, Hiroyuki Takei, et al. 2000. 'Atypical Cystic Lobule of the Breast: An Early Stage of Low-Grade Ductal Carcinomain-Situ'. *Breast Cancer* 7 (4): 326–31. https://doi.org/10.1007/BF02966399.

Pajares, Bella, Marina Pollán, Miguel Martín, et al. 2013. 'Obesity and Survival in Operable Breast Cancer Patients Treated with Adjuvant Anthracyclines and Taxanes According to Pathological Subtypes: A Pooled Analysis'. *Breast Cancer Research* 15 (6): R105. https://doi.org/10.1186/bcr3572.

Pakhira, Suman, and Sib Sankar Roy. 2025. 'Altered Fatty Acid Oxidation via CPT1A Promotes Epithelial-to-mesenchymal Transition in Ovarian Cancer'. *The FEBS Journal* 292 (23): 6283–306. https://doi.org/10.1111/febs.70193.

Palty, Raz, William F. Silverman, Michal Hershfinkel, et al. 2010. 'NCLX Is an Essential Component of Mitochondrial Na^+ /Ca^{2+} Exchange'. *Proceedings of the National Academy of Sciences* 107 (1): 436–41. https://doi.org/10.1073/pnas.0908099107.

Pan, Sijing, Ming Fan, Zhangnan Liu, Xia Li, and Huijuan Wang. 2020. 'Serine, Glycine and One-carbon Metabolism in Cancer (Review)'. *International Journal of Oncology* 58 (2): 158–70. https://doi.org/10.3892/ijo.2020.5158.

Park, E. A., R. L. Mynatt, G. A. Cook, and K. Kashfi. 1995. 'Insulin Regulates Enzyme Activity, Malonyl-CoA Sensitivity and mRNA Abundance of Hepatic Carnitine Palmitoyltransferase-I'. *Biochemical Journal* 310 (3): 853–58. https://doi.org/10.1042/bj3100853.

Park, Jun Hyoung, Sajna Vithayathil, Santosh Kumar, et al. 2016. 'Fatty Acid Oxidation-Driven Src Links Mitochondrial Energy Reprogramming and Oncogenic Properties in Triple-Negative Breast Cancer'. *Cell Reports* 14 (9): 2154–65. https://doi.org/10.1016/j.celrep.2016.02.004.

Pascual, Gloria, Alexandra Avgustinova, Stefania Mejetta, et al. 2017. 'Targeting Metastasis-Initiating Cells through the Fatty Acid Receptor CD36'. *Nature* 541 (7635): 41–45. https://doi.org/10.1038/nature20791.

Patel, Angana A. H., Jozefina J. Dzanan, Kevin X. Ali, et al. 2026. 'Ageing Promotes Metastasis via Activation of the Integrated Stress Response'. *Nature* 652 (8112): 1339–48. https://doi.org/10.1038/s41586-026-10216-0.

Patel, Roshni, Lutfi H. Alfarsi, Rokaya El-Ansari, et al. 2024. 'ATF4 as a Prognostic Marker and Modulator of Glutamine Metabolism in Oestrogen Receptor-Positive Breast Cancer'. *Pathobiology* 91 (6): 411–21. https://doi.org/10.1159/000539564.

Patra, Srimanta, Kewal Kumar Mahapatra, Prakash Priyadarshi Praharaj, et al. 2021. 'Intricate Role of Mitochondrial Calcium Signalling in Mitochondrial Quality Control for Regulation of Cancer Cell Fate'. *Mitochondrion* 57 (March): 230–40. https://doi.org/10.1016/j.mito.2021.01.002.

Paumard, Patrick, Jacques Vaillier, Bénédicte Coulary, et al. 2002. 'The ATP Synthase Is Involved in Generating Mitochondrial Cristae Morphology'. *The EMBO Journal* 21 (3): 221–30. https://doi.org/10.1093/emboj/21.3.221.

Pavitt, Graham D., Kolluru V. A. Ramaiah, Scot R. Kimball, and Alan G. Hinnebusch. 1998. *eIF2 Independently Binds Two Distinct eIF2B Subcomplexes That Catalyze and Regulate Guanine-Nucleotide Exchange*. www.genesdev.org.

Pavlova, Natalya N., and Craig B. Thompson. 2016. 'The Emerging Hallmarks of Cancer Metabolism'. *Cell Metabolism* 23 (1): 27–47. https://doi.org/10.1016/j.cmet.2015.12.006.

Pei, Zhuo, Yifei Qin, Xianghui Fu, et al. 2022. 'Inhibition of Ferroptosis and Iron Accumulation Alleviates Pulmonary Fibrosis in a Bleomycin Model'. *Redox Biology* 57 (November): 102509. https://doi.org/10.1016/j.redox.2022.102509.

Perea, Valerie, Christian Cole, Justine Lebeau, et al. 2023. 'PERK Signaling Promotes Mitochondrial Elongation by Remodeling Membrane Phosphatidic Acid'. *The EMBO Journal* 42 (15): e113908. https://doi.org/10.15252/embj.2023113908.

Perocchi, Fabiana, Vishal M. Gohil, Hany S. Girgis, et al. 2010. 'MICU1 Encodes a Mitochondrial EF Hand Protein Required for Ca2+ Uptake'. *Nature* 467 (7313): 291–96. https://doi.org/10.1038/nature09358.

Perou, Charles M., Therese Sørlie, Michael B. Eisen, et al. 2000. 'Molecular Portraits of Human Breast Tumours'. *Nature* 406 (6797): 747–52. https://doi.org/10.1038/35021093.

Pestova, Tatyana V., Sergei I. Borukhov, and Christopher U. T. Hellen. 1998. 'Eukaryotic Ribosomes Require Initiation Factors 1 and 1A to Locate Initiation Codons'. *Nature* 394 (6696): 854–59. https://doi.org/10.1038/29703.

Philpott, Caroline C., Sarju J. Patel, and Olga Protchenko. 2020. 'Management versus Miscues in the Cytosolic Labile Iron Pool: The Varied Functions of Iron Chaperones'. *Biochimica et Biophysica Acta (BBA) - Molecular Cell Research* 1867 (11): 118830. https://doi.org/10.1016/j.bbamcr.2020.118830.

Pich, Sara, Daniel Bach, Paz Briones, et al. 2005. 'The Charcot–Marie–Tooth Type 2A Gene Product, Mfn2, up-Regulates Fuel Oxidation through Expression of OXPHOS System'. *Human Molecular Genetics* 14 (11): 1405–15. https://doi.org/10.1093/hmg/ddi149.

'PIIS0960982206000480'. n.d.

Pike, Linda J., Xianlin Han, Koong-Nah Chung, and Richard W. Gross. 2002. 'Lipid Rafts Are Enriched in Arachidonic Acid and Plasmenylethanolamine and Their Composition Is Independent of Caveolin-1 Expression: A Quantitative Electrospray Ionization/Mass Spectrometric Analysis'. *Biochemistry* 41 (6): 2075–88. https://doi.org/10.1021/bi0156557.

Pizato, Nathalia, Meg Schwarcz Hoffmann, Clarissa Hoffman Irala, Maria Imaculada Muniz-Junqueira, Elemarcia Martins Da Silva Paixao, and Marina Kiyomi Ito. 2021. 'Serum Fatty Acid Synthase Levels and N-3 Fatty Acid Intake in Patients with Breast Cancer'. *Clinical Nutrition ESPEN* 42 (April): 142–47. https://doi.org/10.1016/j.clnesp.2020.12.027.

Pope, Lauren E., and Scott J. Dixon. 2023. 'Regulation of Ferroptosis by Lipid Metabolism'. *Trends in Cell Biology* 33 (12): 1077–87. https://doi.org/10.1016/j.tcb.2023.05.003.

Possemato, Richard, Kevin M. Marks, Yoav D. Shaul, et al. 2011. 'Functional Genomics Reveal That the Serine Synthesis Pathway Is Essential in Breast Cancer'. *Nature* 476 (7360): 346–50. https://doi.org/10.1038/nature10350.

Powell, Catherine A., Mohd W. Nasser, Helong Zhao, et al. 2015. 'Fatty Acid Binding Protein 5 Promotes Metastatic Potential of Triple Negative Breast Cancer Cells through Enhancing Epidermal Growth Factor Receptor Stability'. *Oncotarget* 6 (8): 6373–85. https://doi.org/10.18632/oncotarget.3442.

Powers, Eric, Georgia Sofia Karachaliou, Chester Kao, et al. 2020. 'Novel Therapies Are Changing Treatment Paradigms in Metastatic Prostate Cancer'. *Journal of Hematology & Oncology* 13 (1): 144. https://doi.org/10.1186/s13045-020-00978-z.

Protani, Melinda, Michael Coory, and Jennifer H. Martin. 2010. 'Effect of Obesity on Survival of Women with Breast Cancer: Systematic Review and Meta-Analysis'. *Breast Cancer Research and Treatment* 123 (3): 627–35. https://doi.org/10.1007/s10549-010-0990-0.

Puthalakath, Hamsa, Lorraine A. O'Reilly, Priscilla Gunn, et al. 2007. 'ER Stress Triggers Apoptosis by Activating BH3-Only Protein Bim'. *Cell* 129 (7): 1337–49. https://doi.org/10.1016/j.cell.2007.04.027.

Pytel, Dariusz, Yan Gao, Katarzyna Mackiewicz, et al. 2016. 'PERK Is a Haploinsufficient Tumor Suppressor: Gene Dose Determines Tumor-Suppressive

Versus Tumor Promoting Properties of PERK in Melanoma'. *PLOS Genetics* 12 (12): e1006518. https://doi.org/10.1371/journal.pgen.1006518.

Qureshi, Saba, Stefan Y. Kim, Stephanie Lee, et al. 2026. 'ATF4 Regulates Mitochondrial Dysfunction and Mitophagy, Contributing to Corneal Endothelial Apoptosis'. *Scientific Reports* 16 (1): 5960. https://doi.org/10.1038/s41598-026-36453-x.

Rambold, Angelika S., Brenda Kostelecky, Natalie Elia, and Jennifer Lippincott-Schwartz. 2011. 'Tubular Network Formation Protects Mitochondria from Autophagosomal Degradation during Nutrient Starvation'. *Proceedings of the National Academy of Sciences* 108 (25): 10190–95. https://doi.org/10.1073/pnas.1107402108.

Ramsay, Rona R., Richard D. Gandour, and Feike R. Van Der Leij. 2001. 'Molecular Enzymology of Carnitine Transfer and Transport'. *Biochimica et Biophysica Acta (BBA) - Protein Structure and Molecular Enzymology* 1546 (1): 21–43. https://doi.org/10.1016/S0167-4838(01)00147-9.

Reda, Asmaa, Alaa Refaat, Ahmed A. Abd-Rabou, et al. 2019a. 'Role of Mitochondria in Rescuing Glycolytically Inhibited Subpopulation of Triple Negative but Not Hormone-Responsive Breast Cancer Cells'. *Scientific Reports* 9 (1): 13748. https://doi.org/10.1038/s41598-019-50141-z.

Reda, Asmaa, Alaa Refaat, Ahmed A. Abd-Rabou, et al. 2019b. 'Role of Mitochondria in Rescuing Glycolytically Inhibited Subpopulation of Triple Negative but Not Hormone-Responsive Breast Cancer Cells'. *Scientific Reports* 9 (1): 13748. https://doi.org/10.1038/s41598-019-50141-z.

Reed, Alex, Timothy Ware, Haoxin Li, J. Fernando Bazan, and Benjamin F. Cravatt. 2023. 'TMEM164 Is an Acyltransferase That Forms Ferroptotic C20:4 Ether Phospholipids'. *Nature Chemical Biology* 19 (3): 378–88. https://doi.org/10.1038/s41589-022-01253-7.

Ren, T., H. Zhang, J. Wang, et al. 2017. 'MCU-Dependent Mitochondrial Ca2+ Inhibits NAD+/SIRT3/SOD2 Pathway to Promote ROS Production and Metastasis of HCC Cells'. *Oncogene* 36 (42): 5897–909. https://doi.org/10.1038/onc.2017.167.

Riggio, Alessandra I., Katherine E. Varley, and Alana L. Welm. 2021. 'The Lingering Mysteries of Metastatic Recurrence in Breast Cancer'. *British Journal of Cancer* 124 (1): 13–26. https://doi.org/10.1038/s41416-020-01161-4.

Riley, Joel S., Giovanni Quarato, Catherine Cloix, et al. 2018. 'Mitochondrial Inner Membrane Permeabilisation Enables Mt DNA Release during Apoptosis'. *The EMBO Journal* 37 (17): e99238. https://doi.org/10.15252/embj.201899238.

Rimessi, A., S. Marchi, S. Patergnani, and P. Pinton. 2014. 'H-Ras-Driven Tumoral Maintenance Is Sustained through Caveolin-1-Dependent Alterations in Calcium Signaling'. *Oncogene* 33 (18): 2329–40. https://doi.org/10.1038/onc.2013.192.

Rizzuto, Rosario, Saverio Marchi, Massimo Bonora, et al. 2009. 'Ca2+ Transfer from the ER to Mitochondria: When, How and Why'. *Biochimica et Biophysica Acta (BBA) - Bioenergetics* 1787 (11): 1342–51. https://doi.org/10.1016/j.bbabio.2009.03.015.

Rochette, Luc, Geoffrey Dogon, Eve Rigal, Marianne Zeller, Yves Cottin, and Catherine Vergely. 2022. 'Lipid Peroxidation and Iron Metabolism: Two Corner Stones in the Homeostasis Control of Ferroptosis'. *International Journal of Molecular Sciences* 24 (1): 449. https://doi.org/10.3390/ijms24010449.

Rodemer, C., T. P. Thai, B. Brugger, et al. 2003. 'Inactivation of Ether Lipid Biosynthesis Causes Male Infertility, Defects in Eye Development and Optic Nerve Hypoplasia in Mice'. *Human Molecular Genetics* 12 (15): 1881–95. https://doi.org/10.1093/hmg/ddg191.

Rojas, Margarito, Gabriel Vasconcelos, and Thomas E. Dever. 2015. 'An eIF2α-Binding Motif in Protein Phosphatase 1 Subunit GADD34 and Its Viral Orthologs Is Required to Promote Dephosphorylation of eIF2α'. *Proceedings of the National Academy of Sciences* 112 (27). https://doi.org/10.1073/pnas.1501557112.

Rosen, Mark D., Craig R. Woods, Steven D. Goldberg, et al. 2009. 'Discovery of the First Known Small-Molecule Inhibitors of Heme-Regulated Eukaryotic Initiation Factor 2α (HRI) Kinase'. *Bioorganic & Medicinal Chemistry Letters* 19 (23): 6548–51. https://doi.org/10.1016/j.bmcl.2009.10.033.

Roy, Madhuchhanda, Amy M. Fowler, Gary A. Ulaner, and Aparna Mahajan. 2023. 'Molecular Classification of Breast Cancer'. *PET Clinics* 18 (4): 441–58. https://doi.org/10.1016/j.cpet.2023.04.002.

Ryoo, Hyung Don. 2024. 'The Integrated Stress Response in Metabolic Adaptation'. *Journal of Biological Chemistry* 300 (4): 107151. https://doi.org/10.1016/j.jbc.2024.107151.

Sahin, U., M. Schmidt, E. Derhovanessian, et al. 2026. 'Individualized mRNA Vaccines Evoke Durable T Cell Immunity in Adjuvant TNBC'. *Nature* 651 (8107): 1088–96. https://doi.org/10.1038/s41586-025-10004-2.

Saleh, Lubaid, Caroline Wilson, and Ingunn Holen. 2021. 'CDK4/6 Inhibitors: A Potential Therapeutic Approach for Triple Negative Breast Cancer'. *MedComm* 2 (4): 514–30. https://doi.org/10.1002/mco2.97.

Sammarco, Alessandro, Giorgia Guerra, Katharina M. Eyme, et al. 2024. 'Targeting SCD Triggers Lipotoxicity of Cancer Cells and Enhances Anti-Tumor Immunity in Breast Cancer Brain Metastasis Mouse Models'. Preprint, Cancer Biology, May 9. https://doi.org/10.1101/2024.05.06.592766.

Sancak, Yasemin, Andrew L. Markhard, Toshimori Kitami, et al. 2013. 'EMRE Is an Essential Component of the Mitochondrial Calcium Uniporter Complex'. *Science* 342 (6164): 1379–82. https://doi.org/10.1126/science.1242993.

Sánchez-Alvarez, Rosa, Ernestina Marianna De Francesco, Marco Fiorillo, Federica Sotgia, and Michael P. Lisanti. 2020. 'Mitochondrial Fission Factor (MFF) Inhibits Mitochondrial Metabolism and Reduces Breast Cancer Stem Cell (CSC) Activity'. *Frontiers in Oncology* 10 (October): 1776. https://doi.org/10.3389/fonc.2020.01776.

Santa-Maria, Cesar A., Maureen O'Donnell, Raquel Nunes, Jean L. Wright, and Vered Stearns. 2022. 'Integrating Immunotherapy in Early-Stage Triple-Negative Breast Cancer: Practical Evidence-Based Considerations'. *Journal of the National Comprehensive Cancer Network* 20 (7): 738–44. https://doi.org/10.6004/jnccn.2022.7025.

Schmitz, Emily A., Hirohide Takahashi, and Erkan Karakas. 2022. 'Structural Basis for Activation and Gating of IP3 Receptors'. *Nature Communications* 13 (1): 1408. https://doi.org/10.1038/s41467-022-29073-2.

Schwab, Annemarie, Zhigang Rao, Jie Zhang, et al. 2024. 'Zeb1 Mediates EMT/Plasticity-Associated Ferroptosis Sensitivity in Cancer Cells by Regulating Lipogenic Enzyme Expression and Phospholipid Composition'. *Nature Cell Biology* 26 (9): 1470–81. https://doi.org/10.1038/s41556-024-01464-1.

Seiler, Alexander, Manuela Schneider, Heidi Förster, et al. 2008. 'Glutathione Peroxidase 4 Senses and Translates Oxidative Stress into 12/15-Lipoxygenase Dependent- and AIF-Mediated Cell Death'. *Cell Metabolism* 8 (3): 237–48. https://doi.org/10.1016/j.cmet.2008.07.005.

Sen, Utsav, Charles Coleman, and Triparna Sen. 2023. 'Stearoyl Coenzyme A Desaturase-1: Multitasker in Cancer, Metabolism, and Ferroptosis'. *Trends in Cancer* 9 (6): 480–89. https://doi.org/10.1016/j.trecan.2023.03.003.

Shah, Sohrab P., Andrew Roth, Rodrigo Goya, et al. 2012. 'The Clonal and Mutational Evolution Spectrum of Primary Triple-Negative Breast Cancers'. *Nature* 486 (7403): 395–99. https://doi.org/10.1038/nature10933.

Shen, Liangliang, John M. O'Shea, Mohan R. Kaadige, et al. 2015. 'Metabolic Reprogramming in Triple-Negative Breast Cancer through Myc Suppression of TXNIP'. *Proceedings of the National Academy of Sciences* 112 (17): 5425–30. https://doi.org/10.1073/pnas.1501555112.

Shenoy, Brahmi, Miloni Mandani, Meena Chintamaneni, and Sonal M. Manohar. 2025. 'Combination of the First-in-Class Imipridone ONC201 and Standard Anticancer Therapies as a Rational Approach for Therapeutic Benefit'. *Current Issues in Molecular Biology* 47 (9): 775. https://doi.org/10.3390/cimb47090775.

Sheva, Kim, Sangita Roy Chowdhury, Nataly Kravchenko-Balasha, and Amichay Meirovitz. 2024. 'Molecular Changes in Breast Cancer Induced by Radiation Therapy'. *International Journal of Radiation Oncology*Biology*Physics* 120 (2): 465–81. https://doi.org/10.1016/j.ijrobp.2024.03.019.

Siegel, Rebecca L., Kimberly D. Miller, and Ahmedin Jemal. 2015. 'Cancer Statistics, 2015'. *CA: A Cancer Journal for Clinicians* 65 (1): 5–29. https://doi.org/10.3322/caac.21254.

Sinha, Krishnendu, Joydeep Das, Pabitra Bikash Pal, and Parames C. Sil. 2013. 'Oxidative Stress: The Mitochondria-Dependent and Mitochondria-Independent Pathways of Apoptosis'. *Archives of Toxicology* 87 (7): 1157–80. https://doi.org/10.1007/s00204-013-1034-4.

Sinn, Hans-Peter, and Hans Kreipe. 2013. 'A Brief Overview of the WHO Classification of Breast Tumors, 4th Edition, Focusing on Issues and Updates from the 3rd Edition'. *Breast Care* 8 (2): 149–54. https://doi.org/10.1159/000350774.

Smirnova, Elena, Lorena Griparic, Dixie-Lee Shurland, and Alexander M. Van Der Bliek. 2001. 'Dynamin-Related Protein Drp1 Is Required for Mitochondrial Division in Mammalian Cells'. *Molecular Biology of the Cell* 12 (8): 2245–56. https://doi.org/10.1091/mbc.12.8.2245.

Sodi, V. L., Z. A. Bacigalupa, C. M. Ferrer, et al. 2018. 'Nutrient Sensor O-GlcNAc Transferase Controls Cancer Lipid Metabolism via SREBP-1 Regulation'. *Oncogene* 37 (7): 924–34. https://doi.org/10.1038/onc.2017.395.

Song, Zhiyin, Mariam Ghochani, J. Michael McCaffery, Terrence G. Frey, and David C. Chan. 2009. 'Mitofusins and OPA1 Mediate Sequential Steps in Mitochondrial Membrane Fusion'. *Molecular Biology of the Cell* 20 (15): 3525–32. https://doi.org/10.1091/mbc.e09-03-0252.

Sørlie, Therese, Robert Tibshirani, Joel Parker, et al. 2003. 'Repeated Observation of Breast Tumor Subtypes in Independent Gene Expression Data Sets'. *Proceedings of the National Academy of Sciences* 100 (14): 8418–23. https://doi.org/10.1073/pnas.0932692100.

Spinelli, Jessica B., and Marcia C. Haigis. 2018. 'The Multifaceted Contributions of Mitochondria to Cellular Metabolism'. *Nature Cell Biology* 20 (7): 745–54. https://doi.org/10.1038/s41556-018-0124-1.

St. Paul, Michael, Samuel D. Saibil, Meghan Kates, et al. 2024. 'Ex Vivo Activation of the GCN2 Pathway Metabolically Reprograms T Cells, Leading to Enhanced Adoptive Cell Therapy'. *Cell Reports Medicine* 5 (3): 101465. https://doi.org/10.1016/j.xcrm.2024.101465.

Stein, Mark N., Joseph R. Bertino, Howard L. Kaufman, et al. 2017. 'First-in-Human Clinical Trial of Oral ONC201 in Patients with Refractory Solid Tumors'. *Clinical Cancer Research* 23 (15): 4163–69. https://doi.org/10.1158/1078-0432.CCR-16-2658.

Stephan, Till, Christian Brüser, Markus Deckers, et al. 2020. 'MICOS Assembly Controls Mitochondrial Inner Membrane Remodeling and Crista Junction Redistribution to

Mediate Cristae Formation'. *The EMBO Journal* 39 (14): e104105. https://doi.org/10.15252/embj.2019104105.

Stockwell, Brent R. 2022. 'Ferroptosis Turns 10: Emerging Mechanisms, Physiological Functions, and Therapeutic Applications'. *Cell* 185 (14): 2401–21. https://doi.org/10.1016/j.cell.2022.06.003.

Sun, Qin, Xiaorui Xing, Huanyu Wang, et al. 2024. 'SCD1 Is the Critical Signaling Hub to Mediate Metabolic Diseases: Mechanism and the Development of Its Inhibitors'. *Biomedicine and Pharmacotherapy* 170 (January). https://doi.org/10.1016/j.biopha.2023.115586.

Sun, Xiangyu, Mozhi Wang, Mengshen Wang, et al. 2020. 'Metabolic Reprogramming in Triple-Negative Breast Cancer'. *Frontiers in Oncology* 10 (March): 428. https://doi.org/10.3389/fonc.2020.00428.

Suresh, Shruthy, BeiBei Chen, Jingfei Zhu, et al. 2020. 'eIF5B Drives Integrated Stress Response-Dependent Translation of PD-L1 in Lung Cancer'. *Nature Cancer* 1 (5): 533–45. https://doi.org/10.1038/s43018-020-0056-0.

Swanda, Robert V., Quanquan Ji, Xincheng Wu, et al. 2023. 'Lysosomal Cystine Governs Ferroptosis Sensitivity in Cancer via Cysteine Stress Response'. *Molecular Cell* 83 (18): 3347-3359.e9. https://doi.org/10.1016/j.molcel.2023.08.004.

Szabò, Ildikò, Luigi Leanza, Erich Gulbins, and Mario Zoratti. 2012. 'Physiology of Potassium Channels in the Inner Membrane of Mitochondria'. *Pflügers Archiv - European Journal of Physiology* 463 (2): 231–46. https://doi.org/10.1007/s00424-011-1058-7.

Szutowvicz, A., J. Kwiatkowski, and S. Angielski. n.d. *LIPOGENETIC CARCINOMA AND GLYCOLYTIC ENZYME ACTIVITIES IN AND NONMALIGNANT DISEASES OF THE HUMAN BREAST*.

Tameire, Feven, Ioannis I. Verginadis, Nektaria Maria Leli, et al. 2019. 'Author Correction: ATF4 Couples MYC-Dependent Translational Activity to Bioenergetic Demands during Tumour Progression'. *Nature Cell Biology* 21 (8): 1052–1052. https://doi.org/10.1038/s41556-019-0370-x.

Tan, Jay X., and Toren Finkel. 2020. 'Mitochondria as Intracellular Signaling Platforms in Health and Disease'. *Journal of Cell Biology* 219 (5): e202002179. https://doi.org/10.1083/jcb.202002179.

Tan, Miduo, Yazhou He, Jiansheng Yi, et al. 2024. 'WTAP Mediates NUPR1 Regulation of LCN2 Through m6A Modification to Influence Ferroptosis, Thereby Promoting Breast Cancer Proliferation, Migration and Invasion'. *Biochemical Genetics* 62 (2): 876–91. https://doi.org/10.1007/s10528-023-10423-8.

Tang, Colin P., Owen Clark, John R. Ferrarone, et al. 2022. 'GCN2 Kinase Activation by ATP-Competitive Kinase Inhibitors'. *Nature Chemical Biology* 18 (2): 207–15. https://doi.org/10.1038/s41589-021-00947-8.

Tang, Hu, Rui Kang, Jiao Liu, and Daolin Tang. 2024. 'ATF4 in Cellular Stress, Ferroptosis, and Cancer'. *Archives of Toxicology* 98 (4): 1025–41. https://doi.org/10.1007/s00204-024-03681-x.

Tesfay, Lia, Bibbin T. Paul, Anna Konstorum, et al. 2019. 'Stearoyl-CoA Desaturase 1 Protects Ovarian Cancer Cells from Ferroptotic Cell Death'. *Cancer Research* 79 (20): 5355–66. https://doi.org/10.1158/0008-5472.CAN-19-0369.

Teske, Brian F., Michael E. Fusakio, Donghui Zhou, et al. 2013. 'CHOP Induces Activating Transcription Factor 5 (ATF5) to Trigger Apoptosis in Response to Perturbations in Protein Homeostasis'. *Molecular Biology of the Cell* 24 (15): 2477–90. https://doi.org/10.1091/mbc.e13-01-0067.

Thayer, Julia A., Jennifer D. Petersen, Xiaoping Huang, et al. 2025. 'A Unified Mechanism for Mitochondrial Damage Sensing in PINK1-Parkin–Mediated Mitophagy'. *The EMBO Journal* 45 (1): 64–105. https://doi.org/10.1038/s44318-025-00604-z.

The Cancer Genome Atlas Network. 2012. 'Comprehensive Molecular Portraits of Human Breast Tumours'. *Nature* 490 (7418): 61–70. https://doi.org/10.1038/nature11412.

Timmerman, Luika A., Thomas Holton, Mariia Yuneva, et al. 2013. 'Glutamine Sensitivity Analysis Identifies the xCT Antiporter as a Common Triple-Negative Breast Tumor Therapeutic Target'. *Cancer Cell* 24 (4): 450–65. https://doi.org/10.1016/j.ccr.2013.08.020.

Timms, Kirsten M., Victor Abkevich, Elisha Hughes, et al. 2014. 'Association of BRCA1/2defects with Genomic Scores Predictive of DNA Damage Repair Deficiency among Breast Cancer Subtypes'. *Breast Cancer Research* 16 (6): 475. https://doi.org/10.1186/s13058-014-0475-x.

Tosatto, Anna, Roberta Sommaggio, Carsten Kummerow, et al. 2016. 'The Mitochondrial Calcium Uniporter Regulates Breast Cancer Progression via HIF -1α'. *EMBO Molecular Medicine* 8 (5): 569–85. https://doi.org/10.15252/emmm.201606255.

Tracz-Gaszewska, Zuzanna, and Pawel Dobrzyn. 2019. 'Stearoyl-CoA Desaturase 1 as a Therapeutic Target for the Treatment of Cancer'. *Cancers* 11 (7): 948. https://doi.org/10.3390/cancers11070948.

Tufail, Muhammad, Can-Hua Jiang, and Ning Li. 2024. 'Altered Metabolism in Cancer: Insights into Energy Pathways and Therapeutic Targets'. *Molecular Cancer* 23 (1): 203. https://doi.org/10.1186/s12943-024-02119-3.

Tulodziecka, Karolina, Barbara B. Diaz-Rohrer, Madeline M. Farley, et al. 2016. 'Remodeling of the Postsynaptic Plasma Membrane during Neural Development'. *Molecular Biology of the Cell* 27 (22): 3480–89. https://doi.org/10.1091/mbc.e16-06-0420.

Turner, Nicholas C. 2017. ‘Signatures of DNA-Repair Deficiencies in Breast Cancer’. *New England Journal of Medicine* 377 (25): 2490–92. https://doi.org/10.1056/NEJMcibr1710161.

Tutt, Andrew, Holly Tovey, Maggie Chon U. Cheang, et al. 2018. ‘Carboplatin in BRCA1/2-Mutated and Triple-Negative Breast Cancer BRCAness Subgroups: The TNT Trial’. *Nature Medicine* 24 (5): 628–37. https://doi.org/10.1038/s41591-018-0009-7.

Twig, Gilad, Alvaro Elorza, Anthony J. A. Molina, et al. 2008. ‘Fission and Selective Fusion Govern Mitochondrial Segregation and Elimination by Autophagy’. *The EMBO Journal* 27 (2): 433–46. https://doi.org/10.1038/sj.emboj.7601963.

Ubellacker, Jessalyn M., Alpaslan Tasdogan, Vijayashree Ramesh, et al. 2020. ‘Lymph Protects Metastasizing Melanoma Cells from Ferroptosis’. *Nature* 585 (7823): 113–18. https://doi.org/10.1038/s41586-020-2623-z.

Ursini, F., M. Maiorino, M. Valente, L. Ferri, and C. Gregolin. 1982. ‘Purification from Pig Liver of a Protein Which Protects Liposomes and Biomembranes from Peroxidative Degradation and Exhibits Glutathione Peroxidase Activity on Phosphatidylcholine Hydroperoxides’. *Biochimica et Biophysica Acta (BBA) - Lipids and Lipid Metabolism* 710 (2): 197–211. https://doi.org/10.1016/0005-2760(82)90150-3.

Ursini, Fulvio, and Matilde Maiorino. 2020. ‘Lipid Peroxidation and Ferroptosis: The Role of GSH and GPx4’. *Free Radical Biology and Medicine* 152 (May): 175–85. https://doi.org/10.1016/j.freeradbiomed.2020.02.027.

Ursini, Fulvio, Matilde Maiorino, and Carlo Gregolin. 1985. ‘The Selenoenzyme Phospholipid Hydroperoxide Glutathione Peroxidase’. *Biochimica et Biophysica Acta (BBA) - General Subjects* 839 (1): 62–70. https://doi.org/10.1016/0304-4165(85)90182-5.

Vander Heiden, Matthew G., Lewis C. Cantley, and Craig B. Thompson. 2009. ‘Understanding the Warburg Effect: The Metabolic Requirements of Cell Proliferation’. *Science* 324 (5930): 1029–33. https://doi.org/10.1126/science.1160809.

Vani Raju, Manikandan, Meenakshi Kaniyur Chandrasekaran, Lavanya Loganathan, et al. 2026. ‘Lipid Remodeling and Ferroptosis in Phosphatidylcholine-Mediated Tumor–Stroma Crosstalk’. *Frontiers in Molecular Biosciences* 13 (January): 1742305. https://doi.org/10.3389/fmolb.2026.1742305.

Vecchia, Sofia La, Saurav Doshi, Petros Antonoglou, et al. 2025. ‘Small-Molecule OPA1 Inhibitors Reverse Mitochondrial Adaptations to Overcome Therapy Resistance in Acute Myeloid Leukemia’. *Science AdVAnceS*.

Venkatesh, Divya, Nicholas A. O'Brien, Fereshteh Zandkarimi, et al. 2020. 'MDM2 and MDMX Promote Ferroptosis by PPARα-Mediated Lipid Remodeling'. *Genes & Development* 34 (7–8): 526–43. https://doi.org/10.1101/gad.334219.119.

Verginadis, Ioannis I., Harris Avgousti, James Monslow, et al. 2022. 'A Stromal Integrated Stress Response Activates Perivascular Cancer-Associated Fibroblasts to Drive Angiogenesis and Tumour Progression'. *Nature Cell Biology* 24 (6): 940–53. https://doi.org/10.1038/s41556-022-00918-8.

Verma, Nandini, Yaron Vinik, Ashish Saroha, et al. 2020. 'Synthetic Lethal Combination Targeting BET Uncovered Intrinsic Susceptibility of TNBC to Ferroptosis'. *Science Advances* 6 (34): eaba8968. https://doi.org/10.1126/sciadv.aba8968.

Vidra, Radu, Adina Nemes, Andreea Vidrean, et al. 2021. 'Pathological Complete Response Following Cisplatin or Carboplatin-based Neoadjuvant Chemotherapy for Triple-negative Breast Cancer: A Systematic Review and Meta-analysis'. *Experimental and Therapeutic Medicine* 23 (1): 91. https://doi.org/10.3892/etm.2021.11014.

Vinayak, Shaveta, and James M. Ford. 2010. 'PARP Inhibitors for the Treatment and Prevention of Breast Cancer'. *Current Breast Cancer Reports* 2 (4): 190–97. https://doi.org/10.1007/s12609-010-0026-0.

Viswanathan, Vasanthi S., Matthew J. Ryan, Harshil D. Dhruv, et al. 2017. 'Dependency of a Therapy-Resistant State of Cancer Cells on a Lipid Peroxidase Pathway'. *Nature* 547 (7664): 453–57. https://doi.org/10.1038/nature23007.

Vivas-García, Yurena, Paola Falletta, Jana Liebing, et al. 2020. 'Lineage-Restricted Regulation of SCD and Fatty Acid Saturation by MITF Controls Melanoma Phenotypic Plasticity'. *Molecular Cell* 77 (1): 120-137.e9. https://doi.org/10.1016/j.molcel.2019.10.014.

Volmer, Romain, Kattria Van Der Ploeg, and David Ron. 2013. 'Membrane Lipid Saturation Activates Endoplasmic Reticulum Unfolded Protein Response Transducers through Their Transmembrane Domains'. *Proceedings of the National Academy of Sciences* 110 (12): 4628–33. https://doi.org/10.1073/pnas.1217611110.

Voutsadakis, Ioannis A., Khalil Zaman, and Serge Leyvraz. 2011. 'Breast Sarcomas: Current and Future Perspectives'. *The Breast* 20 (3): 199–204. https://doi.org/10.1016/j.breast.2011.02.016.

Wagner, Karina, David U. Mick, and Peter Rehling. 2009. 'Protein Transport Machineries for Precursor Translocation across the Inner Mitochondrial Membrane'. *Biochimica et Biophysica Acta (BBA) - Molecular Cell Research* 1793 (1): 52–59. https://doi.org/10.1016/j.bbamcr.2008.05.026.

Wahida, Adam, and Marcus Conrad. 2023. 'Ferroptosis: Under Pressure!' *Current Biology* 33 (7): R269–72. https://doi.org/10.1016/j.cub.2023.03.009.

Wai, Timothy, and Thomas Langer. 2016. 'Mitochondrial Dynamics and Metabolic Regulation'. *Trends in Endocrinology & Metabolism* 27 (2): 105–17. https://doi.org/10.1016/j.tem.2015.12.001.

Wan, Mengting, Shuaikang Pan, Benjie Shan, et al. 2025. 'Lipid Metabolic Reprograming: The Unsung Hero in Breast Cancer Progression and Tumor Microenvironment'. *Molecular Cancer* 24 (1): 61. https://doi.org/10.1186/s12943-025-02258-1.

Wang, Diyu, Lei Yin, Jinrong Wei, Zhixue Yang, and Guoqin Jiang. 2017. 'ATP Citrate Lyase Is Increased in Human Breast Cancer, Depletion of Which Promotes Apoptosis'. *Tumor Biology* 39 (4): 101042831769833. https://doi.org/10.1177/1010428317698338.

Wang, Shang-Jui, Dawei Li, Yang Ou, et al. 2016. 'Acetylation Is Crucial for P53-Mediated Ferroptosis and Tumor Suppression'. *Cell Reports* 17 (2): 366–73. https://doi.org/10.1016/j.celrep.2016.09.022.

Wang, Sheng-Fan, Chih-Hsuan Wung, Meng-Shian Chen, et al. 2018. 'Activated Integrated Stress Response Induced by Salubrinal Promotes Cisplatin Resistance in Human Gastric Cancer Cells via Enhanced xCT Expression and Glutathione Biosynthesis'. *International Journal of Molecular Sciences* 19 (11): 3389. https://doi.org/10.3390/ijms19113389.

Wang, Yufei, Lu Yang, Xiaojun Zhang, et al. 2019. 'Epigenetic Regulation of Ferroptosis by H2B Monoubiquitination and P53'. *EMBO Reports* 20 (7): e47563. https://doi.org/10.15252/embr.201847563.

Wang, Yuqi, Mangze Hu, Jian Cao, et al. 2025. 'ACSL4 and Polyunsaturated Lipids Support Metastatic Extravasation and Colonization'. *Cell* 188 (2): 412-429.e27. https://doi.org/10.1016/j.cell.2024.10.047.

Wang, Zongyi, Fei Yin, Jing Xu, et al. 2019. 'CYT997(Lexibulin) Induces Apoptosis and Autophagy through the Activation of Mutually Reinforced ER Stress and ROS in Osteosarcoma'. *Journal of Experimental & Clinical Cancer Research* 38 (1): 44. https://doi.org/10.1186/s13046-019-1047-9.

Warburg, Otto. 1956. *On the Origin of Cancer Cells*. 123.

Warner, Gregory J., Marla J. Berry, Mohamed E. Moustafa, Bradley A. Carlson, Dolph L. Hatfield, and Jerry R. Faust. 2000. 'Inhibition of Selenoprotein Synthesis by Selenocysteine tRNA[Ser]Sec Lacking Isopentenyladenosine'. *Journal of Biological Chemistry* 275 (36): 28110–19. https://doi.org/10.1074/jbc.M001280200.

Watanabe, Takao, Hiroko Ninomiya, Takashi Saitou, et al. 2020. 'Therapeutic Effects of the PKR Inhibitor C16 Suppressing Tumor Proliferation and Angiogenesis in Hepatocellular Carcinoma in Vitro and in Vivo'. *Scientific Reports* 10 (1): 5133. https://doi.org/10.1038/s41598-020-61579-x.

Weaver, David, Verónica Eisner, Xingguo Liu, et al. 2014. 'Distribution and Apoptotic Function of Outer Membrane Proteins Depend on Mitochondrial Fusion'. *Molecular Cell* 54 (5): 870–78. https://doi.org/10.1016/j.molcel.2014.03.048.

Wei, Yingying, Zhihui Zhu, Hongtao Hu, Jiaqi Guan, Bo Yang, and Huajun Zhao. 2022. 'Eupaformosanin Induces Apoptosis and Ferroptosis through Ubiquitination of Mutant P53 in Triple-Negative Breast Cancer'. *European Journal of Pharmacology* 924 (June): 174970. https://doi.org/10.1016/j.ejphar.2022.174970.

Weingarten-Gabbay, Shira, Shani Elias-Kirma, Ronit Nir, et al. 2016. 'Systematic Discovery of Cap-Independent Translation Sequences in Human and Viral Genomes'. *Science* 351 (6270): aad4939. https://doi.org/10.1126/science.aad4939.

Wek, Ronald C., Tracy G. Anthony, and Kirk A. Staschke. 2023. 'Surviving and Adapting to Stress: Translational Control and the Integrated Stress Response'. *Antioxidants & Redox Signaling* 39 (4–6): 351–73. https://doi.org/10.1089/ars.2022.0123.

Wohlhieter, Corrin A., Allison L. Richards, Fathema Uddin, et al. 2020. 'Concurrent Mutations in STK11 and KEAP1 Promote Ferroptosis Protection and SCD1 Dependence in Lung Cancer'. *Cell Reports* 33 (9). https://doi.org/10.1016/j.celrep.2020.108444.

Wu, Dan, Yi Yang, Yiran Hou, et al. 2022. 'Increased Mitochondrial Fission Drives the Reprogramming of Fatty Acid Metabolism in Hepatocellular Carcinoma Cells through Suppression of Sirtuin 1'. *Cancer Communications* 42 (1): 37–55. https://doi.org/10.1002/cac2.12247.

Wu, Ke, Meisi Yan, Tong Liu, et al. 2023. 'Creatine Kinase B Suppresses Ferroptosis by Phosphorylating GPX4 through a Moonlighting Function'. *Nature Cell Biology* 25 (5): 714–25. https://doi.org/10.1038/s41556-023-01133-9.

Xiao, Chengmei, Yipu Li, Yushuang Liu, et al. 2024. 'Overcoming Cancer Persister Cells by Stabilizing the *ATF4* Promoter G-quadruplex'. *Advanced Science* 11 (35): 2401748. https://doi.org/10.1002/advs.202401748.

Xie, Ting, Wing Yan So, Xing Yu Li, and Po Sing Leung. 2019. 'Fibroblast Growth Factor 21 Protects against Lipotoxicity-Induced Pancreatic β-Cell Dysfunction via Regulation of AMPK Signaling and Lipid Metabolism'. *Clinical Science* 133 (19): 2029–44. https://doi.org/10.1042/CS20190093.

Xie, Yizhao, Biyun Wang, Yannan Zhao, et al. 2022. 'Mammary Adipocytes Protect Triple-Negative Breast Cancer Cells from Ferroptosis'. *Journal of Hematology & Oncology* 15 (1): 72. https://doi.org/10.1186/s13045-022-01297-1.

Xiong, Nating, Heming Wu, and Zhikang Yu. 2024. 'Advancements and Challenges in Triple-Negative Breast Cancer: A Comprehensive Review of Therapeutic and Diagnostic Strategies'. *Frontiers in Oncology* 14 (May): 1405491. https://doi.org/10.3389/fonc.2024.1405491.

Xiong, Yiquan, Zeming Liu, Xiangwang Zhao, et al. 2018. 'CPT1A Regulates Breast Cancer-Associated Lymphangiogenesis via VEGF Signaling'. *Biomedicine & Pharmacotherapy* 106 (October): 1–7. https://doi.org/10.1016/j.biopha.2018.05.112.

Xu, Shangcheng, Pei Wang, Huiliang Zhang, et al. 2016. 'CaMKII Induces Permeability Transition through Drp1 Phosphorylation during Chronic β-AR Stimulation'. *Nature Communications* 7 (1): 13189. https://doi.org/10.1038/ncomms13189.

Xu, Shuo, Tingting Chen, Lihua Dong, et al. 2020. 'Fatty Acid Synthase Promotes Breast Cancer Metastasis by Mediating Changes in Fatty Acid Metabolism'. *Oncology Letters* 21 (1): 1–1. https://doi.org/10.3892/ol.2020.12288.

Yagoda, Nicholas, Moritz Von Rechenberg, Elma Zaganjor, et al. 2007. 'RAS–RAF–MEK-Dependent Oxidative Cell Death Involving Voltage-Dependent Anion Channels'. *Nature* 447 (7146): 865–69. https://doi.org/10.1038/nature05859.

Yan, Xing, and Changhong Liu. 2025. 'The ATF4-Glutamine Axis: A Central Node in Cancer Metabolism, Stress Adaptation, and Therapeutic Targeting'. *Cell Death Discovery* 11 (1): 390. https://doi.org/10.1038/s41420-025-02683-7.

Yang, Fan, Yi Xiao, Jia-Han Ding, et al. 2023. 'Ferroptosis Heterogeneity in Triple-Negative Breast Cancer Reveals an Innovative Immunotherapy Combination Strategy'. *Cell Metabolism* 35 (1): 84-100.e8. https://doi.org/10.1016/j.cmet.2022.09.021.

Yang, Tinglin, Wenhui Li, Tao Huang, and Jun Zhou. 2023. 'Immunotherapy Targeting PD-1/PD-L1 in Early-Stage Triple-Negative Breast Cancer'. *Journal of Personalized Medicine* 13 (3): 526. https://doi.org/10.3390/jpm13030526.

Yang, Wan Seok, Katherine J. Kim, Michael M. Gaschler, Milesh Patel, Mikhail S. Shchepinov, and Brent R. Stockwell. 2016. 'Peroxidation of Polyunsaturated Fatty Acids by Lipoxygenases Drives Ferroptosis'. *Proceedings of the National Academy of Sciences* 113 (34). https://doi.org/10.1073/pnas.1603244113.

Yang, Wan Seok, Rohitha SriRamaratnam, Matthew E. Welsch, et al. 2014. 'Regulation of Ferroptotic Cancer Cell Death by GPX4'. *Cell* 156 (1–2): 317–31. https://doi.org/10.1016/j.cell.2013.12.010.

Yang, Wan Seok, and Brent R. Stockwell. 2008. 'Synthetic Lethal Screening Identifies Compounds Activating Iron-Dependent, Nonapoptotic Cell Death in Oncogenic-RAS-Harboring Cancer Cells'. *Chemistry & Biology* 15 (3): 234–45. https://doi.org/10.1016/j.chembiol.2008.02.010.

Ye, Jiangbin, Monika Kumanova, Lori S. Hart, et al. 2010. 'The GCN2-ATF4 Pathway Is Critical for Tumour Cell Survival and Proliferation in Response to Nutrient Deprivation'. *The EMBO Journal* 29 (12): 2082–96. https://doi.org/10.1038/emboj.2010.81.

Yerbes, Rosario, Rocío Mora-Molina, F. Javier Fernández-Farrán, Laura Hiraldo, Abelardo López-Rivas, and Carmen Palacios. 2022. 'Limiting Glutamine Utilization Activates a GCN2/TRAIL-R2/Caspase-8 Apoptotic Pathway in Glutamine-Addicted Tumor Cells'. *Cell Death & Disease* 13 (10): 906. https://doi.org/10.1038/s41419-022-05346-y.

Yi, Junmei, Jiajun Zhu, Jiao Wu, Craig B. Thompson, and Xuejun Jiang. 2020. 'Oncogenic Activation of PI3K-AKT-mTOR Signaling Suppresses Ferroptosis via SREBP-Mediated Lipogenesis'. *Proceedings of the National Academy of Sciences* 117 (49): 31189–97. https://doi.org/10.1073/pnas.2017152117.

Yin, Lijun, Shuo Qi, and Zhiqiang Zhu. 2023. 'Advances in Mitochondria-Centered Mechanism behind the Roles of Androgens and Androgen Receptor in the Regulation of Glucose and Lipid Metabolism'. *Frontiers in Endocrinology* 14 (October): 1267170. https://doi.org/10.3389/fendo.2023.1267170.

Yorek, Matthew, Xingshan Jiang, Shanshan Liu, et al. 2024. 'FABP4-Mediated Lipid Accumulation and Lipolysis in Tumor-Associated Macrophages Promote Breast Cancer Metastasis'. *eLife* 13 (November): RP101221. https://doi.org/10.7554/eLife.101221.

Young, Sara K., Jeffrey A. Willy, Cheng Wu, Matthew S. Sachs, and Ronald C. Wek. 2015. 'Ribosome Reinitiation Directs Gene-Specific Translation and Regulates the Integrated Stress Response'. *Journal of Biological Chemistry* 290 (47): 28257–71. https://doi.org/10.1074/jbc.M115.693184.

Yu, Chen-Lin, Shun-Fa Yang, Tung-Wei Hung, Chia-Liang Lin, Yi-Hsien Hsieh, and Hui-Ling Chiou. 2019. 'Inhibition of eIF2α Dephosphorylation Accelerates Pterostilbene-Induced Cell Death in Human Hepatocellular Carcinoma Cells in an ER Stress and Autophagy-Dependent Manner'. *Cell Death & Disease* 10 (6): 418. https://doi.org/10.1038/s41419-019-1639-5.

Zagami, Paola, and Lisa Anne Carey. 2022. 'Triple Negative Breast Cancer: Pitfalls and Progress'. *Npj Breast Cancer* 8 (1): 95. https://doi.org/10.1038/s41523-022-00468-0.

Zeng, Feng, Mingkang Yao, Yun Wang, et al. 2022. 'Fatty Acid β-Oxidation Promotes Breast Cancer Stemness and Metastasis via the miRNA-328-3p-CPT1A Pathway'. *Cancer Gene Therapy* 29 (3–4): 383–95. https://doi.org/10.1038/s41417-021-00348-y.

Zhang, Chenliang, Ting Zhang, Qiulin Tang, Yu Zeng, and Dan Cao. 2026. 'The Integrated Stress Response in Cancer: Paradox and Therapeutic Promise'. *Comprehensive Physiology* 16 (1): e70105. https://doi.org/10.1002/cph4.70105.

Zhang, Hao, Shuangli Zhu, Haiting Zhou, Rui Li, Xiaohui Xia, and Huihua Xiong. 2023. 'Identification of MTHFD2 as a Prognostic Biomarker and Ferroptosis Regulator in Triple-Negative Breast Cancer'. *Frontiers in Oncology* 13 (January): 1098357. https://doi.org/10.3389/fonc.2023.1098357.

Zhang, Jingyue, Yawen Song, Qianqian Shi, and Li Fu. 2021. 'Research Progress on FASN and MGLL in the Regulation of Abnormal Lipid Metabolism and the Relationship between Tumor Invasion and Metastasis'. *Frontiers of Medicine* 15 (5): 649–56. https://doi.org/10.1007/s11684-021-0830-0.

Zhang, Nan, Xin Yang, Fengjie Yuan, Wei-Guo Zhu, and Ying Zhao. 2018. 'Autophagy-Deficient Tumor Cells Rely on Extracellular Amino Acids to Survive upon Glutamine Deprivation'. *Autophagy* 14 (9): 1652–53. https://doi.org/10.1080/15548627.2018.1493314.

Zhang, Yilei, Jiejun Shi, Xiaoguang Liu, et al. 2018. 'BAP1 Links Metabolic Regulation of Ferroptosis to Tumour Suppression'. *Nature Cell Biology* 20 (10): 1181–92. https://doi.org/10.1038/s41556-018-0178-0.

Zhang, Yilei, Robert V. Swanda, Litong Nie, et al. 2021. 'mTORC1 Couples Cyst(e)Ine Availability with GPX4 Protein Synthesis and Ferroptosis Regulation'. *Nature Communications* 12 (1): 1589. https://doi.org/10.1038/s41467-021-21841-w.

Zhao, Haixin, Teng Li, Kai Wang, et al. 2019. 'AMPK-Mediated Activation of MCU Stimulates Mitochondrial Ca2+ Entry to Promote Mitotic Progression'. *Nature Cell Biology* 21 (4): 476–86. https://doi.org/10.1038/s41556-019-0296-3.

Zhao, J., J. Zhang, M. Yu, et al. 2013. 'Mitochondrial Dynamics Regulates Migration and Invasion of Breast Cancer Cells'. *Oncogene* 32 (40): 4814–24. https://doi.org/10.1038/onc.2012.494.

Zhao, Xiaofang, Chunyan Zhang, Hong Zhou, et al. 2016. 'Synergistic Antitumor Activity of the Combination of Salubrinal and Rapamycin against Human Cholangiocarcinoma Cells'. *Oncotarget* 7 (51): 85492–501. https://doi.org/10.18632/oncotarget.13408.

Zhao, Y., X. Ruan, J. Cheng, X. Xu, M. Gu, and A. O. Mueck. 2023. 'PGRMC1 Promotes Triple-Negative Breast Cancer Cell Growth via Suppressing Ferroptosis'. *Climacteric* 26 (2): 135–42. https://doi.org/10.1080/13697137.2023.2170225.

Zhou, Qian, Yu Meng, Daishi Li, et al. 2024. 'Ferroptosis in Cancer: From Molecular Mechanisms to Therapeutic Strategies'. *Signal Transduction and Targeted Therapy* 9 (1): 55. https://doi.org/10.1038/s41392-024-01769-5.

Zhou, Zhike, Ye Hua, Jun Ma, et al. 2025. 'Inhibition of RACGAP1 Sensitizes Triple-Negative Breast Cancer Cells to Ferroptosis by Regulating CPT1A-Dependent Fatty Acid Metabolism'. *Journal of Experimental & Clinical Cancer Research* 44 (1): 323. https://doi.org/10.1186/s13046-025-03568-4.

Zhu, Shan, Qiuhong Zhang, Xiaofan Sun, et al. 2017. 'HSPA5 Regulates Ferroptotic Cell Death in Cancer Cells'. *Cancer Research* 77 (8): 2064–77. https://doi.org/10.1158/0008-5472.CAN-16-1979.

Zhu, Yaqin, Yue Wang, Ying Li, et al. 2023. 'Carnitine Palmitoyltransferase 1A Promotes Mitochondrial Fission by Enhancing MFF Succinylation in Ovarian Cancer'.

Communications Biology 6 (1): 618. https://doi.org/10.1038/s42003-023-04993-x.

Zou, Peng, Longhua Liu, Louise D. Zheng, et al. 2016. 'Coordinated Upregulation of Mitochondrial Biogenesis and Autophagy in Breast Cancer Cells: The Role of Dynamin Related Protein-1 and Implication for Breast Cancer Treatment'. *Oxidative Medicine and Cellular Longevity* 2016 (1): 4085727. https://doi.org/10.1155/2016/4085727.

Zou, Wei, Ping Yue, Fadlo R. Khuri, and Shi-Yong Sun. 2008. 'Coupling of Endoplasmic Reticulum Stress to CDDO-Me–Induced Up-Regulation of Death Receptor 5 via a CHOP–Dependent Mechanism Involving JNK Activation'. *Cancer Research* 68 (18): 7484–92. https://doi.org/10.1158/0008-5472.CAN-08-1318.

Zou, Yilong, Whitney S. Henry, Emily L. Ricq, et al. 2020. 'Plasticity of Ether Lipids Promotes Ferroptosis Susceptibility and Evasion'. *Nature* 585 (7826): 603–8. https://doi.org/10.1038/s41586-020-2732-8.

Zou, Yilong, Haoxin Li, Emily T. Graham, et al. 2020. 'Cytochrome P450 Oxidoreductase Contributes Tophospholipid Peroxidation in Ferroptosis'. *Nature Chemical Biology* 16 (3): 302–9. https://doi.org/10.1038/s41589-020-0472-6.

Zou, Ying, Yi-Na Wang, Hong Ma, et al. 2020. 'SCD1 Promotes Lipid Mobilization in Subcutaneous White Adipose Tissue'. *Journal of Lipid Research* 61 (12): 1589–604. https://doi.org/10.1194/jlr.RA120000869.

Zubair, M., S. Wang, and N. Ali. 2021. 'Advanced Approaches to Breast Cancer Classification and Diagnosis'. *Frontiers in Pharmacology* 11 (February): 632079. https://doi.org/10.3389/fphar.2020.632079.

Zyryanova, Alisa F., Kazuhiro Kashiwagi, Claudia Rato, et al. 2021. 'ISRIB Blunts the Integrated Stress Response by Allosterically Antagonising the Inhibitory Effect of Phosphorylated eIF2 on eIF2B'. *Molecular Cell* 81 (1): 88-103.e6. https://doi.org/10.1016/j.molcel.2020.10.031.